QUANTUM MECHANICAL STUDY OF DIFFERENT TYPES OF PROTEIN SENSORS

THESIS SUBMITTED FOR THE AWARD OF THE DEGREE OF

Doctor of Philosophy

in

Applied Physics

By

Dharmveer Singh

Enrolment No.: 431/10

Under the Supervision of

Dr. Devesh Kumar

Department of Applied Physics

School for Physical Sciences

Babasaheb Bhimrao Ambedkar University, Lucknow

U.P., (India) – 226025

2017

DEDICATED TO

MY FAMILY

DECLARATION

I declare that the thesis titled **"Quantum Mechanical Study of Different Types of Protein Sensors"** has been prepared by me under the supervision of Dr. Devesh Kumar, Associate Professor, Department of Applied Physics, School for Physical Sciences, Babasaheb Bhimrao Ambedkar University, Lucknow. No part of this thesis has formed the basis for the award of any degree, diploma or fellowship previously. Further, I declare that the material embodied in the present work is based on original research work and the indebtedness to others has been duly acknowledged at relevant places.

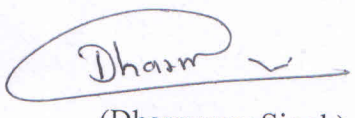

(Dharmveer Singh)

Department of Applied Physics
School for Physical Sciences
Babasaheb Bhimrao Ambedkar University
Vidya Vihar, Raebareili Road
Lucknow, (U.P.), India- 226025

Date: 12th October, 2017
Place: Lucknow

CERTIFICATE

This is to certify that the thesis titled **"Quantum Mechanical Study of Different Types of Protein Sensors"** submitted by Mr. Dharmveer Singh is an original research work and has not been previously submitted in part or full for the award of any other degree or diploma to this or any other university.

The thesis submitted to Babasaheb Bhimrao Ambedkar University, Lucknow satisfies all the requirements as stipulated in the Doctor of Philosophy (Ph.D.) Regulations – 1999 as amended in 2010 and it is fit for submission and evaluation for the award of the degree of Doctor of Philosophy of the University.

Date: 12th October, 2017

Supervisor

Head of the Department

ACKNOWLEDGEMENT

I would like to thank the Almighty for giving me strength, knowledge and opportunity for doing this research work guiding me throughout for its successful completion. I shall always be grateful and thankful to Him.

I would like to express my gratitude towards my supervisor and mentor **Dr. Devesh Kumar**, Associate Professor and Head, Department of Applied Physics. He has been a role model, a good teacher and acted as pillar of support providing me inspiration and guidance without bounds of time. His tireless effort in giving concrete inputs and feedback has helped reached a point from where first draft of this thesis proved so complete in itself that it rapidly evolved into a thesis in such apt shape.

I would like to take this opportunity to expressing my heartfelt reverences to my parents. Without their blessings, I would not have been able to pursure quest of knowledge to this length. I am also grateful to unwavering and unselfish love and support given to me by all my family members especially in times of despair without which I could not have smoothly sailed through the storm. A special mention to support of my younger sister **Miss Pushpa Kumari** must be necessarily included here, she acted as constant motivator and torch bearer guiding through my journey.

I am highly grateful to the help and support provided by faculties of the department: **Dr. B. C. Yadav, Dr. Ramesh Chandra, Dr. A. K. Yadav, Dr. Devendra Singh** and **Dr. K. B. Thapa** for helping me complete this task. They were always available for fruitful discussions that helped enormously in advancing towards research goals.

My acknowledgement would be incomplete without mentioning the help provided by my research group. Dr. Jitendra Kumar, Dr. Pranav Upadhyay, Dr. Suresh Kumar, Mr. Deep Kumar, Mr. Asheesh Kumar, Mr Narinder Kumar, Mr. Ankur Trivedi, Miss Anamika Singh Gaur, Miss Ruchi Mishra and Miss Rolly Yadav were ever willing to extend helping hand round the clock. They were always willing to help during course of Ph.D. research and manuscript preparation. Mr. Anwesh Panday is also thanked for his help. It is not possible for me to mention names of other researchers of the department who supported me through their academic discussions and moral support. I thank one and all who have directly or indirectly helped me or inspired me towards achievement of my goal.

Finally I would like to appreciate support and facilities extended by staff at Library and Computer Center of the Department as well as the University for necessary literature survey and other requirements.

(Dharmveer Singh)

ABSTRACT

Proteins are polymers of amino acids connected by dipeptide bonds. Amino acids play central roles both as building blocks of proteins and as intermediates in metabolism. They are essential for the structure, function, and regulation of the body's tissues and organs. Proteins are made up of hundreds of smaller units called amino acids that are attached to one another by peptide bonds, forming a long chain. There are 20 common amino acids found in proteins, and depending on their sequencing, and the overall protein structure, they convey an extensive array of chemical properties.

Graphene is the youngest known allotrope of carbon which is a two-dimensional and one-thick materials consisting sp^2 hybridized carbon atoms arranged in honeycomb structure. These honeycomb structure are the reasons for the extraordinary properties of graphene, which include a very large surface area [2630m^2/g, it is double that of single-walled carbon nanotube (SWCNT)], a tunable band gap, room temperature Hall effect, high mechanical strength (200 times greater than steel), high elasticity and high thermal conductivity. The exceptional electrical properties of graphene (such as, high charge mobility and capacity, highly tunable conductance) endow it as an ideal sensing element in electronic sensors. Carbon nanostructures [CNSs] exhibit non-covalent interaction such as the XH-π, cation-π, anion-π and π-π interaction towards the small gas molecules, metal ions and bio molecules. The XH-π weak interactions were extensively studied in recent years. These interactions are considered as a unique type of hydrogen bonding interaction in which π electron acts as the proton acceptor. Graphene is a sensitive nano material which detects all the individual events when a biomolecule is adsorbed to or deadsorbed from its surface. The adsorption of various substrates such as amino acids, nucleic acids, antibodies, gas molecules, metal

ions, polymers, organic molecules etc. on grapheme/CNT surfaces has attracted considerable attention because of the fundamental importance and potential industrial applications. In particular, the protein and graphene/CNT interaction has gained significant attention because of its application in various fields such as DNA sequencing, DNA sensing, amino acids sensing, drug delivery etc. Recently, it has been found that the determination of a patient's DNA sequence can reveal one's risk of falling ill with a particular disease and also help to design "personalized medicine", and thus the DNA sequencing appears to be one of most potential applications. The density functional theory (DFT) B3LYP with basis 6-31G** reproduced the proper geometry of the molecules under study. M062X method also provides other properties with accuracy. The charge, geometrical parameters etc. thus obtained can be used for further calculations and interpretations of molecular properties. It has been observed that the interaction energy, adsorption and chemical reactivity varies significantly for alkaline earth metal ions and amino acids with CNTs and graphene. It is expected that the current study will help in development of carbon material based biosensors.

PREFACE

Biosensor exhibits unique specificities towards analytes of biological origin such as proteins, DNAs, glucose, antibodies, antigens of contaminated or infected organisms, pollutants etc. A device for biological recognition event is necessary for such biosensors. This is called process of transduction and involves detection of appropriate signal when given substance interacts with probe of biosensor. As nanomaterials have shown high specificity and sensitivity even at low concentrations of given sample, they are known to act as promising candidates for biosensors. In this work, an attempt has been made towards understanding interaction between carbon nanostructures (carbon nanotube and graphene) with rare earth ions and amino acids. By charting out the corresponding changes occurring due to such interaction, they may serve as potential biosensor material.

Chapter 1 presents a literature survey of work done so far on biological molecules and carbon nanostructures with a focus on various computational quantum mechanical techniques prevalent in the area.

Chapter 2 discusses mathematical details of quantum mechanical methods. It also gives a glimpse of the theoretical methods helpful in study of bio-molecules, metal ions, small molecules and carbon nanostructures complexes.

Chapter 3 hints that the binding energy preferences of aromatic amino acids are different in both exterior and interior positions. The significant changes occur in the HOMO-LUMO energy gap of the CNT (12, 0) on the aromatic amino acids, which are used to design the new nano-bio composite carbonaceous material.

Chapter 4 is focused on study of the Al-doped graphene to improve its gas sensing efficiency and selectivity towards the various gas molecules. The gas molecule CCl_4, CH_4, NH_3, CO_2, CO, NO_2, CCl_2F_2, SO_2, CF_4 and N_2O are all of great practical interest for industrial, environmental and medical applications and have been theoretically investigated in present work. On the other hand, the effect of doping of the graphene sheet on the binding strength has also been estimated.

Chapter 5 describes the effect of binding strength of metal ions (Be^{+2}, Mg^{+2}, Ca^{+2}) at different position inside the carbon nanotube. The interaction energy with CNT(10,0) is compared and effect of metal ions on HOMO-LUMO gap of CNT has been studied.

Chapter 6 describes the effect of binding strength of aromatic amino acids such as histidine, phenylalanine, tyrosine and tryptophan at different position inside the carbon nanotube. It has been established that CNT(12,0) may serve as biosensing material for amino acids.

Chapter 7 presents a computational study of interaction of amino acid with graphene and effect of doping graphene with aluminium. Dramatic changes in electronic properties and related characteristics have been observed.

Chapter 8 summarises general conclusions drawn from research work of this thesis.

LIST OF ABBREVIATIONS

1	AFM	Atomic Force Microscope
2	BDE	Bond Dissociation Energy
3	BDFE	Bond Dissociation Free Energy
4	C-N	Carbon Nitrogen
5	CNS	Carbon Nanostructure
6	CNT	Carbon Nanotube
7	CI	Configuration-Interaction
8	CT	Charge-Transfer
9	DFT	Density Functional Theory
10	DFT-DC	Density Functional Theory Dispersion Correction
11	DFA	Density Functional Approximations
12	DNA	Deoxyribonucleic acid
13	EA	Electron Affinity
14	Ad E	Adsorption Energy
15	EB	Ethyl Benzene
16	ECP	Effective Core Potential
17	EPR	Electron Paramagnetic Resonance
18	GTO	Gaussian type Orbital
19	GC	Gradient Corrected
20	GGA	Generalised Gradient Approximations
21	GNR	Graphene Nano Ribbon
22	Graphene@Al	Al doped in Graphene Sheet
23	HAT	Hydrogen Atom Abstraction
24	HF	Hartree-Fock
25	HOMO	Highest Occupied Molecular Orbital
26	IE	Ionization Energy
27	LACVP	Basis sets that include effective core potential
28	LCAO	Linear Combination of Atomic Orbital
29	LDA	Local Density Approximations

30	LYP	Lee-Yang-Parr
31	LUMO	Lowest Occupied Molecular Orbital
32	MDB	Metalloprotein Databank
33	MM	Molecular Mechanics
34	MMO	Methane Monooxygenase
35	MO	Molecular orbital
36	MOEC	Molecular Orbital Expansion Coefficient
37	MS	Mass Spectrometry
38	MCSCF	Multi-Configuration Self Consistent Field
39	1D CNT	One Dimensional Carbon Nanotube
40	PG	Pure Graphene
41	PDB	Protein Data Bank
42	PES	Potential Energy Surface
43	PTFE	Proton Transfer Gibbs Free Energy
44	QM	Quantum Mechanics
45	RC	Reactant Complex
46	RHF	Restricted Hartree-Fock
47	RNA	Ribonucleic Acid
48	RR	Ribonucleotide Reductase
49	SCF	Self Consistent Field
50	SET	Single Electron Transfer
51	SORCI	Spectra Oriented Configuration Interaction
52	STO	Slater Type Orbital
53	SWCNT	Single Walled Carbon Nanotube
54	TF	Thomas-Fermi
55	TFD	Thomas Fermi Dirac
56	TPSS	Tao-Perdew-Staroverou-Scuseria
57	UB3LYP	Unrestricted Becke Lee Yang Parr basis set
58	UHF	Unrestricted Hartree-Fock
59	VWN	Vecko-Wilk-Nusair
6	VdW-DFz	Vander waals Density Functional-Second
61	ZPE	Zero Point Energy

62	0D CNT	Zero Dimensional Carbon Nanotube
63	3D CNT	Three Dimensional Carbon Nanotube
64	6MR	Six – Membered Ring
65		

LIST OF AMINO ACID ABBREVIATIONS

S. No.	Amino Acid	Three letter code
1	Alanine	Ala
2	Arginine	Arg
3	Asparagine	Asn
4	Aspartic Acid	Asp
5	Cysteine	Cys
6	Glutamine	Gln
7	Glutamic Acid	Glu
8	Glycine	Gly
9	Histidine	His
10	Isoleucine	Ile
11	Leucine	Leu
12	Lysine	Lys
13	Methionine	Met
14	Phenylalanine	Phe
15	Proline	Pro
16	Serine	Ser
17	Threonine	Thr
18	Tryptophan	Trp
19	Tyrosine	Tyr
20	Valine	Val

LIST OF TABLES

LIST OF FIGURES

TABLE OF CONTENTS

CHAPTER 1

INTRODUCTION

CHAPTER 1

INTRODUCTION

1.1. Proteins

Proteins play major roles in all biological processes. These include structural roles, mechanical support, growth and differential, enzymatic catalysis, immune defence, contractile processes, thrombosis and transport of matter and charge. Twenty L-amino acids are the basic building blocks of nanturally occurring proteins. Amino acids differs from each other structurally and functionally owing to the structure and chemical nature of their side chains. Under physiological conditions amino acids exist in zwitter-ionic form and they can be categorised as aliphatic, aromatic, basic, and neutral species, based on the chemical nature of their side chains. The functional diversity and versatility of proteins are due to the structural and chemical diversity of their side chains. Proteins are linear polymers of amino acids, covalently linked through peptide (C-N) bonds.

1.1.1. Amino acids

Amino acids are the basic structural constitutions of naturally occurring proteins. They all consists of an amino group (NH_3^+), a carboxylate group (COO^-), a hydrogen atom and a substituent group (R) called a side chain, bonded to a central carbon atom (C_α) as shown in Figure 1.1.

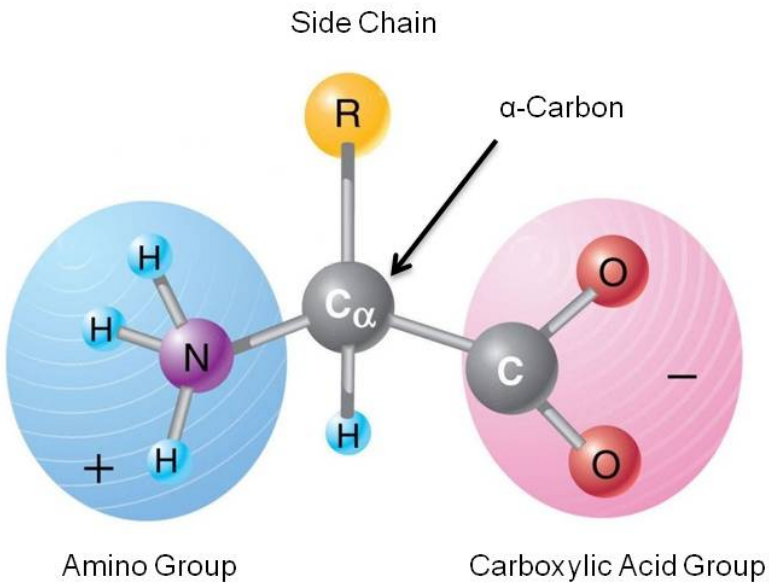

Figure 1.1: Basic unit structure for Amino Acid.

1.1.2. Classification of amino acids

Amino acids can be categorised based on the shape, size and the nature of their side chains. There are three types of amino acids due to this nature (1) charged, (2) neutral and (3) nonpolar R-groups.

(1) There are five amino acids with charged R-groups under physisorbed conditions. These are : basic amino acids such as lysine, arginine and histidine, and acidic amino acids such as aspartic and glutamic acids.

(2) Neutral amino acids are: asparagines, glutamine, cystein, serine and threonine.

(3) Non-polar amino acids are: glysine, alanine, leucine, isoleucine, valine, methionine, proline, phenylalanine, tryptophan and tyrosine (uncharged).

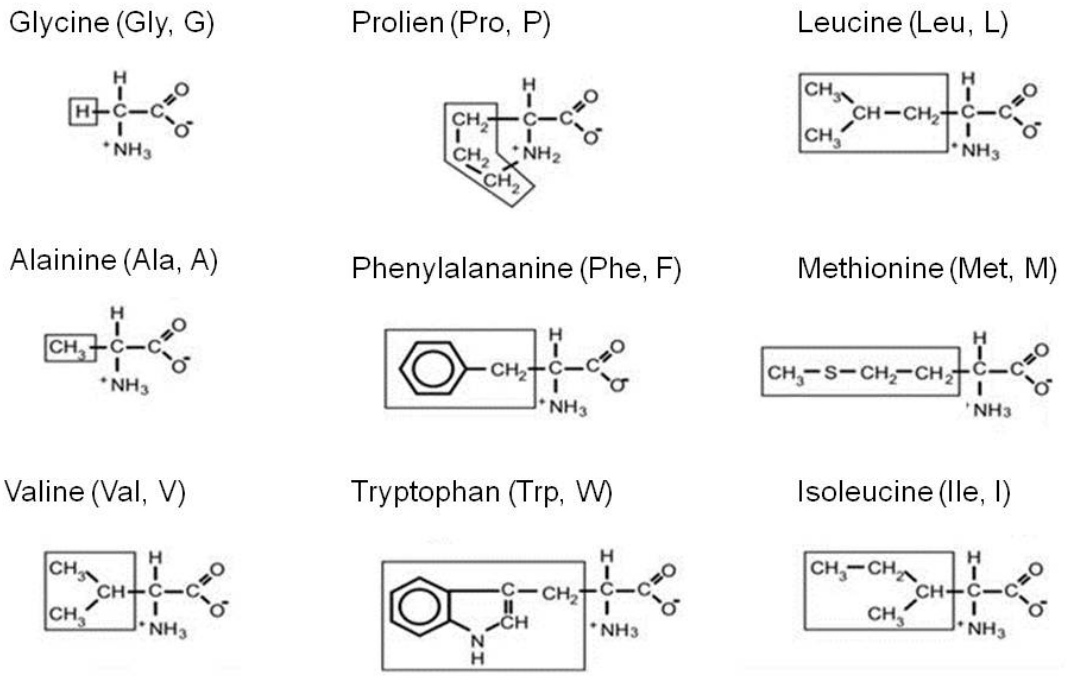

Figure 1.2: Non-polar amino acids.

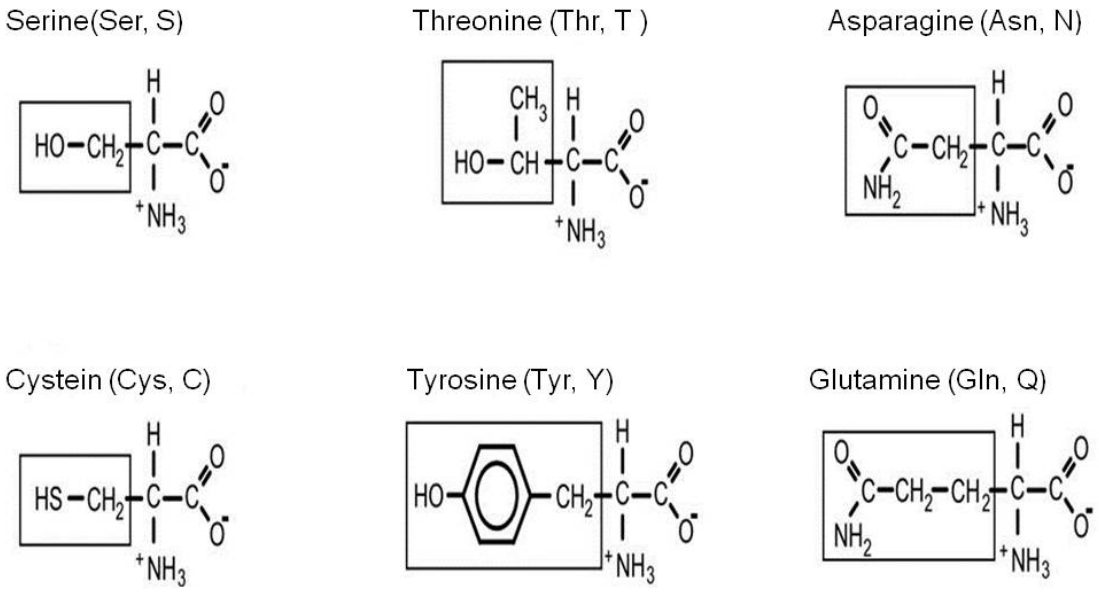

Figure 1.3: Polar, non-charged amino acids.

Figure 1.4: Negatively Charged amino acids.

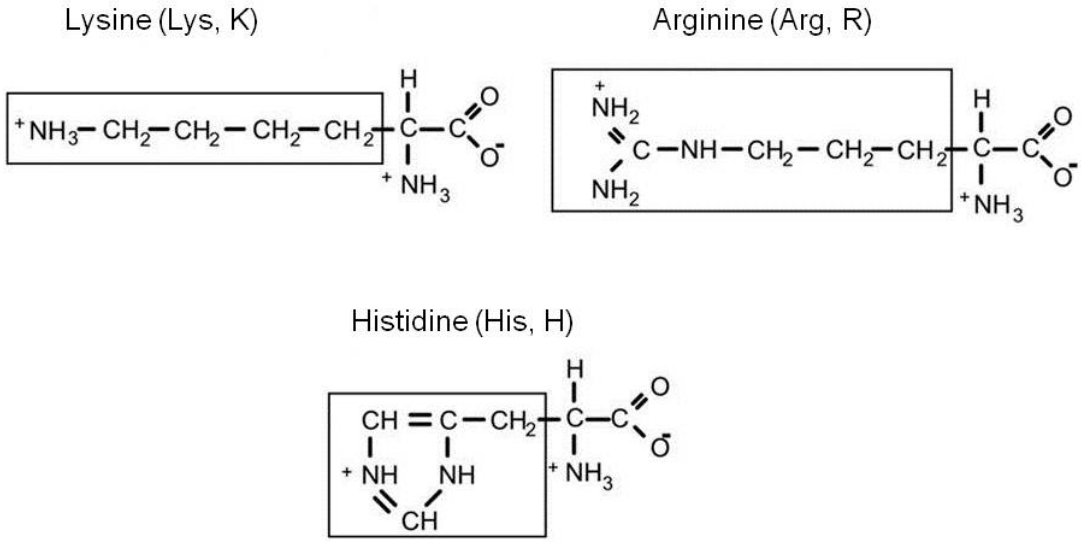

Figure 1.5: Positively Charged amino acids.

1.1.3. Structure of Proteins

Proteins are linear polymers of amino acids, synthesised from a library of twenty amino acids, covalently linked through peptide (C-N) bonds by the hydrolysis between α-amino and α-carboxyl of successive amino acids (Figure 1.6).

A single diamino acid is termed a peptide, and a polymer of several peptides an oligopeptide. A polymer in the range 20-50 amino acid residues is termed either a peptide or a small protein and a polypeptide above 50 amino acid residues is called a protein. A polypeptide consists of repeating peptide units (main chain) with chains(R_1, R_2, R_3, etc). The structure and functional features of proteins and protein complexes are addressed at four levels of hierarchal organisation. There are: (1) primary structure (1^o-structure), (2) secondary(2^o-structure), (3) tertiary structure (3^o-structure) and (4) Quaternary structure (4^o-structure).

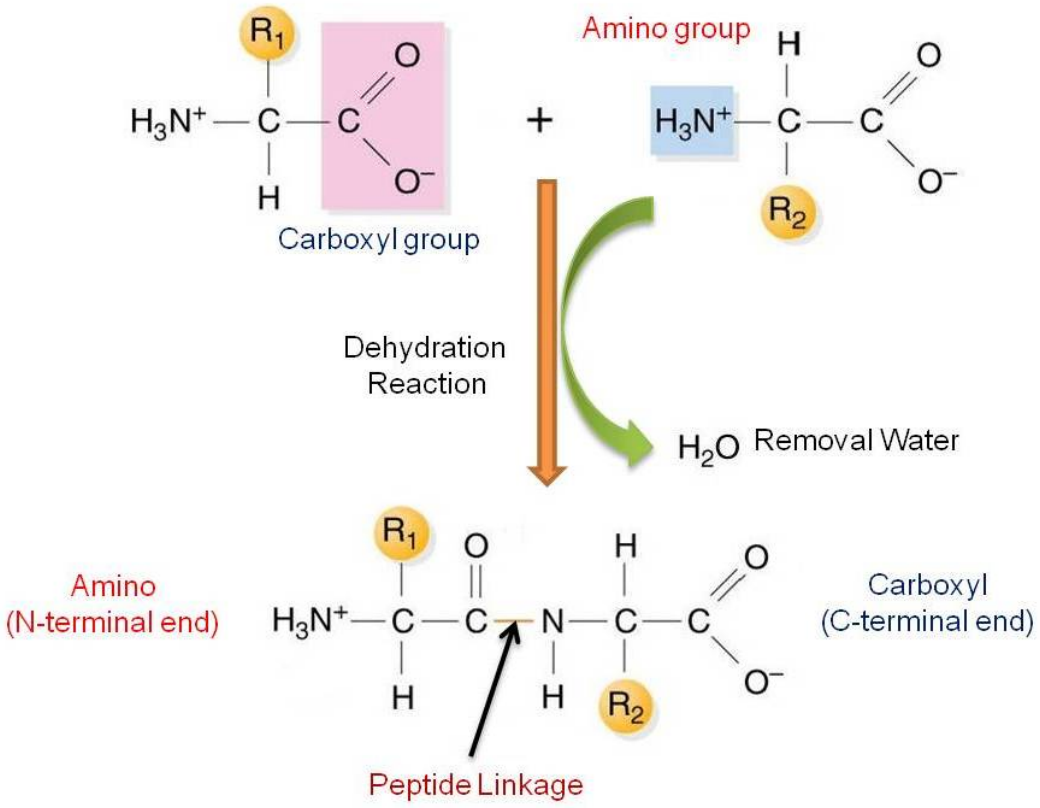

Figure 1.6: Formation of a dipeptide from two monopeptides (R1 and R2 are side chains).

1.1.3.1. The Primary Structure (1^o-Structure) of Proteins

The amino acids sequence of a polypeptide chain constitutes the primary structure of proteins. The convention for the amino acids is that the N-terminal end (free-α-amino group) is to the left (and the number 1-amino acid) and the C-terminal (end with the residue containing a free α-carboxyl group) is to the right. Single alphabet nomenclature of amino acids is used in the amino acid sequence data. It is essential to obtain the primary structure of a protein to understand its molecular mechanism of action, to compare with other homologous proteins, to trace evolutionary paths, and to predict secondary and tertiary structures from the sequence homologies with related proteins (structure prediction). Primary structure data of a protein is generally a indispensable for its structure determination by X-ray diffraction and NMR spectroscopic techniques.

1.1.3.2. The Secondary Structure (2^o-Stucture) of Proteins

The secondary structure of a protein deals with the ordered segments (helices, sheet), reverse turns and loops, and local hydrogen bonding of the polypeptides backbone. The secondary structure elements constitute the building blocks of the folding units in the globular proteins. The secondary structure of a polypeptide (protein) is determined largely by local sequence information. Analysis of structure parameters as bond lengths and bond angles of mono- and dipeptides, obtained from X-ray diffraction studies and Linus Pauling's study conducts to propose the essential features of the peptide unit and polypeptide backbone.

1.1.3.3. The Tertiary Structure (3^o-Structure) of Proteins

The three-dimensional structure (spatial folding) of a protein, consisting of only one polypeptide chain, is reffered to as the tertiary structure. The tertiary structure (protein folding) of a protein is unique and specific to each protein (Figure 1.7). The structure and functional features of protein-binding sites of ligands (protein-drug iteractions), the active sites of enzymes, or the binding sites for other proteins (protein-protein associations) depends on their tertiary structure, and therefore, knowledge of the spatial folding of any protein is indispensable to understand its structure and biochemical functions.

The unique folding of a protein is the result of non-bonded interactions between the polypeptide backbone and the side chains, acting cooperatively. The non-bonded interactions that stabilise the proper folding of macromolecules are ionic (salt bridges), dipole-dipole, van der waal and hydrophobic interactions and hydrogen bonds. Ions, dipoles and induced-dipole have electrical effects on one another by categories of electro-static interactions: ion/ion, ion/dipole, dipole/induced-dipole and induced-dipole/induced-dipole.

1.1.3.4. The Quaternary Structure (4^o-Structure) of Proteins

The structural organisation of proteins consisting of single polypeptides, such as myoglobins, lysozymes, cytochrome c, trypsin and chymotrysine etc., is complete at the tertiary level. However, In the case of proteins and protein complexes that comprise two or more polypeptide chains (poly-subunit proteins), such as hemoglobins, cytochrome oxidase, ATPases and collagen and viruses etc., another level of organisation, namely quarternary structure, deals with the specific

arrangements of the subunits with respect to one another in the protein complex and the interactions that stabilise these arrangements and associations. Non-polar interactions, which are weak , non-directional and driven by entropy factors, play a major role in the structural organisation and stability of quaternary structures in macro-molecular complexes.

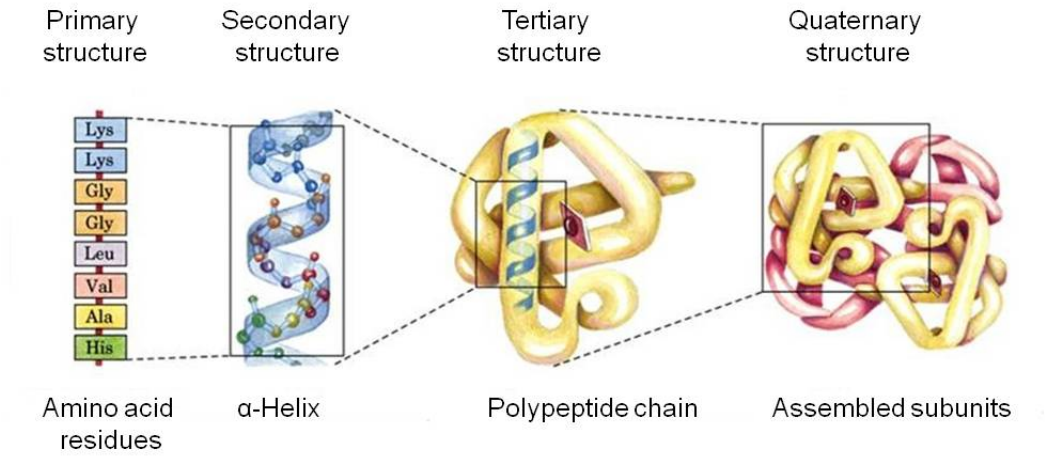

Figure 1.7: Structure of Protein.

1.2. Biosensors and Nanostructures

A biosensor is defined by its unique specificities toward analytes of biological origin. These analytes may be DNAs or proteins generated from antibodies, antigens of contaminated or infected organism. The analytes may also be simple molecules such as, glucose or pollutants. The main challenge in the development of a biosensor is the effective signal capture unit for the biological recognition event i.e., transduction. The transducer translates the recognition of the analyte into electrochemical, magnetic, gravimetric, electrochemiluminescent or optical signals. The nanomaterials are

potential candidates in order to lower detection limits to individual molecules and also to increase sensitivities, gold nanoparticles, carbon nanotubes, graphene, polymer nanoparticles, nanodiamonds, and semiconductor quantum dots are intensively studied nanomaterials.[1]

The nanomaterials have shown appropriateness of their potential applications for biosensing. The use of nano objects led to increased performances with enhanced sensitivities and lowered limits of detection by several orders of magnitudes. The general advantage of nanomaterials is its high specific surface which enables the immobilization of an increased amount of bioreceptor units. One of the main challenges for the immobilization scheme used to conjugate the bio-specific entity on such nanomaterials. Therefore, development of a reliable biosensor technique is the key factors to immobilize the enzyme.

The non-covalent approaches representing interactions such as π–π stacking, entrapment in polymers, van-der Waal forces or electrostatic forces between the biological entity and the nanomaterial are the principles to preserve specific properties of nanomaterials and biomolecules. Putzbach et al. have summarized efficient methods of the biofunctionalization in the nanomaterials.[2] The strategy to attach biomolecules covalently to nanomaterials has a great advantage in terms of reproducibility and stability of the surface functionalization. The uncontrolled anchoring of the biomolecules can affect the domain, which is responsible for the recognition event, is one of the drawback.

The technique for the immobilization of biomolecules through supramolecular or coordinative interactions is widely accepted in recent years for binding of biological species to surfaces. The biotin avidin system is most famous example in the area of biosensor engineering.[3] The biotinylated substrates can be attached to biotinylated

biomolecules through avidin (orstreptavidin) bridges. The nitrilotric-acetic-acid (NTA)/ Cu^{2+}/-histidine complex is another reported affinity systems [4] or adamantane/ β-cyclodextrin, the host-guest system.[5] The advantage of these systems over the other immobilization methods is the reversibility, and the possibility to regenerate/ restore the transducer element. Furthermore, the modified bio-receptor may be characterized individually which assured the reproducibility of the biosensor and the functionalized transducer surface.

According to the chemical composition, most of the nanomaterials are equipped with appropriate functions through direct functionalization, or through coating of functional polymers without changing their specific properties.[6] This type of functionalization allows not only the reproducible immobilization of bio-recepts or units but may also enhances the biocompatibility of materials.

1.2.1. Gold Nanoparticles

Gold nanoparticles are popularly used for biosensor application amongst the noble metal nanoparticles.[6] because of their biocompatibility, their electronic and optical properties, as well as their reasonably simple production and modification.[7]

The phenomenon of resonant surface plasmons, i.e. vibration of the electrons present in the conduction band in response to irradiation of one specific wavelength of light, is the interesting optical properties of gold surfaces. When the incident wavelength is much larger than particle size, the propagation of the vibrating electrons along the surface is not possible and it is termed as Surface Plasmon Resonance (SPR) setups. Then the electron density is polarized on one side of the nanoparticle where the plasmons vibrate in resonance with the frequency of light (Figure 1.8).

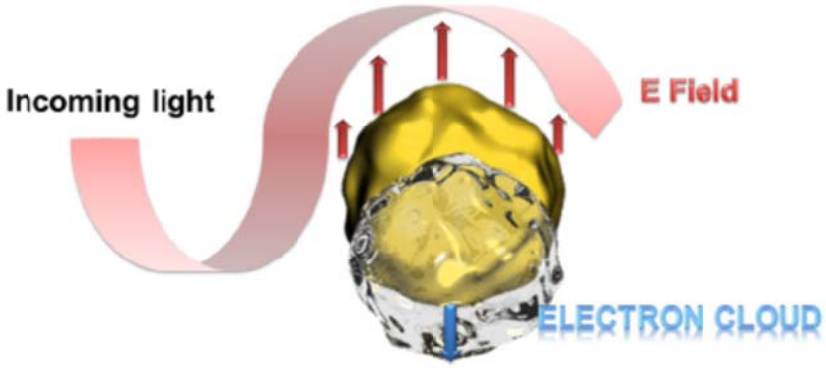

Figure 1.8: Schematic representation of the polarized electron density at the resonant excitation wavelength.

By applying the Mie theory, this phenomenon can be described [8,9] and this is strongly dependent on the dielectric constant of environment as well as the size and shape of the nanoparticle.[10] This dependency on environment is advantageous for (bio)-analytics because the recognition event can happen in a change of the vibration frequency and therefore to a change in color of the gold nanoparticles can be observed with bare eye. A wide series of proficient colorimetric-biosensors were designed for oligonucleotide or DNA or detection, or immunosensors.[11-14]

Wijaya et al., and Guo have demonstrated advantages in bioanalysis using SPR transduction of gold nanoparticles.[15] They have recorded the detection of the analyte in different ways such as the changes of the intensity, angle of incidence, or phase of reflected light with the change of the dielectic constant of propagating surface plasmons' environment of gold films.[15,16] Pedersen and Duncan have used a pure gold nanoparticle based SPR transduction replacing the gold film [17] and demonstrated a clear SPR signal enhancement when gold films and gold nanoparticles are used in a sandwich configuration. Zeng et al., used gold nanoparticles smaller than 40nm at a distance to the gold film surface of 5nm.[18]

Veitch used gold nanoparticles via biotin streptavidin linkage to immobilize the model enzyme horse radish peroxidise (HRP) which is widely used as label in biosensing applications.[19] Chen et al., showed the attachement of single HRP molecule to the gold nonoparticle.[20] Moskovits, Nie and Emory, Hossain et al., Lim et al., Saha et al., have studied the enhanced Raman Spectroscopy based on surface plasmon assisted signal amplification.[21-25]

Xu et al., 2006 have showed that efficient wiring can be obtained using enzymes (HRP) where metal ions are involved in the catalytic redox process.[26] Several group of researchers such as Mena et al., Willner et al., and Pingarrón et al., have also studied to wire the enzymes glucose oxidase (GOx) since its active center is deeply embedded inside the protein structure and contains no metal ion which would facilitate electron transfer.[27-29] Eustis and El-Sayed have reviewed nicely the outstanding properties of gold nanoparticles which made them useful not only for bioanalytics but also for other research fields.[30]

1.2.2. Carbon nanotubes

Nanotubes are derived from a graphene carbon lattice (i.e., the same as in graphite) and were discovered in 1991 by the Japanese electron microscopist Sumio Iijima who was studying the material deposited on the cathode during the arc-evaporation synthesis of fluerenes. They are described as closed cylindrical shape obtained by wrapping a graphene sheet.[31-36] There are mainly two types of CNTs which depends on the number of walls. Single walled carbon nanotube[SWCNTs] can be defined as a single rolled-up graphene sheet(Figure 1.9). They were found in 1993

and the diameter is between 1 to 3nm.[37,38] They self-organize forming bundles comprising even hundreds of tube.

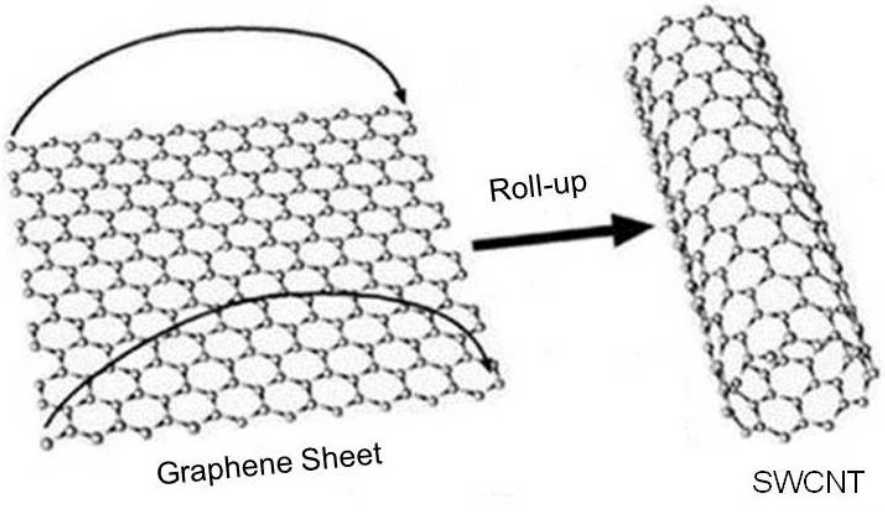

Figure 1.9: Carbon nanotube are obtained by wrapping a graphene sheet.

Multi walled carbon nanotubes[MWCNTs] can be defined as several concentric rolled-up graphene sheets [Figure 1.9], perfectly graphitized and closed at the ends by carbon atom pentagons. The inner diameter varies from 1 to 3nm, and the outer diameter is usually between 2–25nm which depends on the number of walls of graphene sheets. The space between two graphene surfaces is around 3.4Å which is slightly higher than the value of graphite (3.35Å). Iijima suggested that this difference is due to the combination of the graphene sheet curvature, the weak van-der waal forces between concentric tube.[33,39] The length of both types of carbon nanotubes are shown in Figure 1.10.

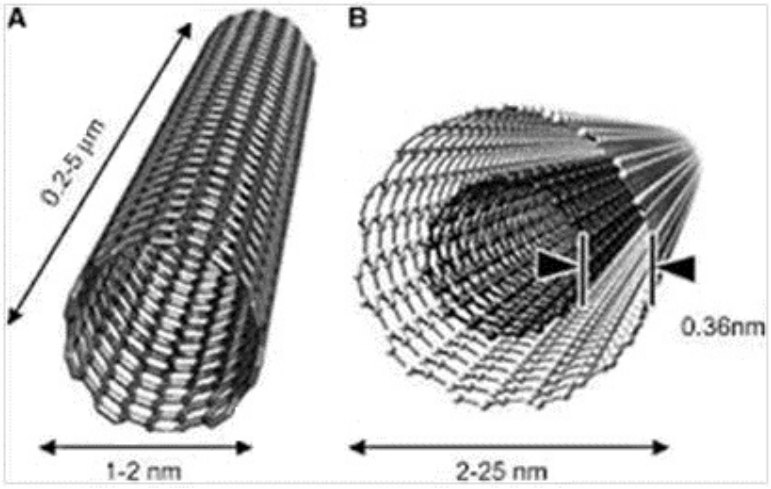

Figure 1.10: Curvature, diameter and length of the SWCNT and MWCNTs.

1.2.2.1. Electronic Structure and properties of carbon nanotubes

Carbon nanotube is the most important allotrope of carbon which is a one dimensional tube of atoms in hexagonal configuration with atoms by sp^2 bond. There are different possible ways to roll a graphene to form a tube giving rise to the different chiral or achiral dispositions. Nanotube can be classified into different types on the basis of their chiral indices, and their structures can be specified through their chiral vectors represented by the chiral indices (n,m). The chiral indices and structure of CNTs depends upon their configuration. In the armchair configuration, the C-C bonds of two opposite sides of the hexagon are perpendicular to the tube axis while in the zig-zag configuration, those bonds are parallel to the tube axis which are shown in figure 1.8. The rest of position configurations, where the C-C bonds form an angle θ respective to the tube axis, are known as chiral structure which are shown in Figure 1.10. The chirality of nanotube can be expresses by the chiral vector C.

$$\vec{C} = n\vec{a} + m\vec{b} \qquad (1.1)$$

Where $\vec{a}$ and $\vec{b}$ are the unit cell base vectors of the graphene sheet, and n≥m. This vector defines the rolling direction of the graphene sheet, with a point (m,n) superimposed over a defined origin (0,0) as shown in figure 1.8. The diameter of the tube can be expressed as:

$$D = \frac{a\sqrt{m^2 + nm + m^2}}{\pi} \qquad (1.2)$$

where $\left|\vec{a}\right| = \left|\vec{b}\right| = a = 1.42\sqrt{3}$ Å corresponding to the constant distance in the graphene sheet. It must be taken into account that this distance is 0.142nm for the sp^2 hybridization of carbon.[40]

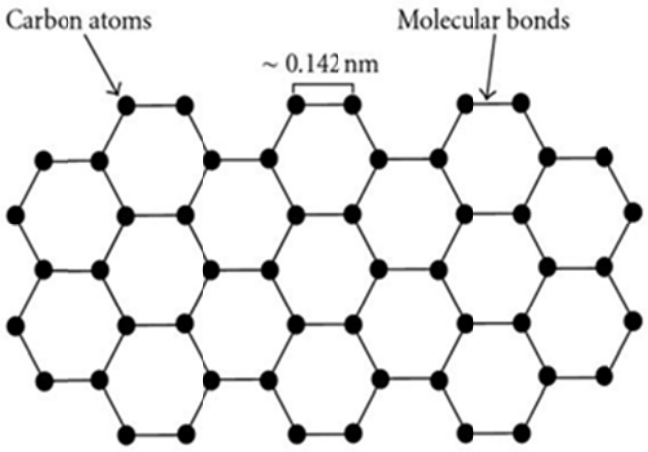

Figure 1.11: Structure of hexagonal graphite showing the unite cell.

Since the magnitude of $\vec{a}$ and $\vec{b}$ are equally 0.246nm, and the diameter of C in nanometer is $0.246(n^2+nm+m^2)^{1/2}$, and the diameter d_t is given by

$$d_t = 0.246(n^2+nm+m^2)^{1/2}$$

The chiral angle θ, the angle between the chiral vector and the rolling direction of the graphene sheet, is defined as

$$\theta = \arctan\left[-\frac{\sqrt{3n}}{2m+n}\right] \tag{1.3}$$

For the zig-zag structure, $\theta = 0^{\circ}$, and the values (n,m) results in (n,0) or (0,m).

For the armchair structure, $\theta = \pm 30^{\circ}$, and the values (n,m) results in (n,n).

The rest of values (n, m) stand for chiral structures.

The physical, chemical, and electronic properties of CNTs largly depend on their curvature and chirality. The armchair (n, n) nanotube shows metallic behaviour, while the zig-zag (n, 0) nanotubes exhibit semiconducting properties. The chiral (n, m) nanotubes perform metallic behaviour if the difference between n and m is a multiple of 3; otherwise, they behave as semiconductors.[41,42] The formation of carbon nanotubes from graphene is illustrated in Figure 1.10. According to the above statement, one third of the SWNTs are metallic, and two thirds are semiconductive. This fact has been confirmed by conductance measurements with Atomic Force Microscope (AFM) over individual nanotubes.[43]

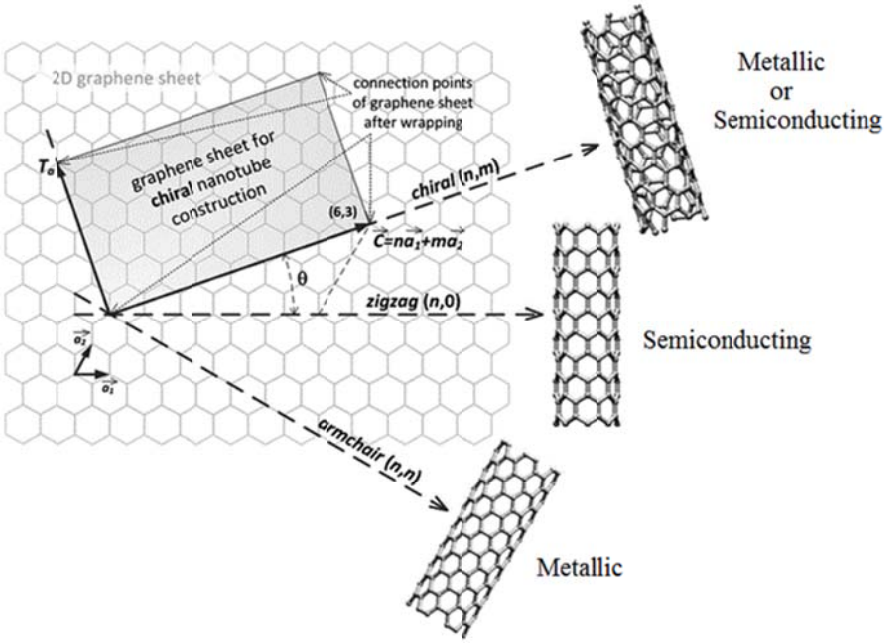

Figure 1.12: Chiral vectors $\vec{C}$ and m, n are defined as chiral indices show on graphene sheet. $\vec{a}$ and $\vec{b}$ are the unit cell vectors of the two dimentional hexagonal graphene nanostructure. d is the diameter of carbon nanotube. The θ is chiral angle which is defined between chiral vector and $\vec{C}$ and the zigzag axis.

1.2.2.2. Non-covalent interactions

The non-covalent interactions are diverse phenomena in the fields of biology, supramoleculecular chemistry and material sciences such as structure, stability, solvation, and crystal packing.[44, 45] Non-covalent interactions play major roles in understanding various biological problems ranging from protein folding to nucleobase packing and stacking.[46-48] An accurate description of non-covalent interactions is also a key in predicting binding and structures in proteins, DNA and RNA. Undersdanding the various factors influence, the unique physical, chemical, and electronic properties of CNSs (carbon nanostructures) making them appropriate for various potential applications in areas ranging from electronic to medicine. It has been shown in the literature that these CNSs exhibit non-covalent type of interactions with

many cases.[49] Hence, it has become important to quantify these non-covalent interactions and also to identify the factors that govern their strength. Besides, as nanomaterials show promising applications in biology and medicine, it is extremely essential to know how they interact with living organisms and environment.[47]

Thus the non-covalent interactions lead to the formation of supramolecular assembly, whereas the covalent interactions lead to the formation of a classical molecule. Among the various existing non-covalent interactions cation-π, π-π interaction and XH-π interactions are most common in the case of CNSs.

1.2.2.2.1. Cation-π interactions

Cation-π interactions are arguably the strongest non-covalent interactions and they have been extensively studied in recent years. Exprimental and theoretical studies done in recent years, have clearly demonstrated that cation-π interactions play an important role in diverse chemical and biological processes.[48-51] In 1981, Kebarele has done the interaction of K^+ with water and benzene in the gas phase. In systematic study of ion solvation by various solvents, Kebarle investigated the puzzling fact that benzene stabilizes K^+ ions better in the gas phase than water does.[52] In 1993, Dougherty has been investigated the cation-π interactions in Li^+, Na^+, K^+, and Rb^+ interaction with various biological molecules.[53] Cation-π interaction has also invoked to rationalize specific drug-receptor interactions.[51,52] and to design both novel receptor binding pockets and more protein ligands.[53-55] It is also recognized as contributing significant to protein.[56-59] and DNA stability.[60,61] Both experimental and theoretical studies have been carried out on cation-π interactions, and have provided valuable insights into their nature.[48,62] The experimental and

theoretical study of cation-π interaction have demonstrated to be a powerful tool for studying such interactions at the atomic and electronic levels, and have proved capable of accurately predicting binding energies. Hence, quantum mechanical methods are now widely accepted as being complementary to experimental measurements on cation-π systems. Cation-π intractions are very sensitive to the nature of metal ion and size of π-system.[63]

1.2.2.2.2. π-π interactions

π-π interactions are one of the weak interaction in nature which have been recognized to impart both structure and functional properties to materials as well as biomolecules.[64] Carbon nanostructures have been shown to exhibits π-π interactions with different aromatic groups in various biomolecules.[65] The π-π stacking interactions of CNSs with aromatic molecules appears to be significant because of their extended π-conjugation, and they seem to play a significant role in explaining the versatile applications of CNTs and graphene.

1.2.2.2.3. Anion-π interactions

Anion-π interaction are one of the non covalent interaction in which the interaction of halides sush as Cl, F, Br and I with the simple aromatic compounds, are not very strong in nature. In recent study on anion-π interactions, these interaction between halides ions and graphene flakes have been found to be stronger than those with simple aromatic compounds like benzene. This unexpected strong binding interaction is an attribute to the effective donor-acceptor interaction between the halide ions and the CNSs.[66]

1.2.2.2.4. X-π interactions

X-π interaction is also a weak interaction which are produced between the (X=C, O, N, S etc) and π-system. These unique interaction is a hydrogen- binding interaction in which π electron acts as the proton acceptor.[67] There are some group which has been done a series of studies of XH-π interactions involving various molecular cations and small molecules.[68-73]

1.2.3. Graphene

Graphene is an allotrope of carbon which was discovered by Adrew Geim in 2004. Graphene is the youngest known allotropes of carbon which is a two-dimentional and one-thick material consisting sp^2 hybridized carbon atoms arranged in honeycomb structure.[74] These allotropes of carbon recently used in research area interest from biomedical to environment applications due to the unique physical and chemical properties. The exceptional properties of carbon nano-materials such as electronic, thermal, optical, mechanical and transport properties make them promising candidates for various potential applications. Graphene has been studied for the past sixty years in order to describe the properties of various carbon-based materials. It also provides an excellent condensed-matter analogue of (2+1)-dimensional quantum electrodynamics which makes graphene the most theoretically studied material in the recent years. Typically important properties of graphene are fractional quantum hall effect at room temperature.[75-77] an ambipolar electric field effect along with ballistic conduction of charge carriers,[78] tunable band gap [79] and high elasticity.[80]

In graphene, the energy of the electrons is linearly dependent on the wave vector near the crossing points in the Brillouin zone which is a significant property of this upcoming material. In this 2D material, Dirac equation finds more utility compared to the frequently used Schrödinger equation to describe the charge carriers which imitate relativistic particles.[81-83]. Although graphene is expected to be perfectly flat, ripples occur because of thermal fluctuations.[74]

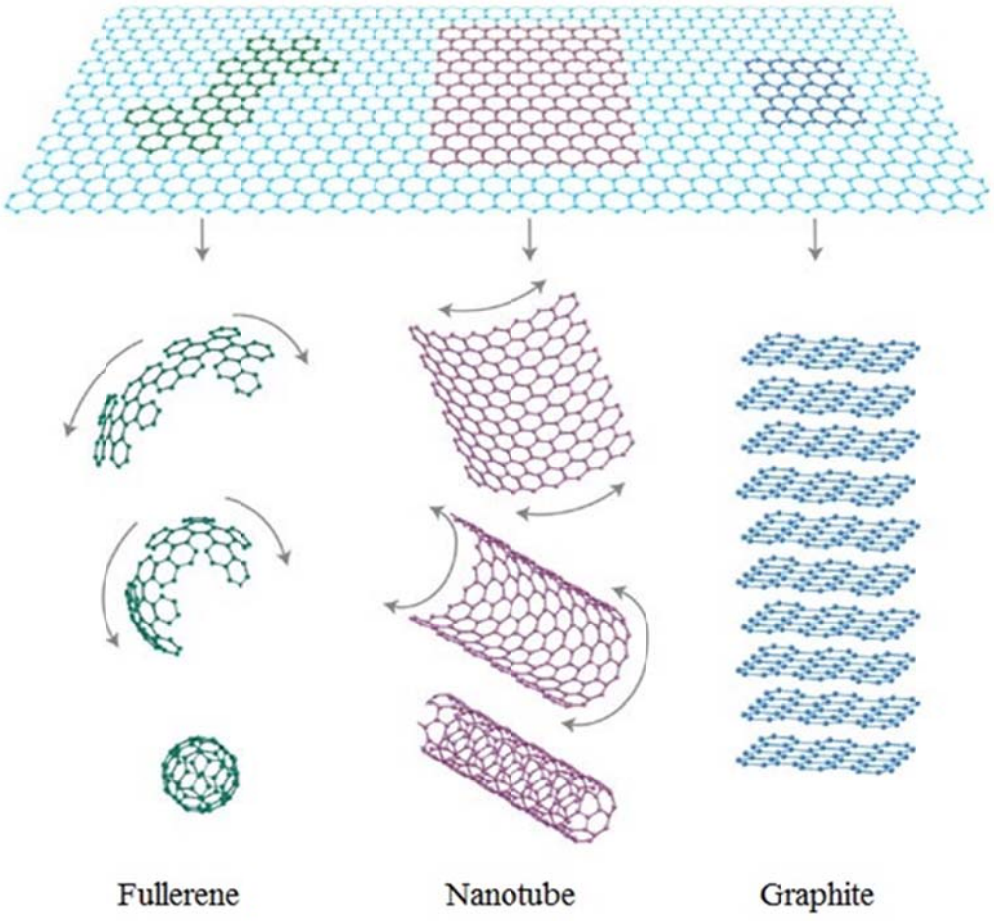

Figure 1.13: Graphene: mother of all graphitic forms. It can be wrapped up 0D buckywalls, rolled into nanotubes 1D nanotubes or stacked into 3D graphite.

Ideally graphene is a single-layer material, but graphene samples with two or more layers are being investigated with equal interest. One can define three different types

of graphene: single-layer graphene (SG), bilayer graphene (BG) and few-layer graphene (number of graphene layers ≤ 10). Although SG and BG were first obtained by micro-mechanical cleavage.[78] since then, graphenes containing different number of layers have been prepared using diverse strategies.[81] There are a few reports on some of the properties of few-layer graphenes, but, there are not many studies reporting changes in properties brought about the number of layers. The widespread applications of graphene have interested scientists wordwide. There are many experimental and theoretical studies in research interest on graphene nano materials. In these present work, it is theoretically investigated the graphene is used to improve its bio-sensing efficiency and selectivity towards the amino acids, nucleoacids, metal ions and various gas molecules. It is very important for graphene to interact with the differents molecular structures so that its electronic properties get changed. These theoretical studies are all of great practical interest for industrial, environmental and medical applications. On the other hand, the effect of molecular structure towards the graphene/CNTs sheet on the binding strength has been estimated.

1.3. Review of Literature

There are several reviews [82-86] which nicely review the electron transfer, biomedical applications, optical properties, imaging and use as biosensor of cabon nanostructures. Graphene has two main advantages over CNT regarding its application in electrochemical sensors and biosensors that are graphene does not contain metallic impurities and the production of graphene is cheap and easily accessible.[87-89] Graphene can easily connect to biomolecules via π-π stacking and hydrophobic interactions.[88,90]

Ruecha et al., has demonstrated the application of graphene as biosensor for the cholesterol.[91] Yang et al., demonstrated the application of graphene to detect pesticides.[92] The graphene-based sensors was used for detection of heavy metal ions such as Pb^{+2} and Cd^{+2}.[93-95] Wang et al., have used graphene based sensor with the CdS quantum dots and molecularly imprinted polymers to detect 4-Aminophenol.[96] The graphene based sensors have been reported for the detection of erythromycin [97] and tryptamine [98] with electrochemical sensors, and for the detection of S. Aureus with a piezoelectric sensor.[99,100]

Several researchers have investigated the biodistribution of SWCNTs in several animal studies with pristine, covalently modified and non-covalently functionalized nanotube samples.[101-104] Some researcher have also reported that pristine and covalently modified SWCNTs that was found accumulated in animal body and caused inflammation, pulmonary/cardiovascular toxicity and oxidative stress.[101,105,106] Biopolymers (e.g. oligonucleotide strands and peptides) and organic polymers were used for the screening of corona phase recognition on SWCNTs and the corona phase structure can be screened for target specificity.[107-111] Several group of researchers have demonstrated SWCNT as sensors for short peptides and proteins.[112-115]

An important application of SWCNTs is biomedical imaging agents. It is a ideal imaging probe in complex biological environments that needs to be biocompatible, bright and stable.[116-124] Fakhri et al., [125] studied of intracellular motion fluctuations by conjugating SWCNTs with kinesin-1 motor proteins in COS-7 cells. SWCNTs is also popular as super-resolution probes.[126-128]

Graphene as biosensor was first demonstrated by Clark and Lyon in 1962.[129] There are several excellent reviews which focus on the synthesis, properties and biosensing performance of graphene and its derivatives for biomedical applications.[130-140]

The *in vivo* toxicity studies shown that biocompatibility of graphene and its derivatives largely depends on its lateral size, dosage, functionalization, charge, and reactive oxygen species.[141-144] The optical properties of graphene and its derivatives over other nanomaterials were nicely reviewed by the several groups.[146-150] Several variety of graphene based electrochemical biosensors have been designed, which lead to a bright way for electrochemical biosensors.[151-155] There are many electrochemical graphene-based device schemes which were proposed for use *in vivo* for monitoring the dopamine, H_2O_2, L-Dopa (an intermediate precursor of the neurotransmitter dopamine), glucose, L-lactate, β-galactosidase-gene expressions.[156-160]

1.4. References

1. Holzinger, M., Goff, A. L. and Cosnier, S., *Frontiers in Chemistry* **2014**, *2*, Article 63.
2. Putzbach, W. and Ronkainen, N., *Sensors* **2013**, *13*, 4811.
3. Wilchek, M. and Bayer, E., *Anal. Biochem.* **1988**, *171*, 1
4. Haddour, N., Cosnier, S. and Gondran, C., *J. Am.Chem.Soc.* **2005**, *127*, 5752.
5. Holzinger, M., Bouffier, L., Villalonga, R. and Cosnier, S., *Biosens.Bioelectron.* **2009**, *24*, 1128.
6. Biju, V., *Chem. Soc. Rev.* **2014**, *43*, 744.
7. Li, Y., Schluesener, H., and Xu, S., *Gold Bull.* **2010**, *43*, 29.
8. Mulvaney, P., *Langmuir* **1996**, *12*, 788.
9. Hao, E., Schatz, G. C. and Hupp, J. T., *J. Fluoresc.* **2004**, *14*, 331.
10. Kelly, K. L., Coronado, E., Zhao, L. L. and Schatz, G. C., *J. Phys. Chem. B* **2002**, *107*, 668.
11. Reynolds, R. A., Mirkin, C. A. and Letsinger, R. L., *J. Am. Chem. Soc.* **2000**, *122*, 3795.
12. Oldenburg, S. J., Genick, C. C., Clark, K. A. and Schultz, D. A. *Anal. Biochem.* **2002**, *309*, 109.
13. Liu, J. and Lu, Y., *J. Fluoresc.* **2004**, *14*, 343.
14. Xu, W., Xue, X., Li, T., Zeng, H. and Liu, X., *Angew. Chem. Int. Ed.* **2009**, *48*, 6849.
15. Wijaya, E., Lenaerts, C., Maricot, S., Hastanin, J., Habraken, S., Vilcot, J. P., Boukherroub, R., Szunerits, S., *Curr. Opin. Solid State Mater. Sci.* **2011**, *15*, 208.
16. Guo, X., *J. Biophotonics* **2012**, *5*, 483.
17. Pedersen, D. B. and Duncan, E. J. S., *Technical Report*, *DRDC Suffield TR* 2005-109.

18. Zeng, S., Yu, X., Law, W. -C., Zhang, Y., Hu, R., Dinh, X. -Q., Hoe, H., -P., Yong, K., -T., *Sens. Actuators B Chem.* **2013**, *176*, 1128.

19. Veitch, N. C., *Phytochemistry* **2004**, *65*, 249.

20. Chen, S., Svedendahl, M., Duyne, R. P. V. and Kaíll, M., *NanoLett.* **2011**, *11*, 1826.

21. Moskovits, M., *J. Chem. Phys.* **1978**, *69*, 4159.

22. Nie, S. and Emory,S. R., *Science* **1997**, *275*, 1102.

23. Hossain, M. K., Huang, G. G., Kaneko, T. and Ozaki, Y., *Phys.Chem.Chem.Phys.* **2009**, *11*, 7484.

24. Lim, D.-K., Jeon, K.-S., Hwang, J.-H., Kim, H., Kwon, S., Suh,Y. D., Nam, J.-M., *Nat.Nano* **2011**, *6*, 452.

25. Saha, K., Agasti, S. S., Kim, C., Li, X. and Rotello, V. M., *Chem.Rev.* **2012**, *112*, 2739.

26. Xu, Q., Mao, C., Liu, N.-N., Zhu, J.-J. and Sheng, J., *Biosens.Bioelectron.* **2006**, *22*, 768.

27. Mena, M. L., Yáñez-Sedeño, P. and Pingarrón, J. M., *Anal.Biochem.* **2005**, *336*, 20.

28. Willner, B., Katz, E. And Willner, I., *Curr.Opin.Biotechnol.* **2006**, *17*, 589.

29. Pingarrón, J. M., Yáñez-Sedeño, P. and González-Cortés, A., *Electrochim.Acta.* **2008**, *53*, 5848.

30. Eustis, S. and El-Sayed, M. A., *Chem. Soc. Rev.* **2006**, *35*, 209.

31. Hirsch, A., *Nat. Mater.* **2010**, *9*, 868.

32. Rao, C. N. R., Sood, A. K., Subrahmanyam, K. S. and Govindaraj, A., *Angew. Chem.,Int. Ed.* **2009**, *48*, 7752.

33. Iijima, S., *Nature* **1991**, *354*, 56.

34. Dinadayalane, T. C. and Leszczynski, J., *Struct. Chem.* **2010**, *21*, 1155.

35. Liang, F. and Chen, B., *Curr. Med. Chem.*, **2010**, *17*, 10.

36. Zhu, Y., Murali, S., Cai, W., Li, X., Suk, J. W., Potts, J. R. and Ruoff, R. S., *Adv. Mater.*, **2010**, *22*, 3906.

37. Bethune, D. S., Kiang, C. H., Devries, M. S., Gorman, G., Savoy, R., Vazquez, J. and Beyers, R., *Nature* **1993**, *363*,605.

38. Iijima, S. and Ichihashi, T., *Nature* **1993**, *363*, 603.

39. Iijima, S., *Materials Science and Engineering B* **1993**, *19*, 172.

40. Saito, R., Dresselhaus, G. and Dresselhaus, M. S., *Carbon* **1995**, *33*, 883.

41. Charlier, J. C., *Acc. Chem. Res.* **2002**, *35*, 1063.

42. Saito, R., Dresselhaus, G. and Dresselhaus, M. S., *Physical Review B* **1996**, *53*, 2044.

43. Kim, W., Choi, H. C., Shim, M., Li, Y., Wang, D. and Dai, H., *Nano Letters* **2002**, *2(7)*, 703.

44. Mahadevi, A. S. and Sastry, G. N., *Chem. Rev.* **2013**, *113*, 2100.

45. Song, G. M., Saraboji, K., Ahmad, S., Ponnusswamy, M. N. and Suwa, M., *Biophys. Chem.* **2004**, *107*, 263.

46. Weber, G., *Protein Interactions* (Chapman and Hall, London, 1992); Rubin, H., *Touchstone of Life: Molecular Information, Cell Communication, and the Foundation of Life* (Oxford University Press, New York, 1999).

47. Jones, S. and Thronton, J. M., *Proc. Natl. Acad. Sci. USA.* **1996**, *96*, 13.

48. Dougherty, D. A., *Science* **1996**, *271*, 163.

49. Zhao, Y. L. and Stoddart, J. F., *Acc. Chem. Res.* **2009**, *42*, 1161.

50. Leszczynski, J., *Nat. Nanotechnol.* **2010**, *5*, 633.

51. Ma, J. C., Doughatery, D. A., *Chem. Rev.* **1997**, *97*, 1303.

52. Kebarle, *J. Phys. Chem.* **1981**, *85*, 1814.

53. Dougherty, *Science* **1996**, *271*, 163.

54. Ward, S. D., Curtis, C. A. and Hulme, E. C., *Mol. Pharmcol.* **1996**, *56*, 1031.

55. Carlier, P. R., Chow, E. S., Han, Y., Liu, J., Yazal, J. El and Pang, Y. P., *J. Med. Chem. Phys.* **1999**, *42*, 4225.

56. Cabarcos, O. and Weinheimer, C., *J. Chem. Phys.* **1999**, *110*, 8429.

57. Choi, H. S., Suh, S. B., Cho, S. J. and Kim, K. S., *Proc. Natl. Acad. Sci. USA* **1998**, *95*, 12094.

58. Roelens, S. and Torriti, R., *J. Am Chem. Soc.* **1998**, *120*, 12443.

59. Gallivan, J. P. and Dougherty, D. A., *Proc. Natl. Acad. Soc. USA* **1996**, *96*, 9459.

60. Macias, A ., Rajamani, R. and Evanseck, J., *Abst. Papers Am. Chem. Soc.* **1997**, *214*, 105.

61. Minoux, H. and Chipot, C., *J. Am. Chem. Soc.* **1999**, *121*, 10366.

62. Wintjens, R., Lievin, J., Rooman, M. and Buisine, E., *J. Mol. Biol.* **2000**, *302*, 395.

63. McFail-Isom, L., Shui, X. and Williams, L.D., *Biochemistry* **1998**, *37*, 17105.

64. Kim, K. S., Tarakeshwar, P. and Lee, J. Y., *Chem. Rev.* **2000**, *100*, 4145.

65. Wounters, J., *Protein Sci.* **1998**, *7*, 2472.

66. Ready, A. S. and Sastry, G. N., *J. Phys. Chem.* **2005**, *109*, 8893.

67. Meyer, E. A., Castellano, R. K. and Diederich, F., *Angew. Chem. Int. Ed.* **2003**, *42*, 1210.

68. Umadevi, D.and Sastry, G. N., *Chem. Phys. Chem.* **2013**, *14*, 2570.

69. Shi, G., Ding, Y and Fang, H., *J. Comput. Chem.* **2012**, *33*, 1328.

70. Grabowski, S. J. and Lipkowski, P. *J. Phys. Chem. A*, **2011**, *115*, 4765.

71. Reddy, A. S. and Sastry, G. N., *J. Phys. Chem. A* **2005**, 8893.

72. Vijay, D. and Sastry, G. N., *Chem. Phys. Lett.* **2010**, *485*, 235.

73. Vijay, D., Sakurai, H. and Sastry, G. N., *Int. J. Quantum Chem.* **2011**, *111*, 1893.

74. Geim, A. K. and Novoselov, K. S., *Nat. Matter* **2007**, *6*, 183.

75. Novoselov, K. S., Geim, A. K., Voggu, R. and Subhrahmanyam, K. S., *J. Phys. Chem. Lett.* **2010**, *1*, 572.

76. Zhang, Y., Tan, J. W., Stormer, H. L. and Kim, P., *Nature* **2005**, *438*, .201.

77. Novoselov, K. S., Jiang, Z., Zhang, Y., Morozov, S. V., Stormer, H. L., Zeitler, U., Maan, J. C., Boebbinger, G. S., Kim, P. and Geim, A.K., *Science* **2007**, *315*, 1379.

78. Novoselov, K. S., Geim, A. K., Morozov, S. V., Jiang, D., Zhang, Y., Dubonos, S. V., Grigorieva, I. V. and Firsov, A. A., *Science* **2004**, *306*, 666.

79. Han, M. Y., Oezyilmaz, B., Zhang, Y. and Kim, P., *Phys, Rev. Lett.* **2007**, *98*, 206805.

81. Lee, C., Wei, X., Kysar, J. W. and Hone, J., *Science* **2008**, *321*, 385.

81. Park, S. and Ruoff, R. S., *Nature Nanotube* **2009**, 217.

82. Kaplan, A., Yuan, Z., Benck, J. D., Rajan, A. G., Chu, X. S., Wang Q. H. and Strano, M. S., *Chem. Soc. Rev.* **2017**, *46*, 4530.

83. Reina, G., González-Domínguez, J. M., Criado, A., Vázquez, E., Bianco A. and Prato, M., *Chem. Soc. Rev.* **2017**, *46*, 4400.

84. Pan, J. Li F. and Choi, J. H., *J. Mater. Chem. B* **2017**, *5*, 6511.

85. Liu, H., Zhang, L., Yanac M. and Yu, J., *J. Mater. Chem. B* **2017**, *5*, 6437.

86. Martín, N., Ros T. D. and Nierengarten, J.-F., *J. Mater. Chem. B* **2017**, *5*, 6425.

87. Bahadir, E. B. and Sezgintürk, M. K., *Trends Anal. Chem.* **2015**, *76*, 1.

88. Deng, X., Tang, H. and Jiang, J., *Anal. Bioanal. Chem.* **2014**, *406*, 6903.

89. Pumera, M., Ambrosi, A., Bonanni, A., Chng, E. L. K. and Poh, H. L., *Trends Anal. Chem.* **2010**, *29*, 954.

90. He, Q., Wu, S., Yin, Z. and Zhang, H., *Chem. Sci.* **2012**, *3*, 1764.

91. Ruecha, N., Rangkupan, R., Rodthongkum, N. and Chailapakul, O., *Biosens. Bioelectron.* **2014**, *52*, 13.

92. Yang, L., Wang, G., Liu, Y. and Wang, M., *Talanta* **2013**, *113*, 135.

93. Huangfu, C., Fu, L., Li, Y., Li, X., Du, H., Ye, J., *Electroanalysis* **2013**, *25*, 2238.

94. Chen, M., Chao, M. and Ma, X., *J. Appl. Electrochem.* **2014**, *44*, 337.

95 Chaiyo, S., Mehmeti, E., Zagar, K., Siangproh, W., Chailapakul, O. and Kalcher, K., *Anal. Chim. Acta* **2016**, *918*, 26.

96. Wang, R., Yan, K., Wang, F. And Zhang, J., *Electrochim. Acta* **2014**, *121*, 102.

97. Lian, W., Liu, S., Yu, J., Xing, X., Li, J., Cui, M. and Huang, J., *Biosens. Bioelectron.* **2012**, *38*, 163.

98. Xing, X., Liu, S., Yu, J., Lian, W. and Huang, J., *Biosens. Bioelectron.* **2012**, *31*, 277.

99. Lian, Y., He, F., Wang, H. and Tong, F., *Biosens. Bioelectron.* **2015**, *65*, 314.

100. Justino, C. I. L., Gomes, A. R., Freitas, A. C., Duarte, A. C., Rocha-Santos, T. A. P., *Trends in Analytical Chemistry* **2017**, *91*, 53.

101. Ema, M., Gamo, M. and Honda, K., *Regul. Toxicol. Pharmacol.* **2016**, *74*, 42.

102. Schipper, M. L., Nakayama-Ratchford, N., Davis, C. R., Kam, N. W., Chu, P., Liu, Z., Sun, X., Dai, H. and Gambhir, S. S., *Nat. Nanotechnol.* **2008**, *3*, 216.

103. Liu, Z., Cai, W., He, L., Nakayama, N., Chen, K., Sun, X., Chen, X. and Dai, H., *Nat. Nanotechnol.* **2007**, *2*, 47.

104. Liu, Z., Davis, C., Cai, W., He, L., Chen, X. and Dai, H., *Proc. Natl. Acad. Sci. USA* **2008**, *105*, 1410.

105. Lanone, S., Andujar, P., Kermanizadeh, A. and Boczkowski, J., *Adv. Drug Delivery Rev.* **2013**, *65*, 2063.

106. Yang, S.-T., Guo, W., Lin, Y., Deng, X.-Y., Wang, H.-F., Sun, H.-F., Liu, Y.-F., Wang, X., Wang, W. and Chen, M., *J. Phys. Chem. C* **2007**, *111*, 17761.

107. Zhang, J. Q., Landry, M. P., Barone, P. W., Kim, J. H., Lin, S. C., Ulissi, Z. W., Lin, D. H., Mu, B., Boghossian, A. A., Hilmer, A. J., Rwei, A., Hinckley, A. C., Kruss, S., Shandell, M. A., Nair, N., Blake, S., Sen, F., Sen, S., Croy, R. G., Li, D. Y., Yum, K., Ahn, J. H., Jin, H., Heller, D. A., Essigmann, J. M., Blankschtein, D. and Strano, M. S., *Nat. Nanotechnol.* **2013**, *8*, 959.

108. Kuang, Z., Kim, S. N., Crookes-Goodson, W. J., Farmer, B. L. and Naik, R. R., *ACS Nano* **2009**, *4*, 452.

109. Heller, D. A., Jin, H., Martinez, B. M., Patel, D., Miller, B. M., Yeung, T. K., Jena, P. V., Hobartner, C., Ha, T., Silverman, S. K. and Strano, M. S., *Nat. Nanotechnol.* **2009**, *4*, 114.

110. Heller, D. A., Pratt, G.W., Zhang, J., Nair, N., Hansborough, A. J., Boghossian, A. A., Reuel, N. F., Barone, P. W. and Strano, M. S., *Proc. Natl. Acad. Sci. USA* **2011**, *108*, 8544.

111. Giraldo, J. P., Landry, M. P., Kwak, S. Y., Jain, R. M., Wong, M. H., Iverson, N. M., Ben-Naim, M. and Strano, M. S., *Small* **2015**, *11*, 3973.

112. Cha, T.-G., Baker, B. A., Sauffer, M. D., Salgado, J., Jaroch, D., Rickus, J. L., Porterfield, D. M. and Choi, J. H., *ACS Nano* **2011**, *5*, 4236.

113. Yoo, C.-H., Jung, S., Bae, J., Kim, G., Ihm, J. and Lee, J., *Chem. Commun.* **2016**, *52*, 2784.

114. Bisker, G., Dong, J., Park, H. D., Iverson, N. M., Ahn, J., Nelson, J. T., Landry, M. P., Kruss, S. and Strano, M. S., *Nat. Commun.* **2016**, *7*, 10241.

115. Ahn, J.-H., Kim, J.-H., Reuel, N. F., Barone, P. W., Boghossian, A. A., Zhang, J., Yoon, H., Chang, A. C., Hilmer, A. J. and Strano, M. S., *Nano Lett.* **2011**, *11*, 2743.

116. Thomas, J. A., *Chem. Soc. Rev.* **2015**, *44*, 4494.

117 Lim, Y. T., Kim, S., Nakayama, A., Stott, N. E., Bawendi, M. G. and Frangioni, J. V., *Mol. Imaging* **2003**, *2*, 50.

118. Medintz, I. L., Uyeda, H. T., Goldman, E. R. and Mattoussi, H., *Nat. Mater.* **2005**, *4*, 435.

119. Keren, S., Zavaleta, C., Cheng, Z., de La Zerda, A., Gheysens, O. and Gambhir, S., *Proc. Natl. Acad. Sci. USA* **2008**, *105*, 5844.

120. Chen, M. and Yin, M., *Prog. Polym. Sci.* **2014**, *39*, 365.

121. Liu, Z., Tabakman, S., Welsher, K. and Dai, H., *Nano Res.* **2009**, *2*, 85.

122. Hong, H., Gao, T. and Cai, W., *Nano Today* **2009**, *4*, 252.

123. Liu, Z., Yang, K. and Lee, S.-T., *J. Mater. Chem.* **2011**, *21*, 586.

124. Gong, H., Peng, R. and Liu, Z., *Adv. Drug Delivery Rev.* **2013**, *65*, 1951.

125. Fakhri, N., Wessel, A. D., Willms, C., Pasquali, M., Klopfenstein, D. R., MacKintosh, F. C. and Schmidt, C. F., *Science* **2014**, *344*, 1031.

126. Godin, A. G., Varela, J. A., Gao, Z., Danne, N., Dupuis, J. P., Lounis, B., Groc, L. and Cognet, L., *Nat. Nanotechnol.* **2017**, *12*, 238.

127. Cognet, L., Tsyboulski, D. A. and Weisman, R. B., *Nano Lett.* **2008**, *8*, 749.

128. Pan, J., Cha, T.-G., Li, F., Chen, H., Bragg, N. A. and Choi, J. H., *Sci. Adv.* **2017**, *3*, e1601600.

129. Clark, L.C. and Lyons C., *Ann. N. Y. Acad. Sci.* **1962**, *102*, 29.

130. Feng, L., Wu, L. and Qu, X., *Adv. Mater.* **2013**, *25*, 168.

131. Sharma, D., Kanchi, S., Sabela, M. I. and Bisetty, K., *Arabian J. Chem.* **2016**, *9*, 238.

132. Park, C. S., Yoon, H. and Kwon, O. S., *J. Ind. Eng. Chem.* **2016**, *38*, 13.

133. Du, D., Yang, Y. and Lin, Y., *MRS Bull.* **2012**, *37*, 1290.

134. Celik, N., Balachandran, W. and Manivannan, N.,:*IET Circ. Device. Syst.* **2015**, *9*, 434.

135. Morales-Narváez, E., Baptista-Pires, L., Zamora-Gálvez, A. and Merkoçi. A., *Adv. Mater.* **2016**, *29*, doi: 10.1002/adma. 201604905.

136. Cruz, S. M. A,. Girão, A. F., Gonçalves, G. and Marques P. A. A. P., *Sensors* **2016**, *16*, E137.

137. Pumera, M., *Mater. Today* **2011**, *14*, 308

138. Lee, J., Kim, J., Kim, S. and Min, D -H., *Adv. Drug Delivery Rev.* **2016**, *105(Part B)*, 275.

139. Liu, Y., Dong, X. and Chen, P., *Chem. Soc. Rev.* **2012**, *41*, 2283.

140. Zhu, X., Liu, Y., Li, P., Nie, Z. and Li, J., *Analyst* **2016**, *141*, 4541.

141. Yang, K., Li, Y., Tan, X., Peng, R. and Liu, Z.,: *Small* **2013**, *9*, 1492.

142. Bianco, A., *Angew. Chem., Int. Ed.* **2013**, *52*, 4986.

143. Ou, L., Song, B., Liang, H., Liu, J., Feng, X., Deng, B., Sun, T. andShao, L., *Part. Fibre Toxicol.* **2016**, *13*, 57.

144. Pelin, M., Fusco, L., León, V., Martín, C., Criado, A., Sosa, S., Vázquez, E., Tubaro, A. and Prato, M., *Sci. Rep.* **2017**, *7*, 40572.

145. Loh, K. P., Bao, Q., Eda, G. and Chhowalla, M., *Nat. Chem.* **2010**, *2*, 1015.

146. Eda, G., Lin, Y -Y., Mattevi, C., Yamaguchi, H., Chen, H -A., Chen, I -S., Chen, C -W. and Chhowalla, M., *Adv. Mater.* **2010**, 22(4), 505.

147. Shang, J,. Ma, L., Li, J., Ai, W., Yu, T. and Gurzadyan, G. G., *Sci. Rep.* **2012**, 2, 792.

148. Choudhary, R. P., Shukla, S., Vaibhav, K., Pawar, P. B. and Saxena, S., *Mater. Res. Express* **2015**, *2*, 95024.

149. Wang, J., Cao, S., Ding, Y., Ma, F., Lu, W. and Sun, M., *Sci. Rep.* **2016**, *6*, 24850.

150. McGuire, J. A., *Phys. Status Solidi RRL* **2016**, *10*, 91.

151. Du, D., Zou, Z., Shin, Y., Wang, J., Wu, H., Engelhard, M. H., Liu, J., Aksay, I. A. and Lin Y., *Anal. Chem.* **2010**, *82*, 2989.

152. Liang, B., Fang, L., Yang, G., Hu, Y., Guo, X. and Ye, X., *Biosens. Bioelectron.* **2013**, *43*, 131.

153. Wu, Q., Hou, Y., Zhang, M., Hou, X., Xu, L., Wang, N., Wang, J. and Huang, W., *Anal. Methods* 2016, *8*, 1806.

154. Lee, H., Choi, T. K., Lee, Y. B., Cho, H. R., Ghaffari, R., Wang, L. Choi, H. J., Chung, T. D., Lu, N., Hyeon, T., Choi, S. H. and Kim, D -H., *Nat. Nanotechnol*. **2016**, *11*, 566.

155. Gong, Q., Wang, Y. and Yang, H., *Biosens. Bioelectron.* **2017**, *89(Pt 1)*, 565.

156. Zhu, M., Zeng, C. and Ye, J., *Electroanalysis* **2011**, *23*, 907.

157. Gu, H., Yu, Y., Liu, X., Ni, B., Zhou, T. and Shi, G., *Biosens. Bioelectron.* **2012**, *32*, 118.

158. Arvand M. and Ghodsi, N., *J. Solid State Electrochem.* **2013**, *17*, 775.

159. Gu, H., Yang, Y., Zhou, X., Zhou, T. and Shi, G., *J. Electroanal. Chem.* **2014**, *730*, 41.

160. Manibalan, K., Mani, V., Huang, C -H., Huang, S -T. and Chang, P -C., *Analyst* **2015**, *140*, 6040.

CHAPTER 2

METHODOLOGY

CHAPTER 2

METHODOLOGY

2.1. Introduction

Classical Newtonian mechanics is the law of macroscopic objects, but it failed to explain certain properties of microscopic systems. Then quantum mechanics is developed to serve as the law governing the behaviours of both macroscopic, e.g. cosmological systems, and microscopic objects, such as electronics and nuclei. To describe the state of a microscopic system in quantum mechanics, it is postulated that a special function termed wave function exists as a function of the particles' coordinates. Although the wave function has a time- dependent nature in principle, its time-independent, or in other words, its stationary form suffices in many application, specially in quantum chemistry.

Computational chemiatry has become a powerful tool for the chemists in most of the research areas with the development of fast processors. The application of computational chemistry based methods has emerged in many areas such as molecular modelling, nanotechnology, pharmaceutical chemistry and matrials science. There are theoretical methods and principles are descried in this chapter which are use in our studies. In our studies, we have used appropriate many methods as ab initio methods, density functional theory, semi-empirical methods etc.

2.2 *ab initio* methods

2.2.1. Quantum mechanical calculations

The molecules are composed of the atoms and atoms are composed of nucleus as well as the electrons. Many atom has one electron in outer most orbits as hydrogen (H), helium

ion (He^{+}), lithium ion (Li^{+2}) etc.. The solution of Schrödinger equation are simple for hydrogen like atoms but other atom much complicated. For large number of electrons, the solution of Schrödinger equation has become simple for using computantional methods.

The fundamental principle of quantum mechanics is to find a solution of the time-independent, non-relativistic Schrödinger equation for any chemical system,[1] and that appropriate system.[2-7] The wave function, Ψ exists for any chemical system, and that appropriate operators (functions), which act upon Ψ return the observable properties of the system. The operator, that returns the system energy, E, as an eigenvalue is called the Hamiltonian operator, $\hat{H}$. Therefore, by solving Schrödinger equation, electronic structure and properties of any molecule may be deremined:

$$\hat{H}\,\Psi = \mathrm{E}\,\Psi \tag{2.1}$$

The wave function represents nuclear as well as electronic motion together, the electronic wave function is separated from total wave function using Born Oppenheimer approximation[8-10]. When the nuclei are fixed at a particular distance, the electronic wave function can sufficiently provide all properties of the molecule. For a multi electron system electronic part of Hamiltonain operator of Schrödinger equation is written as:

$$H_e = -\sum_p \frac{1}{2}\nabla_p^2 - \sum_A \sum_P Z_A r_{AP}^{-1} + \sum_{p<q} r_{pq}^{-1} \tag{2.2}$$

This equation is written in atomic unit and the first term in eq. 2.2 is the kinetic energy of electron and nuclei whereas the third term is potential energy due to inter-electron interaction. Thus the modified Schroendiger wave equation for n electronic system is written as:[11]

$$H_e(1,2,...,n)\psi_e(1,2,....,n) = E_e\psi_e(1,2,...,n) \tag{2.3}$$

Where Ψ_e is the electronic part of the wave function. The complete treatment of quantum mechanical problem involving electronic structure is equivalent to comlete solution of the appropriate Schrödinger equation. Because of the inter electronic repulsion term, the Schrödinger equation for single atom is not separable so we obtain the solution Ψ_0 for n electron is product of n single electronic wave function function. The product wave function is known as Hartree Product:[12]

$$\Psi_0 = \Psi_1(r_1,\theta_1,\varphi_1)\Psi_2(r_2,\theta_2,\varphi_2) \ldots\ldots\ldots\ldots\Psi_n(r_n, \theta_n, \varphi_n) \qquad (2.4)$$

Where Ψ_0 is initial wave function starting from, accuracy of the calculated result that depends upon the choice of Ψ_0. The electrons are fermions obeying the half spin Fermi-Durac statistics.[13] One electron wave function are the molecular orbital which are the products of the spatial orbitals times the spin functions (α or β),[14] to satisfy the Pauli's exclusion principle, the wave function must be antisymmetric.[15] The antisymmetric wave function may be derived from Slater Determinants.[16] The spin orbital Slater determinant for n electrons is written as:

$$\Psi = \frac{1}{\sqrt{N}}\begin{vmatrix} \varphi_1^{(1)}\alpha^{(1)} & \varphi_2^{(1)}\beta^{(1)} & \ldots\ldots\ldots\ldots \varphi_n^{(1)}\beta^{(1)} \\ \varphi_1^{(2)}\alpha^{(2)} & \varphi_2^{(1)}\beta^{(2)} & \ldots\ldots\ldots\ldots \varphi_n^{(1)}\beta^{(2)} \\ \varphi_1^{(n)}\alpha^{(n)} & \varphi_2^{(n)}\beta^{(n)} & \ldots\ldots\ldots\ldots \varphi_n^{(1)}\beta^{(n)} \end{vmatrix} \qquad (2.5)$$

The solution of equation 2.5 is obtained by using perturbation over the solution Ψ_0 and a trial wave function is constructed with the help of Slater determinant by applying the variation principle. The equation of energy of the system given below is written in form of Dirac notation.[17-19]

$$E_e = \frac{\langle \psi_i^{'} \mid H_e^{'} \mid \psi_i^{'} \rangle}{\langle \psi_i^{'} \mid \psi_i^{'}} \qquad (2.6)$$

2.2.2. Hartree Self-Consistent Field Method

The solution of the electronic Schrödinger wave equation of molecule, which is formed by writing the Slater type determinant. This determinant consists of the nuclear-nuclear interaction energy, which has constant value for a given geometry, the nuclear-electron attraction, which is dependent on one electron co-ordinate and the electron-electron repulsion, which depends on two electron co-ordinates.[20,21]

The Hamiltonian is

$$H_e = \sum_{p}^{N} h + \sum_{i=1}^{N}\sum_{j>i}^{N} g_{ij} + V_{nm} \tag{2.7}$$

Where,

$$H_e = -\frac{1}{2}\nabla^2 - \sum_{a}\frac{Z_a}{|R_a - r_p|} \tag{2.8}$$

and

$$g_{ij} = \frac{1}{|r_i - r_j|} \tag{2.9}$$

where one electron operator h_e describes the motion of i^{th} electron in field of all nuclei, g_{ij} is two electron operator giving the repulsion between two electrons while V_{nm} is the nuclear-nuclear interaction energy. The energy can be expressed as

$$E = \sum_{i}^{N}\langle\varphi_i \mid h_i \mid \varphi_i\rangle + \frac{1}{2}\sum_{ij}^{N}(\langle\varphi_j \mid J_i \mid \varphi_j\rangle - \langle\varphi_j \mid K_i \mid \varphi_j\rangle + V_{nm}) \tag{2.10}$$

$$J = \langle\varphi_1^{(1)}\varphi_2^{(2)} \mid g_{12} \mid \varphi_1^{(1)}\varphi_2^{(2)}\rangle \tag{2.11}$$

Where, J operator represents the classical repulsion between the two charge distribution described by $\varphi_{12}(1)$ and $\varphi_{21}(2)$

The K operator represents the exchange internal that has no classical analogue.[22]

To determine the set of MO (Molecular Orbital) which has minimum energy or is stationary in respect to change orbital, variation is carried out in a manner that the MOs should remain orthogonal and normalized. This type of optimization is a termed as constrained and this can be achieved by means of Lagrange multipliers.[20,23] The Lagrange function is stationary with respect to the orbital variation:

$$L = E - \sum_{ij}^{N} \lambda_{ij} (\langle \varphi_i \mid \varphi_j \rangle - \delta_{ij}) \tag{2.12}$$

Where L is the Lagrange function. Variation of the Lagrange function is written as

$$\delta L = \delta E - \sum_{ij}^{N} (\langle \delta\varphi_i \mid \varphi_j \rangle + \langle \varphi_i \mid \delta\varphi_j \rangle) = 0 \tag{2.13}$$

$$\mathrm{F_i} = \mathrm{h_i} + \sum_{j}^{N} (J_j - K_j) \tag{2.14}$$

Where, F_i is the Fock Operator, whreas operator J is the electron repulsion term, known as the coulomb Operator while K is term as the exchange Operator. Hence, the Hartree Fock Equation can be written as below:[20,24]

$$F_i \varphi_i = \varepsilon_i \varphi_i \tag{2.15}$$

A set of functions that are the solutions of eq. 2.15 are called Self-Consistent Field Orbital and are determined through through an iterative method. The Hartree Fock method is known as mean field approximation in which the average electron-electron repulsion is taken into account.[25]

2.2.3. Roothaan Hall Equation

The direct solution of Hartree Fock Equation for molecular system of any size is not pratical so certain approximation methods are required. For achieving it, the MOs are expanded in term of basis functions, conveniently called atomic orbitals. The expression of orbital in terms of atomic orbitals has an advantage in the interpretability of the results. Since the nature of the chemical problems frequently involves relating properties of molecules with those of constitution atoms.

$$\phi_i = \sum c_{\mu i} \chi_\mu \tag{2.16}$$

The optimum value of the coefficient $c_{\mu i}$ is obtained by using the criteria of lowest calculated total energy. This leads to a set of self consistent LCAO molecular orbitals φ_i. Such an orbital will be best for any particular set of basis function. The application of the variational technique leads to Roothan Hall equation.[26]

$$\sum_{\nu} (F_{\nu\mu} - \varepsilon_i S_{\nu\mu}) C_{\mu i} = 0 \tag{2.17}$$

Where $F_{\nu\mu}$ is the fock operator and $S_{\nu\mu}$ is the overlap integral

$$F_{\nu\mu} = \langle \chi_\nu \mid h \mid \chi_\mu \rangle + \sum_{\gamma}^{AO} \sum_{\delta}^{AO} D_{\gamma\delta} (\langle \chi_\nu \chi_\gamma \mid g \mid \chi_\mu \chi_\delta \rangle) - \langle \chi_\nu \chi_\gamma \mid g \mid \chi_\delta \chi_\mu \rangle) \tag{2.18}$$

The density matrix is defined as

$$D_{\gamma\delta} = \sum_{j}^{occ.MO} C_{\gamma j} C_{\delta j} \tag{2.19}$$

Roothan-Hall equations are set of algebraic equation as HF equations are differential equations. They were set by Hall [27] and Roothan[26] independently. The molecular orbitals expanded in the form of atomic orbital are not orthogonal, so by the method of

standard digitization technique we obtained a new set set of basis function χ' and the solution is iteratively.[20]

2.2.4. Computational scheme for solving Roothaan- Hall equation

Hartree Fock method provides the solution of the Schrödinger equation considering average interaction of electrons i.e. distance between electrons and nucleus is taken into account and not the distance between electrons. Hence, the motion of the electron is not corrected in HF equation.[28] The electron correlation is included in Configuration Interaction (CI)[29,30] and Moller-Plesset[31] perturbation theory.

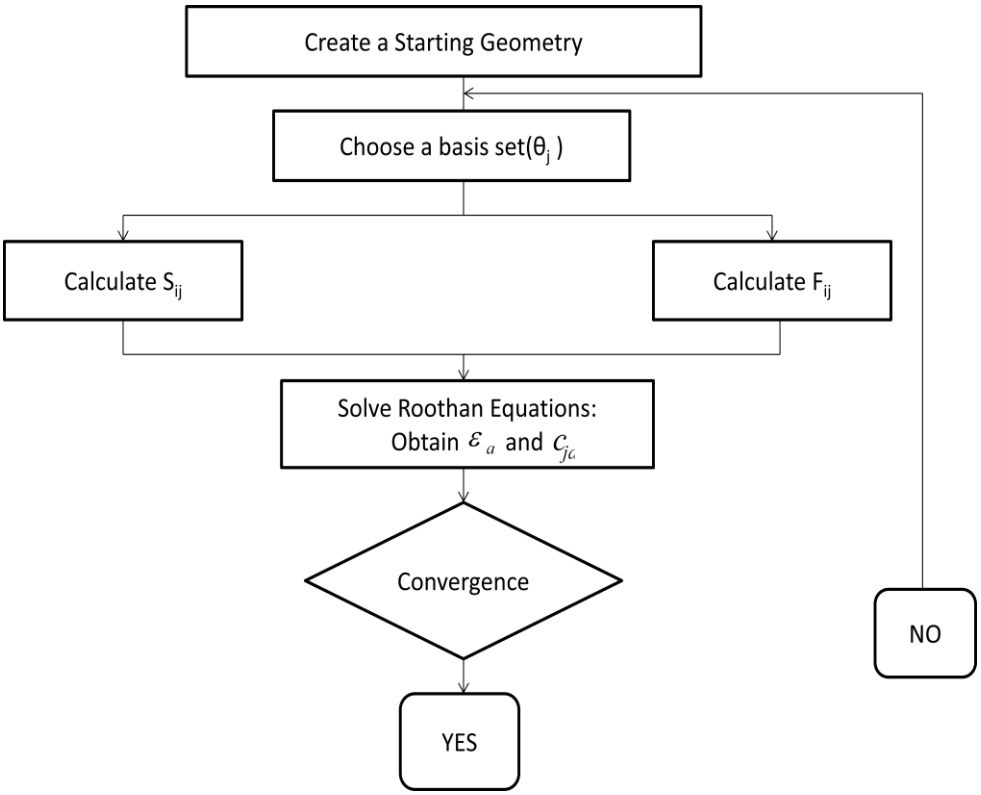

Figure 2.1: Flow chart for a typical quantum-mechanical calculation.

2.3. Basis Set

A basis set represents a set of functions used to describe the shape of orbitals in an atom. To solve the Schrödinger equation one has to optimize the wave function with the help of perturbations from the Hamiltonian operator to find the eigenvalues or associated energies with the equation. There is no straightforward method to obtain wave function of molecules as well as that of atoms in which distinct levels of orbital can easily be identified, i.e. 1s, 2s, 2p etc. To overcome this problem, the Linear Combination of Atomic Orbitals(LCAO) approach[31] is used to describe the molecular wave function through molecular orbitals. In Linear Combination of Atomic Orbitals (LCAO) approach each molecular orbital (one electron function) ϕ_i is expressed as a linear combination of n basis function χ_a

$$\phi_i = \sum_{\alpha=1}^{n} c_{\alpha i}\chi_\alpha \tag{2.20}$$

Where $c_{\alpha i}$ are called Molecular Orbital Expansion Coefficient or simply MO coefficients.

Generally the basis-functions are located at the centre of atoms and are therefore often called atomic basis functions. They are mathematical functions desined to give the maximum flexibility to the molecular orbitals.

Basis set is a set of mathematical functions used to expand the molecular orbitals in order to help solve the Schrödinger equation with each function centred(has its origin) at some point in the molecule (usually on the nuclei). All ab initio methods inherited basis set approximation for their calcaulations. An unknown Molecular Orbital(MO) can be considered as a function in the infinite coordinate system spanned by the complete basis

set. Expansion of an unknown molecular orbital function an unknown function in a set of known functions is not an approximation if using the complete basis set. Although, a complete basis set will mean involvement of an infinite number of functions, which will be impossible to calculate. On employing a finite basis set, only the component of the Molecular Orbital along with those coordinate axes can be represented which corresponds to the selected basis set, the poorer the representstion. The type of basis set function used also influences the performance.

There are two general classes of basis set i.e. Slater Type Orbitals (STOs)[32, 33] and Gaussian Type Orbitals [GTOs].[20, 34] A Slater Type Orbital for an s-type atomic orbital has the form.

$$S(\alpha) = N_s e^{-\xi\alpha^2} \tag{2.21}$$

Where α is radial distance from the nucleus, N_s, is normalization constant, and ζ is a constant known as the orbital exponent, which governs with size of the orbital. A Gaussian Type Orbital for an s-type atomic orbital with the same orbital exponent as STO has the form

$$g(\alpha) = N_g e^{-\xi\alpha^2} \tag{2.22}$$

Where N_g is the normalization constant. The STO basis set has an advantage that they have direct physical interpretation and thus are naturally good basis for molecular orbitals. The STOs have the shortcoming that most of the required integrals needed for the SCF procedure must be calculated numerically, hence it is computationally expensive whereas wave functions with GTO basis set are much easier to compute.

The smallest basis set, which represent one function for each type of occupied orbital in the separated atoms, are called minimal basis set.[35] The most used minimal basis set is

the the STO-3G set. This notation indicates that the basis set approximate the shape of a STO orbital by using a single contaction of three GTO orbital. One such contraction would then be used for each orbital, which is definition of a minimal basis. There are STO-nG basis set n=2-6. The Pople basis set [36,37] are another family of basis set and they can written by the notation 6-31G*. This means that each core orbit is described by a single contraction of six GTO primitives which describes each core orbital and two contractions, of which one with three primitives and another with one primitive describe each valence shell orbital. The Pople basis sets are very popular for organic molecules. The Pople basis set notation can be modified by adding one or two asterisks(*), such as 6-31G* or 6-311G**. A single asterisk means that a set of d primitives has added to atoms to atoms other than hydrogen as well. These are called polarization functions because they give the wave function more flexibility to change shape. One or two plus signs can also be added, such as 6-31+G* or 6-31++G*. A single plus sign indicates that diffuse functions have been added to atoms other than hydrogen. The second plus sign indicates that diffuse functions are far being used for all atoms. These diffuse functions far from the nucleus. Diffuse functions are used for anions, which have larger electron density distributions. Diffuse functions are used for describing interactions at long distances, such as vander waals interactions. The effect of adding diffuse functions is usually to change the relative energies of the various geometries associated with these systems. Basis sets with diffuse functions are also called augmented basis set.

2.4. Density Functional Theory

Density functional method is the alternative method which are based on the wave function based methods. DFT is based on determining the electron density, a physical

observable quantity, rather than wave function. Unlike, in itself DFT contains no approximations. Unlike HF and post-HF methods, there is no a priori way to establish how good a given and systematic way to improve upon it. It has however become clear that DFT methods often produce results of comparable quality to much more expensive post- HF methods that have their origins in the Thomas –Fermi-Dirac model.[38-39] In 1998, Walter Kohn was awarded the Nobel prize in chemistry for his development of the DFT and ever-since DFT has become the most popular and useful computational approach to study many- electron systems. The computational based on DFT attained more reputation over the the years as it gives more information regarding the properties of the system at a lower cost than the wave function based methods. According to density functional theory, the energy functional are divided in three parts which are shown in following equation,

$$E_{DFT}[\rho] = T[\rho] + E_{ne}[\rho] + E_{ee}[\rho] \tag{2.23}$$

Where, $T[\rho]$ indicates the kinetic energy, $E_{ne}[\rho]$ shown as the attraction between the nuclei and electrons and E_{ee} represents the electron-electron repulsion. The electron-electron repulsion term may be divided into coulomb $J[\rho]$ and exchange parts $K[\rho]$ by implicitly including correlation energy in all the terms. Thus the equation becomes,

$$E_{DFT}[\rho] = T[\rho] + E_{ne}[\rho] + J[\rho] + K[\rho] \tag{2.24}$$

The E_{ne} and $J[\rho]$ terms are given by their classical expressions where n represents the number of nuclei,

$$E_{ne}[\rho] = -\sum_{a}^{n} \int \frac{Z_a(R_a)\rho(r)}{|R_a - r|} dr \tag{2.25}$$

$$J[\rho] = \frac{1}{2} \iint \frac{\rho(r)\rho(r')drdr''}{[r - r']} \tag{2.26}$$

One of the earlier attempts to use electron density instead of the conventional wavefunction to calculate the properties of molecules, was done by Thomas and Fermi[40]. In the 1927, based on the uniform electron gas, they proposed the following fundamental for the kinetic energy $T_{TF}[\rho]$.

$$T_{TF} = \frac{3}{10}(3\pi^2)^{\frac{2}{3}} \int \rho^{\frac{5}{3}}(r)dr \tag{2.27}$$

Where, $T_{TF}[\rho]$ denotes the kinetic energy functional of the Thomas-Fermi(TF model. The expression from the exchange part $K[\rho]$ is given by the Dirac notation and hence the model with inclusion of the exchange term is taken as Thomas-Fermi-Dirac(TFD) model.

$$K[\rho] = -\frac{3}{4}\left(\frac{3}{\pi}\right) \int \rho^{\frac{4}{3}}(r) \tag{2.28}$$

Thus the total enrgy functional of the system $E_{TFD}[\rho]$ is given as,

$$E_{TFD}[\rho] = \frac{3}{10}(3\pi^2)^{\frac{2}{3}} \int \rho^{\frac{5}{3}}(r) - \sum_{a}^{N_{nuclei}} \frac{Z_a(R_a)\rho(r)dr}{|R_a - r|} + \frac{1}{2}\iint \frac{\rho(r)\rho(r')}{|r - r'|}drdr' - \frac{3}{4}\left(\frac{3}{\pi}\right)^{\frac{1}{3}} \int \rho^{\frac{4}{3}}(r)dr \tag{2.29}$$

There are many drawbacks in the Thomas-Fermi model such as the assumption of a uniform electron gas model is poor for representing atoms and molecules. The importance of this simple Thomas-Fermi model is not how well it performs in computing the ground state energy, but more as an illustration that the energy can be determined purely using the electron density.

Many density functional approximations(DFA) have been developed for practical applications. There are roughly three categories of density functional methods: (i) Local density approximation (LDA) methods assume that the density of the molecule is uniform throughout the molecules, and is typically not a very popular or useful method.

(ii) Gradient corrected (GC) methods look to account for the non-uniformaly of the electron density. (iii) Hybrid, as the name suggests, attempt to incorporate some of the more useful features from ab initio methods (specifically Hartree-Fock methods) with some of the improvements of DFT mathematics. The most significant advantage to DFT methods is a significant increase in computational accuracy without the additional increase in computing time.[41,42]

A breakthrough in DFT and computational chemistry in generally appeared when Becke developed the hybrid density functional procedures.[43] Thus, Becke benchmarked DFT methods against a test of experimentally known ionization energies, electron affinities and proton affinities with high accuracy. He came up with a three-parameter (hybrid) density functional method to estimate the contributions of the exchange and correlation functions and optimized the values of three fit parameter (A, B, C) against the experimental data in the test set. There are many possibilities of combining the various exchange and correlation functional, but the most popular one has become the B3LYP method. Becke used B3PW91 rather than B3LYP in his original paper, but B3LYP is used as an example since it is the most popular DFT method.[43] Essentially the hybrid density functional method B3LYP has the following form:

$$E_{xc}^{B3LYP} = AX_X^{Slater} + (1-A)E_X^{HF} + B\Delta E_X^{Becke} + E_X^{VWN} + C\Delta E_C^{LYP} \qquad (2.30)$$

Thus, it takes the local density approximation functions of Slater and Vosko-Wilk-Nusair relation, a correction term for the exchange due to Becke and Lee-yang-parr correction for nonlocal correction factors. The coefficient A, B, and C are essentially fit parameters obtained through fiting the energies of B3LYP/6-31G* calculations against experimentally obtained ionisation energies and electron affinities. These fit parameters

have created an accurate and low-cost computational method and as a result B3LYP has become one the widest used techniques in science over the past decade.

The DFT functional used for the study of this thesis are as below:

(i) B3LYP: Its detail is already discussed above. It is hybrid functional with 15% HF exchange: It is good performer for geometry optimization.[44]

(ii) M06: This functional is based on meta-GGA approximations, because this include all terms that depend on the kinetic energy density, and are all based on flexible functional forms parametrized on high-quality benchmark databases. It is global hybrid functional with 27% HF exchange. It is good performer for main group thermochemistry, kinetics, excited states, non-covalent interactions and transitions elements. This method described the dispersive interaction.[45]

2.5. Dispersion corrected DFT

Dispersion forces are ubiquitous long range attractive forces acting between instantaneous dipole and induced dipole that result from electron correlation between interacting systems. London developed the first modern theory on dispersion and explained them as arising from simultaneous electron correlation of the separated subsystems. These dispersion forces arise due to purely correlation effect and hence they cannot be reproduced in the HF level. The lack of an exact and explicit form for the exchange-correlation functional is the major drawback of DFT. Hence various dispersion correction methods have been invoked to obtain better and reliable density functionals.

In order to tackle the dispersion correction several approaches have been adopted such as the nonlocal vdW density functionals, conventional and parameterized density functionals, and the semiclassical corrections DFT-D methods. In the year 2004, Dion et al. proposed a vdW-DF which is a non-local correlation functional that approximately accounts for dispersion interactions.[46] The exchange–correlation energy E_{xc} of a system is expressed as,

$$E_{xc} = E_x^{LDA/GGA} + E_c^{LDA/GGA} + E_c^{NL} \quad (2.31)$$

The nonlocal term E_c^{NL} that describes the dispersion energy which contributes at short electron–electron distances to the correlation energy. Though it could successfully describe dispersion in a range of systems, the vdW-DF overestimates equilibrium separations and underestimates hydrogen-bond strength. In order to overcome this drawback Langreth and Lundqvist in 2010, proposed a second version of van der Waals density functional (vdW-DF2) by employing a more accurate semilocal exchange functional PW86.[46] The other vdW-DF functionals which are in use are VV09 and VV10.[47]

Parameterization of standard DFT functionals to account for the exchange-correlation energy is another popular approach in developing functionals. The Wilson–Levy correlation functional has been used together with Hartree–Fock theory to evaluate interaction energies at intermediate separations for several weakly-bonded systems.[48] Tao-Perdew-Staroverov-Scuseria (TPSS) is a meta-GGA density functional for the exchange-correlation energy that satisfies exact constraints without empirical parameters.[49-50] Truhlar and co-workers developed M05 class of functionals using a semiempirical approach and various constraints such as the functionals are in uniform electron gas limit and assumed to be free of self correlation error.[51] Among the

Minnesota functional series, the M06-2X functional is considered to be the most accurate dispersion-uncorrected functional that gives good results for various noncovalent interactions.

Grimme's approach involves the semiclassical treatment of difficult dispersion interactions and combines the resulting potential with DFT which is termed as DFTD.[52, 53-55] The general form for the dispersion energy to be added with the Kohn–Sham DFT energy is

$$E_{disp}^{DFT-D} = -\sum_{AB}\sum_{n=6,8,10...} s_n \frac{C_n^{AB}}{R_{AB}^n} f_{damp}(R_{AB}) \qquad (2.32)$$

Where, C_n^{AB} is the averaged (isotropic) nth-order dispersion coefficient for atom pair AB, R_{AB} refers to the internuclear distance, s_n denotes the scaling factors typically used to adjust the correction to the repulsive behaviour of the chosen density functional and the term f_{damp} corresponds to the damping function which determines the range of the dispersion correction to be included in the given functional. One of the limitations in empirical addition of the dispersion correction term is that the dispersion coefficients are assumed to be constants for different molecular environments. This limitation was addressed by Grimme in the revised DFT-D3 method where the dispersion coefficients are sensitive to the hybridization state of atoms in molecules.[54] B97D, B3LYP-D3, wB97xD and B2PLYPD are some of the dispersion corrected DFT functionals.

2.6. The Hohenberg-Kohn Existence Theorem

Hohenberg and Kohn established two fundamental theorems that marked the beginning of modern DFT.[56] The Hohenberg-Kohn theorem states the total energy of a non-

degenerate ground state is a unique functional of the electron density of the system. Thus all properties of a system can be calculated from the ground-state density. The electron density can be integrated over all space to obtain the total number of electrons.

$$\int \rho_0(r)dr = N \tag{2.33}$$

The second Hohenberg-Kohn theorem states the ground state energy E_0 that can be obtained by applying variational principle. Accordingly, for every trial density function that satisfies the equation and $\rho_{tr}(r) \geq 0$ for all r, the following inequality holds, where, E_υ is the energy function.

Later Kohn-Sham introduced a procedure, where iterative process analogous to the one-electron wave function in HF is involved to reach the self consistency, which is popularly known as Kohn-Sham approach.

2.7. Koopman's Theorem

In a system of 2N electrons for occupied orbitals, λ_i are estimates of the energy necessary to remove an electron from orbital i; for vacant orbitals, λ_i are estimates of the energy attending the addition of an electron to that orbital *i*.[57]

The second assertion is easier to demonstrate. If we add an electron to a previously empty orbital M in a system of 2N electrons, that electron will have an energy composed of an one electron term h_{MM}. It will also repel all the 2N electrons and exchange with N of them- those who have like spin.

$$\langle M \mid F \mid M \rangle = h_{MM} + \sum_{l=1}^{M} 2J_{MI} - K_{MI} \tag{2.34}$$

This is precisely the orbital energy for the previously vacant orbital M.

If an electron is removed from one of the occupied orbitals P, it loses not only its kinetic energy and attraction for the nuclear framework (h_{PP}) but also all repulsions with the pairs of electrons in the other (N-1) orbitals and exchanges with those electrons in the other orbitals that shares its shares its spin.

So far we have

$$-\left[h_{pp} + \sum_{I \neq P} 2J_{PI} - K_{PI} \right] \tag{2.35}$$

We have not taken account of the loss of a repulsion in MOP, which could be written

$$J_{PP} = 2J_{PP} - K_{PP} \tag{2.36}$$

Adding this term, we have the desired result for the ionization energy

$$IE_P = -\langle P \mid F \mid P \rangle = -\lambda_P \tag{2.37}$$

Koopman's theorem provides a first- order approximation to ionization energies and electron affinities. There is no provision for relaxation of the charge distribution when an electron is added or removed.

2.8. Electron Correlation

The Hartree-Fock theory fails to expain the the electron correlation. This is the drawback of HF theory. One of the important limitations of HF calculations is that is takes account

for the average effect of electron repulsion but does not consider explicity electron-electron interaction. In HF theory, the probability of finding an electron around an atom is determined by the electron to nucleus distance by between two electrons. The term electron correlation[58, 59-61] refers to the coupling or correlation of electronic motions with one another. The electron correlation leads to a reduction in the electron-electron repulsion energy. Electron correlation can generally be classified into three types: a) exchange b) dynamic c) non-dynamic electron correlation. The HF theory account for the exchange correlation which arises due to pairs of electrons having parallel spin. That is why the HF function satisfies the antisymmetry requirement of the Pauli principle due to which it vanishes when two electrons with the same spin have the same spatial coordinates. This basic correlation prevents two parallel-spin electrons from being found at the same position in space, this is often called Fermi correlation. The difference between the exact nonrelativistic energy (E_{exact}) and the HF energy (E_{HF}) at the HF limit is the correlation energy (E_{corr}).

$$E_{corr} = E_{exact} - E_{HF} \tag{2.38}$$

As the SCF wavefunction takes into account the interactions between electrons only in a average way (mean field approximation), it fails to incorporate the entire instantaneous (dynamic) interactions between electrons. Dynamic electron correlation arises due to the improper treatment of the electron repulsion between the electrons in motion leading to the accumulation of electrons around the nuclei of the system thereby overestimating the stabilization between the electron and nuclei. This results in the underestimation of the bond lengths in the molecules, and overestimation of the harmic force constants and harmonic frequencies.[62-63]

There are a variety of theoretical methods that have been developed to include the electron correlation effects. These methods in general are reffered to as post –SCF methods as they add correlation corrections to the bases HF model. The popular theoretical methodologies which take account for the electron for the electron correlation are configuration (CI), multi configurational self consistent field (MCSCF) and Minnesota functional theory. The currently most popular pure and hybrid density functional theory (DFT) derives approaches which take care for electron correlation with a less computational effort compared to the other post-HF methods.

2.9. References

1. Schrödinger, E. *Ann. Physik*, **1926**, *79*, 361.
2. Jensen, F., *Introduction to Computational Chemistry*, (Wiley, 1999).
3. Foresman, B. J. and Frisch, A., *Exploring Chemistry with Electronic Structure Methods*, Second Edition, (Gaussian Inc. 1996).
4. Leach, A. R., *Molecular Modelling, Principles and Applications*, (Longmann, 1996).
5. Atkins, P. W. and Friedman, R. S., *Molecular Quantum Mechanics*, Third Edition, (Oxford, 1997).
6. Szabo, A. and Ostlund, N. S., *Modern Quantum Chemistry, Introduction to Advanced Electronic Structure Theory*, (Dover, 1996).
7. Levine, I. N., *Quantum Chemistry*, Fourth Edition, (Prentice-Hall, 1991).
8. Born, M. and Oppenheimer, J. R., Ann. Physik. **1927**, *84*, 457.
9. Kolos, W. and Wolniewicz, L., *J. Chem. Phys.* **1964**, *41*, 3663.
10. Sutsliffe, B.T., *Adv. Quantum Chem.* **1997**, *28*,65.
11. Pople J. A. and Beveridge, D. L., *Approximate Molecular Orbital Theory*, McGraw-Hill Book Co., New York(1970).
12. Hartree, D.R., *Proc. Cambridge Phil. Soc.* **1928**, *24*,89; *111*, 426.
13. Uhlenbeck, G. and Goudsmit, S., *Nature wissenschaften* **1925**, *13*, 953.
14. Pople, J. A., Beveridge, D. L. and Dobosh, P. A., *J. Chem. Phys.* **1967**, *47*, 2026.
15. Pauli, W., *Z. Physik.* **1925**, *31*, 765.
16. Slater, J. C., *Phys, Rev.* **1930**, *35*, 509; *34*, 1239.
17. Dirac, P. A. M., *The Principle of Qunatum mechanics*, Oxford University Press, London(1958)
18. McDonald, J. K. L., *Phys. Rev.* **1933**, *43*, 830.
19. Young, R. H., *Int. J. Qunat. Chem.* **1972**, *6*, 596.
20. Jenson, F., *Introduction to computational Chemistry*, 2nd edition, John Wiley & Sons Ltd., Chichester (2007)
21. Levine, I. N., *Quantum Chemistry*; Chapter, " *The Hatree Fock Self-Consistent Method*", Person, Fifth edition (2000)
22. Levine, I. N., *Quantum Chemistry.*, Chapter-8, "*Pertarbation Theory*", Pearson, Fifth edition (2000).
23. Pople, J. A. and Beveridge, D. L., *Z. Physik.* **1930**, *61*, 126.
24. Lennard-Jones, J. E., *Proc. Roy. Soc. (London)* **1949**, *A 198*, 14.

25. Edimiston, C. and Ruedenberg, K., *Rev. Mol. Phys.***1963**, *34*, 457; *J. Chem. Phys.* **1965**, *43*, 597.
26. Roothan, C. C., *J. Rev. Mod. Phys.* **1951**, *23*, 69.
27. Hall, G. G., *Poc. Roy. Soc., (London)* **1951**, *A205*, 541.
28. Hehre, W. J., Radom, L., Pople, J. A. and Schleyer, P.V.R., *Ab Initio Molecular Orbital Theory*, Wiley (1986)
29. Roos, B. O. (eds.) *Lecture Notes in Quantum Chemistry*, Spring- Verleg(1992)
30. Olsen, J., Christiansen, O., Koch, H., Jorgensen, P., *J. Chem. Phys. Lett.* **1996**, *261*, 369.
31. Huckel, E., *Z. Physik.* **1931**, *70*, 204.
32. Feller, D. and Davidson, E.R., *Rev. Comp. Chem.* **1990**, 1.
33. Helgaker, T. and Taylor, P. R., *Modern Electronic Structure Theory*, PartII (D. Yarkony ed.), World Schientific , pp. 727(1995).
34. Boys, S. F., *Proc. Roy. Soc.,(London)* **1950**, *A 200*, 542.
35. Hehre, W. J., Stewart, R. F. and Pople, J. A., *J. Chem. Phys.* **1969**, *51*, 2657.
36. Binkley, J. S. and Pople, J. A., *J. Am. Chem. Soc.* **1980**, *102*, 939.
37. Frisch, M. J., Pople, J. A. and Binkley, *J. Chem. Phys.* **1984**, *80*, 3265.
38. Block, F., *Z. Physik* **1929**, *57*, 545.
39. Dirac, P. A. M., *Proc. Cambridge Phil. Soc.* **1930**, *26*, 376.
40. Thomas, L. H. *Math. Procc. Cambridge* **1929**, *23*, 542.
41. Cohen, A. J., Mori-Sanchez, P. and Yang W., *Chem. Rev.* **2012**, *112*, 289.
42. Zhang, G. and Musgrave C. B., *J. Phys. Chem. A* **2007**, *111*, 1554.
43. Becke, A. D., *J. Chem. Phys.* **1993**, *98*, 5648.
44. Yanai, T., Tew, D. P. and Handy, N. C., *Chem. Phys. Lett.* **2004**, *393*, 51.
45. Zhao Y. and Truhlar, D. G., *Acc. Chem. Res.* **2008**, *41*, 157.
46. Dion, M., Rydberg, H., Schröder, E., Langreth, D. C. and Lundqvist, B. I., *Phys. Rev. Lett.* **2004**, *92*, 246401.
47. Lee, K., Murray, É. D., Kong, L., Lundqvist, B. I. and Langreth, D. C., *Phys. Rev. B: Condens. Matter* **2010**, *82*, 081101.
48. Wilson, L. C. and Levy, M., *Phys. Rev. B* **1990**, *41*, 12930.

49. Tao, J. and Perdew, J. P., *J. Chem. Phys.* **2005**, *122*, 114102.

50. Tao, J., Perdew, J. P., Staroverov, V. N. and Scuseria, G. E., *Phys. Rev. Lett.* **2003**, *91*, 146401.

51. Zhao, Y. and Truhlar, D. G., *Theor. Chem. Acc.* **2008**, *120*, 215.

52. Grimme, S., *J. Chem. Phys.* **2006**, *124*, 034108.

53. Antony, J. and Grimme, S., *Phys. Chem. Chem. Phys.* **2008**, *10*, 2722.

54. Ehrlich, S., Moellmann, J. and Grimme, S., *Acc. Chem. Res.* **2012**, *46*, 916.

55. Grimme, S., *J. Comput. Chem.* **2006**, *27*, 1787.

56. Hohenberg, P. and Kohn, W., *Phys. A: At. Mol. Opt. Phys.* **1964**, *136*, B864.

57. Koopmans, T., *Physics* **1933**, *1*,104.

58. Hehre, W. J., *A Guide to molecular Mechanics and Quantum Chemical Calulations*, Wavefunction, Inc.: Irvine, CA (2003).

59. Szabo A. and Ostlund, N. S., *Modern Quantum Chemistry: Introduction to Advanced Electronics Structure Theory*, McGraw-Hall: New York (1982).

60. Raghavachari K. and Anderson, J. B., *J. Phys. Chem.* **1996**, *100*, 12960.

61. Head-Gordon, M., *J. Phys. Chem.* **1996**, *100*, 13213.

62. Pople, J. A., Raghavachari, K., Schlegel, H. B., DeFrees, D., Binkley, J. S., Hout, R. F. and Hehre, W., *J. Int. J. Qunatum Chem. Symp.* **1981**, *15*, 269.

63. Pople, J. A., Scott, A. P., Wong, M. W. and Radom, L., *Israel J. Chem.* **1993**, 33, 345.

CHAPTER 3

INTERACTION OF AMINO ACIDS WITH SINGLE WALLED CARBON NANOTUBE: A QUANTUM MECHANICAL STUDY

CHAPTER 3

INTERACTION OF AMINO ACIDS WITH SINGLE WALLED CARBON NANOTUBE: A QUANTUM MECHANICAL STUDY

3.1. Introduction

The carbon nano-structures(CNSs) such as graphene and carbon nanotube have emerged as the promising nanomaterials for biomedical and environmental applications due to unique physical and chemical properties such as a tunable band gap, room temperature Hall effect, high mechanical strength (200 times greater than steel), and high elasticity, thermal conductivity and high entangle network structure. The exceptional electrical properties of graphene (such as, high charge mobility and capacity, highly tunable conductance) makes it as an ideal for sensing applications.[1-3] Carbon nanostructures (CNSs) exhibit the non-covalent interaction such as cation-π, π-π and CH-π towards the small molecules, metal ions and biomolecules as amino acid, nucleic acids. The non-covalent interaction of amino acids with various substrates and their proton affinity values have been studied.[4-5] The important aromatic amino acid for the interaction between a peptide and a single walled carbon nanotube has also been done in experimental studies.[6] A recent experimental study revealed that π-π noncovalent interactions between CNTs and the aromatic residue (Trp, Phe, Tyr) of the proteins were found to play a significant role in determining the strength of the CNT-protein interaction.[7] Subramanium et al. have brought out new insight to study the interaction of CNT and peptides.[8-13] The interaction between these can be seen in Figure 3.1. The

study of noncovalent carbonaceous materials play a vital role in understanding various carbon nanostructures, such as diagnosis of life threatening diseases (sensors), cancers therapy (drug delivery system), DNA sequencing (personalized medicines).[12-14] Developing sensors based on CNT-biomolecule composites for amplified detection methods is an area of recent interest, and such sensors can be efficiently used for the detection of various carbon nanostructures as well as different biomaterials such as DNA, protein, and so on.[15] Umadevi et al. investigated the adsorption of biological molecules such as amino acids, enzymes, antibodies and nucleic acids, metal ions as Na^{+}, Ka^{+}, Ca^{+2}, Mg^{+2}, Be^{+2} and small molecules as CO_2, H_2O, CO, NH_3, H_2O, CH_4 on the surface of graphene/CNTs along with the significant changes in the energy as well as sensitivity and specificity of biosensor.[16-20] Wang et al.[21] carried out a study to understand the affinity of the specific peptides to CNTs and delineate contribution of the constituents of amino acids to the binding strength of the peptides with CNTs. Further the studies on the structure-function-affinity of the peptides with the CNT have shown that phenylalanine has an important role to play in enhancement of the adsorption of peptides on the CNTs.[22] Li et al. demonstrated that polytryptophan peptides bind more strongly through their aromatic rings with the CNTs compared to the polylysine.[23] However, the role of interaction of these biomolecules with the CNTs and the extent to which the nanotube can be used is not understood much for these biological systems. Other studies on the adsorption of polynuclear aromatic compounds to CNTs, suggest that the π-π interactions play a critical role in the binding strength towards the nanotubes.[24-25] Dai and co-workers have investigated the potential of carbon nanotube to be used as gas sensors for detection of molecules such as NO_2 and NH_3.[26] Schedin et

al. reported their experimental observation that graphene – based sensors could detect even the adsorption of individual gas molecules.[27] Carbon nanostructures can absorb a number of species such as gas molecule, metal ions, polymers, organic molecules, and bio molecules such as proteins, nucleobases and DNA on their surface and these adsorption properties provide opportunities for potential industrial applications.[28-29] Several studies have been carried out on the immobilisation of proteins and nucleic acid on nanotube.[30-32] However recent studies elaborate on the appreciable changes in nanotube conductivity as bio molecules which are immobilised, directly or indirectly, on the CNT sidewalls.[33-35] Roman et al. used DFT method to investigate the adsorption of any few amino acids on (3, 3) CNT.[36] In the present work detailed theoretical calculations has been done between aromatic amino acids and single walled carbon nanotube which is discussed.

3.2. Computational Details

The calculations of the interaction between CNT and aromatic amino acids complex system were carried out using the density functional theory. The geometry of all the structures was optimized using B3LYP/6-31G* method. The both individual structures and complex structures were optimized. In this study, the binding energy of the complex system is calculated using the following equation (3.1).

$$\text{Binding Energy} = E_{CNT\_A} - E_{CNT} - E_A \qquad (3.1)$$

The binding energy is defined as the difference between the total energy of the individual structures (E_{CNT}; enrgy of carbon nanotube and E_A; energy of amino acids) and the total

energy of the complex system (E_{CNT_A}). The geometry of the aromatic amino acid such as histidine, phenylalanine, tyrosine, and tryptophan and carbon nano structures respectively was optimized using Gaussian 09 program suite. These individual aromatic amino acids established adsorption at different position of SWCNT. The individual amino acid was placed parallel to the surface of SWCNT at a distance of 3.0Å. Thereafter the complex structure was optimized using density functional theory by Gaussian 09 program suite. [37]

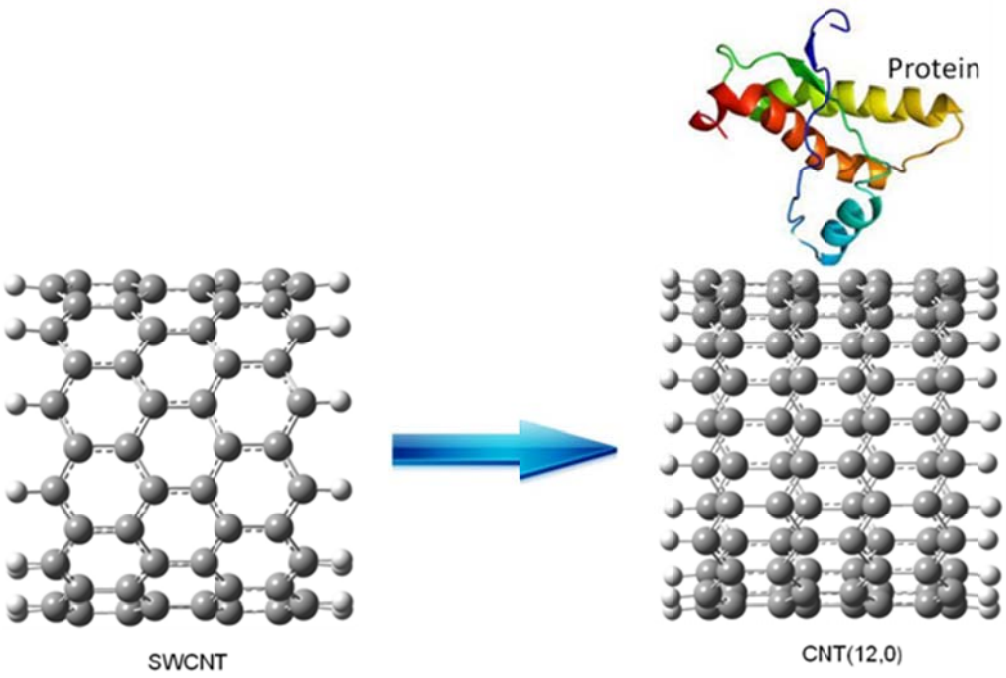

Figure 3.1: The geometrical optimization of zigzag single walled carbon nanotube [CNT (12, 0)] before and after interaction with protein.

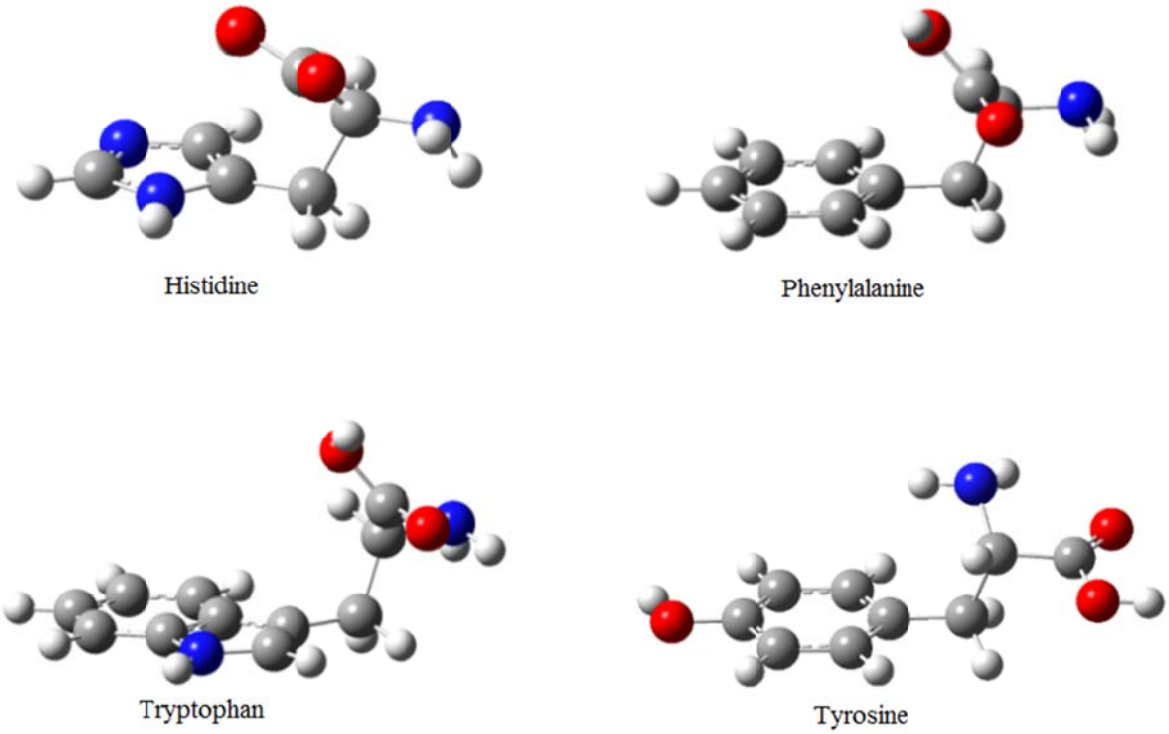

Figure 3.2: The full geometrical optimization of individual structure of aromatic amino acids.

3.3. Results And Discussion

The optimized structures of aromatic amino acids and single walled carbon nanotube are shown in Figure 3.1 and 3.2. The initial configurations of all four aromatic amino acid bases were assigned so that their aromatic rings are oriented exactly parallel to the CNT surface. In this work, zig-zag SWCNT i.e. CNT (12, 0) was considered to study the interaction of aromatic amino acids molecule with their π-surface towards carbon nanostructures. For instance, the Figures 3.3 and 3.4 shows the aromatic amino acid interaction in exterior and interior position of CNT (12, 0). The propensity and nature of aromatic amino acids such as Phenylalanine, Histidine, Tyrosine, and Tryptophan towards the zigzag carbon nanotube have studied. From the results obtained, the zigzag

SWCNT behaves as semiconducting materials. Aromatic amino acid is placed in two different positions i.e. inside the CNT and outside the CNT placed parallel to the surface of CNT at a distance of 3.0Å to make sure that π-π interaction takes place which plays a crucial role in the non-bonded interaction. The binding strength of all the aromatic amino acid in both the positions (i.e. interior and exterior) is found to bind with different affinity. The calculated binding energy of the aromatic amino acids such as histidine, phenylalanine, tyrosine and tryptophan in the exterior position of carbon nanotube is -8.00, -0.17, -0.65 and -0.79 kcal/mole and interior position is -2.89, 4.66, 1.78 and 8.45 kcal/mole respectively. Consequently, the aromatic amino acids have a strong affinity to bind in interior position of the CNT (12, 0). It is also observed from the results that the binding strength for tryptophan is greater in interior position than in the exterior position of the CNT (12, 0).

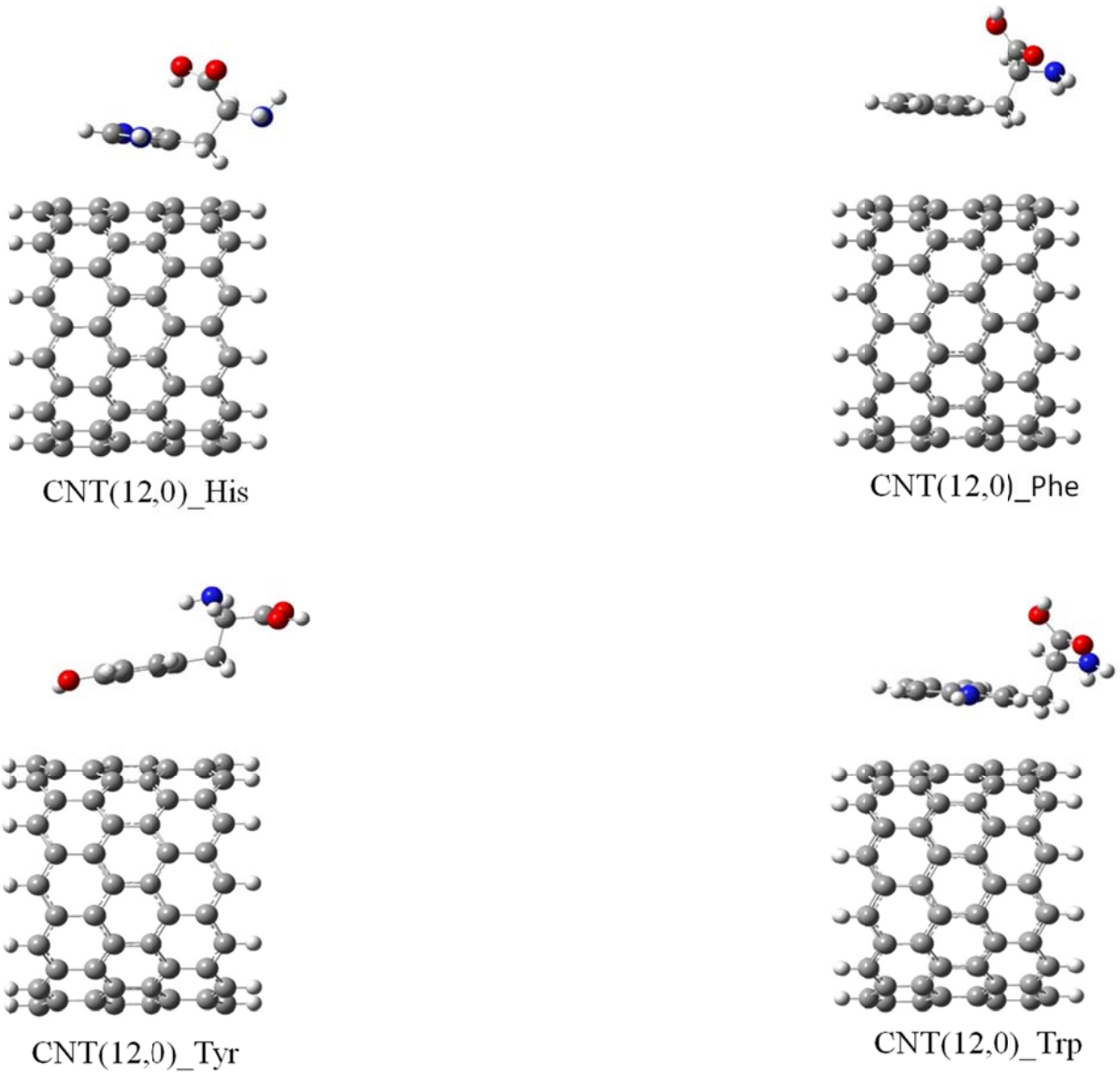

Figure 3.3: Model of aromatic amino acids adsorbed on the exterior position of single walled carbon nanotube [CNT (12, 0)].

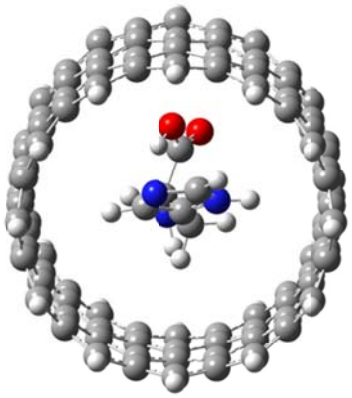

CNT(12,0)_His

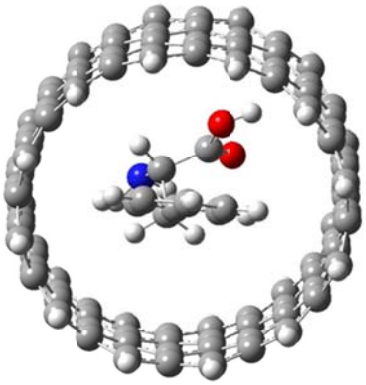

CNT(12,0)_Phe

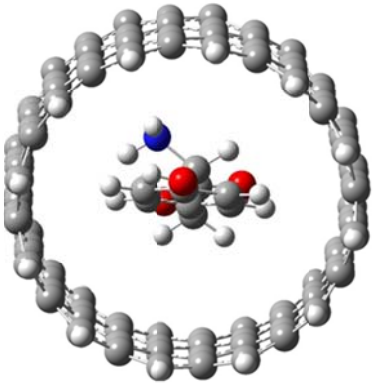

CNT(12,0)_Tyr

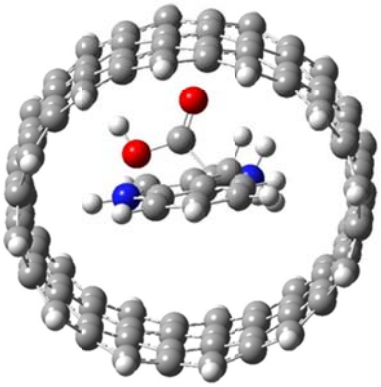

CNT(12,0)_Trp

Figure 3.4: Model of aromatic amino acids adsorbed in the interior position of single walled carbon nanotube [CNT (12, 0)].

Table 3.1: The binding energy and HOMO-LUMO gap of the complex molecular system in the exterior position using B3LYP/6-31G*.

Complex molecular system	Binding Energy (kcal/mole)	HOMO Energy (eV)	LUMO Energy(eV)	HOMO-LUMO Gap (eV)
CNT(12,0)_Histidine	-8.00	-3.88	-3.48	0.40
CNT(12,0)_Phenylalanine	-0.17	-3.85	-3.44	0.41
CNT(12,0)_Tyrosine	-0.65	-3.88	-3.47	0.40
CNT(12,0)_Tryptophan	-0.79	-3.89	-3.48	0.41

Table 3.2: The binding energy, HOMO-LUMO gap of the complex molecular system in the interior position using B3LYP/6-31G*.

Complex Molecular System	Binding Energy (Kcal/mole)	HOMO Energy (eV)	LUMO Energy (eV)	HOMO-LUMO gap (eV)
Cnt(12,0)_Histidine	-2.891	-3.838	-3.481	0.357
CNT(12,0)_Phenylalanine	4.656	-3.895	-3.487	0.408
CNT(12,0)_Tyrosine	1.778	-3.839	-3.436	0.403
CNT(12,0)_Tryptophan	8.447	-3.867	-3.470	0.397

Tables 3.1 and 3.2 also shows that the HOMO-LUMO gap of the various aromatic amino acids in exterior and interior position of single walled carbon nanotube. The HOMO-LUMO gap for the interaction of histidine with CNT (12, 0) varies from 0.36 to 0.40 eV for the interior and exterior position respectively. The binding energy of histidine increases with decreasing HOMO-LUMO gap of CNT (12, 0). The binding energy of phenylalanine and tyrosine is greater in interior position than in the exterior position of

CNT (12, 0) but there is no significant change of HOMO-LUMO gap of CNT(12,0) with increase in binding energy for phenylalanine. On the other hand the binding energy of tryptophan vary from -0.79 to 8.5 kcal/mole and the HOMO-LUMO gap of CNT (12, 0) vary from 0.41 to 0.40eV. So, it is clear that the binding energy of tryptophan is increasing with decrease in the HOMO-LUMO gap for CNT (12, 0) in interior position. Therefore, we can conclude that the tryptophan have strongest binding energy in interior position of single walled carbon nanotube.

3.4. Conclusion

The binding of a series of different aromatic amino acids with carbon nanotube has been comprehensively analysed. These calculations reveals that the binding energy preferences of aromatic amino acids are different in both positions respectively i.e. in exterior and interior positions. The binding energy of aromatic amino acid is greater in interior than the exterior position of single walled carbon nanotube. For the exterior position the preferential order of the interaction for the aromatic amino acids with single walled carbon was histidine<tyrosine<tryptophan<phenylalanine while for the interior position the order is histidine<tyrosine<phenylalanine<tryptophan. The tryptophan prefers to bind to the inner side wall of carbon nanotube. The significant changes occur in the HOMO-LUMO gap of the CNT(12,0) on the aromatic amino acids. This study can also be applied to develop novel bio- sensors, new carbon based drug delivery systems and sensing applications, focusing particularly on the mechanism of binding between biomolecule and carbon nanotube.

3.5. References

1. Dinadayalane, T. C. and Leszczynski, J., *Struct. Chem.* **2010**, *21*, 1155.
2. Liang, F. and Chen, B., *Curr. Med. Chem.* **2010**, *17*, 10.
3. Zhu, Y., Murali, S., Cai, W., Li, X., Suk, J. W., Potts, J. R. and Ruoff, R. S., *Adv. Mater.* **2010**, *22*, 3906.
4. Ready, A. S., Sastry, G. N., *J. Phys. Chem. A.* **2005**, *109*, 8893.
5. Dinadayalane, T. C., Sastry, G. N. and Leszczynski, J., *Int. J. Quantum Chem.* **2006**, *106*, 2920.
6. Zorbas, V., Smith, A. L., Xie, H., Ortiz-Acevedo, A., Dalton, A. B., Dieckmann, G. R., Draper, R. K., Baughman, R. H. and Musselman, I. H., *J. Am. Chem. Soc.* **2005**, *127*, 12323.
7. Ge, C., Du, J., Zhao, L., Wang, L., Li, Y., Yang, Y., Zhou, R., Chai, Z. and Chen, C., *Proc. Natl. Acad. Sci. USA* **2011**, *108*, 16968.
8. Balamurugan, K., Gopalakrishnan, R., Raman, S. S. and Subramanian, V., *J. Phys. Chem. B* **2010**, *114*, 14048.
9. Balamurugan, K., Singham, E. R. A., Subramanian, V., *J. Phys. Chem. C* **2011**, *115*, 8886.
10. Gopalakrishnan, R., Balamurugan, K., Singham, E. R. A., Sundaraman, S. and Subramanian, V., *Phys. Chem. Chem. Phys.* **2011**, *13*, 13046.
11. Balamurugan, K. and Subramanian, V., *Biopolymers* **2013**, *99*, 357.
12. Liu, Z., Sun, X., Nakayama-Ratchford, N. and Dai, H., *ACS Nano* **2007**, *1*, 50.
13. Khan, M. A. K., Kerman, Prtryk M. and Kraatz, H., *Anal. Chem.* **2008**, *80*, 2574.
14. Kuang, Z., Kim, S. N., Crookes-Goodson, W. J., Farmer, B. L. and Naik, R.R., *ACS Nano* **2010**, *4*, 452.
15. Barone, P. W., Baik, S., Heller, D.A. and Strano, M. S., *Nat. Mater.* **2005**, *4*, 86.
16. Umadevi, D. and Sastry, G.N., *J. Phys. Chem. C* **2011**, *115*, 9656.

17. Umadevi, D. and Sastry, G. N., *J. Phys. Chem. Lett.* **2011**, *2*, 1572.

18. Umadevi, D., Panigrahi, S. and Sastry, G. N., *Acc. Chem. Res.* **2014**, *47*, 2574.

19. Umadevi, D. and Sastry, G. N., *Curr. Sci.* **2014**, *106*, 1224.

20. Umadevi, D. and Sastry, G. N., *Chem. Phys. Lett.* **2012**, *549*, 39.

21. Kong. J., Franklin, N. R., Zhou, C. W., Chapline, M. G., Peng, S., Cho, K. J., and Dai, H., *Science* **2000**, *287*, 622; Collins, P. G., Bradley, K., Ishigami, M. and Zettl, A., *Science* **2000**, *287*,1801; Shim, M., Javey, A., Wong Shi Kam, N. and Dai, H., *J. Am. Chem.Soc.* **2001**, *123*,11512.

22. Zorbas, V., Smith, A. L., Xie, H., Ortiz-Acevedo, A., Dalton, A. B., Dieckmann, G. R., Draper, R. K., Baughman, R. H., and Musselman, I. H., *J. Am. Chem. Soc.* **2005**, *127*, 12323.

23. Lie, X., Chen, W., Zhan, Q., Sowards, L., Pender, M., and Naik, R. R., *J. Phys. Chem. B* **2006**, *110*, 12621.

24. Chen, R. J., Zhan, Y., Wang, D., and Dai, H., *J. Am. Chen. Soc.* **2001**, *123*, 3838.

25. Zhan, J., Lee, J. K., Wu, Y., and Murray, R. W., *Nano Lett.* **2003**, *3*, 403.

26. Kong, J., Franklin, N., Zhou, C., Chapline, M., Peng, S., Cho, K. and Dai, H., *Science* **2000**, *287*, 622.

27. Schedin, F., Geim, A. K., Morozov, S. V., Hill, E. W., Blake, P., Katsnelson, M. I. and Novoselove, K. S., *Nature Mater.* **2007**, *6*, 652.

28. Chen, W., Duan, L. and Zhu, D., *Environ. Sci. Technol.* **2007**, *41*, 8295.

29. Panigrahi, S., Bhattacharya, S., Banerjee, S. and Bhattacharyya, D., *J. Phys. Chem. C* **2012**, *116*, 4374.

30. Balavoine, F., Schultz, P., Richard, C., Mallouh, V., Ebbesen, T. and Mioskowski, C., *Angew. Chem. Int. Ed.* **1999**, *38*, 1912.

31. Tsang, S. C., Davis, J. J., Malcolm, L., Green, H., Allen, H., Hill, O., Leung, Y. C. and Sadler, P. J., *J. Chem. Soc. Chem.Commun.* **1995**, *17*, 1803.

32. Tsang, S.C., Guo, Z., Chen, Y.K., Green, M. L. H., Allen, H., Hill, O., Hambley, T.W. and Sadler, P. J., *Angew. Chem. Int. Ed. Engl.***1997**, *36*, 2197.

33. Chen, R. J., Bangsaruntip, S., Drouvalakis, K. A., Kam, N. W. S., Shim, M., Li, Y., Kim, W., Utz, P. and Dai, H., *Proc. Natl. Acad. Sci.* **2003**, *100*, 4984.

34. Besteman, K., Lee, J., Wiertz, F. G. M., Heering, H. and Dekker, C., *Nano Lett.* **2003**, *3*, 727.

35. Star, A., Gabriel, J. C. P., Bradley, K. and Gruner, G., *Nano Lett.* **2003**, *3*, 459.

36. Roman, T., Dino, W. A., Nakanishi, H. and Kasai, H., *Eur. Phys. J. D* **2006**, *38*, 117.

37. Frisch, M. J., Trucks, G. W., Schlegel, H. B., Scuseria, G. E., Robb, M. A., Cheeseman, J. R., Scalmani, G., Barone, V., Mennucci, B., Petersson, G. A., Nakatsuji, H., Caricato, M., Li, X., Hratchian, H. P., Izmaylov, A. F., Bloino, J., Zheng, G., Sonnenberg, J. L., Hada, M., Ehara, M., Toyota, K., Fukuda, R., Hasegawa, J., Ishida, M., Nakajima, T., Honda, Y., Kitao, O., Nakai, H., Vreven T., Montgomery, J. A. Jr., Peralta, J. E., Ogliaro, F., Bearpark, M., Heyd, J. J., Brothers, E., Kudin, K. N., Staroverov, V. N., Keith, T., Kobayashi, R., Normand, J., Raghavachari, K., Rendell, A., Burant, J. C., Iyengar, S. S., Tomasi, J., Cossi, Rega, M., N., Millam, J. M., Klene, M., Knox, J. E., Cross, J. B., Bakken, V., Adamo, C., Jaramillo, J., Gomperts, R., Stratmann, R. E., Yazyev, O., Austin, A. J., Cammi, R., Pomelli, C., Ochterski, J. W., Martin, R. L., Morokuma, K., Zakrzewski, V. G., Voth, G. A., Salvador, P., Dannenberg, J. J., Dapprich, S., Daniels, A. D., Farkas, O., Foresman, J. B., Ortiz, J. V., Cioslowski, J., and Fox, D. J., Gaussian, Inc.,Wallingford CT, 2010.

CHAPTER 4

ADSORPTION OF SMALL GAS MOLECULES ON PURE AND AL-DOPED GRAPHENE SHEET: A QUANTUM MECHANICAL STUDY

CHAPTER 4

ADSORPTION OF SMALL GAS MOLECULES ON PURE AND AL-DOPED GRAPHENE SHEET: A QUANTUM MECHANICAL STUDY

4.1. Introduction

Carbon is a versatile element of the earth's crust and it is found on earth surface in different allotropes such as graphite, diamonds, charcoal and coke. The newer allotropes of carbon such as graphene, carbon nanotubes (CNTs) and fullerenes were gradually discovered.[1-3] Graphene is the youngest known allotrope of carbon which is a two-dimensional and one-atom thick material consisting of sp^2 hybridized carbon atoms arranged in honeycomb structure. These allotropes of carbon are extensively used in research areas from biomedical to environment applications due to their unique physical and chemical properties.[4] The exceptional properties of carbon nano-materials such as electronic, thermal, optical, mechanical and transport properties make them promising candidates for various potential applications.[5-7] It is observed from several experimental and theoretical studies that the transport and electronic properties are extremely sensitive to change in the local chemical environment.[8-10] Carbon nanostructures [CNSs] exhibit non-covalent interaction such as the XH-π, cation-π, anion-π and π-π interactions towards the small gas molecules, metal ions and biomolecules.[11-15] The XH-π weak interactions were extensively studied in recent years.[16-20] These interactions have been considered to be a unique type of hydrogen bonding interaction in which π electron acts as the proton acceptor.[21] Graphene is a

sensitive nano material which detects all the individual events when a gas molecule is adsorbed to or deadsorbed from its surface.[22] However, it is very difficult to prepare a perfect single layer graphene with zero band gap. Doping is one of the most efficient method to improve the electronic properties of the materials. Wang et al., have found that the sp^2- hybridization affects and changes the electronic properties of the system when B, N, B-N is doped with PG (PG).[23] Lherbier et al., showed that the charge mobility and conductivity of graphene changes when B/N impurity atom is added to its surface.[24] Recently, there are several experimental studies on Al, Ga and Pd doped graphene sheets based gas sensor.[25,26] Interestingly, the nanoparticles such as Al, Ga and Pd incorporated the significant changes in the sensitivity and selectivity towards the gas molecules. The structure and physical properties of carbon nanostructures make them potential candidates as sensors to detect different type of gas molecules. Dai and co-workers were the first to report the gas sensors based on carbon nanotubes to detect gas molecules such as NO_2 and NH_3.[27] Recently, Schedin et al., experimentally reported that graphene based gas sensors possess very high sensitivity such that the adsorption of individual gas molecules could be detected.[28] CNSs can absorb a number of species such as gas molecule, metal ions, polymers, organic molecules, and bio molecules such as proteins, nucleobases and DNA on their surface and these adsorption properties provide opportunities for potential industrial applications.[29-32]

Roman et al., studied the adsorption of few amino acids on single walled carbon nanotube [CNT (3,3)] using DFT method. Roman et al., studied the adsorption of few amino acids on single walled carbon nanotube by using DFT method.[33] CNTs have also been found to be suitable candidate for the negative electrode of the Li-ion batteries, where the Li

diffuses between the positive and the negative terminals in ionic state.[34,35] Thus the fundamental understanding of the interaction of metals with CNTs in the ionic state is important. It is also important to know the role of various factors such as solvent and other chemical environment which influence such cation-π interaction.[36-38] Umadevi et al., have found that the charge transfer between graphane and t he molecules is an important factor in determining the binding strength of the complex molecular systems.[39] Zhang et al., studied that doped graphene strongly interacts with CO, NO and NO_2 while NH_3 interacts weakly.[40] Zou et al., found that the SiG has a higher chemical reaction toward the gas molecules due to doping of Silicon atom and shows the higher adsorption energy with CO, O_2, NO_2 and H_2O.[41] In the current study, the Al-doped graphene to improve its gas sensing efficiency and selectivity towards the various gas molecules were theoretically investigated. The gas molecule CCl_4, CH_4, NH_3, CO_2, CO, NO_2, CCl_2F_2, SO_2, CF_4 and N_2O, are all of great practical interest for industrial, environmental and medical applications. On the other hand, the effect of doping of the graphene sheet on the binding strength has been estimated. The charge transfer that occurred during the complex formation has also been explored. The change in the HOMO-LUMO gap of pure graphene and Al-doped graphene upon the binding of these gas molecules has also been estimated.

4.2. Computational Methods

The calculations of the interaction between PG, Al-dopd graphene and gas molecule is carried out using Density Functional Theory (DFT). The geometrical calculations of all structures have been done by using DFT method B3LYP/6-31G*.[45-46] In this study,

the individual gas molecules were adsorbed on the surface of PG and Al-doped graphene, thereafter geometry optimization calculations were accomplished using Gaussian 09 program suite.[47] It is important to note that complete geometrical configuration were tested but those shown are the lowest energy species feasible for the interaction of the compounds. Single point energy calculations have been done at the M06/6-31++G** [48-51] level to fine-tune the energy.

The adsorption energy (E_{ad}) of the small gas molecule (X = CCl_4, CH_4, NH_3, CO_2, N_2, CO, NO_2, CCl_2F_2, SO_2, CF_4, H_2) on the pure and Al-doped graphene is calculated by following equation:

$$E_{ad} = E_{graphene\_X/graphene@Al\_X} - (E_{graphene/Al@graphene} + E_X) \quad (4.1)$$

Here $E_{graphene\_X/graphene@Al\_X}$ represents the total energy of complex molecular system. $E_{graphene/graphene@Al}$ and E_X represent the total energies of the graphene and gas molecule respectively. The individual small gas molecule was placed parallel to the surface of graphene and doped graphene at the 3Å distance. The variation of the charge on gas molecules as well as on pure and doped graphene when the individual gas molecules are kept at the 3Å distance from its surface was calculated. The charge transfer has been considered as the sum of the all atoms in the pure and Al-doped graphene model system. Positive charge transfer values indicate the transfer of charge from graphene to the molecules, while negative charge values indicate the transfer of charge from the molecules to the pure and Al-doped graphene. The HOMO-LUMO gap of pure and Al-doped graphene as well as their complexes at M06/6-31++G** level of theory were also calculated. All calculations were carried out using the Gaussian09 program suite.

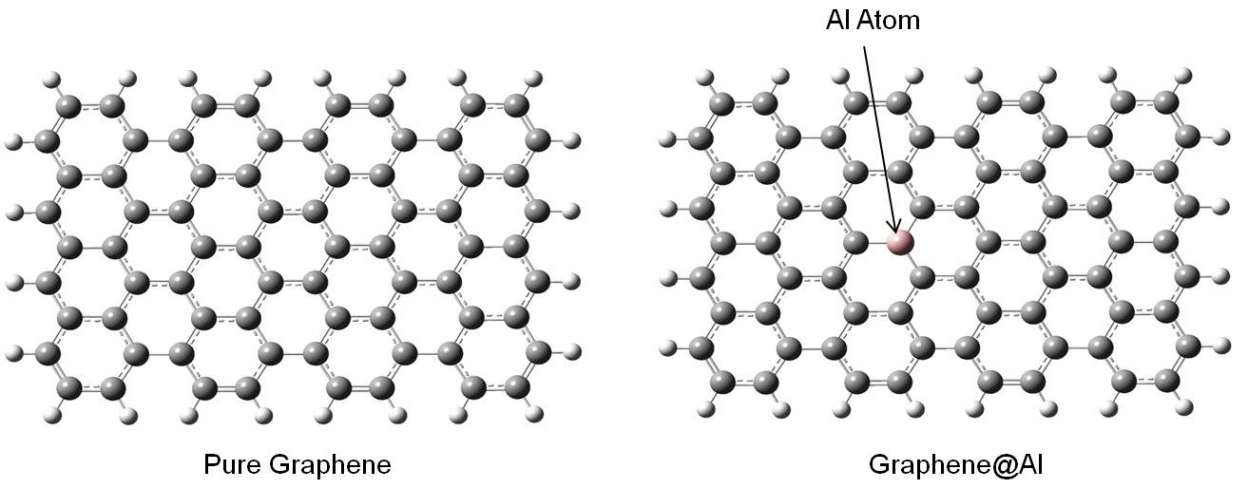

Figure 4.1: Top view of the geometrical optimized structure of pure and Al-doped graphene (Graphene@Al) model system considered in this study.

4.3. Results and Discussion

The optimized structure of pure and Al-doped graphene and their complexes with small molecules are shown in Figure 4.1, 4.2 and 4.3. The initial configuration of all small gaseous molecules were assigned so that these are oriented exactly parallel to the pure and Al-doped graphene at 3Å from its surface. In the present study, pure and Al-doped graphene was considered to study the interaction of small gas molecule with X-π noncovalent interaction towards carbon nano materials. Table 4.1 and 4.2 summarizes our results on the adsorption energy, equilibrium graphene-molecule distance (d, defined as the distance of nearest atoms between graphene and molecule), the charge transfer (Q, Mulliken charge) and HOMO-LUMO gap for the most stable configurations of pure and Al-doped graphene adsorbed with various gas molecules in the our calculations as shown in Figure 4.2, 4.3 and Table 4.1, 4.2. Subsequently, we look at the binding of the pure and Al-doped graphene with various gas molecules and the trend in the charge transfer.

The HOMO-LUMO gap of pure and Al-doped graphene with adsorption of various gas molecules were also investigated. When one impurity atom as Al is substituted for one C atom in graphene sheet, the optimized configuration of graphene sheet is dramatically distorted. The Al atom introduces the deformation of the six-membered ring (6MR) near the doping site to relieve stress as a result the Al atom protrudes out of the graphene sheet. The optimized carbon-dopant atom distance (Al-C) is 1.751Å at B3YP/6-31G* which is in agreement with the previous study.[42]

4.3.1. Adsorption energy and charge transfer

The small gas molecules form X-π type complex with the pure and Al-doped graphene that are shown in Figure 4.2 and Figure 4.3. It observed the adsorption energy of small gas molecules complexes with pure and Al-doped graphene when the gas molecules are kept parallel to the graphene surface at 3Å distance. Table 4.1, 4.2 and Figure 4.4 displays the adsorption energy, charge transfer and molecule sheet distance of the small gas molecules complexes with pure and Al-doped graphene at M06/6-31++G** level of theory.

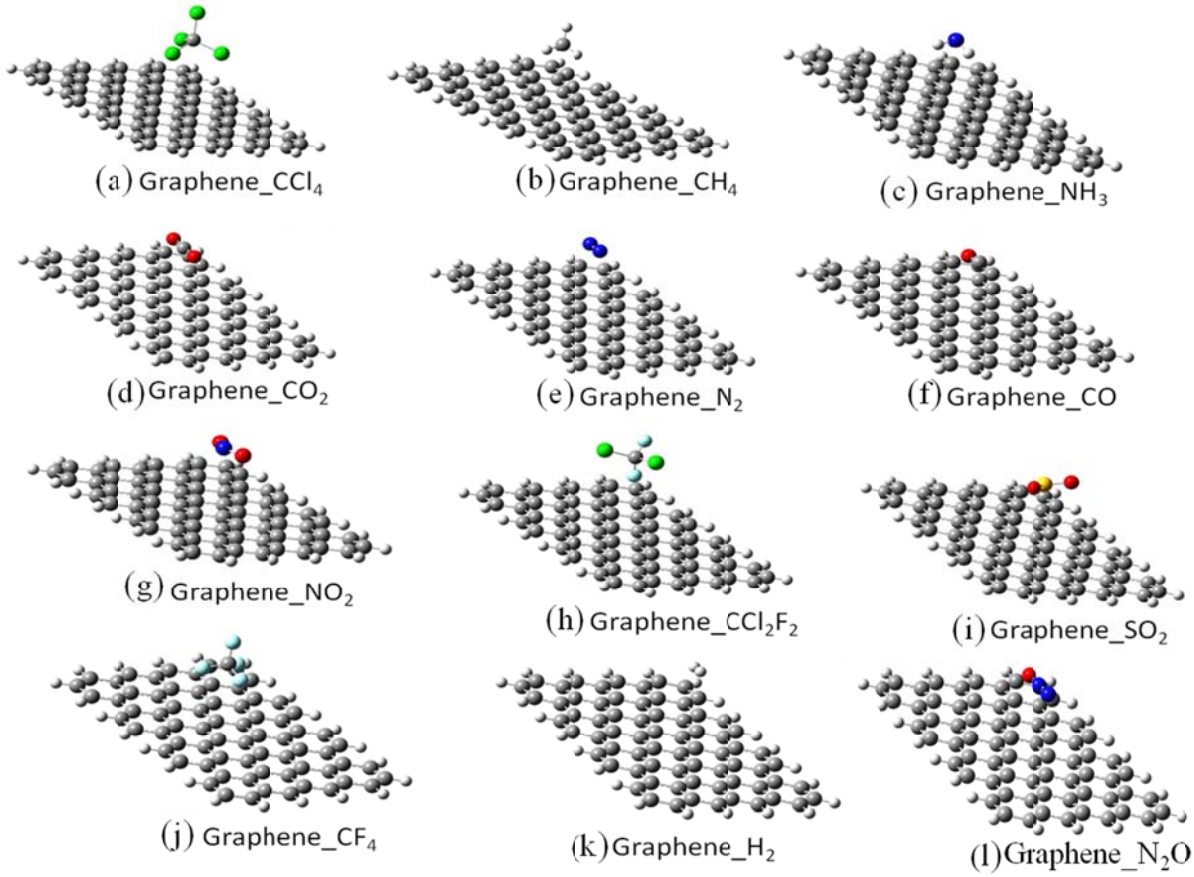

Figure 4.2: Optimized geometries of PG with small gas molecule adsorbed (a) CCl_4, (b) CH_4, (c) NH_3, (d) CO_2, (e) N_2, (f) CO, (g) NO_2, (h) CCl_2F_2, (i) SO_2, (j) CF_4, (k) H_2 and (l) N_2O by M06/6-31++G** method.

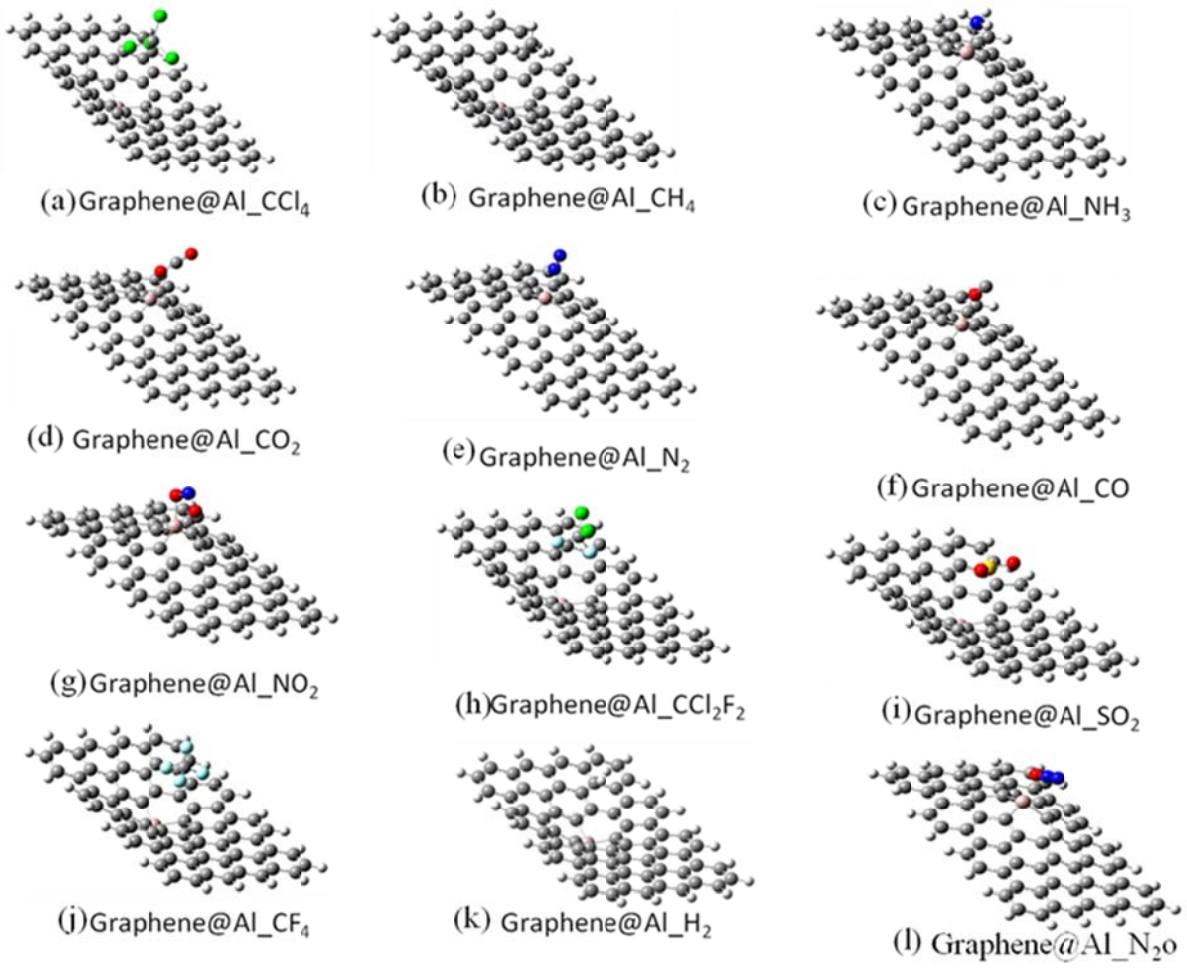

Figure 4.3: Optimized geometries of Aluminum doped graphene@Al(@ shown as Al doping in PG) adsorbed with small gas molecule (a) CCl_4, (b) CH_4, (c) NH_3, (d) CO_2, (e) N_2, (f) CO, (g) NO_2, (h) CCl_2F_2, (i) SO_2, (j) CF_4, (k) H_2 and (l) N_2O by M06/6-31++G** method.

Table 4.1. The Adsorption Energy (eV), Molecule Sheet Distance(Å), Charge Transfer (a.u.) and HOMO-LUMO Energy Gap (eV) at M06/6-31++G** level of theory.

Carbon nano material	Small gas molecule	Adsorption Energy (eV)	Molecule sheet distance (Å)	Charge on gas molecule(a.u.)	HOMO-LUMO gap(eV)
Pure Graphene	CCl_4	-0.394	4.498	-0.0196	0.3339
	CH_4	-0.067	3.784	-0.0133	0.3336
	NH_3	-0.145	3.357	0.0334	0.3336
	CO_2	-0.122	3.626	0.0169	0.3336
	N_2	-0.083	3.828	0.014	0.3339
	CO	-0.110	3.732	0.0098	0.3336
	NO_2	-0.996	3.573	0.025	0.8727
	CCl_2F_2	-0.119	3.355	0.0039	0.3336
	SO_2	-0.279	3.578	0.0254	0.3339
	CF_4	-0.150	3.404	0.0552	0.3336
	H_2	-0.013	4.946	0.0006	0.3339
	N_2O	-0.123	3.634	0.0180	0.3340

Table 4.2: The Adsorption energy (eV), Molecule sheet distance (Å), Charge transfer (a.u.), and HOMO-LUMO Gap(eV) at M06/6-31++G** level of theory.

Carbon nano material	Small Gas molecule	Adsorption Energy(eV)	Molecule Sheet distance(Å)	Charge on gas molecule	HOMU-LUMO Gap(eV)
Graphene @Al	CCl_4	-1.354	3.920	-0.007	0.661
	CH_4	-1.242	4.300	0.004	0.616
	NH_3	-2.948	2.053	0.493	1.080
	CO_2	-2.019	2.158	0.423	1.574
	N_2	-1.279	2.210	0.837	0.444
	CO	-1.255	2.344	0.276	0.494
	NO_2	-3.867	1.894	-0.065	0.330
	CCl_2F_2	-1.361	3.956	0.020	0.579
	SO_2	-1.608	3.579	0.045	0.599
	CF_4	-1.354	3.920	0.138	0.662
	H_2	-1.637	6.306	0.001	1.512
	N_2O	-1.409	2.163	0.518	0.453

Interestingly, a different trend in the case of small gas molecule interacting with pure and Al-doped graphene is observed, the adsorption energy of small gas molecules towards the Al-doped graphene is greater than PG. From Table 4.2 and Figure 4.2, the adsorption energy of all gas molecules is higher for the Al-doped graphene than that of pure graphite.

For CCl_4 and CH_4 adsorbed on PG, the most energetically favorable configuration (Graphene_CCl_4) is also identical. The adsorption of CCl_4 and CH_4 on PG is non-covalent interaction with the adsorption energy of -0.394eV and -0.067eV and the molecule sheet distance of 4.498Å and 3.784Å, respectively. The charge transfer from graphene to CCl_4 and CH_4 molecule is -0.0196a. u. and -0.0133a.u. which indicates that the PG acts as a donor while gas molecule as an acceptor. Therefore PG is less sensitive to the CCl_4 than CH_4 molecule. The most stable configuration of CCl_4 and CH_4 on graphene@Al is a configuration with the CCl_4 and CH_4 molecule parallel to the graphene sheet and a Cl atom of CCl_4 and H atom of CH_4 adsorbed on the top of an Al atom which is shown in Figure 4.3(a) and Figure 4.3(b), where the molecular sheet distance is 3.920 and 4.300Å, respectively. The calculated E_{ad} value is -1.354eV and -1.242eV which indicates that the graphene@Al has higher adsorption energy than PG with CCl_4 and CH_4.

The NH_3 molecule shows different adsorption configurations on pure and Al-doped graphene, showing a more complicated adsorption mechanism than the other molecules. On the PG, the configuration with the three hydrogen atoms of NH_3 pointing towards the graphene plane is the favorable one [Figure 4.3(c)] which gives an adsorption energy and molecule distance of -0.145eV and 3.357Å, respectively. This result is consistent with

previous reports about NH_3 adsorbed on carbon nanotubes(-0.14eV) and NH_3 adsorbed on graphene(0 ~ -0.17eV) [43-44] which indicates a weak interaction between NH_3 and the PG. On the Al-doped graphene, NH_3 is attached to the Al atom with the N atom pointing at the sheet, which gives an adsorption energy of -2.948eV and an Al-N distance of 2.053Å [as shown in Figure 4.3(c) and Table 4.2]. The charge transfer from NH_3 to graphene is 0.493a.u. which indicates that the graphene behaves as charge acceptor and NH_3 molecule as charge donor. The adsorption energy of NH_3 on Al-graphene (-2.948eV) is much higher than that on the PG, which attributes to the strong interaction between the electron –deficient Al atom and the electron –donating N atom of NH_3. It is also investigated that the Al-doped graphene undergoes an obvious distortion upon NH_3 adsorption [Figure 4.3(c)], indicating that the B site is transformed from sp^2 to sp^3 hybridization which matched the previous study.[37] The molecular distance between Al and N is 2.053Å. This strong interaction is also evident in the electronic total charge density on Al-doped graphing system, which shows the large electron density overlap.

The adsorption energy of this complex system is -0.122eV and molecule-sheet distance is 3.626Å which are shown in Table 4.1 and Figure 4.2(d). The low adsorption energy and long molecule sheet distance indicate a weak interaction. When the CO_2 molecule is adsorbed on PG, the calculated charge transfer of CO_2 is 0.0169a.u. In this configuration, the CO_2 molecule acts as charge donor. When the CO_2 molecule is adsorbed on Al-doped graphene, the one oxygen atom of CO_2 shows most stable configuration towards the Al atom of graphene@Al sheet. In this configuration, the adsorption energy and molecule sheet distance (O-Al) is -2.019eV and 2.158Å respectively. This result indicates that the interaction of CO_2 with graphene@Al is much stronger than that of the PG due to large

transfer of charge. In this configuration, the charge transfer from CO_2 to the graphene@Al is 0.423a.u. which means that the CO_2 molecule acts as charge donor and graphene@Al acts as charge acceptor.

In case of graphene_N_2 configuration, the N-N axis gets aligned parallel to the graphene plane along the axis of two opposite C atoms of the 6MR which was found to be the most stable configuration. The adsorption energy and the molecule sheet distance of this complex system is -0.083eV and 3.828Å, respectively as shown in Figure 4.4(a), Figure 4.4(c) and Table 4.1. The charge transfer between N_2 and graphene was calculated from Mulliken population analysis which are shown in Table 4.1. This result indicates that the interaction is weak in nature due to very small adsorption energy and charge transfer. When adsorbed on Al-doped graphene (graphene@Al), N_2 adopts perpendicular oreintation with Al atom of graphene sheet. In this configuration, the one N atom of N_2 and Al atom of graphene@Al is very close as shown in Figure 4.3(e). The adsorption energy and the molecule sheet distance is -1.279eV and 2.210Å respectively [as shown in Figure 4.4(a) and Figure 4.4(c)]. The charge transfer from N_2 to graphene@Al is 0.837a.u. which indicates the N_2 acts as charge donor. In this configuration, the adsorption energy of the complex system is higher than the graphene_N_2 due to large transfer of charge which are responsible for strong interaction.

The most stable configuration of CO molecule is similar to the CO_2 and N_2 which are aligned parallel to the PG plane along the axis of two opposite C atoms of the 6MR in the complex molecular structure. The adsorption energy and molecule sheet distance is -0.110eV and 3.732 Å, respectively[as shown in Table 4.1]. When the CO molecule is adsorbed on PG, the charge calculated on the C and O atoms of the CO molecule are

0.100a.u. and -0.090a.u., respectively, while there is no charge on the carbon atoms of the PG. So, we can say that a very small charge is transferred from CO to the PG. Therefore, the low adsorption energy and very small charge transfer indicates weak physisorption. When the CO molecule is adsorbed on Al-doped graphene, CO molecule adopts a tilted oreintation with respect to the plane of the Al-containing 6MR, with the O atom close to graphene@Al. In this complex structure, the adsorbed energy and molecule sheet distance are found be -1.255eV and 2.344Å, respectively. The charge transfer from CO molecule to graphene@Al is 0.275au. In this configuration, the adsorption energy of graphene@Al_CO is higher than graphene_CO complex [as shown in and Table 4.2 and Figure 4.4(a)].

The shortest distance and adsorption energy from PG to the nearest O atom of NO_2 are 3.573Å and -0.996eV respectively, which indicates a weak interaction between the NO_2 and PG. However, the adsorption energy of NO_2 on PG can remarkably change the electronic properties of PG and the charge transferred from NO_2 to PG is about 0.02504a.u. It is clear that the PG behaves as charge acceptor. In other words, the PG is more sensitive to the NO_2 molecule than any other gas molecule. For NO_2 adsorbed on Graphene@Al (Al-doped graphene), the most stable configuration (Graphene@Al_NO_2) is similar to that of graphene_NO_2. But the oxygen atom of NO_2 is bonded to the Graphene@Al as shown in Figure 4.2(g). The O-Al bond length is 1.894Å and the adsorption energy for Graphene@Al_NO_2 is -3.867eV, which indicates that NO_2 is chemisorbed on the Graphene@Al. In this configuration, the adsorption energy is greater than graphene_NO_2 due to large charge transferred from Graphene@Al to NO_2, about -

0.064582a.u. which is shown in Table 4.2 and Figure 4.4(b). It is clear that the graphene@Al behave as charge donor while interacting with the NO_2.

For CCl_2F_2 adsorption on PG, the most energetically favorable configuration is similar to the graphene_CCl_4 and graphene_CH_4. In this configuration, the CCl_2F_2 is adsorbed to PG with one F atom of CCl_2F_2 pointing downwards as shown in Figure 4.2(h) and Table 4.1. The adsorption of CCl_2F_2 on PG shows interaction with the adsorption energy of -0.119eV with molecule sheet distance of 3.355Å, indicating the weak physisorption nature. The calculated charge transfer from CCl_2F_2 is only 0.004a.u. Therefore, the PG is not senstive to the CCl_2F_2. When the CCl_2F_2 is adsorbed on Al-doped graphene, both florine atoms of CCl_2F_2 gets close to the grapehe@Al. In this configuration, the adsorption energy, molecule sheet distance and charge transfer is -1.361eV, 3.956Å and 0.02a.u., respectively which indicates that interaction is weak in nature due to very small charge transfer[as shown in Figure 4.4(b) and Table 4.2].

In the graphene_SO_2 complex structure, the S atom of SO_2 is close to the C atom of PG. The adsorption energy E_{ad} and shortest distance from PG to the S atom of SO_2 are -0.279eV and 3.578Å, respectively, which are suggesting weak interaction between the SO_2 and PG [as shown in Figure 4.4(c) and Table 4.1]. However, there is no change in the electronic properties of PG due to the low charge transfer, about 0.025a.u. from SO_2 to the PG. Therefore, PG is not sensitive to the SO_2 molecule. As shown in Figure 4.3(i), the SO_2 is adsorbed on Al-doped graphene, the S atom of SO_2 gets close to the graphene@Al because the Al atom is negatively charged and S atom is positively charged. The charge on Al, S, O(98) and O(99) are -0.283, 0.796, -0.373 and -0.378 a.u., respectively which indicates that Al atom repel both oxygen atom but attracts the S atom

because S atom becomes more positively charged. In this complex structure, the adsorption energy and molecule sheet distance between S and Al is -1.608eV and 3.579Å as shown in Figure 4.3(i) and Table 4.2. However, the charge transfer is very low from SO_2 to grahene@Al, about 0.045a.u.

For CF_4 adsorption on PG, the most energetically favorable configuration is similar to the graphene_CCl_4 and graphene_CH_4. In this configuration, the CF_4 is adsorbed to PG with one F atom of CF_4 pointing downward as shown in Figure 4.2(j) and Table 4.1. The adsorption of CF_4 on PG is the non-covalent interaction with the adsorption energy of -0.150eV and the molecule sheet distance of 3.404Å, indicating the weak physisorption. The calculated charge transfer from CF_4 is only 0.055a.u. Therefore, the PG is not senstive to the CF_4. When the CF_4 is adsorbed on Al-doped graphene, one florine atom of CF_4 gets close to the grapehe@Al. In this configuration, the adsorption energy, molecule sheet distance and charge transfer is -1.354eV, 3.404Å and 0.135a.u. respectively. So we can say that the graphene@Al is more sensitive than PG towards the CF_4 molecule [Figure 4.3(j) and Table 4.2]. In this complex, the graphene@Al acts as charge acceptor.

The H_2 molecule was initially placed parallel to the graphene. After full relaxation, a configuration with the adsorbed H_2 axis gets aligned almost parallel to the graphene surface along the axis of two opposite C atoms of the 6MR and was found to be the most stable one for the PG. The adsorption energy of this system is -0.013eV and the molecule sheet distance is 3.946Å as shown in Figure 4.3(k) and Table 4.1which are suggesting weak interaction between H_2 and graphene. The charge transfer between H_2 and graphene is 0.0007a.u. In this configuration, PG is not sensitive towards the H_2 molecule. When adsorbed on graphene@Al, H_2 is oriented perpendicular to the Al-doped graphene plane,

with one H(97) atom close to the graphene@Al. In this complex structure, the adsorption energy, molecule sheet distance and charge transfer are -1.637eV, 6.306Å and 0.001a.u. respectively. Interestingly, the graphene@Al has more adsorption energy than PG.

As shown in Figure 4.2(l), the most stable configuration of N_2O adsorbed on PG(graphene_N_2O) is similar to graphene_CO_2, where the gas molecule axis is aligned parallel to the graphene plane along the axis of two opposite C atoms of the 6 MR. However, the N_2O in graphene_N_2O is located above the centre of the 6MR. The calculated adsorption energy, molecule sheet distance and mulliken charge are 0.123eV, 3.634Å and 0.018a.u., respectively. The low adsorption energy and long molecule sheet distance are suggesting weak physisorption. However, it is found that the interaction is significantly improved when a C atom in the PG is replaced by an Al atom. Figure 4.3(l) shows that the most stable configuration of N_2O adsorbed on graphene@Al, where the oxygen atom of N_2O is close to the Al atom of graphene@Al. The adsorption energy E_{ad} for graphene@Al_N_2O is -1.409eV, which is clearly higher than that for graphene_N_2O. The interaction distance between the N_2O molecule and the graphene@Al decreases to 2.163 Å, which indicates strong interaction. The charge transfer from N_2O to the graphene is 0.518a.u. The large transferred of charge suggests that the local electronic properties of graphene@Al is remarkably changed due to the adsorption of N_2O on graphene@Al.

The above mentioned results suggest that the PG has weak interaction towards all gas molecules. Introducing dopants like Al atom into the graphene significantly increases the molecule-graphene interaction. The order of adsorption energy for the small gas molecules complexes is $NO_2>CCl_4>SO_2>CF_4>NH_3>N_2O>CO_2>CCl_2F_2>CO>N_2>CH_4>H_2$ with PG while $NO_2>NH_3>CO_2>H_2>SO_2>N_2O>CCl_2F_2>CF_4>CCl_4>N_2>CO>CH_4$ with Al-doped graphene. Interestingly, our results predicted that Al doped graphene are more suitable for gas sensing applications, since they have stronger interactions with all small gas molecule than PG. The Al doped graphene particularly shows the highest sensitivity towards NO_2, NH_3 and CO_2.

4.3.2. HOMO-LUMO gap

The primary requisite for a material to perform as a sensor is to undergo a change in its physical property on interacting with an analyte. Such changes can be monitored and recorded to determine the presence of the analyte. The HOMO-LUMO gap is defined as the energy difference between lowest unoccupied molecular orbital and highest occupied molecular orbital. It is the electronic property of any molecular system which is helpful to design new materials. In order to notice such depiction in the case of carbon materials, we have calculated the HOMO-LUMO gap of the PG and Al-doped graphene in the free state and in with the small gas molecules complexed. In general, in the case of X-π complexes, the HOMO-LUMO gap of SWCNT varies with orientation of small gas molecules on the PG and Al-doped graphene. It has been shown that the energy gap of PG is not significant but when the gas molecules is adsorbed on graphene@Al then

significant changes in HOMO-LUMO gap is observed [as shown in Table 4.2]. So we can say that the variation in HOMO-LUMO energy gap of the graphene upon binding with the the various small gas molecule is significant.

(a)

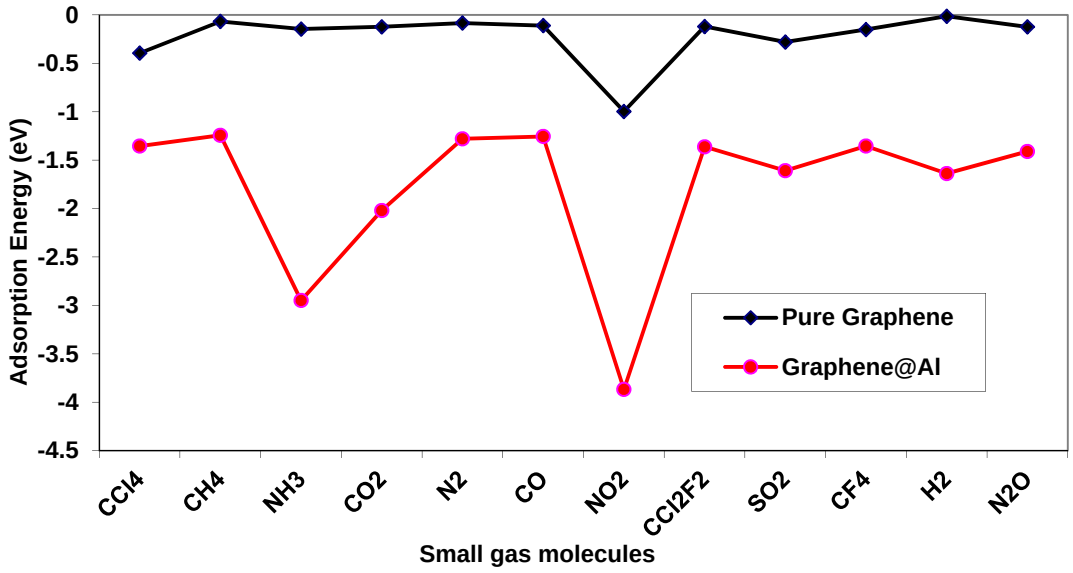

(b)

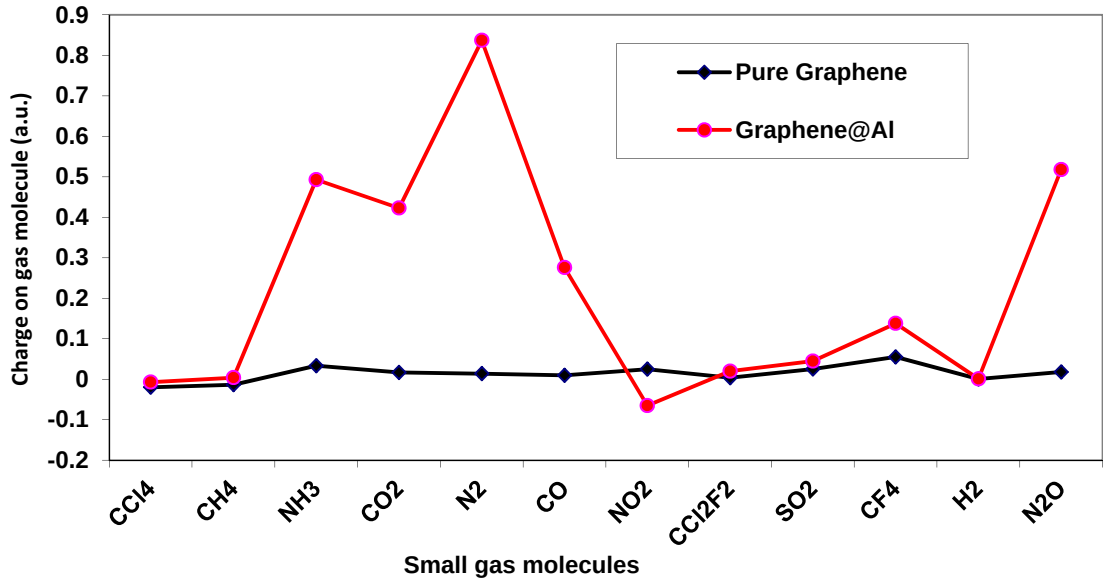
Charge on gas molecule (a.u.)
0.9
0.8
0.7
0.6
0.5
0.4
0.3
0.2
0.1
0
-0.1
-0.2
Pure Graphene
Graphene@Al
CCl4
CH4
NH3
CO2
N2
CO
NO2
CCl2F2
SO2
CF4
H2
N2O
Small gas molecules

(c)

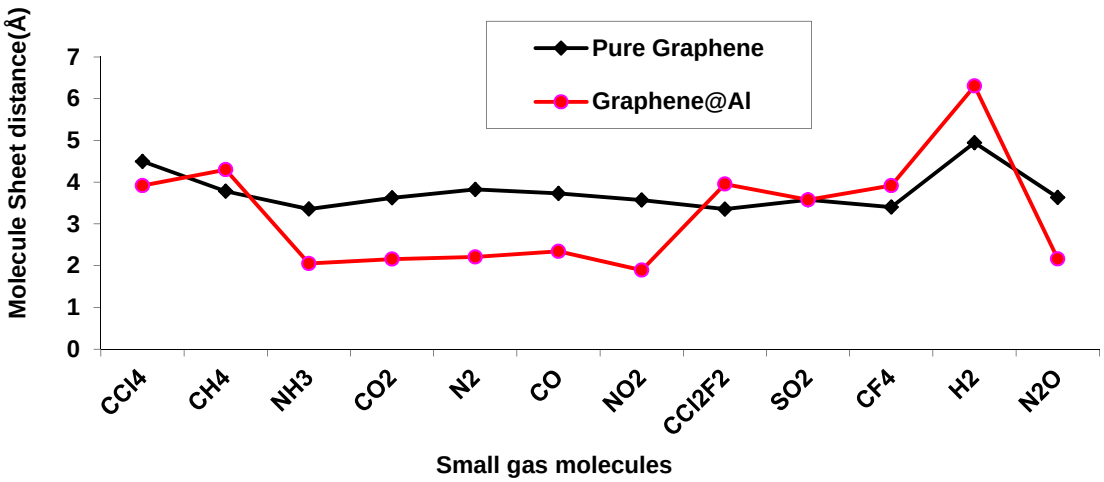
Molecule Sheet distance(Å)
7
6
5
4
3
2
1
0
Pure Graphene
Graphene@Al
CCl4
CH4
NH3
CO2
N2
CO
NO2
CCl2F2
SO2
CF4
H2
N2O
Small gas molecules

(d)

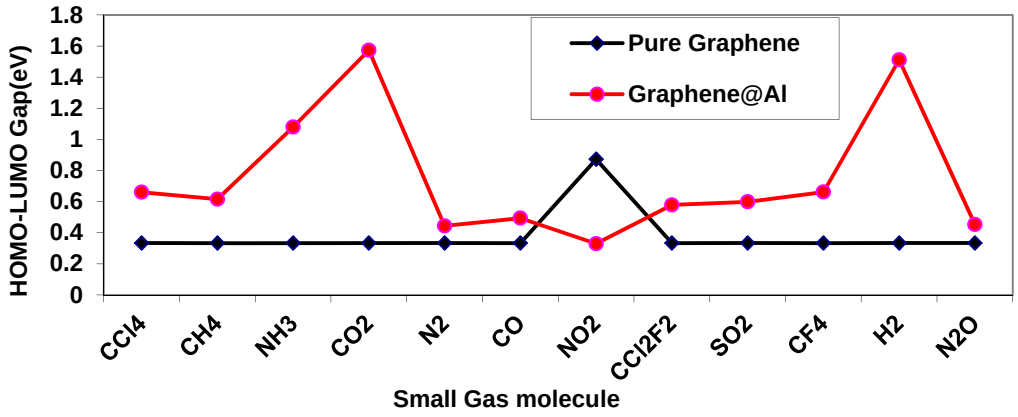

Figure 4.4: (a) The adsorption energy E_{ad}, (b) charge transfer, (c) molecule sheet distance and (d) HOMO-LUMO gap of small gas molecules with pure and Al-doped graphene complexes at the M06/-31++G** level of theory. The red line with solid red circles represents the variation for the aluminium doped graphene while the black line with black solid squares represent the variation for PG. The HOMO-LUMO gap for PG is 0.33 eV and for Al-dope graphene is 0.22 eV without any gas molecules.

4.4. Conclusion

The adsorption energy of various small gas molecules such as CCl_4, CH_4, NH_3, CO_2, CO, NO_2, CCl_2F_2, SO_2, CF_4 and N_2O with the PG and (graphene@Al) has been comprehensively analysed. These calculations reveal that the adsorption energy has preferences of small gas molecules with the doping in graphene as well as molecule sheet distance. It can be seen from the results that the adsorption energy of these gas molecule is higher for the Al-doped graphene than for the PG. PG shows weak sensitivity to the all

gas molecules. Compared with PG, graphene@Al has a higher chemical reactivity towards all gas molecules due to the doping of Al atom and shows the higher adsorption energy with NO_2, NH_3 and CO_2. The strong interactions between graphene@Al and the adsorbed molecules induces dramatic changes in the electronic properties of graphene@Al and make graphene@Al a promising candidates as gas sensing materials for NO_2, NH_3 and CO_2. The Mulliken charge analysis reveals that gas molecule acts as charge donor and acceptor in different configuration towards the pure and Al-doped graphene and influence the physical properties of carbon materials, which leads to the sensitivity. It has also been found that HOMO-LUMO gap of the carbon nanotube is always affected by the binding of the small gas molecules. Significant changes occur in the HOMO-LUMO gap on PG and graphene@Al on interacting with gas molecules, which provides a handle to tune the electronic and conductivity properties of graphene through gas molecule complexation. These studies can also be applied to develop new carbon based materials and sensing applications, focusing particularly on the mechanism of binding of various gas molecule with the graphene. It is hoped that our results would be helpful to develop novel carbon nano material based gas sensors.

4.5. References

1. Hirsch, A., *Nat. Mater* **2010**, *9*, 868.
2. Rao, C. N. R., Sood, A. K., Subrahmanyam, K. S. and Govindaraj, A., *Angew. Chem. Int. Ed.* **2009**, *48*, 7752.
3. Iijima, S., *Nature* **1991**, *354*, 56.
4. Liu, J., Cui, L. and Losic, D., *Acta Biomaterialia* **2013**, *9*, 9243.
5. Dinadayalane, T. C. and Leszcznski, J., *Struct. Chem*. **2010**, *21*, 1155.
6. Liang, F. and Chen, B., *Curr. Med. Chem.* **2010**, *17*, 10.
7. Zhu, Y., Murali, S., Cai, W., Li, X., Suk, J. W., Potts, J. R. and Ruoff, R. S., *Adv. Mater.* **2010**, *22*, 3906.
8. Goldoni, A., Larciprete, R., Petaccia, L. and Lizzit, S., *J. Am. Chem. Soc.* **2003**, *125*, 11329.
9. Guo, Z., Feng, Y., He, S., Qu, M., Chen, H., Liu, H., Wu, Y., and Wang, Y., *Adv. Materials* **2012**, *25*, 584.
10. Zhong, J., Chiou, J., Dong, C., Glans, P. A., Pong, W. F., Chang, C., Wu, Z. and Guo, J., *Appl. Phys. Lett.* **2012**, *100*, 201605.
11. Umadevi, D., Panigrahi, S. and Sastry, G. N., *Acc. Chem. Res.* **2014**, *47*, 2574.
12. Vijay, D. and Sastry, G. N., *Chem. Phys. Lett.* **2010**, *485*, 235.
13. Shi, G., Ding, Y. and Fang, H., *J. Comput. Chem.* **2012**, *33*, 1328.
14. Grabowski, S. J. and Lipkowski, P., *J. Phys. Chem. A* **2011**, *115*, 4765.
15. Mahadevi, A. S. and Sastry, G. N., *Chem. Rev.* **2016**, *116*, 2775.
16. Charlier, J. C., *Acc. Chem. Res.* **2002**, *35*, 1063.
17. Huang, P., Zhu, H., Jing, L., Zhao, Y. and Cao, X., *ACS Nano* **2011**, *5*, 7945.
18. Dougherty, D. A., *Science* **1996**, *271*, 163.
19. Kim, S. K., Hu, S., Tarakeshwar, P. and Lee, J. Y., *Chem. Rev.* **2000**, *100*, 4145.

20. Ready, A. S. and Sastry, G. N., *J. Phys. Chem. A.* **2005**, *109*, 8893.

21. Grabowski, S. J. and Lipkowski, P., *J. Phys. Chem. A* **2011**, *115*, 4765.

22. Schedin, F., Geim, A. K., Morozov, S. V., Hill, E. W., Blake, P., Katsnelson, M. I. and Novoselov, K. S., *Nat. Mater.* **2007**, *6*, 652.

23. Wang, X., Sun, G., Routh, P., Kim, D. H., Huang, and Wand P. Chen, *Chem. Soc. Rev.* **2014**, *43*, 7067.

24. Lherbier, A., Blasé, R. X., Niquet, Y., Triozon, F. and Roche, S., *Phys. Rev. Lett.* **2008**, *101*, 036808.

25. Lv, Y-a, Zhuang, G-l, Wang, J-g, Jia, Y-b and Xie, Q., *Phys. Chem. Chem. Phys.* **2011**, *13*, 12472.

26. Cho, B., Yoon, J., Hahm, M. G., Kim, D. H., Kim, A. R., Kahng, Y. H., Park, S. W., Lee, Y. J., Park, S. G., Kwon, J. D., Kim, C. S., Song, Jeong M. Y., Nam, K. S. and Ko H. C., *J. Mater. Chem.* **2014**, *2*, 5280.

27. Kong, J., Franklin, N., Zhou, C., Chapline, M., Peng, S., Cho, K. and Dai, H., *Science* **2000**, *287*, 622.

28. Schedin, F., Geim, A. K., Morozov, S. V., Hill, E. W., Blake, P., Katsnelson, M. I. and Novoselov, K. S., *Nature Mater.* **2007**, *6*, 652.

29. Umadevi, D. and Sastry, G. N., *J. Phys. Chem. C* **2011**, *115*, 9656.

30. Umadevi, D. and Sastry, G. N., *J. Phys. Chem. Lett.* **2011**, *2*, 1572.

31. Chen, W., Duan, L. and Zhu, D., *Environ. Sci. Technol.* **2007**, *41*, 8295.

32. Panigrahi, S., Bhattacharya, S., Banerjee, S. and Bhattacharyya, D., *J. Phys. Chem. C* **2012**, *116*, 4374.

33. Roman, T., Dino, W. A., Nakanishi, H. and Kasai, H., *Eur. Phys. J. D* **2006**, *38*, 117.

34. Kumar, A., Reddy, A. L. M., Mukherjee, A., Dubey, M., Zhan, X., Singh, N., Ci, L., Edward, W., John, N., Mital, G. and Ajayan, P. M., *ACS Nano* **2011**, *5*, 4345.

35. Reddy, A. L. M., Srivastav, A., Gowda, S. R., Gullapalli, H., Dubey, M. and Ajayan, P. M., *ACS Nano* **2010**, *4*, 6337.

36. Rao, J. S., Zipse, H. and Sastry, G. N., *J. Phys. Chem. B* **2009**, *113*, 7225.

37. Sharma, B., Rao, J. S. and Sastry, G. N., *J. Phys. Chem. A* **2011**, *115*, 1971.

38. Mahadevi, A. S. and Sastry, G. N., *J. Phys. Chem. B* **2011**, *115*, 703.

39. Umadevi, D. and Sastry, G. N., *Phys. Chem.Chem.Phys.* **2015**, 17, 30260.

40. Zhang, Y. H., Chen, Y. B., Zhou, K. C., Liu, C. H., Zeng, J., Zhang, H. L. and Peng, Y., *Nanotechnology* **2009**, *20*, 185504.

41. Zou, Y., Li, F., Zhu, Z. H., Zhao, M. W., Xu, X. G. and Su, X .Y., *Eur. Phys. B.* **2011**, *81*, 475.

42. Dai, J. Y. and Yuan, J. M., *Phys. Rev. B* **2010**, *81*, 165414.

43. Bai, L. and Zhou, Z., *Carbon* **2007**, *45*, 2105.

44. Charles, W., Bauschlicher, J. and Ricca, A., *Phys. Rev. B* **2004**, *70*, 115409.

45. Becke, A. D., *J. Chem. Phys.* **1993**, *98*, 5648.

46. Ditchfield, R., Hehre, W. J, and. Pople, J. A., *J. Chem. Phys.* **1971**, *54*, 724.

47. Frisch, M. J., Trucks, G. W., Schlegel, H. B., Scuseria, G. E., Robb, M. A., Cheeseman, J. R., Scalmani, G., Barone, V., Mennucci, B., Petersson, G. A., Nakatsuji, H., Caricato, M., Li, X., Hratchian, H. P., Izmaylov, A. F., Bloino, J., Zheng, G., Sonnenberg, J. L., Hada, M., Ehara, M., Toyota, K., Fukuda, R., Hasegawa, J., Ishida, M., Nakajima, T., Honda, Y., Kitao, O., Nakai, H., Vreven T., Montgomery, J. A. Jr., Peralta, J. E., Ogliaro, F., Bearpark, M., Heyd, J. J., Brothers, E., Kudin, K. N., Staroverov, V. N., Keith, T., Kobayashi, R., Normand, J., Raghavachari, K., Rendell, A., Burant, J. C., Iyengar, S. S., Tomasi, J., Cossi, Rega, M., N., Millam, J. M., Klene, M., Knox, J. E., Cross, J. B., Bakken, V., Adamo, C., Jaramillo, J., Gomperts, R., Stratmann, R. E., Yazyev, O., Austin, A. J., Cammi, R., Pomelli, C., Ochterski, J. W., Martin, R. L., Morokuma, K., Zakrzewski, V. G., Voth, G. A., Salvador, P., Dannenberg, J. J., Dapprich, S., Daniels, A. D., Farkas,

O., Foresman, J. B., Ortiz, J. V., Cioslowski, J., and Fox, D. J., Gaussian, Inc.,Wallingford CT, 2010.

48. Zhao, Y. and Truhlar, D. G., *Theor. Chem. Acc.* **2008**, *120,* 215.

49. Petersson, G. A., Bennett, A., Tensfeldt, T. G., Al-Laham, M. A, Shirley, W. A. and. Mantzaris, J., *J. Chem. Phys.***1988**, *89,* 2193.

50. Petersson, G. A. and Al-Laham, M. A., *J. Chem. Phys.* **1991**, *94,* 6081.

51. Frisch, M. J., Pople, J. A, and. Binkley, J. S., *J. Chem. Phys.* **1984**, *80,* 3265.

CHAPTER 5

INTERACTION OF ALKALINE EARTH METAL IONS WITH SINGLE WALLED CARBON NANOTUBE: A QUANTUM MECHANICAL STUDY

CHAPTER 5

INTERACTION OF ALKALINE EARTH METAL IONS WITH SINGLE WALLED CARBON NANOTUBE: A QUANTUM MECHANICAL STUDY

5.1. Introduction

Carbonaceous materials such as graphene and carbon nanotube are the promising class of materials for potential application as chemical and and bio-molecule sensors due to their unique physical and chemical properties. These exceptional electrical properties of graphene (such as, high charge mobility and capacity, highly tunable conductance) are used as an ideal sensing element in electronic sensors.[1-3]. The physical, chemical and electronic properties of carbon nanotubes(CNTs) largely depend on their chirality and curvature. The carbon atom forming the structure of CNTs has sp^2 hybridization. The CNTs are made by wrapping the graphene sheets in different ways. Carbon nanotube are classified into three types on the basis of their chirality (n,m) and curvature. m=0 defined as armchair CNT, n=m zigzag CNT and n≠m chiral CNT. Armchair (n, n) shows metallic behaviour, while zigzag (n,0) behaves as semiconductors. Chiral (n, m) nanotube exhibit metallic behaviour if the difference between n and m is a multiple of 3, otherwise, they behave as semiconductor.[4] Since the electronic properties depend upon the tube geometries; CNTs are found to be promosing materials for electronic devices in future.

Carbon nanostructures exhibit the cation-π, anion-π and non-covalent interaction towards the small molecules, metal ions and biomolecules such as amino acid, nucleic acids. The

cation-π interactions were extensively studied in recent years.[4-8] These interactions are very sensitive to the nature of metal ion and size of π-system.[9-13] Lee et al., have observed a conductivity enhancement in CNT bundles doped with K and Br and suggested that doped CNT can represent a new family of synthetic metals.[14] The study of non-covalent fuctionalization of carbonaceous materials play a vital role in understanding various CNSs, such as diagnosis of life threatening diseases (sensors), cancer therapy (drug delivery system), DNA sequencing (personalized medicines).[15-17] Developing sensors based on CNT and biomolecule composites for amplified detection methods is an area of recent interest, and such sensors can be efficiently used in the detection of various CNSs as well as different biomaterials such as DNA, protein, and so on.[18] CNSs can absorb a number of species such as gas molecule, metal ions, polymers, organic molecules, and biomolecules such as proteins, nucleobases and DNA on their surface and these adsorption properties provide opportunities for potential industrial applications.[19-22] Several studies have been carried out on the immobilisation of proteins and nucleic acid on nanotube.[23-25] However recent studies elaborate on the appreciable changes in nanotube conductivity as bio molecules which are immobilised, directly or indirectly, on the CNT sidewalls.[26-28] Roman et al., used DFT method to investigate the adsorption of few amino acids on CNT(3,3).[29] Wang et al., [30] carried out a study to understand the affinity of the specific peptides to CNTs and delineate contributions of the constituents amino acids to the binding strength of the peptides with CNTs. Further the studies on the structure-function-affinity of the peptides with the CNT have shown that phenylalanine has an important role to play in enhancement of the adsorption of peptides on the CNTs.[31] Li et al., demonstrated that

polytryptophan peptides bind more strongly through their aromatic rings with the CNTs compared to the polylysine.[32] However, the nature of interaction of these bio molecules with the CNTs and the extent to which the nanotube can be used as functionalization is not understood much in these biological systems. Other studies on the adsorption of polynuclear aromatic compounds to CNTs, suggest that the π-π interactions can play a critical role in the binding strength towards the nanotube.[33-34] Dai and co-workers have investigated the potential of carbon nanotube to be used as gas sensors for detection of molecules such as NO_2 and NH_3.[35] Schedin et al., reported their experimental observation that graphene – based sensors could detect even the adsorption of individual gas molecules.[36] CNTs have also been found to be suitable candidate for the negative electrode of the Li-ion batteries, where the Li diffuse between the positive and negative in the ionic state.[37-38] Thus the fundamental understanding of the interaction of metals with CNTs in the ionic state is important. It is also important to know the role of various factors such as solvent and other chemical environment which influence such cation-π interactions.[39-41] Umadevi et. al. have been found that the charge transfer between graphane and different molecules and ions is an important factor in determining the binding strength of the complexes.[42] In the current study, first systematic study of a series of di-cationic alkaline earth metal ions (Be^{+2}, Mg^{+2}, Ca^{+2}) inside the single walled carbon nanotube [CNT (10, 0)] at different position has been performed. The effect of binding strength of metal ions at different positions inside the carbon nanotube is explored. The charge transfer during the complex formation and the change in the HOMO-LUMO gap are explored, which provide valuable information in tuning the

electronic and conductivity properties through metal ions complexation with single walled carbon nanotube.

5.2. Computational Details

The calculations of the interaction between CNT and metal ions carried out using the developed density functional theory. The geometrical calculations of all structures have been done by using DFT method B3LYP/6-31G*. In this study, the geometries of alkaline earth metal ions (Ca^{+2}, Mg^{+2}, Be^{+2}) with single walled carbon nanotube (SWCNT) were optimized. Thereafter, the individual metal ions are made to pass through the middle position of CNT and the charge variation of the individual metal ions as well as on SWCNT [CNT (10, 0)] are carried out at each inner point of complexed system. It is important to note that competing geometrical configuration were tested but those shown are the lowest energy species feasible for the interaction of the compounds. The variation of the charge on alkaline earth metal ions as well as single walled carbon nanotube when the metal ions are going gradually inside the CNT (10, 0) was calculated. The charge transfer has been considered as the sum of the all atoms/ions and SWCNT. Positive charge transfer values indicate the transfer of charge from SWCNT to the metal ions; negative charge transfer values indicate the transfer of charge from the metal ions to the SWCNT. The single point energy and HOMO-LUMO gap by using B3LYP/6-31++G** and M06/6-31++G** level of theory was performed. All calculations were carried out using the Gassian09 program package.[43]

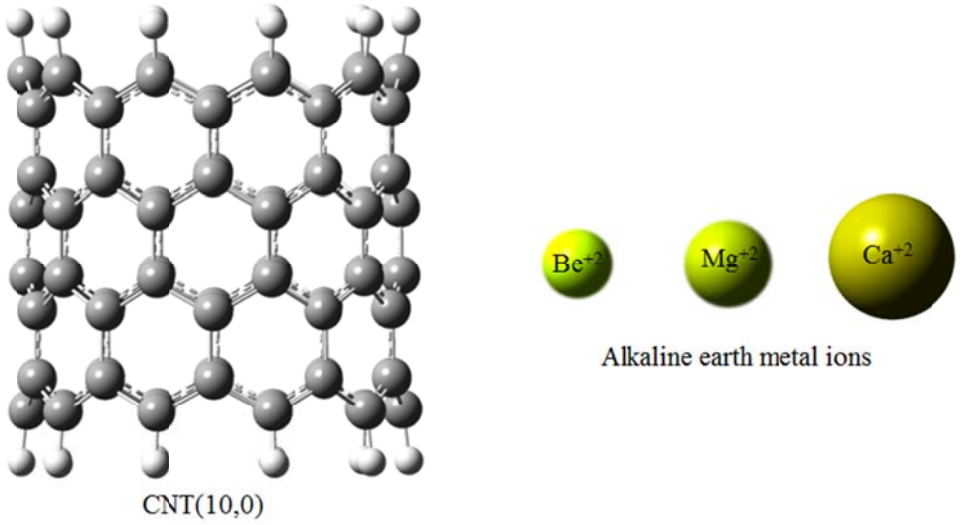

Figure 5.1: The model system of single carbon nanotube [CNT (10, 0)] and alkaline earth ions (Ca^{+2}, Mg^{+2}, Be^{+2}) before interaction.

5.3. Results and discussions

The optimized structures of alkaline metal ions and complex structure are shown in Figure 5.1, 5.2 and 5.3 respectively. A wide range of model system representing single walled carbon nanotube was considered to study the interaction of alkaline earth metals ions with cation-π surface towards carbon nanotube. For instance, the Figure 5.2 and Figure 5.3 shows that the di-cationic alkaline earth metal ions interact at different positions. In this section, at the outset we discuss the orientation of the metal ions on the SWCNT in the optimized structure. Subsequently, we look at the interaction energy of the carbon nanotube with various metal ions and the trends in the charge transfer for all the complexed. It also investigated the HOMO-LUMO gap of SWCNT during the charge transfer at every position of doped metal ions.

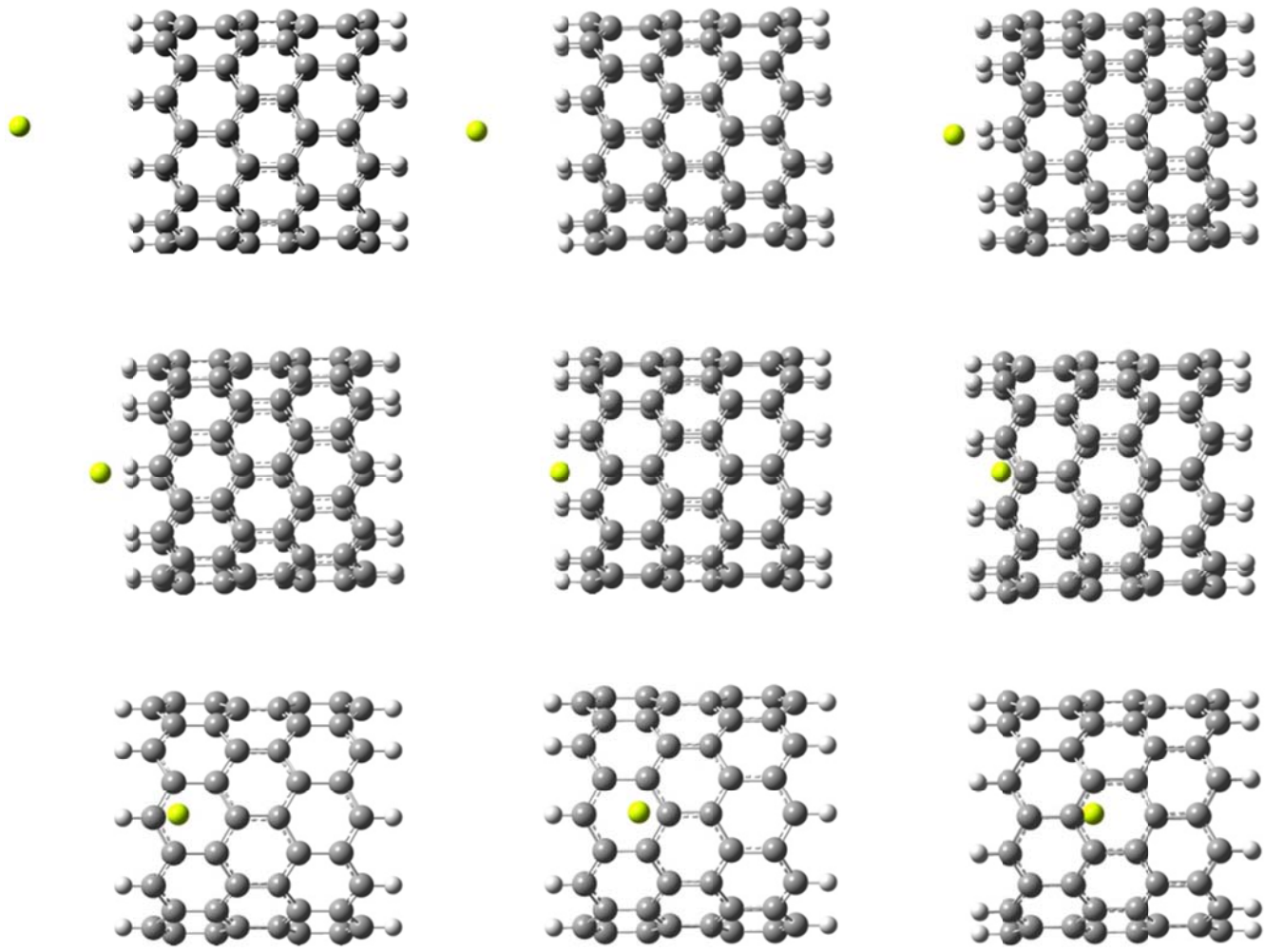

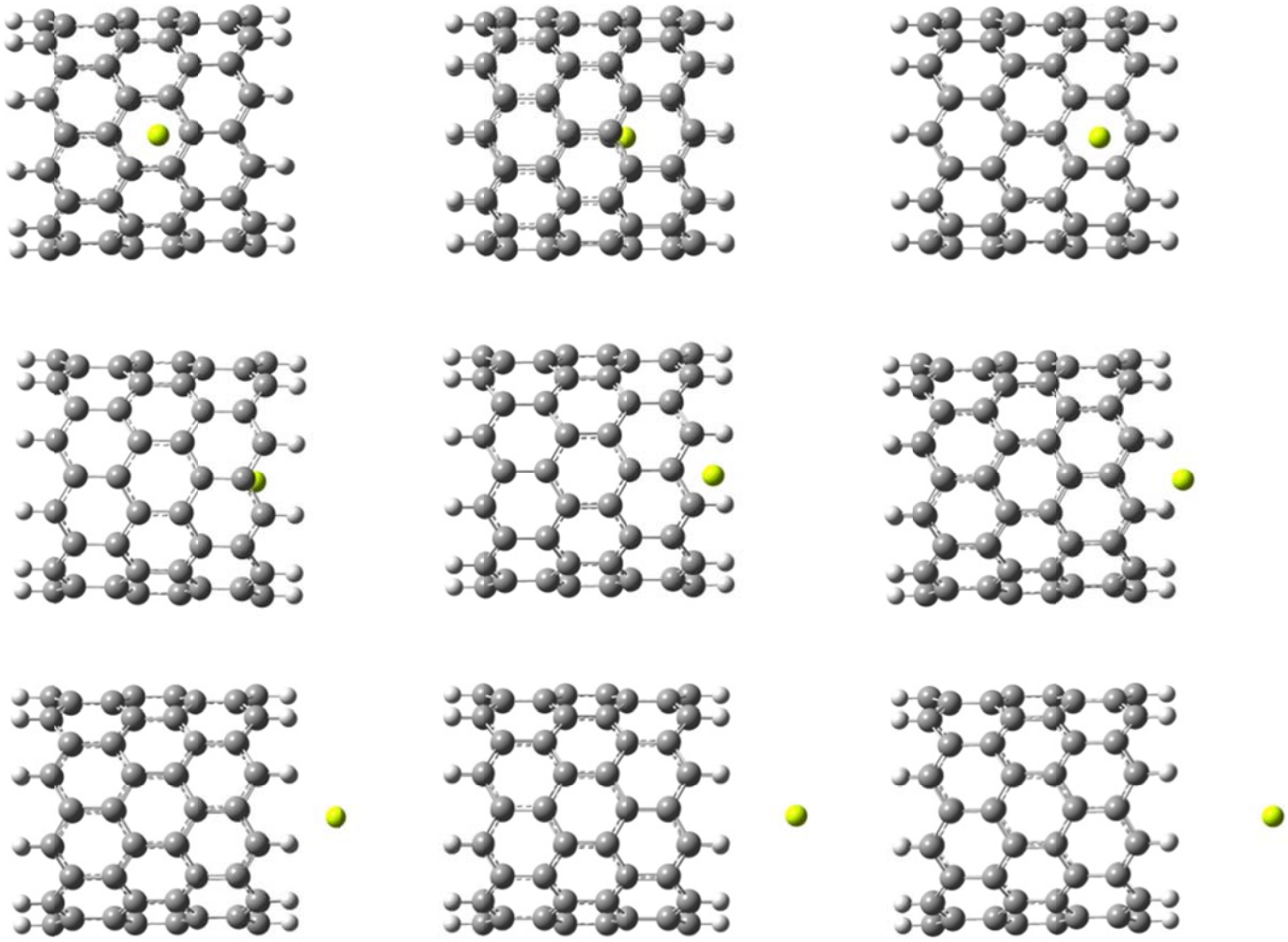

Figure 5.2(a): Optimized geometries of the complexes CNT(10,0) with alkaline earth metal ions (Be^{+2}, Mg^{+2}, Ca^{+2}) by B3LYP/6-31++G** method.

Table 5.1: Calculated interaction energy(ΔE) of complex molecular system, charge on alkaline earth metal ion (Be^{+2}) and carbon nanotube and HOMO-LUMO Energy Gap using B3LYP method and 6-31++G** basis set.

Alkaline Earth metal ion	Different stages of CNT(10,0)	Total energy (kcal/mol)	$\Delta E=E_0-E$ (kcal/mol)	Charge on Earth metal ions (au)	Charge on CNT (au)	HOMO-LUMO Energy Gap (eV)
Be^{+2}	1	-1929464.49	0	-0.01	2.01	0.65
	2	-1929464.52	0.03	-0.01	2.01	0.65
	3	-1929464.13	-0.36	0.01	1.99	0.65
	4	-1929462.77	-1.72	0.07	1.93	0.64
	5	-1929461.16	-3.33	0.09	1.91	0.62
	6	-1929460.46	-4.03	-0.02	2.02	0.62
	7	-1929460.61	-3.88	-0.09	2.09	0.62
	8	-1929461.54	-2.95	-0.12	2.12	0.64
	9	-1929462	-2.49	-0.18	2.18	0.65
	10	-1929462.19	-2.3	-0.20	2.20	0.65
	11	-1929461.79	-2.7	-0.15	2.15	0.64
	12	-1929460.86	-3.63	-0.09	2.09	0.62
	13	-1929460.49	-4.00	-0.08	2.08	0.62
	14	-1929460.81	-3.68	0.05	1.95	0.62
	15	-1929461.89	-2.6	0.09	1.91	0.62
	16	-1929463.37	-1.12	0.04	1.96	0.64
	17	-1929464.39	-0.1	0.00	2.00	0.65
	18	-1929464.54	0.05	-0.01	2.01	0.65

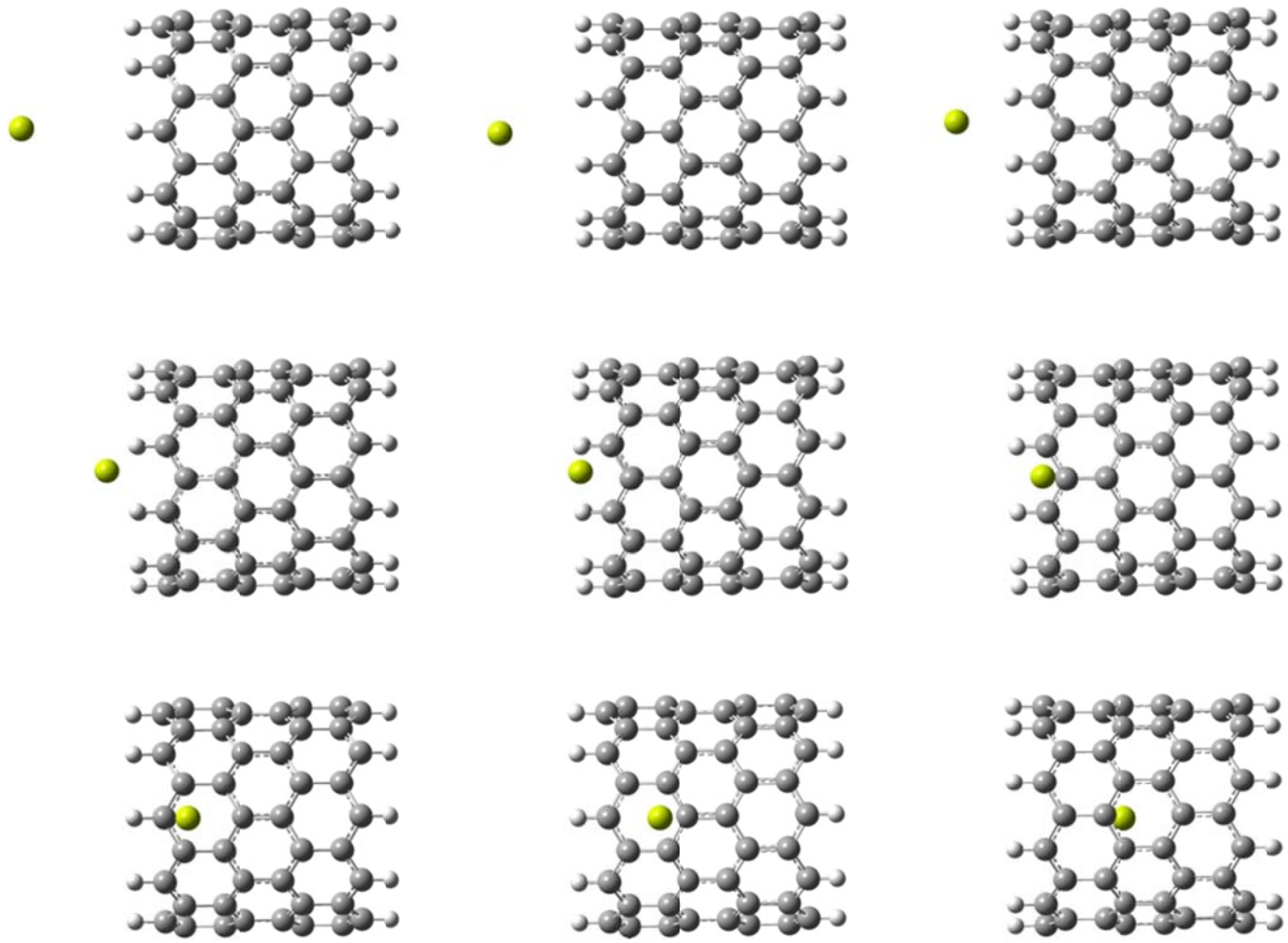

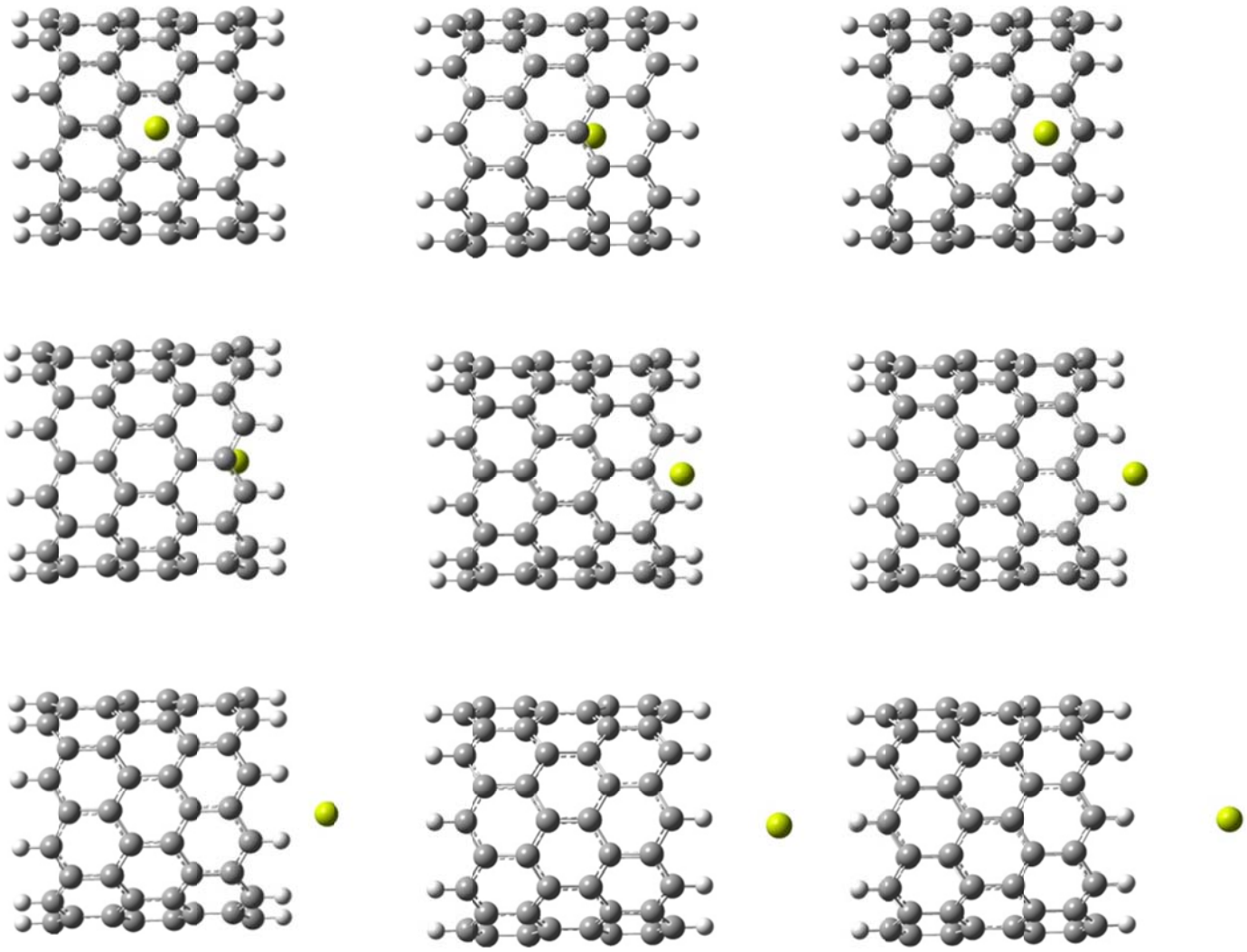

Figure 5.2(b): Optimized geometries of the complexes CNT(10,0) with alkaline earth metal ion (Mg^{+2}) by B3LYP/6-31++G** method.

Table 5.2: Calculated interaction energy(ΔE) of complex molecular system, charge on alkaline earth metal ion (Mg^{+2}) and carbon nanotube and HOMO-LUMO Energy Gap using B3LYP method and 6-31++G** basis set.

Alkaline Earth metal ion	Different stages of CNT(10,0)	Total energy (kcal/mol)	$\Delta E=E_0-E$ (kcal/mol)	Charge on Earth metal ions(au)	Charge on CNT (au)	HOMO-LUMO Gap (eV)
Mg^{+2}	1	-2045808.84	0.00	0.03	1.97	0.44
	2	-2045808.79	-0.05	0.07	1.93	0.65
	3	-2045808.05	-0.79	0.12	1.88	0.65
	4	-2045805.97	-2.87	0.12	1.88	0.64
	5	-2045803.15	-5.69	0.08	1.92	0.62
	6	-2045801.37	-7.46	-0.01	2.01	0.62
	7	-2045801.32	-7.52	0.02	1.98	0.62
	8	-2045802.49	-6.35	0.11	1.89	0.64
	9	-2045803.08	-5.76	0.17	1.83	0.65
	10	-2045803.32	-5.52	0.18	1.82	0.65
	11	-2045802.82	-6.02	0.15	1.85	0.64
	12	-2045801.76	-7.08	0.06	1.94	0.62
	13	-2045801.25	-7.59	-0.01	2.01	0.62
	14	-2045802.36	-6.48	0.04	1.96	0.62
	15	-2045804.61	-4.23	0.11	1.89	0.62
	16	-2045807.07	-1.77	0.12	1.88	0.64
	17	-2045808.54	-0.30	0.09	1.91	0.65
	18	-2045808.88	0.04	0.04	1.96	0.62

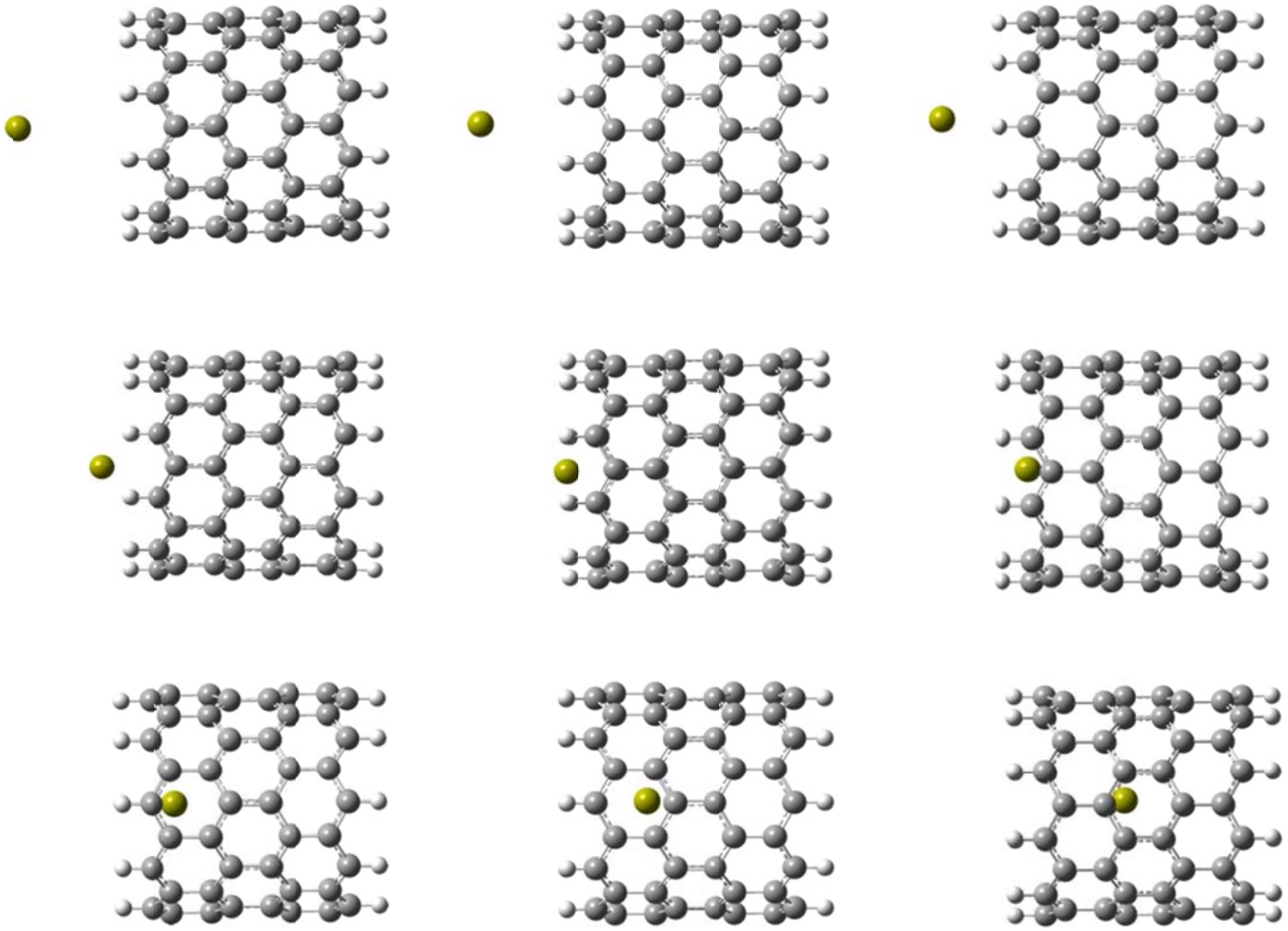

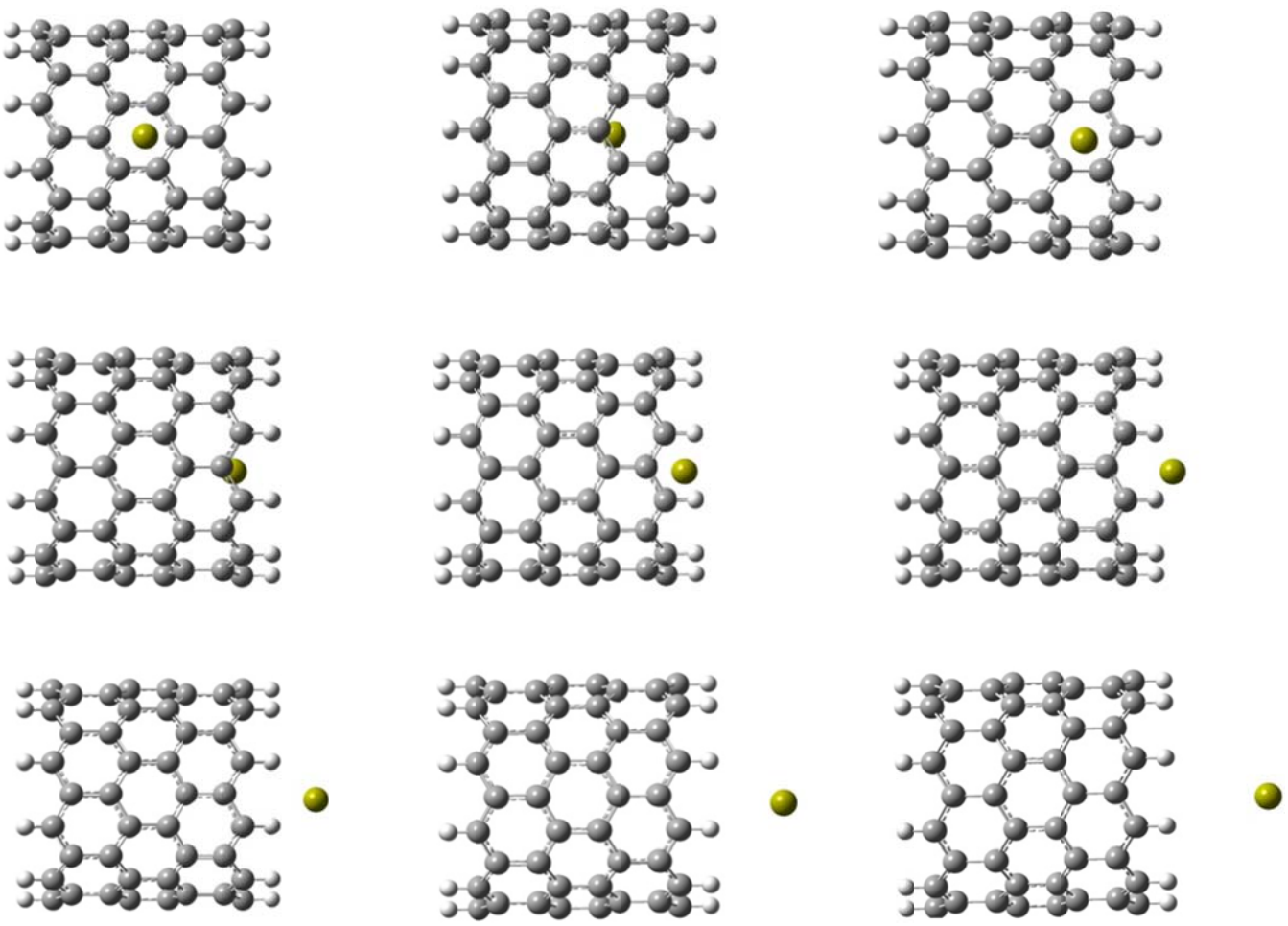

Figure 5.2(c): Optimized geometries of the complexes CNT(10,0) with alkaline earth metal ion (Ca^{+2}) by B3LYP/6-31++G** method.

Table 5.3: Calculated interaction energy(ΔE) of complex molecular system, charge on alkaline earth metal ion (Ca^{+2}) and carbon nanotube and HOMO-LUMO Energy Gap using B3LYP method and 6-31++G** basis set.

Alkaline Earth metal ion	Different stages of CNT(10,0)	Total energy (kcal/mol)	$\Delta E=E_0-E$ (kcal/mol)	Charge on Earth metal ions(au)	Charge on CNT(au)	HOMO-LUMO Gap (eV)
Ca^{+2}	1	-2345419.70	0.00	0.33	1.67	0.41
	2	-2345417.82	-1.88	0.28	1.72	0.47
	3	-2345415.23	-4.47	0.25	1.75	0.54
	4	-2345411.62	-8.08	0.37	1.63	0.60
	5	-2345409.55	-10.15	0.53	1.47	0.65
	6	-2345409.80	-9.90	0.45	1.55	0.64
	7	-2345409.31	-10.39	0.19	1.81	0.60
	8	-2345408.48	-11.22	0.06	1.94	0.55
	9	-2345407.93	-11.77	-0.02	2.02	0.53
	10	-2345407.73	-11.97	-0.03	2.03	0.54
	11	-2345408.12	-11.58	0.02	1.98	0.53
	12	-2345408.68	-11.02	0.12	1.88	0.58
	13	-2345409.64	-10.06	0.32	1.68	0.63
	14	-2345409.55	-10.15	0.53	1.47	0.66
	15	-2345410.28	-9.42	0.45	1.55	0.63
	16	-2345413.53	-6.17	0.28	1.72	0.57
	17	-2345416.76	-2.94	0.26	1.74	0.50
	18	-2345418.93	-0.77	0.30	1.70	0.43

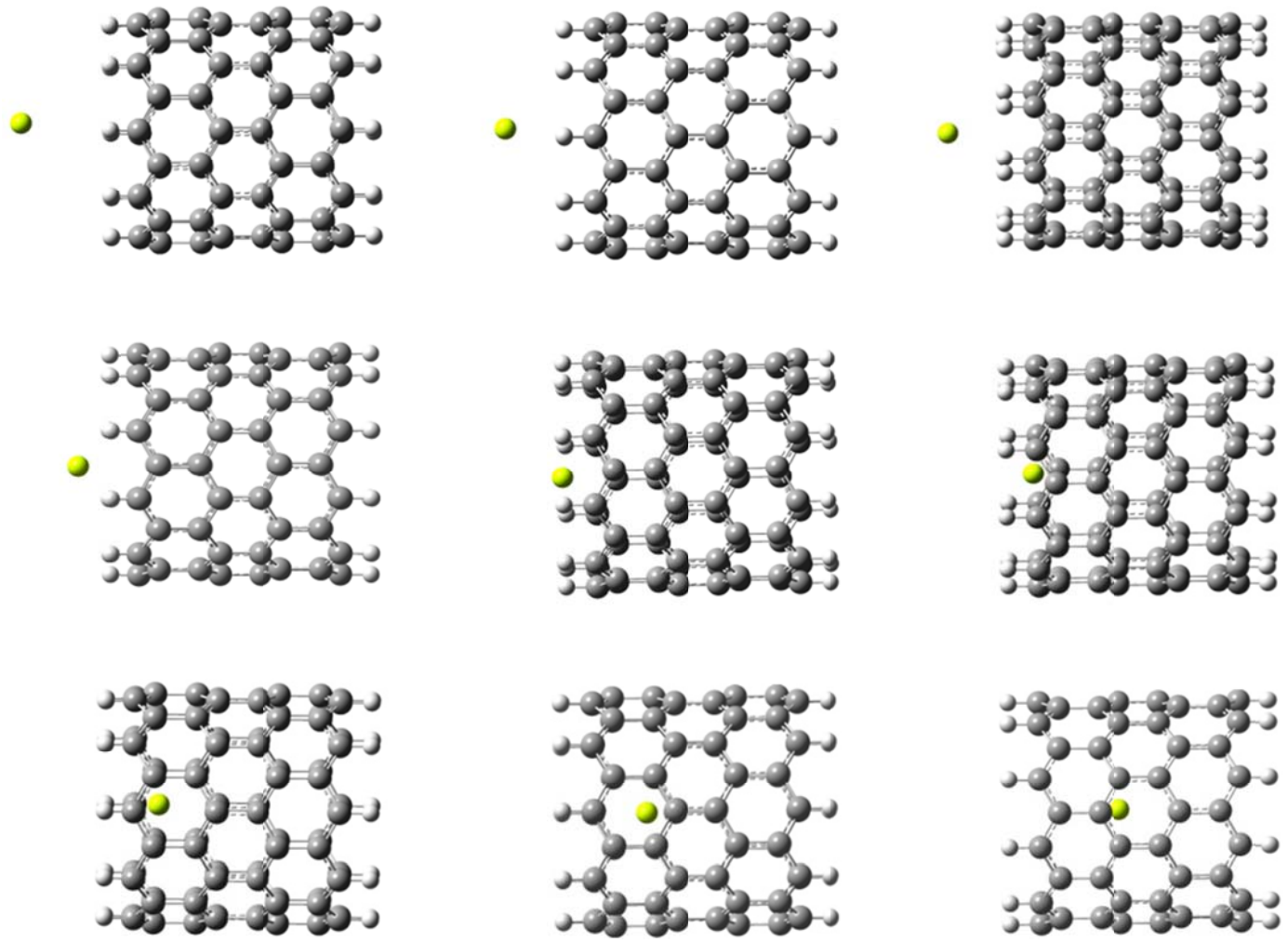

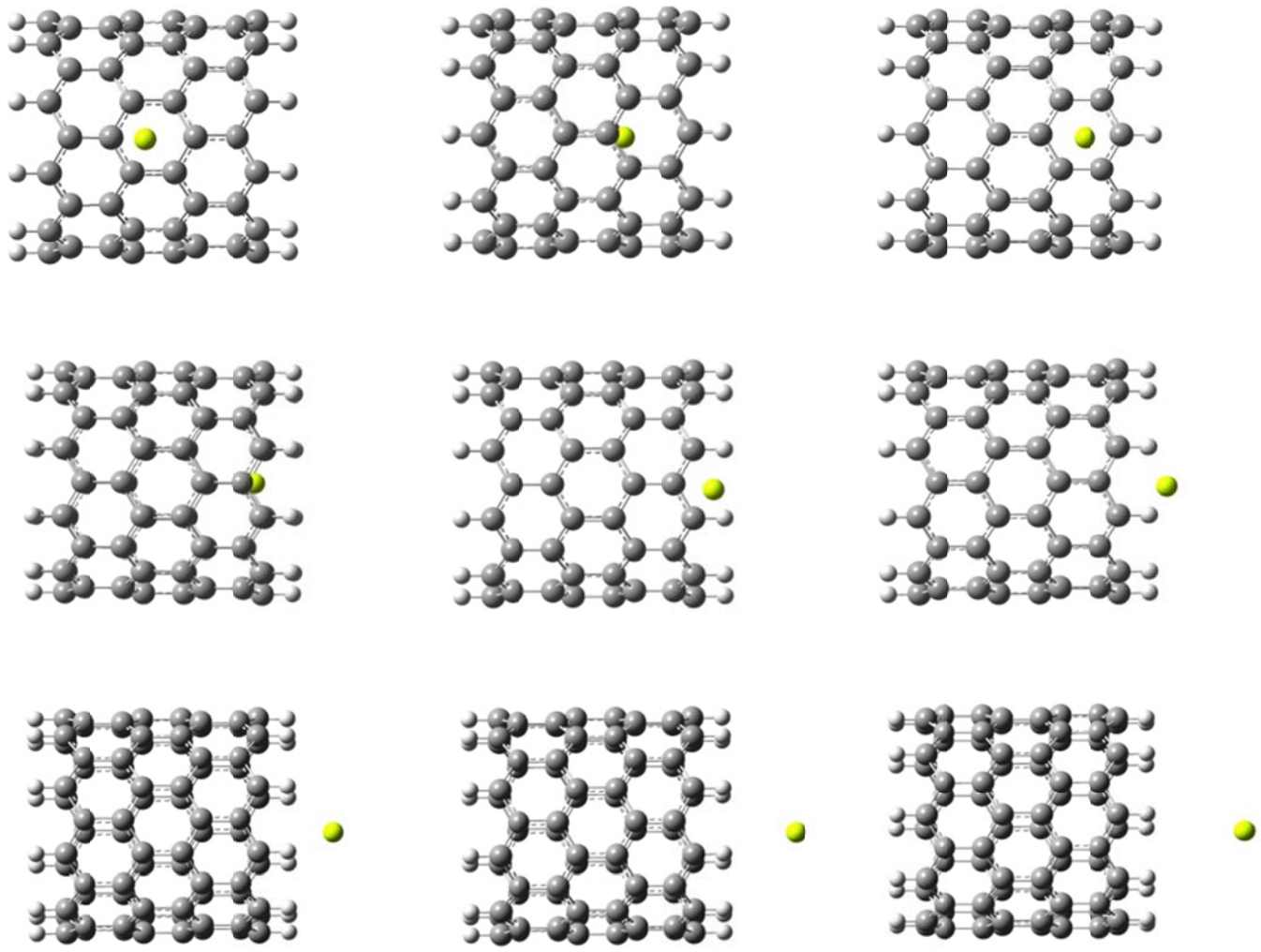

Figure 5.3(a): Optimized geometries of the complexes CNT(10,0) with alkaline earth metal ion (Be^{+2}) by M06/6-31++G** method.

Table 5.4: Calculated interaction energy(ΔE) of complex molecular system, charge on alkaline earth metal ion (Be^{+2}) and carbon nanotube and HOMO-LUMO Energy Gap using M06 method and 6-31++G** basis set.

Alkaline Earth metal ion	Different stages of CNT(10,0)	Total energy (kcal/mol)	$\Delta E=E_0-E$ (kcal/mol)	Charge on Earth metal ions(au)	Charge on CNT(au)	HOMO-LUMO Gap (eV)
Be^{+2}	1	-1928037.53	0.00	0.01	1.99	0.86
	2	-1928038.12	0.59	0.02	1.98	0.86
	3	-1928039.10	1.58	0.04	1.96	0.86
	4	-1928040.36	2.84	0.13	1.87	0.85
	5	-1928041.78	4.25	0.11	1.89	0.83
	6	-1928045.09	7.56	-0.01	2.01	0.83
	7	-1928046.90	9.38	-0.23	2.23	0.83
	8	-1928049.52	12.00	-0.31	2.31	0.84
	9	-1928051.07	13.55	-0.41	2.41	0.86
	10	-1928050.56	13.03	-0.49	2.49	0.86
	11	-1928050.70	13.17	-0.33	2.33	0.85
	12	-1928047.54	10.02	-0.29	2.29	0.83
	13	-1928046.22	8.70	-0.12	2.12	0.83
	14	-1928043.22	5.69	0.05	1.95	0.83
	15	-1928040.79	3.26	0.14	1.86	0.83
	16	-1928039.32	1.79	0.07	1.93	0.85
	17	-1928038.40	0.88	0.02	1.98	0.86
	18	-1928037.76	0.23	0.01	1.99	0.86

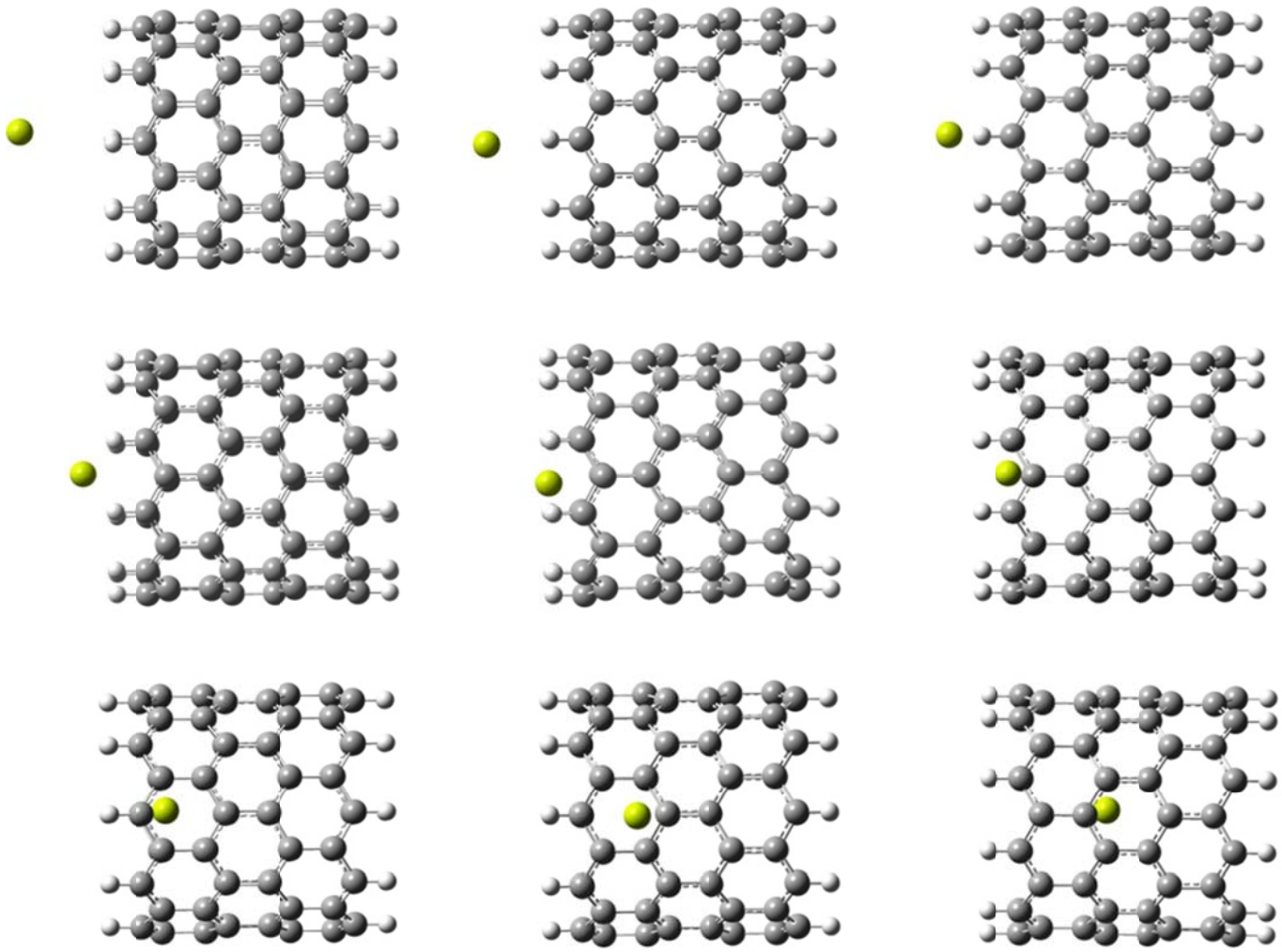

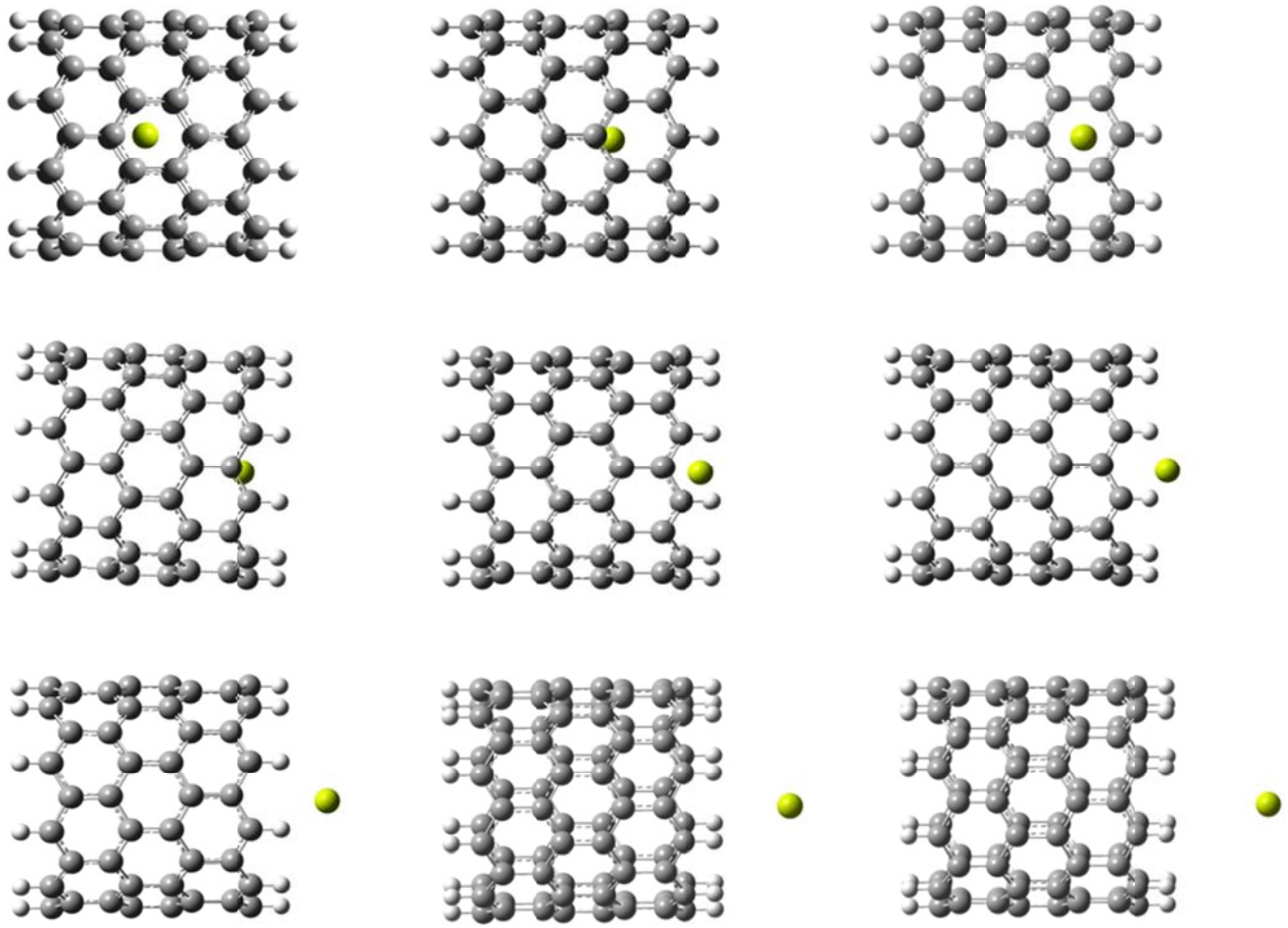

Figure 5.3(b): Optimized geometries of the complexes CNT(10,0) with alkaline earth metal ion (Mg^{+2}) by M06/6-31++G** method.

Table 5.5: Calculated interaction energy(ΔE) of complex molecular system, charge on alkaline earth metal ion (Mg^{+2}) and carbon nanotube and HOMO-LUMO Energy Gap using M06 method and 6-31++G** basis set.

Alkaline Earth metal ion	Different stages of CNT(10,0)	Total energy (kcal/mol)	$\Delta E=E_0-E$ (kcal/mol)	Charge on Earth metal ions(au)	Charge on CNT(au)	HOMO-LUMO Gap (eV)
Mg^{+2}	1	-2044367.65	0.00	0.044	1.99	0.86
	2	-2044368.61	0.96	0.070	1.98	0.86
	3	-2044370.03	2.38	0.072	1.96	0.86
	4	-2044371.21	3.56	0.110	1.87	0.85
	5	-2044372.25	4.60	0.030	1.89	0.83
	6	-2044375.31	7.66	0.035	2.01	0.83
	7	-2044376.91	9.26	-0.050	2.23	0.83
	8	-2044380.19	12.54	0.008	2.31	0.84
	9	-2044382.11	14.46	-0.020	2.41	0.86
	10	-2044381.97	14.32	-0.049	2.49	0.86
	11	-2044381.53	13.88	0.018	2.33	0.85
	12	-2044378.01	10.36	-0.032	2.29	0.83
	13	-2044376.26	8.61	-0.001	2.001	0.83
	14	-2044373.83	6.18	-0.001	1.95	0.83
	15	-2044371.44	3.79	0.085	1.86	0.83
	16	-2044370.45	2.80	0.082	1.93	0.85
	17	-2044369.15	1.50	0.071	1.98	0.86
	18	-2044368.06	0.41	0.058	1.99	0.86

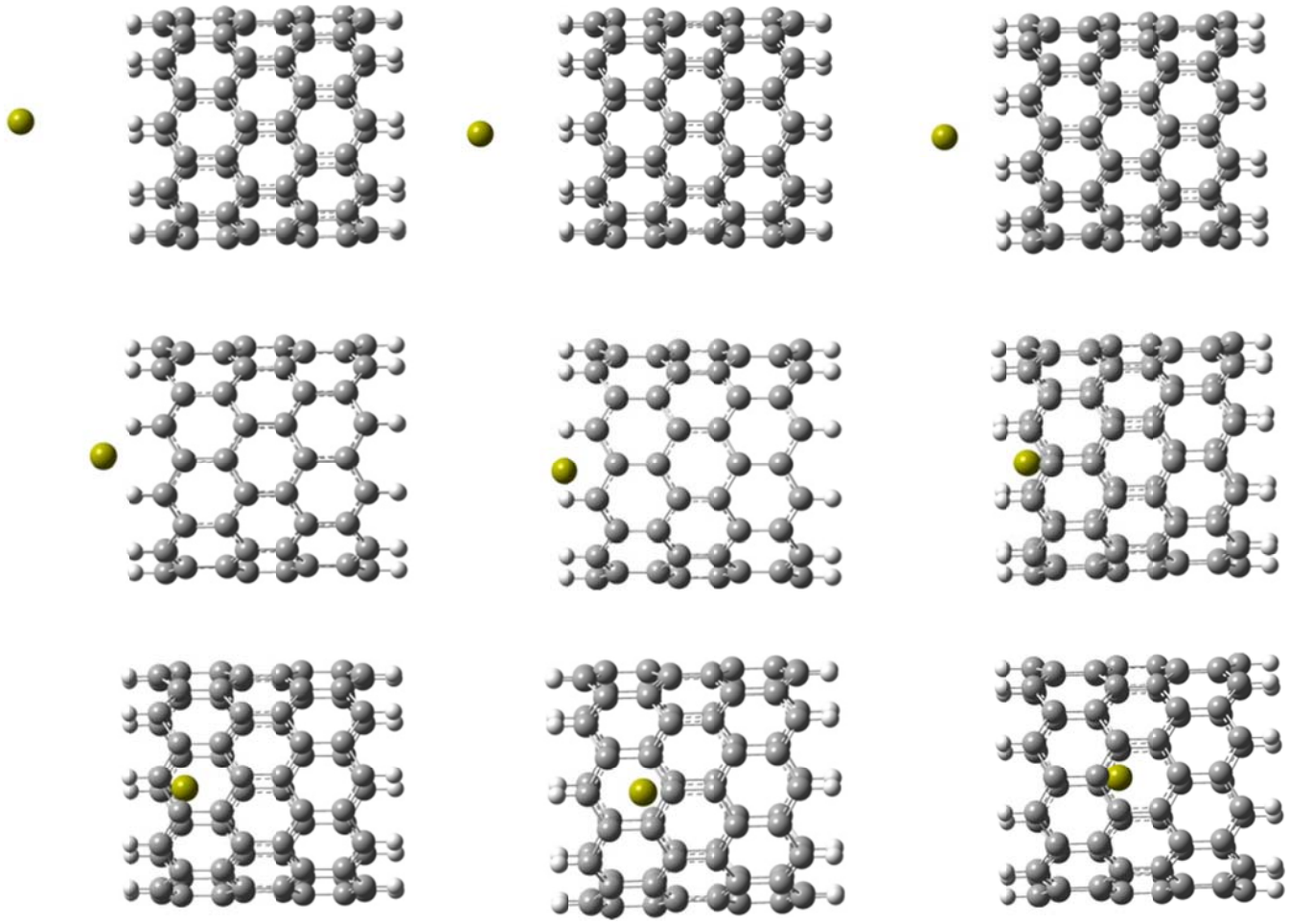

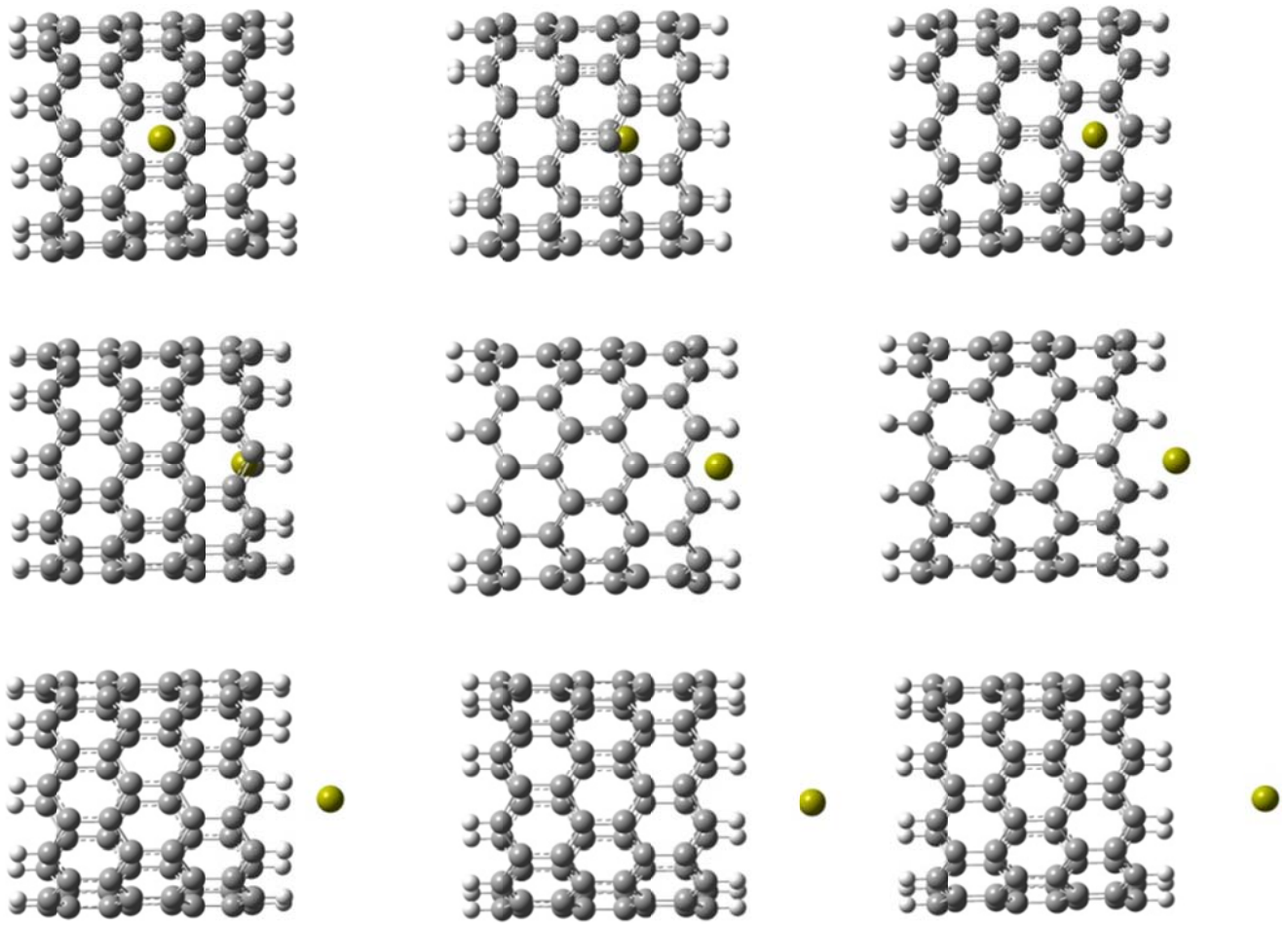

Figure 5.3(c): Optimized geometries of the complexes CNT(10,0) with alkaline earth metal ion (Ca^{+2}) by M06/6-31++G** method.

Table 5.6: Calculated interaction energy(ΔE) of complex molecular system, charge on alkaline earth metal ion (Ca^{+2}) and carbon nanotube and HOMO-LUMO Energy Gap using M06 method and 6-31++G** basis set.

Alkaline Earth metal ion	Different stages of CNT(10,0)	Total energy (kcal/mol)	$\Delta E=E_0-E$ (kcal/mol)	Charge on Earth metal ions(au)	Charge on CNT(au)	HOMO-LUMO Energy Gap (eV)
Ca^{+2}	1	-2343977.37	0.00	0.34	1.66	0.56
	2	-2343977.30	-0.07	0.32	1.68	0.65
	3	-2343978.03	0.66	0.25	1.75	0.75
	4	-2343978.91	1.54	0.33	1.67	0.84
	5	-2343982.34	4.97	0.45	1.55	0.86
	6	-2343987.40	10.03	0.35	1.65	0.88
	7	-2343989.15	11.78	0.00	2.00	0.86
	8	-2343991.16	13.79	-0.12	2.12	0.79
	9	-2343992.28	14.91	-0.29	2.29	0.73
	10	-2343992.38	15.01	-0.34	2.34	0.73
	11	-2343991.80	14.43	-0.20	2.20	0.76
	12	-2343989.87	12.50	-0.06	2.06	0.84
	13	-2343988.47	11.10	0.16	1.84	0.88
	14	-2343984.93	7.56	0.47	1.53	0.87
	15	-2343979.92	2.55	0.34	1.66	0.85
	16	-2343978.24	0.87	0.27	1.73	0.79
	17	-2343977.55	0.18	0.29	1.71	0.69
	18	-2343977.24	-0.13	0.33	1.67	0.60

5.3.1. The interaction energy and charge transfer analysis

The alkaline earth metal ions form cation-π type complexes with the CNT. The interaction energy of metal ions complexes with single walled carbon nanotube when the metal ion passes through from one end to another end of single walled carbon nanotube. Figure 5.2 and Table 5.1 displays the interaction energy of the metal ions complexes with SWCNT at B3LYP/6-31++G** level. It is clear from the Figure 5.2 and Table 5.1 that the interaction energy of alkaline earth metal ions complexes is better at the interior position than both ends of SWCNT. Interestingly, it observed a different trend in the case of metal ions where a strong binding strength is observed when the metal ions are passing in the middle of the SWCNT as compared to other positions. The order of the interaction energy of alkaline metal ions complexes is Ca^{+2} >Mg^{+2}>Be^{+2} with zig-zag single walled carbon nanotube [CNT (10,0)] at B3LYP/6-31++G** level. Figure 5.3 and Table 5.2 shows that the interaction energy of the same alkaline earth metal ions complexes with single walled carbon nanotube at the M06/6-31++G**. Consequently, we observed that the metal ions complexes such as Mg^{+2} and Be^{+2} have strong binding strength at particular position with single walled carbon nanotube. Interestingly, it is observed that a different trend in the case of metal ions where a strong binding strength is observed in interior as compared to the outside of SWCNT. The order of the interaction energy of alkaline metal ions complexes is Be^{+2} > Mg^{+2}> Ca^{+2} with zigzag single walled carbon nanotube [CNT (10, 0)] at M06/6-31++G** level. According to the B3LYP/6-31++G** method the interaction energy (ΔE) of metal ions varies from 0 to -11.97 Kcal/mol but according to M06/6-31++G** the interaction energy (ΔE) of metal ions varies from 0 to 15.01Kcal/mol. The more positive interaction energy indicates the metal ions repels the

six membered ring of CNT(12,0). Due to this, the alkaline earth metal ions shows the weak interactions towards the CNT(12,0). So it can observed that the alkaline earth metal ions exhibit strong binding strength when the metal ions situated inside the SWCNT at B3LYP/6-31++G** level of theory.

In order to gauge the mechanics of these foregoing binding interactions, the Mulliken charge transfer analysis at B3LYP/6-31++G**{ Figure 5.5 and Table 5.1} and M06/6-31++G**{Figure 5.5 and Table 5.2} have done. Charge transfer is a phenomenon in which a large fraction of an electronic charge is transferred from one entity (charge donor) to another (charge acceptor). As result of the charge transfer electronic structure of the sensor materials will be affected, thus leading to changes in their electronic properties. The negative charge values on the alkaline metal ions in the optimized complexes clearly point out that these metal ions act as charge acceptors from the carbon nanotube. It is clear from Table 5.1-5.3 that the charge on CNT(10, 0) varies with alkaline earth metal ions complexes. After the interaction with single CNT(10, 0) within B3LYP/6-31++G** level, the net partial negative charge on the Be^{+2}, Mg^{+2} and Ca^{+2} are -0.20, -0.01 and -0.04au respectively.These are the highest charge transfer to the metal ions from the carbon nanotube. The low interaction energy and small charge transfer indicats weak physisorption. In this way the carbon nanotube becomes positively charged at similar position which are shown in Table1 and Figure 5.5(a), 5.5(b) and 5.5(c). On the other hand within M06/6-31++G** level the net partial negative charge on the Be^{+2}, Mg^{+2}, and Ca^{+2} is -0.49, -0.05 and -0.34 au respectively. It is also noted from Table (5.1-5.3) and Figure 5.5 (a, b and c) that for both methods, the Mg^{+2} metal ions is obtained with less negative charge than Be^{+2} and Ca^{+2}. In the line of observation in the case of

interaction energy, the extend of charge transfer from CNT(10,0) to the alkaline metal ions is dependent of the orientation of metal ions whereas charge transfer is more in the interior than the exterior position of SWCNT. Consequently, a comparative study between the two density functional method i.e. B3LYP and M06 shows that the B3LYP/6-31++G** method gives better accuracy than the M06/6-31++G** method for metal ions complexes with zigzag SWCNT [CNT (10, 0)].

5.3.2. HOMO-LUMO Gap

The material has to undergo through a change in its physical properties on interacting with analyte if it has to perform as a sensor. These changes can be observed and recorded to confirm the presence of the analyte. The primary requisite for a material to perform as a sensor is to undergo a change in its physical property on interacting with an analyte. Such changes can be monitored and recorded to determine the presence of the analyte. The HOMO-LUMO gap is the difference between lowest unoccupied molecular orbital and highest occupied molecular orbital. This is the electronic properties of any molecular system which is helpful to design new materials. In order to notice such depiction in the case of carbon materials, the HOMO-LUMO gap of the CNT (10,0) in the free state and in the alkaline metal ions complexed is calculated. In general, in the case of cation-π complexes, the HOMO-LUMO gap of SWCNT varies with position of alkaline earth metal ions inside the carbon nanotube. It has been shown that the energy gap of CNT decreases when the metal ion such as Ca^{+2} is inside of SWCNT. On the other hand the energy gap of CNT increases when the metal ions such as Be^{+2}, Mg^{+2} is inside SWCNT.

So it can be concluded that the variation in HOMO-LUMO gap of the carbon nanotube upon binding with the alkaline metal ions is significant.

(a)

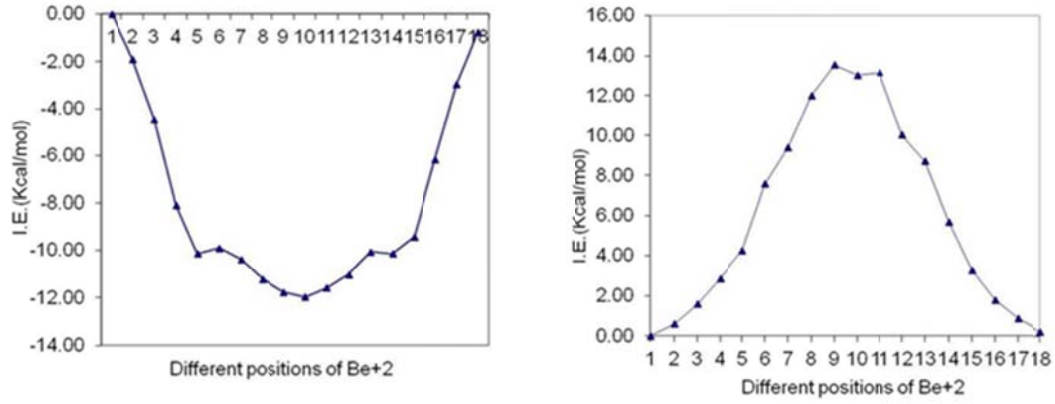

(b)

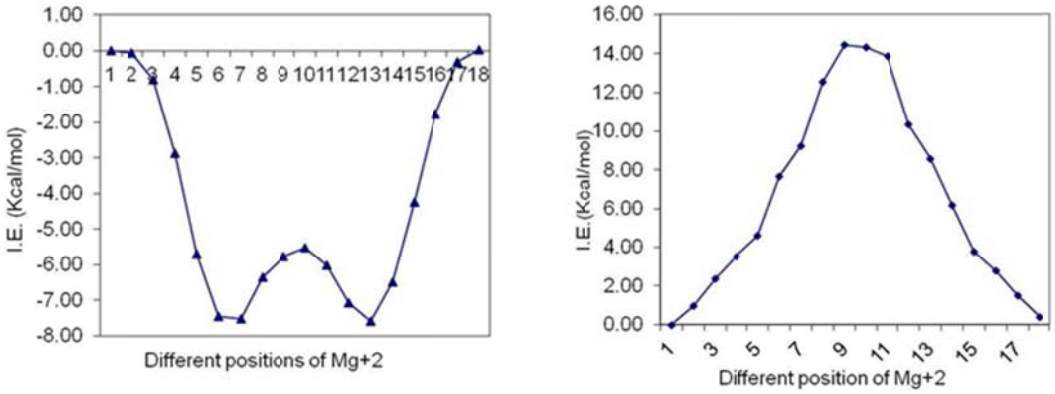

(c)

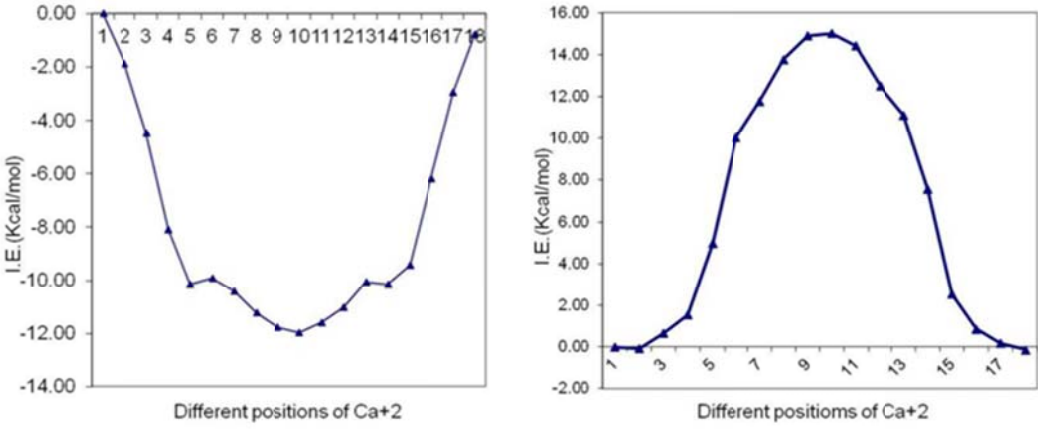

Figure 5.4: Variation of Interaction energy (IE Kcal/mol) with the movement of ion inside the CNT(10,0) (a) Be^{+2} ion, (b) Mg^{+2} ion and (c) Ca^{+2} ion.

(a)

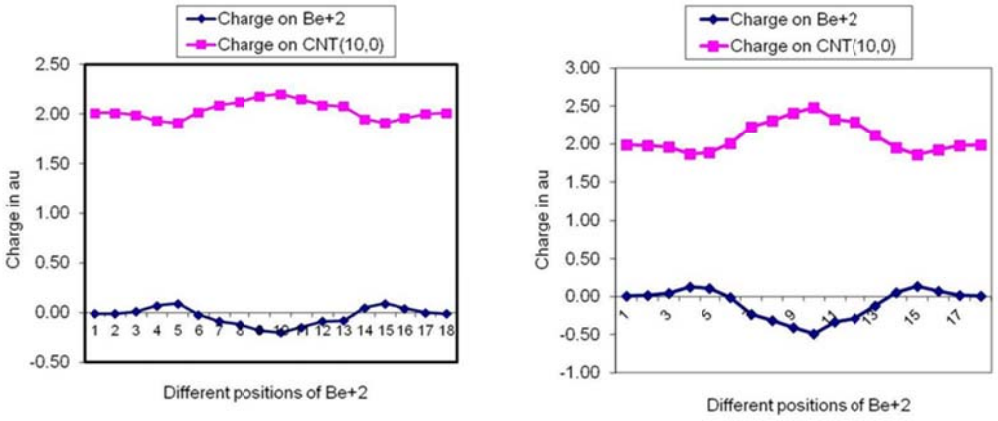

(b)

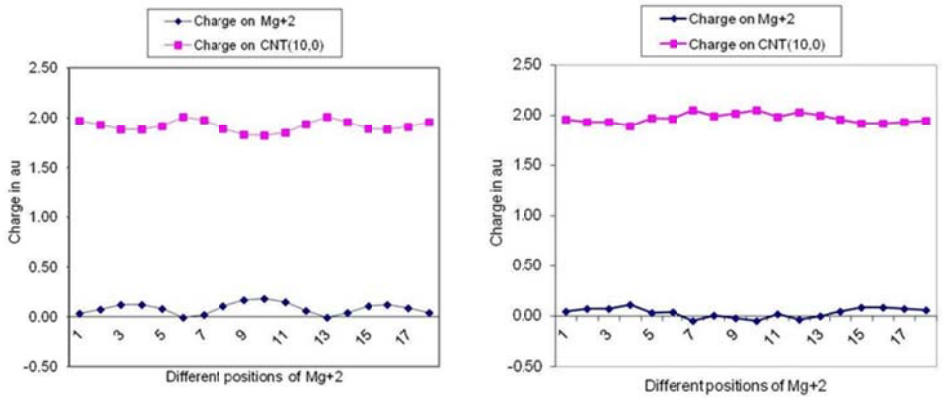

(c)

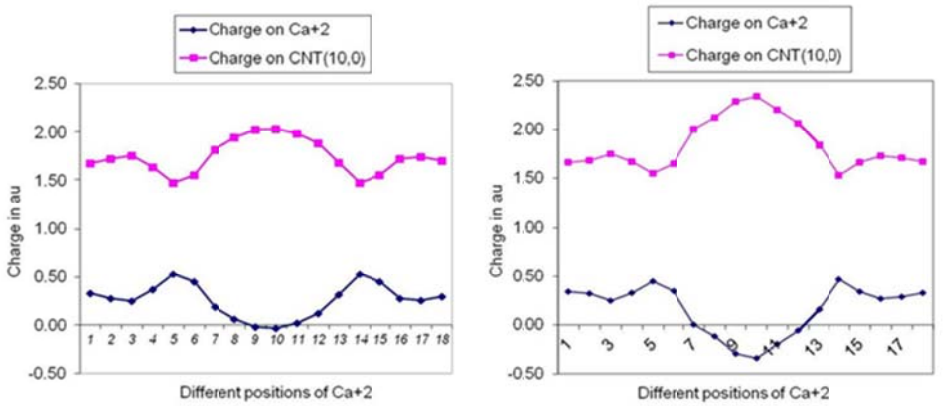

Figure 5.5: Variation of charge on CNT (10,0) and ion with the movement of ion inside the CNT(10,0) (a) Be^{+2} ion, (b) Mg^{+2} ion and (c) Ca^{+2} ion.

(a)

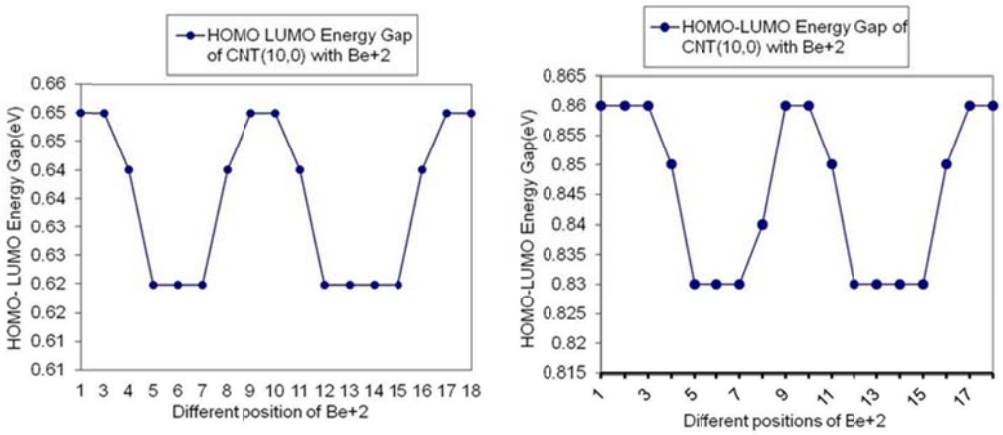

(b)

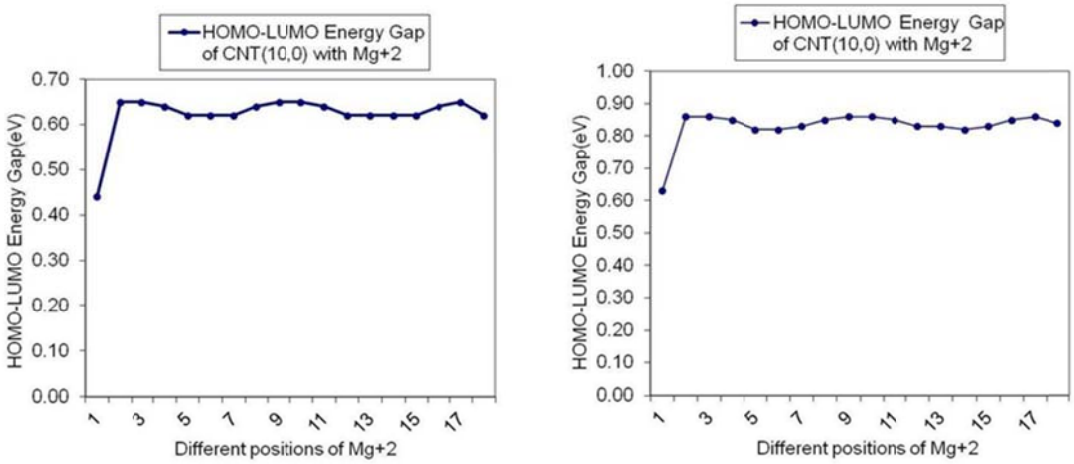

(c)

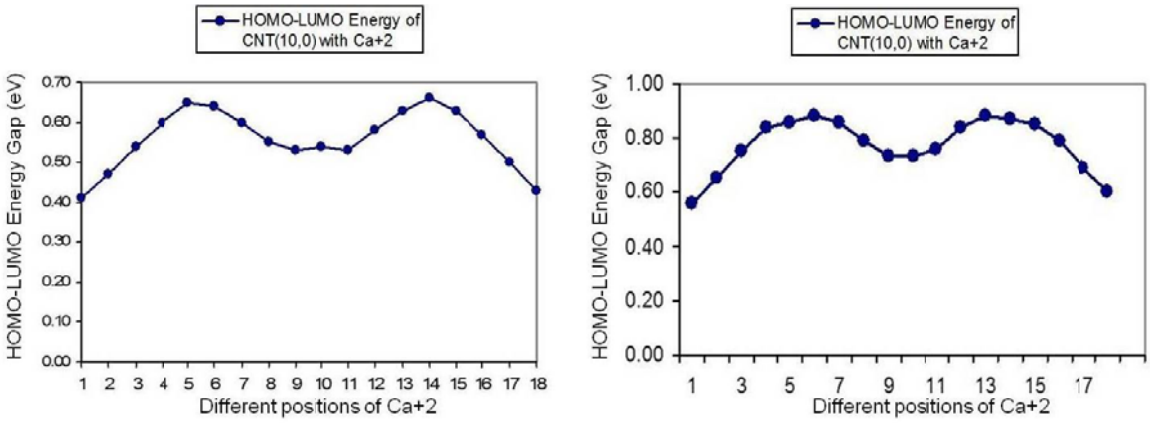

Figure 5.6: Variation of HUMO-LUMO gap with the movement of ion inside the CNT(10,0) (a) Be^{+2} ion, (b) Mg^{+2} ion and (c) Ca^{+2} ion.

5.4. Conclusion

The binding of series alkaline earth metal ions (Be^{+2}, Mg^{+2}, Ca^{+2},) with SWCNT has been comprehensively analysed. Our calculations reveal that the interaction energy preferences of metal ions varies at different positions of CNT (10, 0). It can be seen from our results that the order of interaction energy of these metal ions is Ca^{+2} >Mg^{+2}>Be^{+2}. So, the di-cationic such as calcium ion prefers to bind inside the CNT(10, 0). The Mulliken charge analysis reveals that these metal ions acts as charge acceptors to CNT(10, 0) and influence the physical properties of carbon materials, which leads to the sensitivity. It has also been found that HOMO-LUMO gap of the carbon nanotube is always affected by the binding of these alkaline earth metal ions. Significant changes occur in the HOMO-LUMO gap of the CNT (10, 0) on the metal ions, which provide a handle to tune the electronic and conductivity properties of CNTs through metal ion complexation. These studies can also be applied to develop new carbon based drug delivery systems and sensing applications, focusing particular on the mechanism of binding of metal ions with carbon nanotube.

5.5. References

1. Dinadayalane, T. C. and Leszczynski, J., *Struct. Chem.* **2010**, *21*, 1155.
2. Liang, F. and Chen, B., *Curr. Med. Chem.* **2010**, *17*, 10.
3. Zhu, Y., Murali, S., Cai, W., Li, X., Suk, J. W., Potts, J. R. and Ruoff, R. S., *Adv. Mater.* **2010**, *22*, 3906.
4. Charlier, J. C., *Acc. Chem. Res.* **2002**, *35*, 1063.
5. Huang, P., Zhu, H., Jing, L., Zhao, Y. And Cao, X., *ACS Nano* **2011**, *5*, 7945.
6. Dougherty, D. A., *Science* **1996**, *271*, 163.
7. Kim, S. K., Hu, S., Tarakeshwar, P. and Lee, J. Y., *Chem. Rev.* **2000**, *100*, 4145.
8. Ready, A. S. And Sastry, G. N., *J. Phys. Chem. A.* **2005**, *109*, 8893.
9. Reddy, A. S., Sastry, G. M. and Sastry, G. N., *Protein: Struct. Funct. Bioinf.* **2007**, *67*, 1179.
10. Vijai, D. and Sastry, G. N., *Phys. Chem. Chem. Phys.* **2008**, *10*, 582.
11. Gal, J., Maria, P., Decouzon, M., Mo, O., Yanez, M. and Abboud, J. L. M., *J. Am Chem. Soc.* **2003**, *125*, 10394.
12. Premkumar, J. R., Vijai, D. and Sastry, G. N., *Dalton Trans.* **2012**, *41*, 4965.
13. Vijai, D. and Sastry, G. N., *J. Phys. Chem. A.* **2006**, *110*, 10148.
14. Lee, R. S., Kim, H. J., Fischer, J. E., Thess, A. and Smalley, R. E., *Nature* **1997**, *388*, 255.
15. Liu, Z., Sun, X., Nakayama-Ratchford, N. and Dai, H., *ACS Nano* **2007**, *1*, 50.
16. Khan, M. A. K., Kerman, Prtryk M. and Kraatz, H., *Anal. Chem.* **2008**, *80*, 2574.
17. Kuang, Z., Kim, S. N., Crookes-Goodson, W. J., Farmer, B. L. and Naik, R. R., *ACS Nano* **2010**, *4*, 452.
18. Barone, P. W., Baik, S., Heller, D. A. and Strano, M. S., *Nat. Mater.* **2005**, *4*, 86.
19. Umadevi D. and Sastry, G. N., *J. Phys. Chem. C* **2011**, *115*, 9656.

20. Umadevi, D. and Sastry, G. N., *J. Phys. Chem. Lett.* **2011**, *2*, 1572.

21. Chen., W., Duan, L. and Zhu, D., *Environ. Sci. Technol.* **2007**, *41*, 8295.

22. Panigrahi, S., Bhattacharya, S., Banerjee, S. and Bhattacharyya, D., *J. Phys. Chem. C* **2012**, *116*, 4374.

23. Balavoine, F., Schultz, P., Richard, C., Mallouh, V., Ebbesen, T. and Mioskowski, C., *Angew. Chem. Int. Ed.* **1999**, *38*, 1912.

24. Tsang, S.C., Davis, J. J., Malcolm, L., Green, H., Allen, H., Hill, O., Leung, Y. C. and Sadler, P. J., *J. Chem. Soc. Chem.Commun.* **1995**, *17*, 1803.

25. S.C. Tsang, Z. Guo, Y. K. Chen, M. L. H. Green, H. Allen, O. Hill, T.W. Hambley, P. J. Sadler, Angew. Chem. Int. Ed. Engl.1997, 36, 2197.

26. Chen, R. J., Bangsaruntip, S., Drouvalakis, K. A., Kam, N. W. S., Shim, M., Li, Y., Kim, W., Utz , P. and Dai, H., *Proc. Natl. Acad. Sci.* **2003**, *100*, 4984.

27. Besteman, K., Lee, J., Wiertz, F. G. M., Heering, H. and Dekker, C., *Nano Lett.* **2003**, *3*, 727.

28. Star, A., Gabriel, J. C. P., Bradley, K. and Gruner, G., *Nano Lett.* **2003**, *3*, 459.

29. Roman, T., Dino, W. A., Nakanishi, H. and Kasai, H., *Eur. Phys. J. D.* **2006**, *38*, 117.

30. Wang, S., Humphreys, E. S., Chung, S. Y., Delduco, D. F., Lustig, S. R., Wang, H., Parker, K. N., Rizzo, N. W., Subramoney, S., Chang, Y. M. and Jagota, A., *Nature Mater.* **2003**, *2*, 196.

31. Zorbas, V., Smith, A. L., Xie, H., Ortiz-Acevedo, A., Dalton, A. B., Dieckmann, G. R., Draper, R. K., Baughman, R. H. and Musselman, I. H., *J. Am. Chem. Soc.* **2005**, *127*, 12323.

32. Lie, X., Chen, W., Zhan, Q., Sowards, L., Pender, M. and Naik, R. R., *J. Phys. Chem. B* **2006**, *110*, 12621.

33. Chen, R. J., Zhan, Y., Wang, D. and Dai, H., *J. Am. Chen. Soc.* **2001**, *123*, 3838.

34. Zhan, J., Lee, J. K., Wu, Y. and Murray, R. W., *Nano Lett.* **2003**, *3*, 403.

35. Kong, J., Franklin, N., Zhou, C., Chapline, M., Peng, S., Cho K. and Dai , H., *Science* **2000**, *287*, 622.

36. Schedin, F., Geim, A. K., Morozov, S. V., Hill, E. W., Blake, P., Katsnelson M. I. and Novoselove, K. S., *Nature Mater.* **2007**, *6* , 652.

37. Kumar, A., Reddy, A. L. M., Mukherjee, A., Dubey, M., Zhan, X., Singh, N., Ci, L., Edward Billups, W., Nagurny, J., Mital G. and Ajayan, P.M., *ACS Nano*, **2011**, *5*, 4345.

38. Reddy, A. L. M., Srivastav, A., Gowda, S. R., Gullapalli, H., Dubey, M., Ajayan, P. M., *ACS Nano* **2010**, *4*, 6337.

39. Rao, J. S., Zipse, H. and Sastry, G. N., *J. Phys. Chem. B* **2009**, *113*, 7225.

40. Sharma, B., Rao, J. S. and Sastry, G. N., *J. Phys. Chem. A* **2011**, *115*, 1971.

41. Mahadevi, A. S. and Sastry, G. N., *J. Phys. Chem. B* **2011**, *115*, 703.

42. Umadevi D. and Sastry, G. N., *Phys. Chem.Chem.Phys.* **2015**, *17*, 30260.

43. Frisch, M. J., Trucks, G. W., Schlegel, H. B., Scuseria, G. E., Robb, M. A., Cheeseman, J. R., Scalmani, G., Barone, V., Mennucci, B., Petersson, G. A., Nakatsuji, H., Caricato, M., Li, X., Hratchian, H. P., Izmaylov, A. F., Bloino, J., Zheng, G., Sonnenberg, J. L., Hada, M., Ehara, M., Toyota, K., Fukuda, R., Hasegawa, J., Ishida, M., Nakajima, T., Honda, Y., Kitao, O., Nakai, H., Vreven T., Montgomery, J. A. Jr., Peralta, J. E., Ogliaro, F., Bearpark, M., Heyd, J. J., Brothers, E., Kudin, K. N., Staroverov, V. N., Keith, T., Kobayashi, R., Normand, J., Raghavachari, K., Rendell, A., Burant, J. C., Iyengar, S. S., Tomasi, J., Cossi, Rega, M., N., Millam, J. M., Klene, M., Knox, J. E., Cross, J. B., Bakken, V., Adamo, C., Jaramillo, J., Gomperts, R., Stratmann, R. E., Yazyev, O., Austin, A. J., Cammi, R., Pomelli, C., Ochterski, J. W., Martin, R. L., Morokuma, K., Zakrzewski, V. G., Voth, G. A., Salvador, P., Dannenberg, J. J., Dapprich, S., Daniels, A. D., Farkas, O., Foresman, J. B., Ortiz, J. V., Cioslowski, J., and Fox, D. J., Gaussian, Inc.,Wallingford CT, 2010.

CHAPTER 6

INTERACTION OF AROMATIC AMINO ACIDS WITH ZIG-ZAG CARBON NANOTUBE: A QUATUM MECHANICAL STUDY

CHAPTER 6

INTERACTION OF AROMATIC AMINO ACIDS WITH ZIG-ZAG CARBON NANOTUBE: A QUATUM MECHANICAL STUDY

6.1. Introduction

Graphene, two dimensional allotropes of carbon, is zero band gap semiconductor materials. Another form of carbon is one dimensional carbon nanotube which are made by wrapping of planar graphene.[1] These carbon nanostructures are promising materials for biomedical and environmental applications due to unique electronic, thermal, mechanical, and transport properties.[2-4] Comparing the properties and reactivity of these allotropes, which differ in their curvature, is interesting in its own right. The adsorption of various substrates such as gas molecules, metal ions, polymer, organic molecules and biomolecules such as proteins and DNA on CNT surfaces has attracted considerable attention because of the fundamental importance and potential applications.[5-6] Carbon nanostructures (CNSs) exhibit the non-covalent interactions such as cation-π, π-π and CH-π towards the small molecules, metal ions and biomolecules as amino acid, nucleic acids. The non-covalent interaction of amino acids with various substrates and their proton affinity values have been studied.[7-8] The important aromatic amino acid for the interaction between a peptide and a single walled carbon nanotube has also been done in experimental studies.[9] A recent experimental study revealed that π-π noncovalent interactions between CNTs and the aromatic residue (Trp, Phe, and Tyr) of the proteins were found to play a significant role in determining the strength of the CNT-

protein interaction.[10] Subramanium et. al. have brought out new insight to study the interaction of CNT and peptides.[11-14] M.D. Studied that the zwetterionic-glycine adsorption is bound stronger to the CNT (10, 0) surface in comparision to non-ionic glycine counterparts, as well as on phenylalanine, histidine and cystein side chain groups.[15] A protein can interact with a nanoparticle to form a complex known as protein-corona, which defines the biological identity of the particle.[16-17] Because of further biological response of the body and the biodistribution of the nanoparticle in the body depend on the protein-nanoparticle complex; it is indispensable to understand the interaction of peptides with CNSs. Several experimental and computational studies have been performed to explore the binding strengths of different amino acids on the surfaces of CNTs and graphene.[6,18-21] The structures and unique properties of CNSs make them promising candidates for sensors to detect species with ultimate sensitivity such that the adsorption of individual gas molecules could be detected.[22] The π-π stacking interactions of CNSs with aromatic molecules appeared to be substantial significance due to their extended π orbital, and they seem to play a significant role in explaining the versatile applications of CNTs and graphene. In a recent study, Zou et. al. quantified the contribution of π-π interactions on the adsorption of organic pollutants on finite single-walled CNTs.[23] Further, progress in the biomedical applications of CNTs in imaging and cellular delivery [24-27] is on the go. Bianco et. al. [24] showed that functionalized CNTs can be used as templates for delivering bioactive peptides to the immune system. CNTs as multifunctional biological transporters [28] and near-infrared agents for selective cancer cell destruction have also been demonstrated.[29] Leu et. al. used CNTs as non-viral molecular transporters for the delivery of short interfering RNA (siRNA)

into human T cells and primary cells. It is shown that the electronic structure of the CNT is highly sensitive to its environment.[30] The presence of electrostatic charges and adsorption of various molecules on the surface brings in large changes in conducting properties of the CNT, thus reflecting the perturbations in the electronic structure. More recently, it has further been shown that the electrical conductance of CNTs changes appreciably as promising CNT-based sensors for analytical applications in chemistry and biology.[31] In the current study, it has been theoretically investigated that the CNT(12,0) is used to improve its biosensing efficiency and selectivity towards biomolecules such as histidine, phenylalanine, tyrosine and tryptophan. It is very important for CNT (12,0) to interact with the biomolecules so that its electronic properties gets changed. The aromatic amino acids are all of great practical interest in drug delivery systems, environmental and medical application. The effect of binding strength of aromatic amino acids at different positions inside the carbon nanotube is explored. The charge transfer during the complex formation and the change in the HOMO-LUMO gap are also explored, which provide valuable information in tuning the electronic and conductivity properties through aromatic amino acids complexation with single walled carbon nanotube.

6.2. Computational Details

The calculations of the interaction between single walled zigzag carbon nanotube [CNT (12, 0)] and aromatic amino acids is carried out using the density functional theory. The geometrical calculations of all structures have been done by using one method B3LYP/3-21G*. Initially, the individual aromatic amino acids are made to passing through the

SWCNT and the geometry optimization of all such structures were performed within density functional theory using of Gaussian 09 program suite.[32] It is important to note that competing geometrical configuration was tested, but those shown are the lowest energy species feasible for the interaction of the compounds. Interaction energy has been done at the B3LYP/3-21G* level to fine-tune the energy.

The interaction energy (E_{in}) of the aromatic amino acids such as histidine, phenylalanine, tryptophan and tyrosine with CNT (12, 0) is calculated by the following equation.

$$E_{int} = E_{\circ} - E \tag{6.1}$$

Here $E_{\circ}$ is the total energy of complex molecular systems for the initial position of aromatic amino acid with SWCNT. E represents the variation of total energy at different position of aromatic amino acids with SWCNT respectively. The individual aromatic amino acid was placed parallel inside to the surface of SWCNT. The variation of the interaction energy and charge on amino acids as well as SWCNT when the individual amino acids are passing through the SWCNT is calculated. The charge transfer has been considered as the sum of the all atoms in SWCNT model system and aromatic amino acids. Positive charge transfer values indicate the transfer of charge from SWCNT to amino acids, while negative charge values indicate the transfer of charge from amino acids to the SWCNT. Also the HOMO-LUMO gap of SWCNT- aromatic amino acids complexes at B3LYP/3-21G* level of theory was calculated. All calculations were carried out using the Gaussian09 program suite.

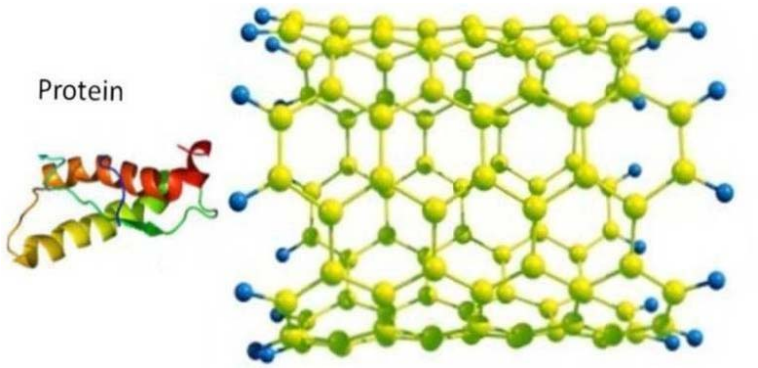

Figure 6.1: Schematic representation of the interaction between a single walled carbon nanotube and a protein. The single walled carbon nanotube and amino acid models used to mimic this interaction are shown in the inset.

6.2.1. Model system considered in the study

In this work, a wide range of model system was considered to study the interaction of aromatic molecules with their π-surfaces. The Figure 6.2 represents the zigzag carbon nanotube [CNT(12,0)] model system which is introduced for interaction with biomolecules. In this interaction, when the aromatic amino acid passes through the CNT (12,0), a fundamental interaction of aromatic acids such as histidine(His), phenylalanine(Phe), tyrosine(Tyr), tryptophan(Trp) with CNT (12,0) is obtained.

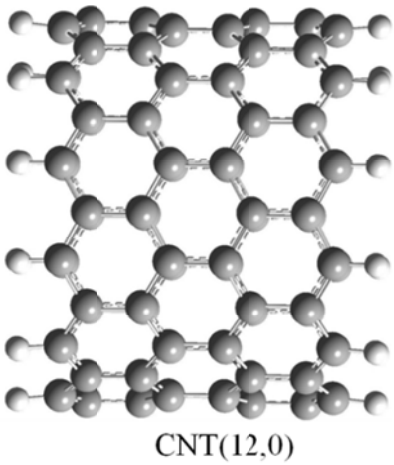

Figure 6.2: Zig-zag single walled carbon nanotube model system.

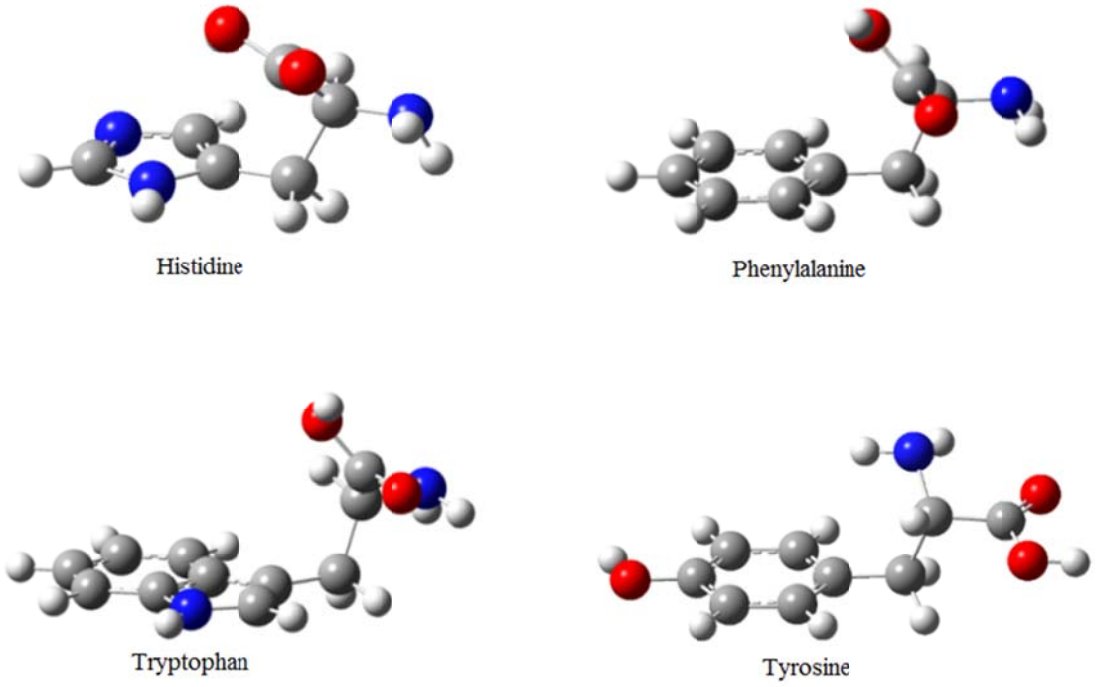

Figure 6.3: The optimized structure of individual aromatic amino acids.

6.3. Results and discussion

The π-complexes formed by CNT (12,0) with various amino acids such as histidine, phenylalanine, tyrosine and tryptophan is considered. The optimized structure of aromatic amino acids and CNT (12,0) and their complexes are shown in Figure **6.2.** The initial configuration of all amino acids was assigned so that these are passing inside from one end to another end of SWCNT. The SWCNT was considered to study the interaction of biomolecules π-π noncovalent interaction towards carbon nano materials. Table 6.1 summarizes results on the interaction energy, the charge transfer (Q, mulliken charge) and HOMO-LUMO gap for the most stable configurations of SWCNT which interacts with various amino acids in our calculations that are shown in Figures (6.3 – 6.6) and

Table 6.1. Subsequently, the binding of the SWCNT with various biomolecules and the trend in the charge transfer is observed. It is also investigated the HOMO-LUMO gap of SWCNT with the interaction of various aromatic amino acids.

6.3.1. The interaction energy and charge transfer analysis

The aromatic amino acids forms π-π complexes with single walled carbon nanotubes [CNT (12,0)]. The investigated interaction energy of amino acid complexes with single walled carbon nanotube when the amino acids as histidine, phenylalanine, tyrosine and tryptophan pass through the CNT (12, 0). Figure 6.4-6.7 displays the optimized structure of the amino acid complexes with SWCNT at B3LYP/3-21G* method. The HOMO-LUMO gap of CNT (12, 0) complexes with aromatic amino acids is calculated. It is clear from our results that the change in interaction energy, charge and HOMO-LUMO energy gap CNT (12, 0) with amino acids are significant. The interaction energies of four amino acids and CNT (12, 0) complexes at B3LYP/3-21G* level is shown in Tables 6.1-6.4, respectively. It is clear that the change of interaction energy of aromatic amino acids is more dramatic with CNT (12, 0). In order to guage the mechanics of these foregoing binding interactions, the Mulliken charge transfer analysis at B3LYP/3-21G*{Figure 6.8 (a-d)} is also calculated. Charge transfer is a phenomenon in which a large fraction of an electronic charge is transferred from one entity (charge donor) to another (charge acceptor). As a result of the charge transfer electronic structure properties of the sensor materials will be affected. The negative charge values on the aromatic amino acids in the optimized complexes clearly points out that these aromatic amino acids act as charge acceptors from the carbon annotate. It is clear from Table 6.1- 6.4 the charge transfer

between amino acids and CNT (12, 0) are significant. Consequently, the aromatic amino acid complexes such as tryptophan has the stronger interaction energy than histidine, phenylalanine and tyrosine. According to B3LYP/3-21G* method, the interaction energy of $\Delta E_{CNT(12,0)\_His}$, $\Delta E_{CNT(12,0)\_Phe}$, $\Delta E_{CNT(12,0)\_Tyr}$ and $\Delta E_{CNT(12,0)\_Trp}$ are greater inside the carbon nanotube. The variation of the interaction energies of aromatic amino acids with CNT (12, 0) is shown in Figure 6.8(a-d).

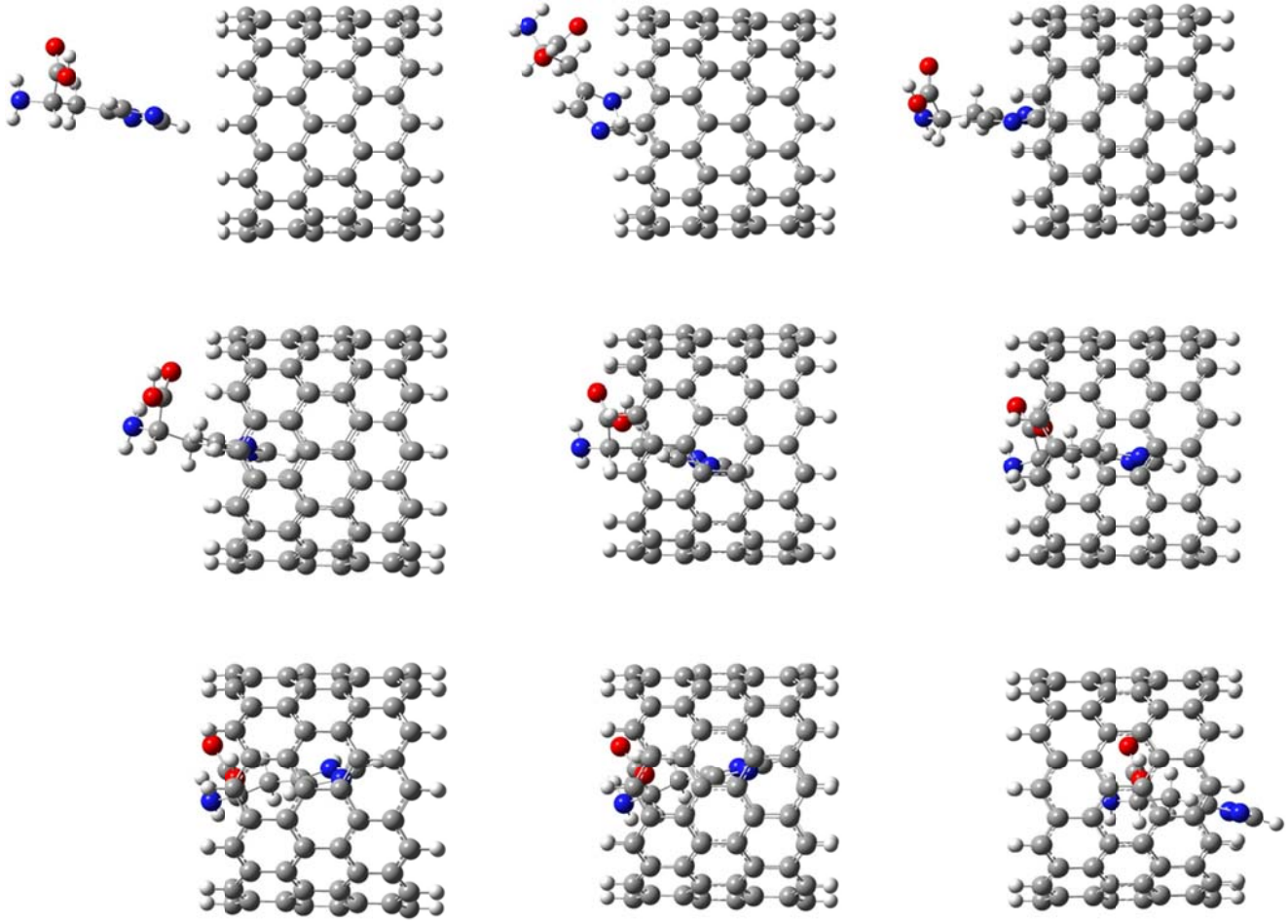

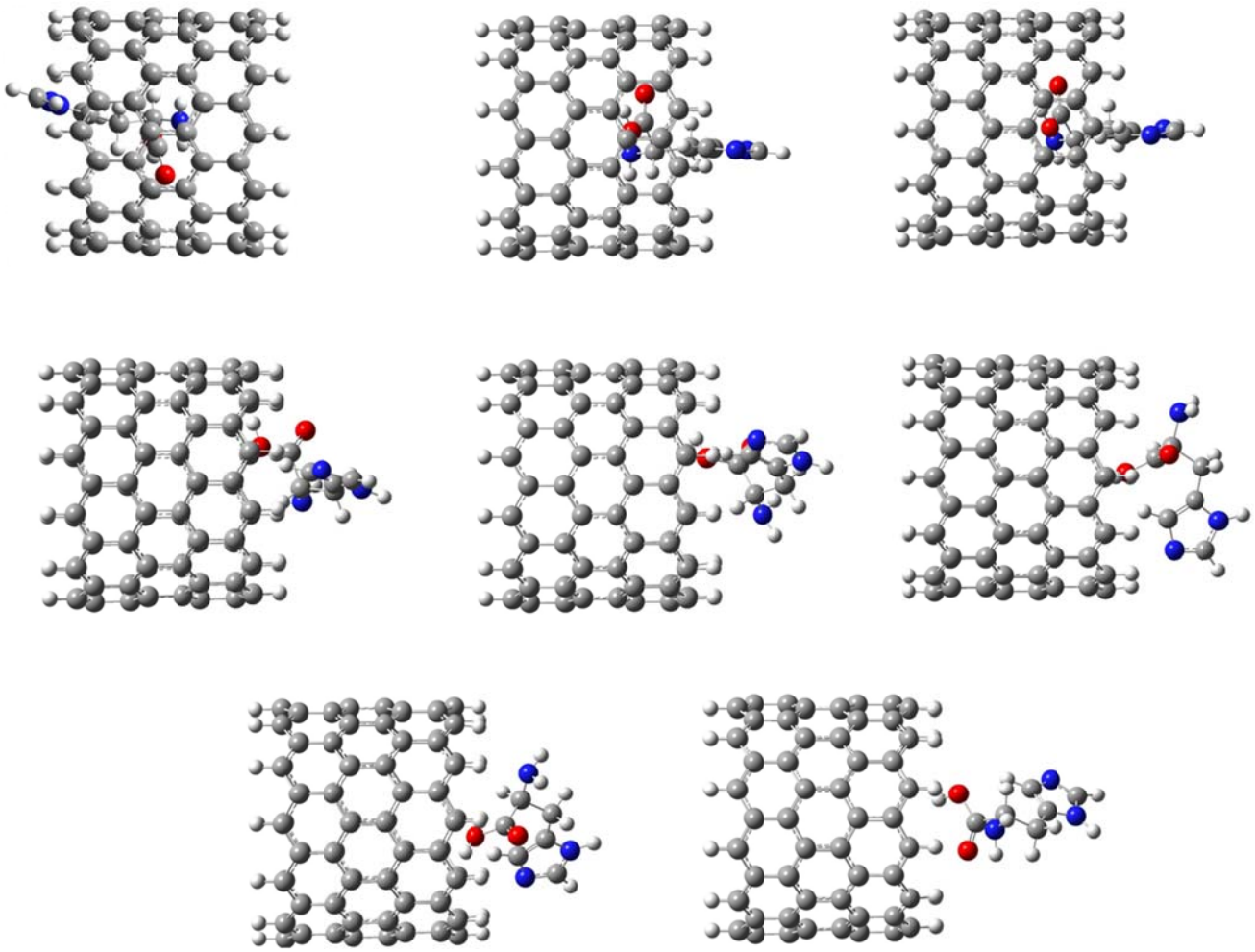

Figure 6.4: Optimized geometries of the complexes formed with CNT (12, 0) and histidine.

Table 6.1. The Interaction Energy (kcal/mol), Charge Transfer (a.u.) and HOMO-LUMO Gap (eV) at B3LYP/3-21G* level of theory.

Aromatic amino acid	Different positions of CNT(12,0)	Total energy (au)	ΔE=E0-E (kcal/mol)	Charge on Histidine (au)	Charge on CNT(12,0) (au)	HOMO-LUMO Gap (eV)
Histidine	CNT(12,0)_His_01	-2634386.18	0.00	0.00	0.00	0.39
	CNT(12,0)_His_02	-2634395.12	8.94	0.00	0.00	0.35
	CNT(12,0)_His_03	-2634393.87	7.69	0.00	0.00	0.34
	CNT(12,0)_His_04	-2634395.00	8.82	-0.01	0.01	0.34
	CNT(12,0)_His_05	-2634393.64	7.46	-0.01	0.01	0.38
	CNT(12,0)_His_06	-2634393.61	7.44	-0.01	0.01	0.38
	CNT(12,0)_His_07	-2634393.87	7.70	0.01	-0.01	0.38
	CNT(12,0)_His_08	-2634393.27	7.09	-0.02	0.02	0.38
	CNT(12,0)_His_09	-2634393.07	6.89	0.06	-0.06	0.34
	CNT(12,0)_His_10	-2634393.57	7.39	0.02	-0.02	0.34
	CNT(12,0)_His_11	-2634395.24	9.06	0.06	-0.06	0.35
	CNT(12,0)_His_12	-2634395.13	8.95	0.04	-0.04	0.35
	CNT(12,0)_His_13	-2634406.28	20.10	0.04	-0.04	0.35
	CNT(12,0)_His_14	-2634406.12	19.94	-0.01	0.01	0.38
	CNT(12,0)_His_15	-2634406.12	19.94	0.00	0.00	0.38
	CNT(12,0)_His_16	-2634406.10	19.92	0.03	-0.03	0.38
	CNT(12,0)_His_17	-2634396.72	10.54	0.00	0.00	0.39

6.3.2. CNT (12, 0) _Histidine optimized Molecular System

The π-π interaction energies of histidine at different binding positions of CNT (12, 0) are summarized in Table 6.1. The variation of interaction energy and charge on histidine and CNT (12, 0) are shown in Figure 6.7 and Figure 6.8, respectively, which indicates a weak

interaction when the tyrosine passes through CNT (12, 0), because the interaction energy of histidine tends to be positive while coming towards the other side of CNT (12, 0). Consequently, the repulsion between histidine and CNT (12, 0) increases from 1 to 17 positions. The maximum repulsion between histidine and CNT(12,0) occurs at position 14 which shows weak interaction. In this configuration, the charge transferred from CNT (12, 0) to histidine at positions 1 to 6, 8, and 14 to 15, so the hisidine acts as charge acceptor and the CNT (12, 0) as donor, but at the position 7, 9 to 13 and 16 to 17, the charge is transferred from histidine to CNT(12,0), so the histidine acts as charge donor and CNT (12, 0) acceptor which are shown in Table 6.1 and Figure 6.8(a).

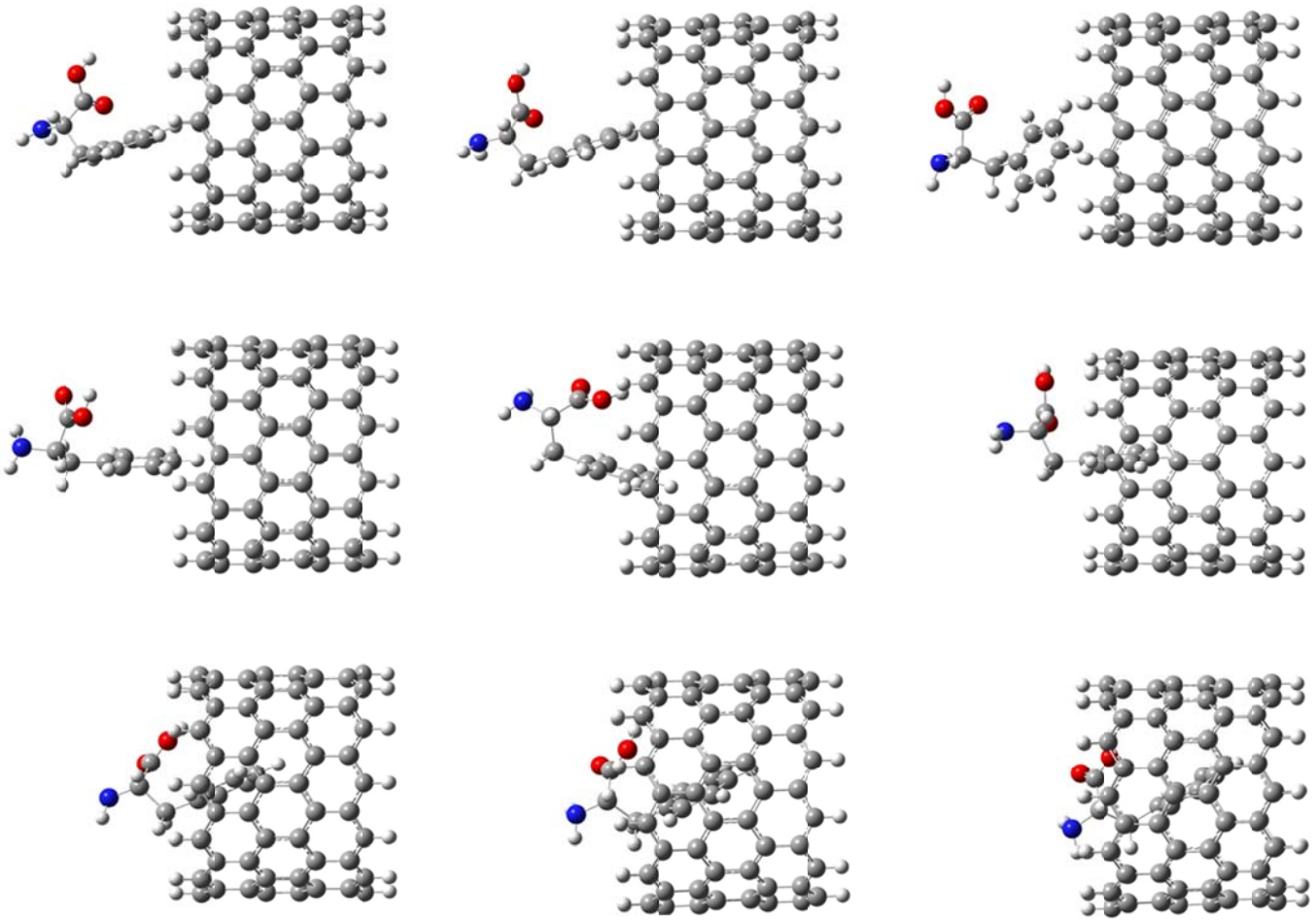

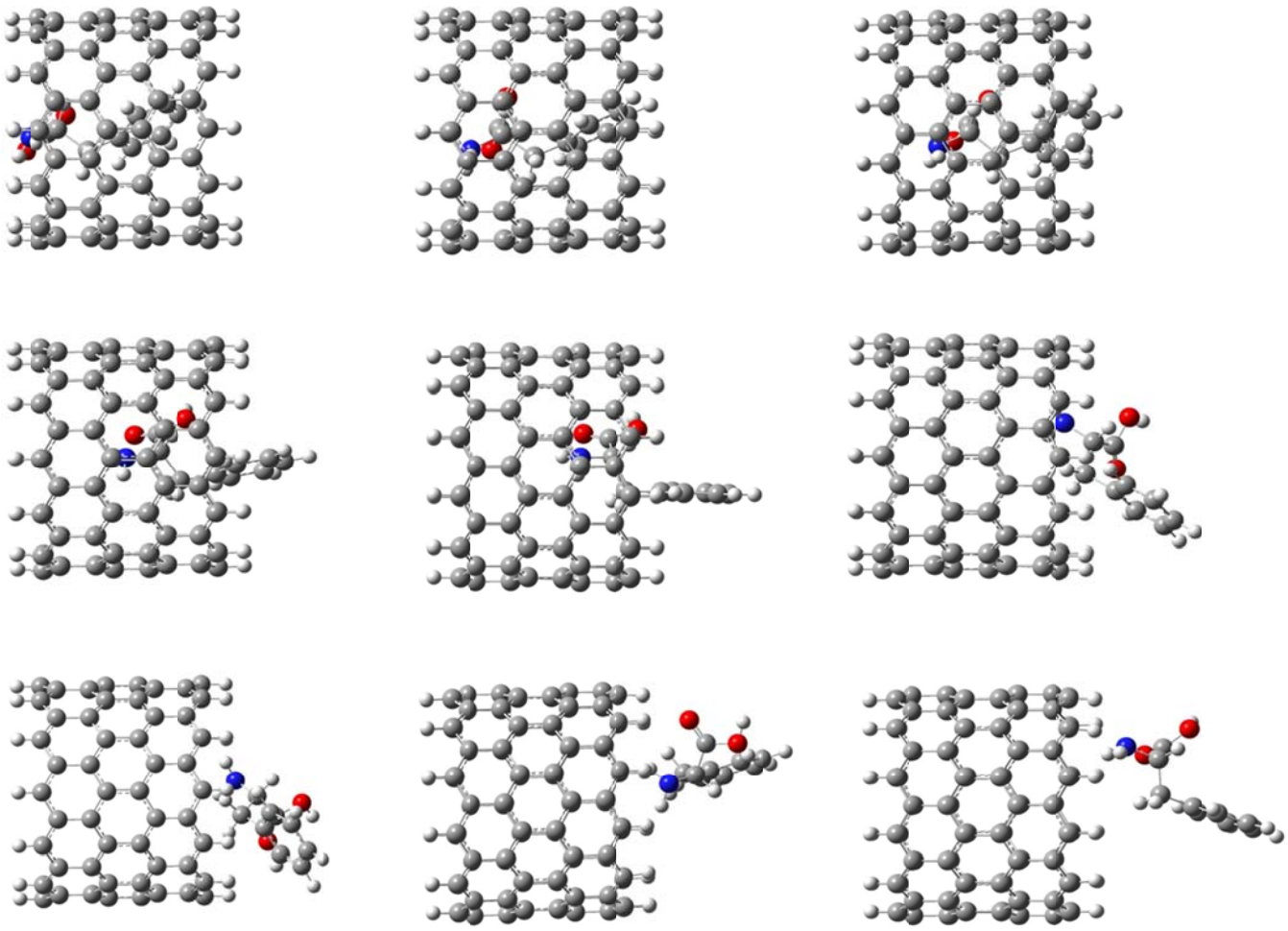

Figure 6.5: Optimized structure of complex formed of CNT(12,0) and Phenylalanine

Table 6.2: The Interaction Energy (kcal/mol), Charge Transfer (a.u.) and HOMO-LUMO Energy Gap (eV) at B3LYP/3-21G* level of theory.

Aromatic amino acid	Different positions of CNT(12,0)	Total energy (kcal/mole)	$\Delta E=E_0-E$ (kcal/mol)	Charge on phenylalanine (au)	Charge on CNT(12,0) (au)	HOMO-LUMO Gap(eV)
Phenylalanine	CNT(12,0)_Phe_01	-2638170.16	0.00	0.000	0.000	0.408
	CNT(12,0)_Phe_02	-2638170.38	0.22	0.000	0.000	0.381
	CNT(12,0)_Phe_03	-2638163.17	-7.00	-0.003	0.003	0.389
	CNT(12,0)_Phe_04	-2638159.16	-11.00	-0.012	0.012	0.395
	CNT(12,0)_Phe_05	-2638168.45	-1.72	-0.002	0.002	0.395
	CNT(12,0)_Phe_06	-2638167.22	-2.95	0.000	0.000	0.387
	CNT(12,0)_Phe_07	-2638167.63	-2.53	0.026	-0.026	0.391
	CNT(12,0)_Phe_08	-2638167.72	-2.45	0.238	-0.238	0.393
	CNT(12,0)_Phe_09	-2638166.35	-3.81	0.034	-0.034	0.394
	CNT(12,0)_Phe_10	-2638165.73	-4.43	0.276	-0.276	0.395
	CNT(12,0)_Phe_11	-2638163.87	-6.29	0.352	-0.352	0.393
	CNT(12,0)_Phe_12	-2638162.61	-7.55	0.018	-0.018	0.393
	CNT(12,0)_Phe_13	-2638164.03	-6.14	0.192	-0.192	0.393
	CNT(12,0)_Phe_14	-2638164.90	-5.26	0.088	-0.088	0.387
	CNT(12,0)_Phe_15	-2638170.77	0.61	0.100	-0.100	0.381
	CNT(12,0)_Phe_16	-2638173.64	3.47	0.042	-0.042	0.380
	CNT(12,0)_Phe_17	-2638171.32	1.15	0.015	-0.015	0.381
	CNT(12,0)_Phe_18	-2638170.62	0.46	0.001	-0.001	0.379

6.3.3. CNT (12, 0)_Phenylalanine optimized Molecular System

The phenylalanine forms π-π type complexes with CNT(12,0) due to the presence of aromatic ring as shown in Figure 6.5. The interaction energy is observed when the phenylalanine passes through the CNT(12,0) which is shown in Figure 65. The interaction energy of this complex system is -11.000Kcal/mole which is shown in Table 6.2. When the phenylalanine interacts with CNT (12, 0), calculated charge on phenylalanine CNT (12, 0) is -0.012 au and 0.012 au, respectively. In this configuration(4^{th} position), the charge transfer is found to be maximum from CNT (12, 0) to the phenylalanine than that of the other positions. At the fourth position of complex molecular system, the phenylalanine acts as charge acceptor and CNT (12, 0) donor, but at all other positions, they are acting as charge donor. The phenylalaine from position 3 to 5 acts as charge acceptor while at other positions it acts as charge donor. The highest interaction energy and large charge transfer (from CNT(12,0) to histidine) indicates strong interactions, which are shown in Table 6.2 and Figure 6.5. Consequently, the phenylalanine exhibits stronger interaction energy due to large charge transfer, which is responsible for high sensitivity and selectivity.

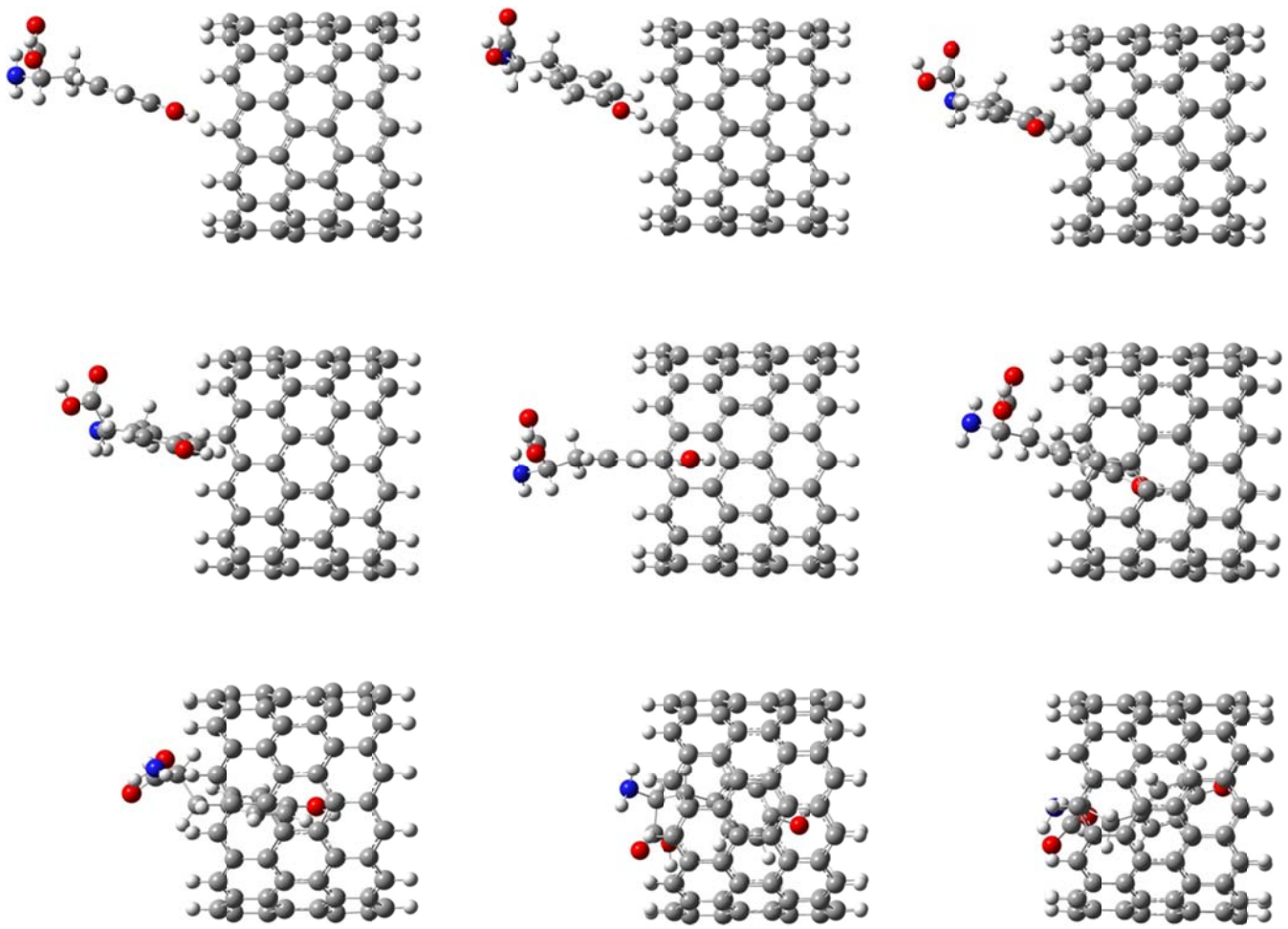

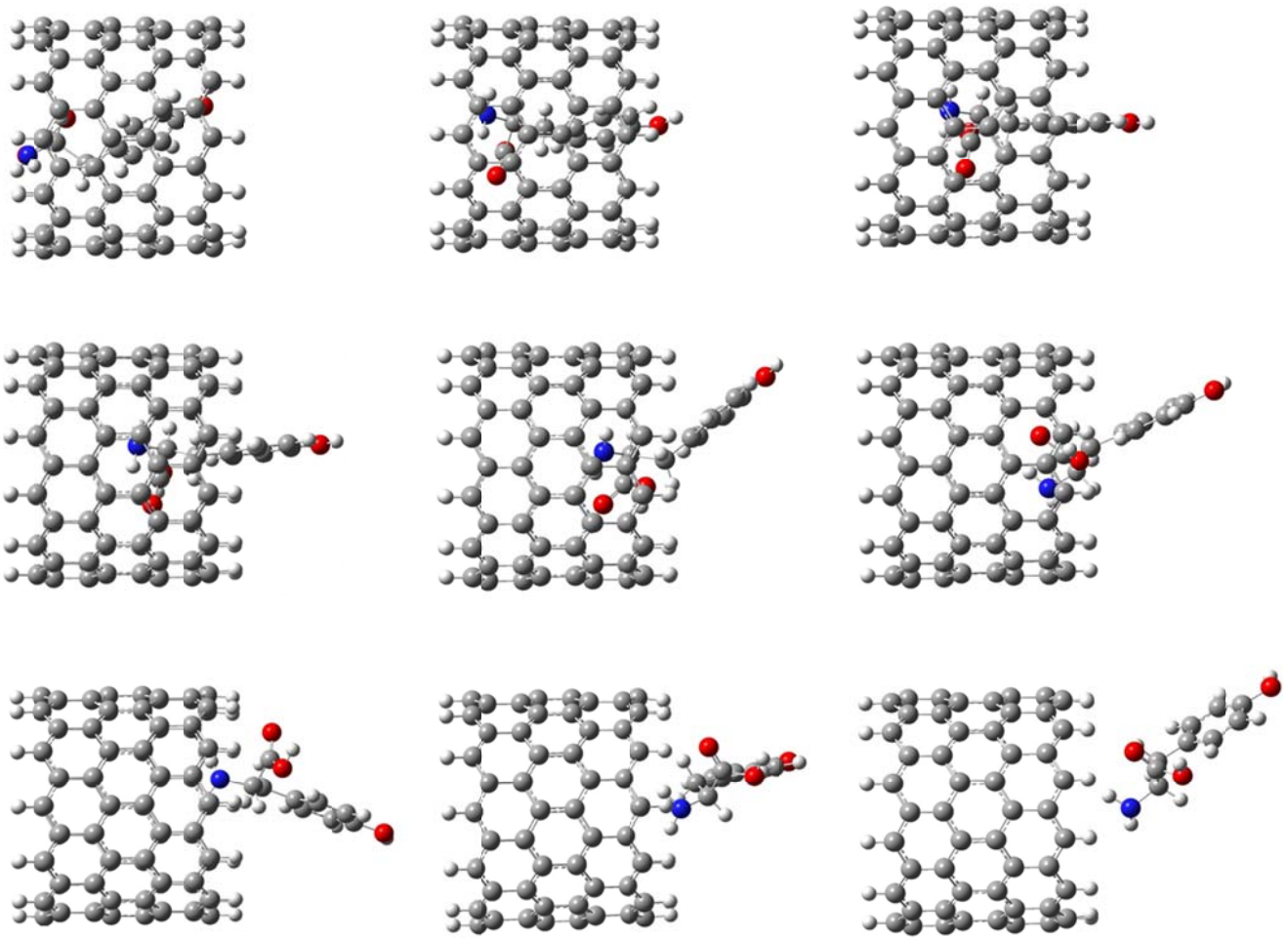

Figure 6.6: Optimized structure of complex formed of CNT (12, 0) and Tyrosine.

Table 6.3: The Interaction Energy (kcal/mol), Charge Transfer (a.u.) and HOMO-LUMO Energy Gap (eV) at B3LYP/3-21G* level of theory.

Aromatic amino acids	Different positions of CNT(12,0)	Total energy (kcal/mole)	$\Delta E=E_0-E$ (kcal/mol)	Charge on tyrosine	Charge on CNT(12,0)	HOMO-LUMO Gap
Tyrosine	CNT(12,0)_Tyro_01	-2685102.81	0.00	0.00	0.00	0.39
	CNT(12,0)_Tyro_02	-2685103.84	1.02	0.04	-0.04	0.39
	CNT(12,0)_Tyro_03	-2685104.21	1.40	0.02	-0.02	0.39
	CNT(12,0)_Tyro_04	-2685103.82	1.00	0.02	-0.02	0.39
	CNT(12,0)_Tyro_05	-2685097.44	-5.37	0.00	0.00	0.39
	CNT(12,0)_Tyro_06	-2685102.47	-0.35	0.02	-0.02	0.38
	CNT(12,0)_Tyro_07	-2685098.53	-4.28	0.04	-0.04	0.38
	CNT(12,0)_Tyro_08	-2685104.57	1.76	0.06	-0.06	0.39
	CNT(12,0)_Tyro_09	-2685103.88	1.06	0.02	-0.02	0.39
	CNT(12,0)_Tyro_10	-2685102.86	0.05	0.10	-0.10	0.38
	CNT(12,0)_Tyro_11	-2685099.73	-3.08	0.09	-0.09	0.39
	CNT(12,0)_Tyro_12	-2685099.91	-2.90	0.05	-0.05	0.39
	CNT(12,0)_Tyro_13	-2685100.83	-1.98	0.03	-0.03	0.39
	CNT(12,0)_Tyro_14	-2685102.53	-0.28	0.01	-0.01	0.38
	CNT(12,0)_Tyro_15	-2685101.44	-1.37	-0.02	0.02	0.39
	CNT(12,0)_Tyro_16	-2685105.12	2.31	-0.02	0.02	0.37
	CNT(12,0)_Tyro_17	-2685106.86	4.05	0.00	0.00	0.38
	CNT(12,0)_Tyro_18	-2685103.73	0.92	0.00	0.00	0.38

6.3.4. CNT (12, 0) _Tyrosine optimized Molecular System

The variation of interaction energy and charge on tyrosine and CNT (12, 0) are shown in Table 6.3 and Figure 6.6, respectively. The interaction energy at position 5 indicates the strongest interaction when the tyrosine is passing inside the CNT (12, 0). However, the interaction energy of tyrosine when it comes out of CNT (12, 0) remarkably changes the electronic properties of CNT (12, 0). In this configuration, the charge is transferred from tyrosine to CNT (12, 0) from position 2 to 14, so the tyrosine acts as charge donor and the CNT (12, 0) acceptor, but at the position 15 to 18, the charge is transferred from CNT (12, 0) to tyrosine, so the tyrosine acts as charge acceptor and CNT (12, 0) donor which are shown in Table 6.3 and Figure 6.9(c).

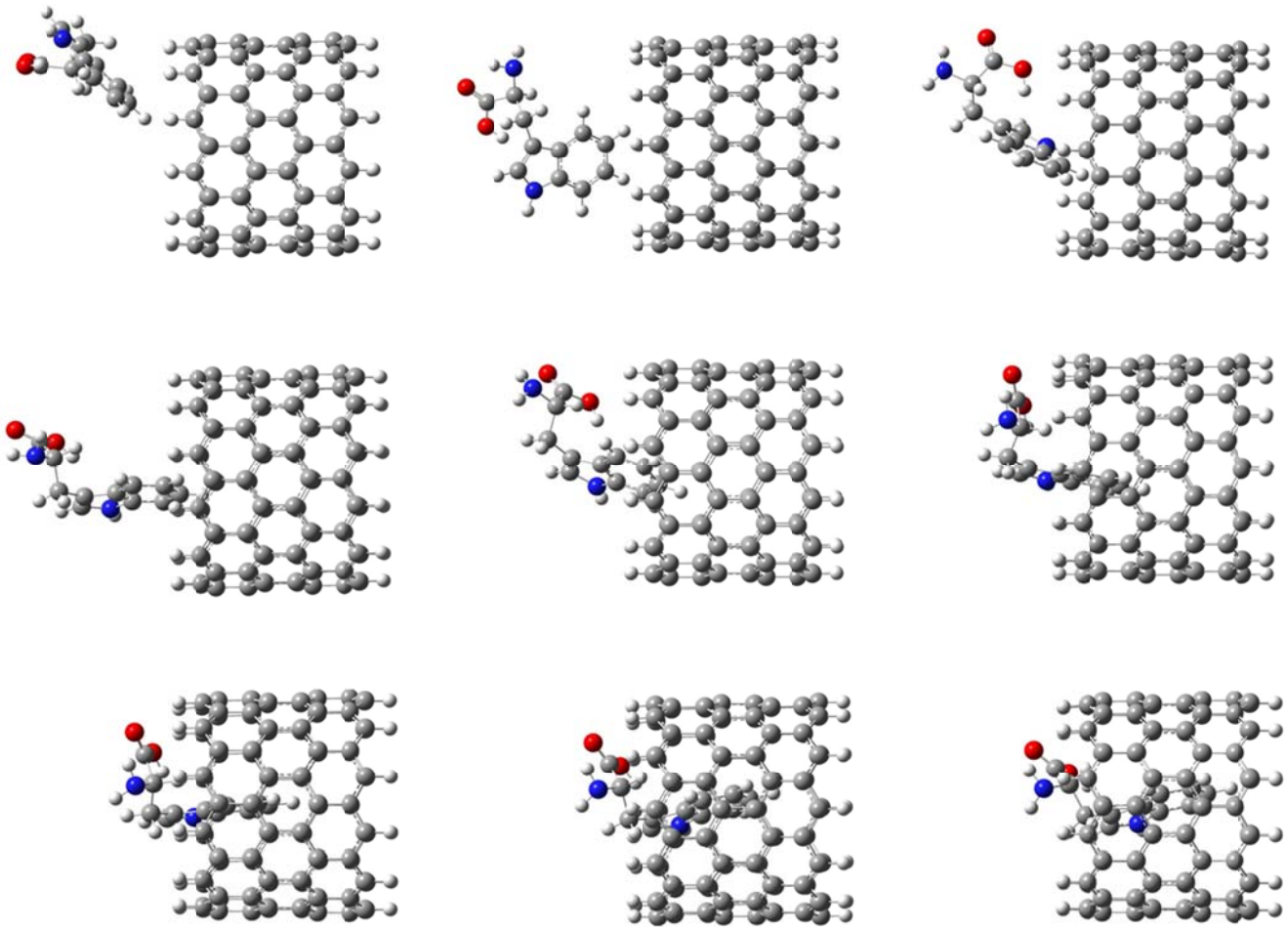

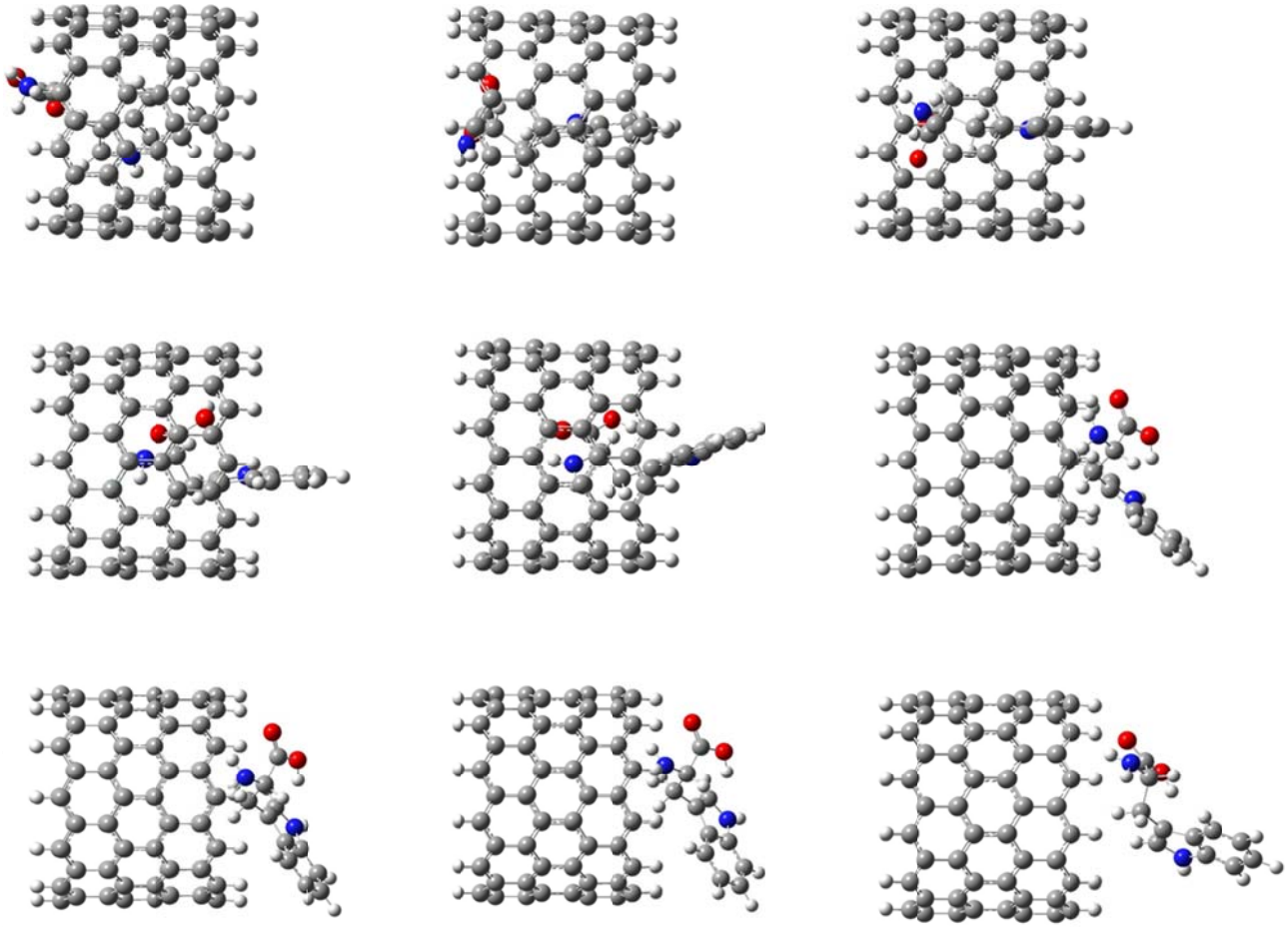

Figure 6.7: Optimized structure of complex formed of CNT(12,0) and Tryptophan.

Table 6.4: The Interaction Energy (kcal/mol), Charge Transfer (a.u.) and HOMO-LUMO Energy Gap (eV) at B3LYP/3-21G* level of theory.

Aromatic amino acids	Different positions of CNT(12,0)	Total energy (kcal/mole)	$\Delta E=E_0-E$ (kcal/mol)	Charge on tryptophan	Charge on CNT(12,0)	HOMO-LUMO Gap
Tryptophan	CNT(12,0)_Trp_01	-2720265.98	0.00	0.00	0.00	0.39
	CNT(12,0)_Trp_02	-2720266.82	0.84	0.00	0.00	0.39
	CNT(12,0)_Trp_03	-2720275.59	9.61	-0.01	0.01	0.35
	CNT(12,0)_Trp_04	-2720265.83	-0.16	-0.01	0.01	0.39
	CNT(12,0)_Trp_05	-2720271.73	5.75	0.01	-0.01	0.37
	CNT(12,0)_Trp_06	-2720274.54	8.55	0.03	-0.03	0.33
	CNT(12,0)_Trp_07	-2720278.38	12.39	0.15	-0.15	0.32
	CNT(12,0)_Trp_08	-2720276.89	10.90	0.22	-0.22	0.34
	CNT(12,0)_Trp_09	-2720270.93	4.95	0.53	-0.53	0.35
	CNT(12,0)_Trp_10	-2720265.49	-0.49	0.50	-0.50	0.35
	CNT(12,0)_Trp_11	-2720262.32	-3.66	0.48	-0.48	0.39
	CNT(12,0)_Trp_12	-2720263.24	-2.74	0.57	-0.57	0.36
	CNT(12,0)_Trp_13	-2720261.27	-4.71	0.50	-0.50	0.37
	CNT(12,0)_Trp_14	-2720265.53	-0.45	0.36	-0.36	0.38
	CNT(12,0)_Trp_15	-2720266.75	0.76	0.39	-0.39	0.38
	CNT(12,0)_Trp_16	-2720275.10	9.12	0.20	-0.20	0.38
	CNT(12,0)_Trp_17	-2720276.14	10.15	0.08	-0.08	0.38
	CNT(12,0)_Trp_18	-2720272.69	6.71	0.01	-0.01	0.35

6.3.5. CNT (12, 0) _Tryptophan optimized Molecular System

In the CNT (12, 0)_Trp complex structure, the tryptophan amino acid consists of two aromatic groups which closely interacts with benzene rings of CNT(12,0), the binding strength of π-π noncovalent interaction is increased when the tryptophan comes in middle position of the CNT (12,0). Due to this reason, the interaction energies of tryptophan tends towards negative, which indicates the strong interaction between them. Interestingly, the CNT (12, 0) exhibits strong interaction energies when the tryptophan is optimized. In this configuration, the charge is transferred from CNT (12,0) to tryptophan at position 3 and 4 but for all remaining positions, the charge is transferred from tryptophan to CNT(12,0). Consequently, the CNT (12,0) acts as a charge donor at 3 and 4 while for remaining positions it behaves as charge acceptor. Due to variation of charge on CNT (12, 0), the change in interaction energies is significant which is showed in Table 6.4 and Figure 6.8(d).

6.3.6. HOMO-LUMO Gap

The necessary conditions for a material to perform as a sensor is to undergo a change in its physical property on interacting with an analyte. These changes may be recorded to confirm the presence of the analyte. The HOMO-LUMO gap defined as the difference between lowest unoccupied molecular orbital and highest occupied molecular orbital. This is the electronic properties of any molecular system which is helpful to design new materials. In order to notice such depiction in the case of carbon nanomaterials, the HOMO-LUMO gap of the CNT (12, 0) in the free state and the aromatic amino acid complexes is calculated. In general, in the case of π-π complexes, the HOMO-LUMO gap

of SWCNT varies with the orientation of aromatic amino acids inside the different positions of CNT (12, 0). In case of histidine complexes, the HOMO-LUMO energy values of CNT (12, 0) vary from 0.3369 to 0.3886eV but for phenylalanine 0.3793 to 0.4084 eV. In case of tyrosine and tryptophan complexes, the HOMO-LUMO energy values vary 0.3736 to 0.3943 eV and 0.3154 to 0.3943 eV. Consequently, there is a similar change in HOMO-LUMO gap of phenylalanine and tyrosine interaction, but HOMO-LUMO gap varies from 0.3154 to 0.3943 eV. It has been shown that the energy gap of CNT (12, 0) undergoes a significant change as shown in Table (6.1 – 6.4) and Figure 6.10, the change in HOMO-LUMO gap is significant [as shown in Table 6.2]. Thus, the HOMO-LUMO energy value and the orbital distribution seems to be good evidence to explain the strength of interaction of the π complexes of CNTs nano-materials. So it can be said that the variation in HOMO-LUMO gap of the carbon nanotube upon binding with the various aromatic amino acids biomolecules is significant.

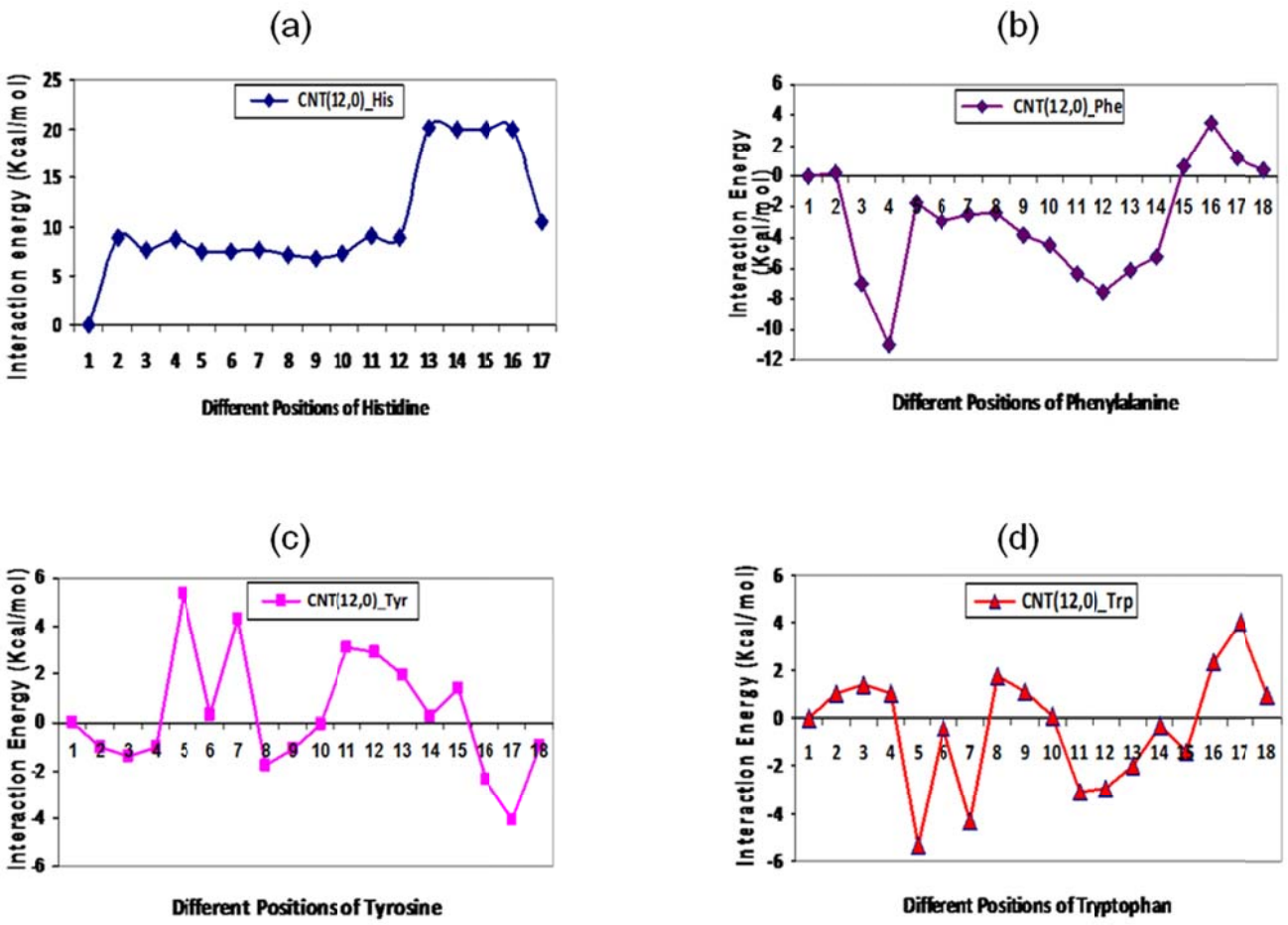

Figure 6.8: The Interaction energy of aromatic amino acids with CNT(12,0) complexes at the B3LYP/3-21G* level of theory.

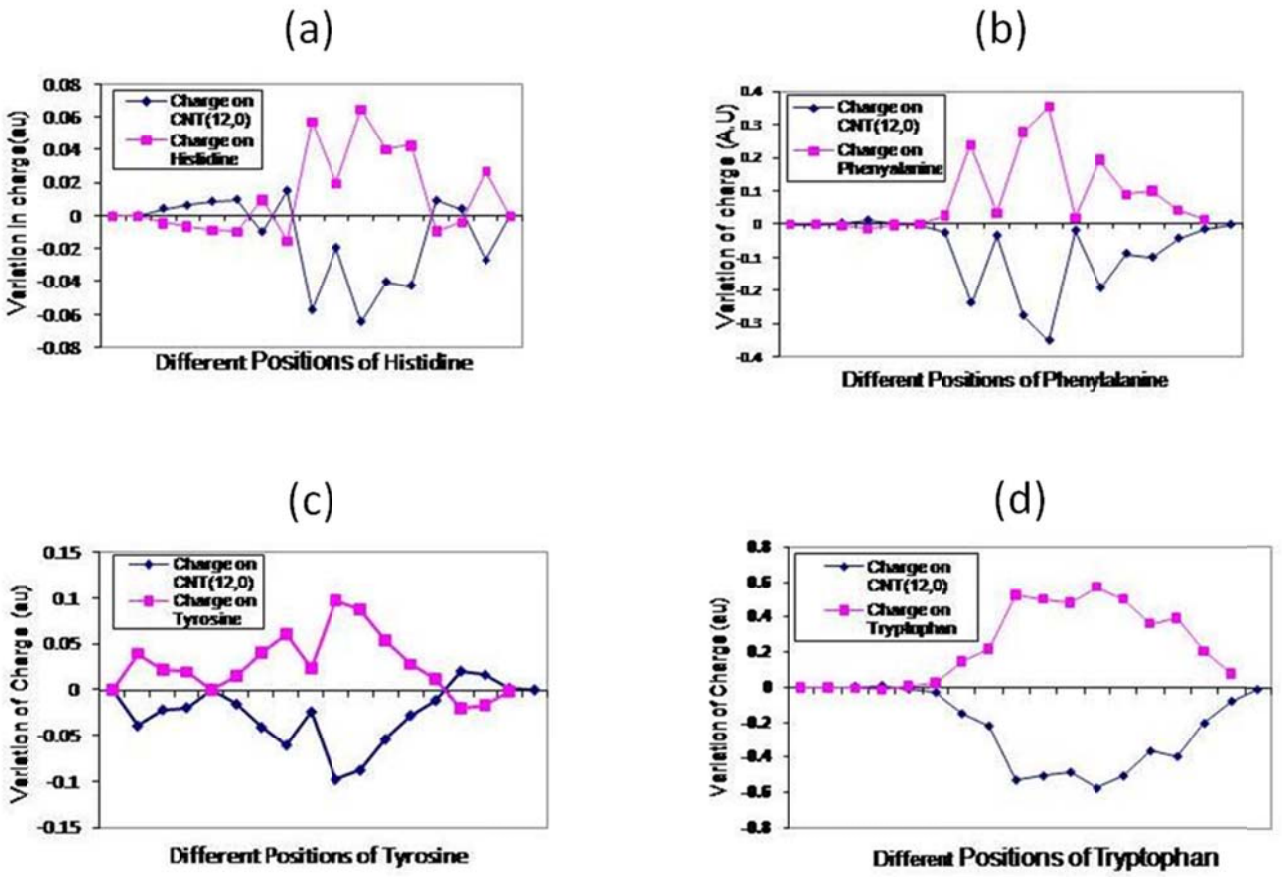

Figure 6.9: Variation of charge on aromatic amino acids and CNT(12,0) at different positions.

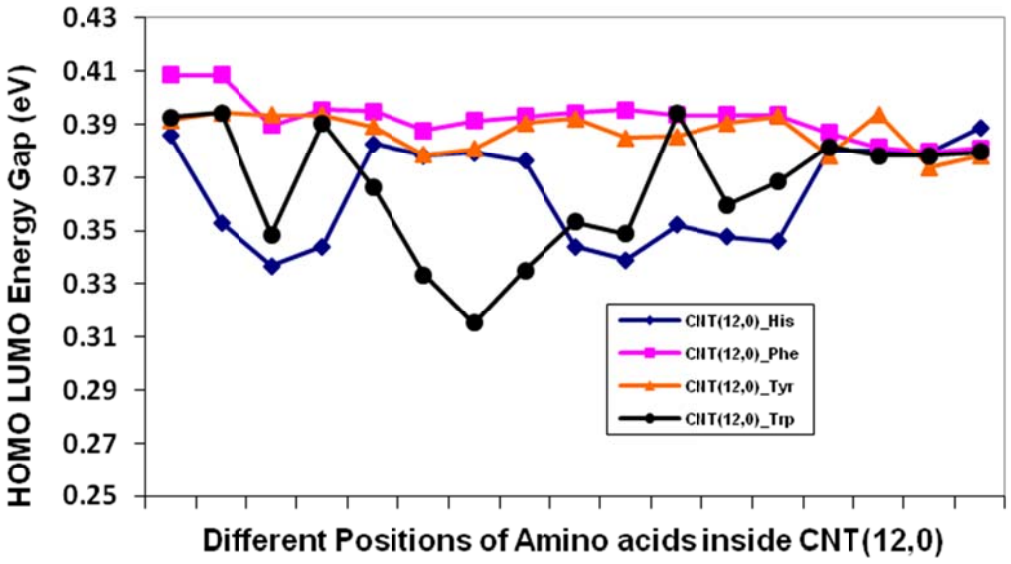

Figure 6.10: The variation of HOMO-LUMO of CNT(12,0) complexes at the B3LYP/3-21G* level of theory.

6.4. Conclusion

The Interaction energies of aromatic amino acids such as histidine, phenylalanine, tyrosine and tryptophan with the single walled carbon nanotube have been comprehensively analyzed. Our calculations reveal that the energy has preferences of aromatic amino acid biomolecule with the doping in CNT (12,0) as well as charge transfer between them. It can be seen from our results that the interaction energy of these biomoleculeS is higher inside CNT (12,0) than that of outside. CNT(12,0) shows weak sensitivity when the aromatic amino acids is oriented outside. On the other hand, compared with all aromatic amino acids, CNT (12,0) has a higher chemical reactivity

towards tryptophan biomolecule due to large π-π orbital distributions and shows the higher interaction energies with tryptophan. The strong interactions between CNT(12,0) and aromatic amino acids induces dramatic changes in the electronic properties of CNT(12,0) and make CNT(12,0) a promising candidate as biosensing materials for amino acids. The Mulliken charge analysis reveals that aromatic amino acids act as charge donor and acceptor in different configuration towards CNT (12,0) and influence the physical properties of carbon materials, which leads to the sensitivity. It has also been found that HOMO-LUMO gap of the carbon nanotube is always affected by the binding of aromatic amino acid biomolecules. Significant changes occur in the HOMO-LUMO gap of CNT (12,0) on biomolecules, which provides a handle to tune the electronic and conductivity properties of CNTs through biomedical complication. These studies can also be applied to develop new carbon based materials and sensing applications, focusing particularly on the mechanism of binding of various biomedical with the CNTs.

6.5. References

1. Allen, M.J., Tung, V.C. and Kaner, R. B., *Chem. Rev.* **2010**, *110*, 132.
2. Hu, J., Odom, T.W. and Lieber, C. M., *Acc. Chem. Res.* **1999**, *32*, 435.
3. Odom, T.W., Huang, J., Kim, P. and Lieber, C. M., *J. phys. Chem. B* **2000**, *104*, 2794.
4. Lui, C. M., Liu, L., Mak, K. F., Flynn, G. W. and Heinz, T. F., *Nature* **2009**, *462*, 339.
5. Umadevi, D., Sastry and G. N., *J. Phys. Chem C.* **2011**, *115*, 9656.
6. Rajesh, C., Majumder, C., Mizuseki, H. and Kaswazoe, Y. A., *J. Chem. Phys.* **2009**, *130*, 124911.
7. Ready, A. S. and Sastry, G. N., *J. Phys. Chem. A.* **2005**, *109*, 8893.
8. Dinadayalane, T. C., Sastry, G. N. and Leszczynski, J., *Int. J. Quantum Chem.* **2006**, *106*: 2920.
9. Zorbas, V., Smith, A. L., Xie, H., Ortiz-Acevedo, A., Dalton, A. B., Dieckmann, G. R., Draper, R. K., Baughman, R. H. and Musselman, I. H., *J. Am. Chem. Soc.* **2005**, *127*, 12323.
10. Ge, C., Du, J., Zhao, L., Wang, L., Li, Y., Yang, Y., Zhou, R., Chai, Z. and Chen, C., *Proc. Natl. Acad. Sci. USA* **2011**, *108*, 16968.
11. Balamurugan, K., Gopalakrishnan, R., Raman, S.S. and Subramanian, V., *J. Phys. Chem. B* **2010**, *114*, 14048.
12. Balamurugan, K., Singham, E. R. A. and Subramanian, V., *J. Phys. Chem. C* **2011**, *115*, 8886.
13. Gopalakrishnan, R., Balamurugan, K., Singham, E. R. A., Sundaraman, S. and Subramanian, V., *Phys. Chem. Chem. Phys.* **2011**, *13*, 13046.
14. Balamurugan, K. and Subramanian, V., *Biopolymers* **2013**, *99*, 357.
15. Ganji, M. D., *Diamond & Related Materials*, **2009**, 18, 662.

16. Lesczynski, J., *Nat. Nanotechnolo.* **2010**, *5*, 633.

17. Stigler, M. Lundqvist, Elia, G., Lynch, I., Cedervall, T. and Dawson, K. A., *Proc. Natl. Acad. Sci. USA* **2008**, *105*, 14265.

18. Jalbout, A. F., *Int. J. Quantum Chem.* **2010**,*110*, 831.

19. Z. Yang, Z. Wang, Z. Tian, P. Xiu and R. zhou, J. chem. Phys. 2012,136, 025103.

20. Wang, C., Li, S., Zhang, R. and Lin, Z., *Nanoscale* **2012**, *4*, 1146.

21. Piao, L., Li, Q. and Li, R., *J. Phys. Chem. Chem. C.* **2012**, *116*, 1724.

22. Schedin, F., Geim, A. K., Morozov, S. V., Hill, E. W., Blake, P., Katsnelson, M. I. and Novoselove, K. S., *Nature Mater.* **2007**, *6*, 652.

23. Zou, M., Zhang, J., Chen, J. and Li, X., *Environ. Sc. Technol.* **2012**, *46*, 8887.

24. Biano, A., Kostarelos, K., Partidos, C. D. and Prato, M., *Chem. Common.(Cambridge)* **2005**, 571.

25. Shi Kam, N. W., Connell, M. O., Wisdom, J. A. and Dai, H., *Proc. Natl. Acad. Sci. U.S.A* **2005**, *102*, 11600.

26. Liu, Z., Cai, W., He, L., Nakayama, N., Chen, K., Sun, X., Chen, X. and Dai, H., *Natl. Nanotechnol.* **2007**, *2*, 47.

27. Rosi, N. L. and Mirkin, C. A., *Chem. Rev.* **2005**,*105*, 1547.

28. Salvador-Morales, C., Townsend, P., Flahaut, E., Venien-Bryan, C., Vlands, A., Green, M. L. H. and Sim, R. B., *Carbon* **2007**, *45*, 607.

29. Liu, Z., Winters, M., Holodniy, M. and Dai, H., *Angew. Chem., Int. Ed.* **2007**, *46*. 2023.

30. Kong, J., Franklin, N. R., Zhou, C. W., Chapline, M. G., Peng, S., Cho, K. J. and Dai, H., *Science* **2000**, *287*, 622; Collings, K., Bradley, M., and Ishigami A., *Zettl.* 2000, *287*, 1801; Shim, M., Javey, A., Wong Shi Kam, N. and Dai, H., *J. Am. Chem. Soc.* **2001**, *123*, 11512.

31. Chem, R. J., Choi, H. C., Bangsaruntip, S., Yenilmez, E., Tang, X., Wang, Q., Chang, Y. and Dai, H., *J. Am. Chem. Soc.* **2004**, *126*, 1563; Beste-man, J., Lee, F., Wiertz, G.

M., Heering H. and Dekker, C., *Nano Lett.* **2003**, *3*, 727; Star, A., Gabriel, J. C. P., Bradley, K. and Gruner, C., *Nano Lett.* **2003**, *3*, 459; Balavoine, F., Schultz, P., Richard, C., Mallouh, V., Ebbesen, T. and Mioskowski, C., *Angew. Chem., Int. Ed.* **1999**, *38*, 1912.

32. Frisch, M. J., Trucks, G. W., Schlegel, H. B., Scuseria, G. E., Robb, M. A., Cheeseman, J. R., Scalmani, G., Barone, V., Mennucci, B., Petersson, G. A., Nakatsuji, H., Caricato, M., Li, X., Hratchian, H. P., Izmaylov, A. F., Bloino, J., Zheng, G., Sonnenberg, J. L., Hada, M., Ehara, M., Toyota, K., Fukuda, R., Hasegawa, J., Ishida, M., Nakajima, T., Honda, Y., Kitao, O., Nakai, H., Vreven T., Montgomery, J. A. Jr., Peralta, J. E., Ogliaro, F., Bearpark, M., Heyd, J. J., Brothers, E., Kudin, K. N., Staroverov, V. N., Keith, T., Kobayashi, R., Normand, J., Raghavachari, K., Rendell, A., Burant, J. C., Iyengar, S. S., Tomasi, J., Cossi, Rega, M., N., Millam, J. M., Klene, M., Knox, J. E., Cross, J. B., Bakken, V., Adamo, C., Jaramillo, J., Gomperts, R., Stratmann, R. E., Yazyev, O., Austin, A. J., Cammi, R., Pomelli, C., Ochterski, J. W., Martin, R. L., Morokuma, K., Zakrzewski, V. G., Voth, G. A., Salvador, P., Dannenberg, J. J., Dapprich, S., Daniels, A. D., Farkas, O., Foresman, J. B., Ortiz, J. V., Cioslowski, J., and Fox, D. J., Gaussian, Inc.,Wallingford CT, 2010.

CHAPTER 7

COMPUTATIONAL STUDY ON THE INTERACTION OF TRYPTOPHAN WITH GRAPHENE AND AL-DOPED GRAPHENE

CHAPTER 7

COMPUTATIONAL STUDY ON THE INTERACTION OF TRYPTOPHAN WITH GRAPHENE AND AL-DOPED GRAPHENE

7.1. Introduction

Graphene, two dimensional new material of carbon, is zero band gap semiconductor materials. The another important form of carbon are one dimensional carbon nanotube and 0 dimensional fullerene which are made by wrapping of planar graphene[1]. These carbon nanostructures are promising materials for biomedical and environmental applications due to unique electronic, thermal, mechanical, and transport properties [2-4]. There are important applications of graphene and its derivatives in different fields such as nanoelectronics, engineering nanocomposite materials, energy storage, field effect transistor, sensors, catalysis, biology, and also medicine have envisaged and that have been investigated [5-13]. The interaction of biomolecules and graphene and its derivatives are also used in biology and medicine applications. The large surface area ($2630 m^2/g$) of graphene facilitates the adsorption of biomolecules and gas molecules.[14-20] Carbon nanostructures such as graphene and CNTs exhibits non-covalent interaction, such as the XH-π, cation-π, anion-π and π-π interaction towards the small gas molecules, metal ions and bio molecules.[21-25] Doping is one of the most efficient method to improve the electronic properties of the materials. The sensitivity of graphene to gas molecules can be enhanced by doping with metal atoms.[26] The detection of adsorbed molecules is possible because of its high conductivity and concordat charge transfer

between the interacting partners[27]. The adsorption strength of molecules on graphene can be tuned by doping graphene with elements such as boron, nitrogen, silicon, aluminum, phosphorus, and sulfur and also by topological defects [28-33]. The usefulness of pristine and doped graphene in the field of catalysis has been widely explored. The adsorption of CO molecules on the intrisinc and Al- doped graphene was studied [26] using DFT method. In these results, the Al-doped graphene (AlG) found strongly chemisorbs CO molecules while intrinsic graphene is weakly adsorbed. Wang et al., have found that the sp2- hybridization affected and changes the electronic properties of the system when B, N, B-N is doped with pure graphene (PG).[34] Lherbier et al., showed that the charge mobility and conductivity of graphene changes when B/N impurity atom is added to its surface.[35] Y. H. Zhang et al., studied that doped graphene strongly interacts with CO, NO and NO_2 while NH_3 interacts weakly.[36] Y. Zou et al., found that the SiG has a higher chemical reactions toward the gas molecules due to doping of silicon atom and shows the higher adsorption energy with CO, O_2, NO_2 and H_2O.[37] The adsorption of modified nucleobases(MBs) on the surface of graphene(G), boron-doped graphene(BG), nitrogen-doped graphene(NG) and silicon-doped graphene(SiG) has been investigated using electronic structure calculation and associated analysis methods. It was found from the calculations that the MBs stack with the surface of G, BG, NG, and SiG models and that the π-π stacking interaction plays a dominant role in the stabilization of the intermolecular complexes[38]. In the present study, the AlG to improve its bio sensing efficiency and selectivity towards the histidine were theoretically investigated. On the other hand, the effect of doping of the graphene sheet on the interaction energy has been estimated. The charge transfer that occurred during the

complex formation has also been explored. The change in the HOMO-LUMO energy gap of graphene and AlG upon the binding of tryptophan (Trp) has also been estimated.

7.2. Computational Methodology

The calculations of the interaction between graphene/AlG and Trp (Trp) were carried out using the recently developed density functional theory. The geometrical calculations of all structures have been done by using B3LYP method and 3-21G* basis set. Initially, the individual Trp amino acids was established on PG and AlG and geometric optimization calculations were performed within density functional theory using Gaussian 09 suite program [39]. It is important to note that competing geometrical configuration was tested, but those shown are the lowest energy species feasible for the interaction of the compounds. The present work is limited to the aromatic amino acids such as Trp. To evaluate the interaction energy (IE) of the Trp(X) on the G and AlG is calculated by following equation.

$$IE = E_{G\_X/AlG\_X} - E_{G/AlG} - E_X \quad (7.1)$$

Here E_{G_X} and E_{AlG_X} represents the total energy of complex molecular system. E_G/E_{AlG} and E_X represent the total energies of the graphene and Trp amino acids, respectively. The individual Trp was placed parallel to the surface of PG and AlG at the 3Å distance. The variation of the charge on Trp as well as on PG and AlG was calculated when the individual Trp molecule is kept at the 3Å distance from its surface. The charge transfer has been considered as the sum of all the atoms in the PG and AlG model system. Positive charge transfer values indicate the transfer of charge from the G and AlG to the

molecules, while negative charge values indicate the transfer of charge from the Trp to the G and AlG. The HOMO-LUMO energy gap of PG and AlG as well as their complexes was considered at B3LYP/3-21g* level of theory were also calculated. All calculations were carried out using the Gaussian09 program package.

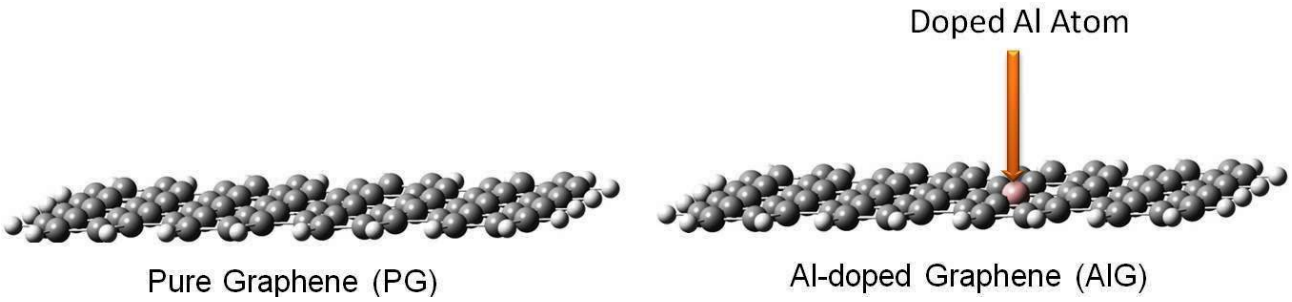

Figure 7.1: Top view of the geometrically optimized structure of pure and AlG model system considered in this study

7.3. Result and discussion

The optimized structure of PG and AlG and their complexes with Trp are shown in Figure 7.1 and 7.2. The initial configuration of Trp was assigned so that these are oriented exactly parallel to the PG and AlG at 3Å from its surface. In this work, PG and AlG were considered to study the interaction of Trp with π-π noncovalent interaction towards carbon nano materials. Table 7.1 and Table 7.2 summarizes our results on HOMO energy, LUMO energy and HOMO-LUMO energy gap of isolated PG (PG) and AlG at B3LYP method and 3-21g* basis set. Table 2 summarizes our results on interaction energy, charge on Trp, PG and AlG (Q, Mulliken charge), HOMO energy, LUMO energy and HOMO-LUMO energy using the same basis set. The visualization of HOMO and LUMO energy density are shown in Figure 7.3 and Figure 7.4.

Subsequently, we look at the binding of the PG and AlG with Trp and the trend in the charge transfer. The HOMO-LUMO energy gap of PG and AlG with the interaction of Trp were also investigated. When one Al atom is substituted for one C atom in graphene sheet, the optimized configuration of graphene sheets is dramatically distorted. The Al atom introduces the deformation of the six-membered ring (6MR) near the doping site to relieve stress as a result the Al atom protrudes out of the graphene sheet. The optimized carbon-dopant atom distance (Al-C) is 1.748Å at B3LYP/3-21G* which in agreement with the previous study.[40]

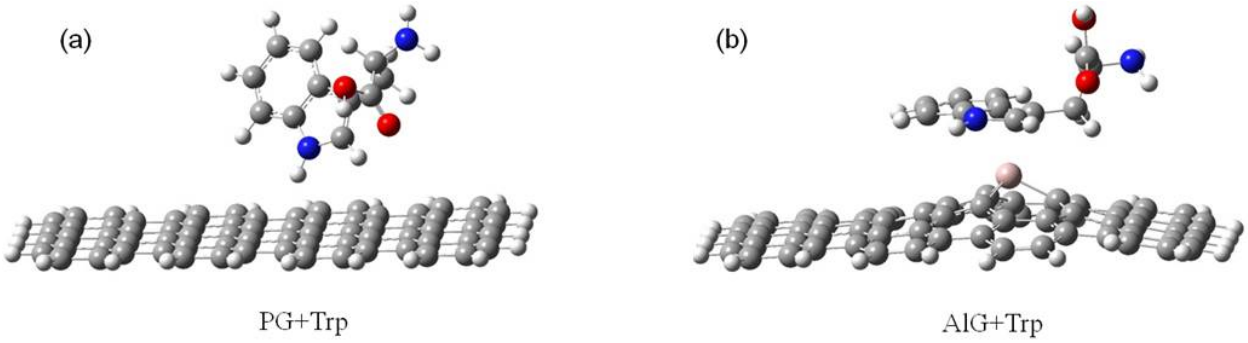

Figure 7.2: The optimized geometry of PG and AlG with Trp biomolecule complexes by B3LYP method and 3-21G* basis set.

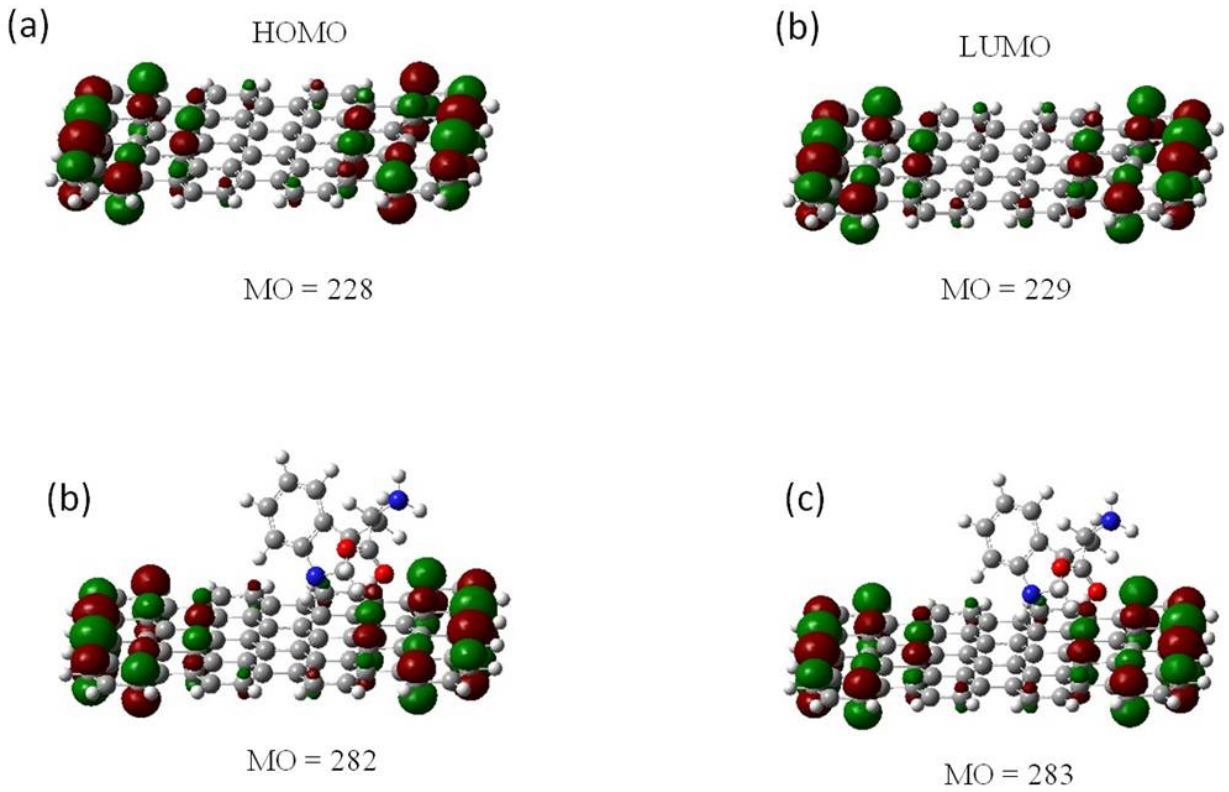

Figure 7.3: The HOMO and LUMO of complexed and non-complexed forms of PG at 0.02 isovalue

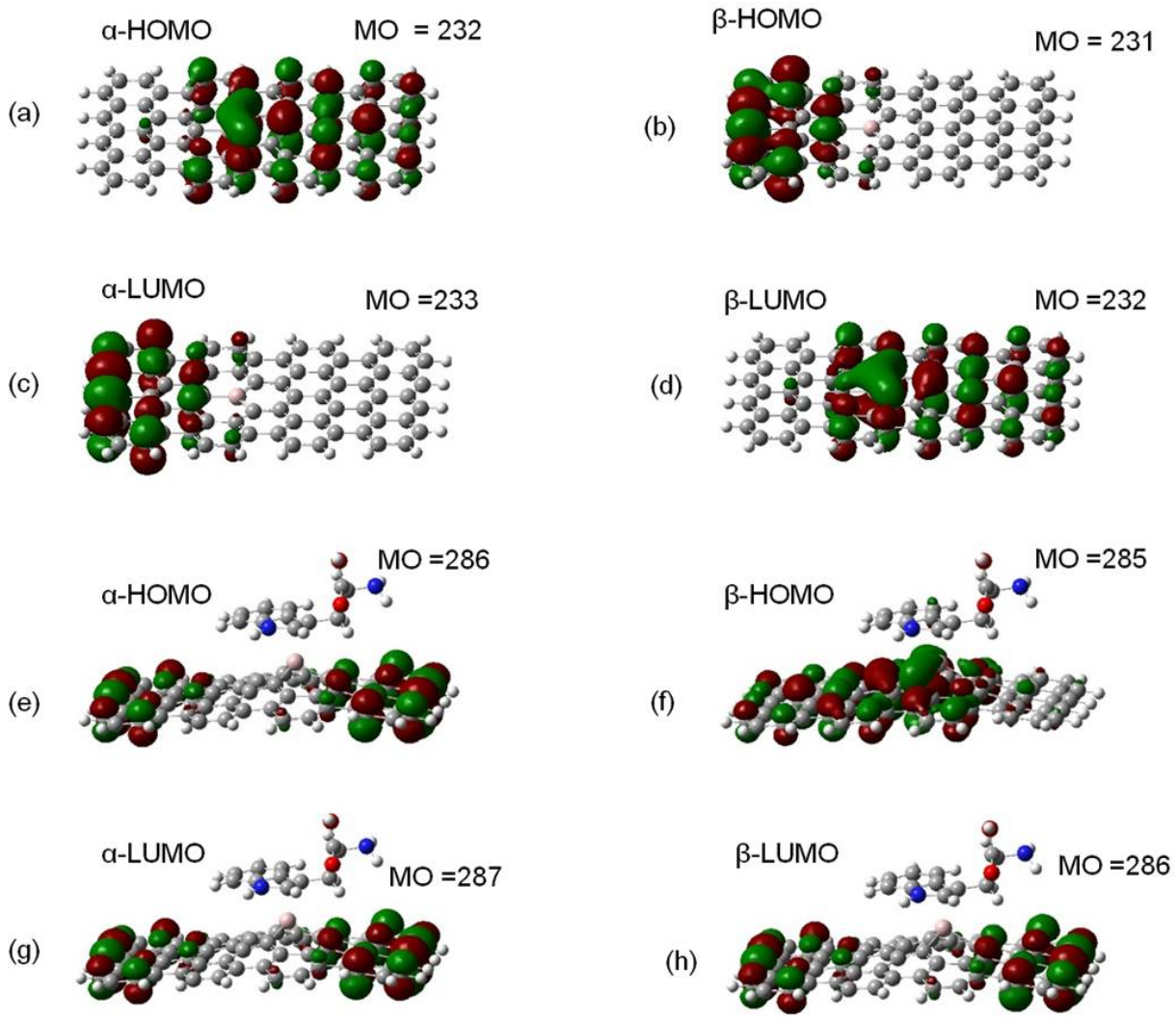

Figure 7.4: The HOMO (α and β) and LUMO (α and β) of complexed and non-complexed forms of AlG at 0.02 isovalue.

Table 7.1: HOMO Energy, LUMO energy and HOMO-LUMO Energy Gap(eV) B3LYP method and 3-21G* basis set.

Molecular structure	HOMO Energy (eV)	LUMO Energy (eV)	HOMO-LUMO Energy Gap(eV)
Pure Graphene (PG)	-3.8431	-3.5778	0.2653
Al-doped Graphene (AlG)	α = - 4.6262 β = - 4.5381	α = - 2.8330 β = - 3.3620	1.4846

Table 7.2: Interaction Energy(kcal/mole), charge transfer, HOMO Energy, LUMO energy and HOMO-LUMO Energy Gap(eV) at B3LYP method and 3-21G* basis set.

Complex Molecular structure	Interaction Energy (kcal/mole)	Charge on Trp (au)	Charge on G/AlG (au)	Molecular Sheet Distance (Å)	HOMO Energy (eV)	LUMO Energy (eV)	HOMO-LUMO Gap (eV)
G + TRP	1.813	-0.0064	+0.0064	5.527	-3.8975	-3.6319	0.2656
AlG +TRP	-48.177	-0.01386	+0.01386	2.489	α = -4.1250 β = -4.3031	α = -2.7799 β = -3.0896	1.2892

7.3.1. Interaction Energy and charge transfer

The Trp form π-π type complex with the PG and AlG that are shown in Figure 7.2. It is observed the interaction energy of Trp complexes with PG and AlG when the Trp molecule is kept parallel to the PG/AlG surface at 3Å distance. Table 7.1 and Table 7.2

displays the interaction energy, charge transfer, molecule sheet distance and HOMO-LUMO energy of Trp complexes with PG and AlG at B3LYP method and 3-21G* basis set.

The Trp biomolecule shows different interaction configurations on PG and AlG, showing a more complicated interaction mechanism. On graphene, the configuration with the one hydrogen atoms of - NH_2 pointing towards the PG plane is the favorable one [Figure 7.2(a)] which gives an interaction energy and molecule distance of 1.813kcal/mole and 5.527Å (distance measured between C73 and C108), respectively which indicates a weak interaction between Trp and the PG. On the AlG, Trp is attached to the Al (90) atom with the C(108) atom pointing at the sheet, which gives an interaction energy of -48.177kcal/mole and an Al-C distance of 2.489Å [as shown in Figure 7.2(b) and Table 7.2]. The charge transfer from graphene to Trp is 0.0064a.u. which indicates that the graphene behaves as charge donor and Trp biomolecule as charge acceptor. This result indicates that the interaction is weak in nature due to very small adsorption energy and charge transfer. The interaction energy of Trp on AlG is much higher than that on the PG, which attributes to the strong interaction between the electron –deficient Al atom and the electron –accepting C atom of Trp. The molecular distance between Al and C is 2.053Å. The high interaction energy and low molecular sheet distance indicates the strong interaction. This strong interaction is also evident in the electronic total charge density on AlG system, which shows the large electron density overlap.

7.3.2. HOMO- LUMO energy gap

The HOMO-LUMO energy gap is defined as the difference between lowest unoccupied molecular orbital and highest occupied molecular orbital. It is the electronic property of any molecular system which is helpful to design new materials. Quantum mechanically, the interaction between two reactants takes place due to the of interaction of frontier molecular orbitals.[41] After interaction of Trp spices on the surface of AlG, some changes occur in its HOMO and LUMO energies. In order to notice such depiction in the case of carbon materials, the calculated HOMO-LUMO energy gap of the PG and AlG in the Free State and in with the Trp complexed. Figure 7.3 and Figure 7.4 shows the HOMO-LUMO outlooks for PG and AlG along with Trp complexes. As seen Figure 3, the HOMO of PG is mostly restricted on the C-C bonds whereas the the LUMO is situated on the conflicted site. After Al is doped on the PG, both α-HOMO and β-LUMO is dislocated on Al atom which results in more reactivity of AlG compared to PG which is shown in Figure 7.4(a) and 7.4(d). In general, in the case of π-π complexes, the HOMO-LUMO energy gap of graphene varies with orientation of Trp on the PG and AlG. It has been shown that the energy gap of PG is not significant but when the Trp is adsorbed on AlG then significant changes in HOMO-LUMO energy gap is observed [as shown in Table 7.1 and Table 7.2]. So it can be said that the variation in HOMO-LUMO energy gap of the graphene upon binding with the the Trp biomolecule is significant.

7.4 Conclusion

The interaction energy of Trp with the PG and AlG has been comprehensively analysed. These calculations reveals preferential order of binding of Trp for pure and AlG. It can be seen from the results that the interaction energy of Trp biomolecule is higher for the AlG than for the graphene. The PG shows weak sensitivity to the Trp biomolecule. AlG has a higher chemical reactivity towards Trp due to the doping of Al atom than PG and as it shows the AlG exhibits strong interaction towards the Trp. The strong interactions between AlG and Trp induces dramatic changes in the electronic properties of AlG and make AlG a promising candidates as bio-sensing materials for biomolecules. The Mulliken charge analysis reveals that Trp acts as charge acceptor and graphene as donor in different configuration towards the PG and AlG and influence the physical properties of carbon materials, which leads to the sensitivity. Significant changes occur in the HOMO-LUMO energy gap on PG and AlG on interacting with biomolecule, which provides a handle to tune the electronic and conductivity properties of graphene through biomolecule complexation. These studies can also be applied to develop new carbon based materials and sensing applications, focusing particularly on the mechanism of binding of Trp biomolecule with the graphene. It is hoped that our results would be helpful to develop novel carbon material based bio sensors.

7.5. References

1. Allen, M.J., Tung, V.C., Kaner, R. B., Chem. Rev. **2010**, 110, 132.

2. Hu, J.; Odom, T.W.; Lieber, C.M., Acc. Chem. Res. **1999**, 32, 435.

3. Odom, T.W., Huang, J., Kim, P., Lieber, C.M., J. phys. Chem. B **2000**, 104, 2794.

4. Lui, C.M., Liu, L., Mak, K.F., Flynn, G.W., Heinz, T.F., Nature **2009**. 462, 339.

5. Xuan, Y., Wu, Y. Q., Shen, T., Qi, M., Capano, M. A., Cooper, J. A., Ye, P. D., Appl. Phys. Lett. **2008**, 92, 013101.

6. Yang, X. M., Tu, Y. F., Li, L., Shang, S., Tao, X. M., ACS Appl. Mater. Interfaces **2010**, 2, 1707.

7. Liu, C., Alwarappan, S., Chen, Z. F., Kong, X. X., Li, C. Z., Biosens. Bioelectron. **2010**, 25, 1829.

8. Stoller, M. D., Park, S. J., Zhu, Y. W., An, J. H., Ruoff, R. S., Nano Lett. **2008**, 8, 3498.

9. Li, X., Wang, X., Zhang, L., Lee, S., Dai, H., Science **2008**, 319, 1229.

10. Lu, C. C., Lin, Y. C., Yeh, C. H., Huang, J. C., Chiu, P. W., ACS Nano **2012**, 6, 4469.

11. Lu, C. H., Yang, H. H., Zhu, C. L., Chen, X., Chen, G. N., Angew. Chem., Int. Ed. **2009**, 48, 4785.

12. Qu, L. T., Liu, Y., Baek, J. B., Dai, L., ACS Nano **2010**, 4, 1321.

13. Liu, Z., Robinson, J. T., Sun, X. M., Dai, H. J., J. Am. Chem. Soc. **2008**, 130, 10876.

14. Qin, Wu., Li, Xin., Bian, W. W., Fan, X. J., Qi, J. Y., **2010**, 31, 1007.

15. Umadevi, D., Sastry, G. N., J. Phys. Chem. Lett. **2011**, 2, 1572.

16. Rajesh, C., Majumder, C., Mizuseki, H., Kawazoe, Y. A., J. Chem. Phys. **2009**, 130, 124911.

17. Romero, H. E., Joshi, P., Gupta, A. K., Gutierrez, H. R., Cole, M. W., Tadigadapa, S. A., Eklund, P. C., Nanotechnology **2009**, 20, 245501.

18. Huang, B., Li, Z., Liu, Z., Zhou, G., Hao, S., Wu, J., Gu, B. L., Duan, W., J. Phys. Chem. C **2008**, 112, 13442.

19. Leenaerts, O., Partoens, B., Peeters, F., Phys. Rev. B: Condens. Matter Mater. Phys. **2008**, 77, 125416.

20. Lee, J., Choi, Y. K., Kim, H. J.; Scheicher, R. H.; Cho, J. H., J. Phpys. Chem. C **2013**, 117, 13435.

21. Umadevi D, Panigrahi S, and Sastry, G.N., Acc. Chem. Res. **2014**, 47, 2574.

22. Vijay, D., Sastry, G. N,. Chem. Phys. Lett., **2010**, 485, 235.

23. Shi G.; Ding Y.; Fang H., J. Comput. Chem. **2012**, 33, 1328.

24. Grabowski S. J, Lipkowski P., J. Phys. Chem. A **2011**, 115, 4765.

25. Mahadevi A. S and Sastry G.N., Chem. Rev. **2016**, 116, 2775.

26. Ao, Z. M.; Yang, J.; Li, S.; Jiang, Q., Chem. Phys. Lett. **2008**, 461, 276.

27. Mohanty, N.; Berry, V,. Nano Lett. **2008**, 8, 4469.

28. Dai, J.; Yuan, J.; Giannozzi, P., Appl. Phys. Lett. **2009**, 95, 232105.

29. Ao, Z.; Li, S.; Jiang, Q. **2010**, 150, 680.

30. Kaniyoor, A., Jafri, R. I., Arokiadoss, T., Ramaprabhu, S., Nanoscale **2009**, 1, 382.

31. Zhang, Y. H.; Chen, Y. B.; Zhou, K. G.; Liu, C. H.; Zeng, J.; Zhang, H. L.; Peng, Y. Nanotechnology **2009**, 20, 185504.

32. Ao, Z. M., Yang, J., Li, S.; Jiang, Q. Chem. Phys. Lett. **2008**, 461, 276−279.

33. Ao, Z. M.; Li, S.; Jiang, Q., Phys. Chem. Chem. Phys. **2009**, 11, 1683.

34. Wang X., Sun G., Routh P., Kim D.H., Huang W.and P., Chem, Chem. Soc. Rev., **2014**, 43 7067.

35. Lherbier A, Blase RX, Niquet Y, Triozon F, Roche S, Phys. Rev. Lett., **2008**, 101, 036808

36. Zhang Y.H., Chen Y.B., Zhou K.C., Liu C.H., Zeng J., Zhang H.L and Peng Y., Nanotechnology, **2009**, 20, 185504.

37. Zou Y, Li F, Zhu ZH, Zhao MW, Xu XG and Su X.Y., Eur. Phys. B. **2011**, 81, 475.

38. Mudedla, S.K.; Balamurugan and Subramanian V., J. Phys. Chem. C **2014**, 118, 16165

39. Frisch, M. J., Trucks, G. W., Schlegel, H. B., Scuseria, G. E., Robb, M. A., Cheeseman, J. R., Scalmani, G., Barone, V., Mennucci, B., Petersson, G. A., Nakatsuji, H., Caricato, M., Li, X., Hratchian, H. P., Izmaylov, A. F., Bloino, J., Zheng, G., Sonnenberg, J. L., Hada, M., Ehara, M., Toyota, K., Fukuda, R., Hasegawa, J., Ishida, M., Nakajima, T., Honda, Y., Kitao, O., Nakai, H., Vreven T., Montgomery, J. A. Jr., Peralta, J. E., Ogliaro, F., Bearpark, M., Heyd, J. J., Brothers, E., Kudin, K. N., Staroverov, V. N., Keith, T., Kobayashi, R., Normand, J., Raghavachari, K., Rendell, A., Burant, J. C., Iyengar, S. S., Tomasi, J., Cossi, Rega, M., N., Millam, J. M., Klene, M., Knox, J. E., Cross, J. B., Bakken, V., Adamo, C., Jaramillo, J., Gomperts, R., Stratmann, R. E., Yazyev, O., Austin, A. J., Cammi, R., Pomelli, C., Ochterski, J. W., Martin, R. L., Morokuma, K., Zakrzewski, V. G., Voth, G. A., Salvador, P., Dannenberg, J. J., Dapprich, S., Daniels, A. D., Farkas, O., Foresman, J. B., Ortiz, J. V., Cioslowski, J., and Fox, D. J., Gaussian, Inc.,Wallingford CT, 2010.

40. Dai, J. Y. and Yuan, J. M., Phys. Rev. B **2010**, 81, 165414.

41. Samadizadeh, M., Rastegar, S.F. and Peyghan , A. A., Phys. E **2015**, 69, 75.

CHAPTER 8

GENERAL CONCLUSION

CHAPTER 8

GENERAL CONCLUSION

The result discussed in the present work lead to some important conclusion which may be summarized as follows:

A. The density functional theory (DFT) B3LYP with basis 6-31G** reproduce the proper geometry of the molecules under study. M062X method also provides other properties with accuracy. These methods can be used for geometry optimization with frequency calculation to check all frequencies must be real. The charge, geometrical parameters etc. thus obtained can be used for further calculations and interpretations of molecular properties.

B. The binding energy preferences of aromatic amino acids are different in both positions respectively i.e. in exterior and interior positions of SWCNTs. The binding energy of aromatic amino acid is greater in interior than the exterior position of SWCNTs. For the exterior position the preferential order of the interaction for the aromatic amino acids with SWCNTs was histidine<tyrosine<tryptophan<phenylalanine while for the interior position the order is histidine<tyrosine<phenylalanine< tryptophan. The tryptophan prefers to bind to the inner side wall of carbon nanotube. The significant changes occur in the HOMO-LUMO gap of the CNT(12,0) on the aromatic amino acids.

C. The adsorption energy of various small gas molecules such as CCl_4, CH_4, NH_3, CO_2, CO, NO_2, CCl_2F_2, SO_2, CF_4 and N_2O with the pure and Al-doped

graphene(graphene@Al) has preferences of small gas molecules with the doping in graphene as well as molecule sheet distance. It can be seen that the adsorption energy of these gas molecule is higher for the Al-doped graphene than for the pure graphene. Pure graphene shows weak sensitivity to the all gas molecules. Compared with pure graphene, graphene@Al has a higher chemical reactivity towards all gas molecules due to the doping of Al atom and shows the higher adsorption energy with NO_2, NH_3 and CO_2. The strong interactions between graphene@Al and the adsorbed molecules induces dramatic changes in the electronic properties of graphene@Al and make graphene@Al a promising candidates as gas sensing materials for NO_2, NH_3 and CO_2. The Mulliken charge analysis reveals that gas molecule acts as charge donor and acceptor in different configuration towards the pure and Al-doped graphene and influence the physical properties of carbon materials, which leads to the sensitivity. It has also been found that HOMO-LUMO gap of the carbon nanotube is always affected by the binding of the small gas molecules. Significant changes occur in the HOMO-LUMO gap on pure graphene and graphene@Al on interacting with gas molecules, which provides a handle to tune the electronic and conductivity properties of graphene through gas molecule complexation.

D. The calculation of binding of a series of alkaline earth metal ions (Be^{+2}, Mg^{+2}, Ca^{+2},) with SWCNT reveal that the interaction energy preferences of metal ions varies at different positions of CNT (10, 0). It was observed that the order of interaction energy of these metal ions is $Ca^{+2} > Mg^{+2} > Be^{+2}$. The HOMO-LUMO gap of the CNT is always affected by the binding of these alkaline earth metal ions.

E. The study of interaction energies of aromatic amino acids such as histidine, phenylalanine, tyrosine and tryptophan with the SWCNT reveal that the energy has preferences of aromatic amino acid biomolecule with the doping in CNT (12,0) as well as charge transfer between them. It can also be observed that the interaction energy of these biomolecule is higher inside CNT (12,0) than that of outside. CNT(12,0) shows weak sensitivity when the aromatic amino acids oriented outside.

F. The study of interaction energy of TRP with the graphene (G) and Al doped graphene (AlG) reveal that the interaction energy has preferences of biomolecule with the doping in graphene as well as molecule sheet distance. Significant changes occur in the HOMO-LUMO gap on PG and AlG on interacting with biomolecule, which provides a handle to tune the electronic and conductivity properties of graphene through biomolecule complexation.

G. Developing chemical and bio sensors based on carbon materials has become an area of significant research interest since the physical and electronic properties of these materials are vulnerable to external enviroment. It is hope that our study will be helpful to develop novel carbon material based bio sensors.

LIST OF PUBLICATIONS

Published Papers:

[1] Adsorption of small gas molecules on pure and Al-doped graphene sheet: a quantum mechanical study

Dharmveer Singh, Asheesh Kumar, Devesh Kumar

Bulletin of Material Science, DOI 10.1007/s12034-017-1478-x.

[2] Interaction of Amino Acids with Single Walled Carbon Nanotube: A Quantum Mechanical Study

Dharmveer Singh, Asheesh Kumar, Devesh Kumar

International Journal of Chemical and Pharmaceutical Analysis, **2016**, *3(2)*, 1.

Communicated Papers:

[1] Quantum Mechanical Study of Nucleic Acid Interaction with Carbon Nanotubes in interior and at exterior positions

Asheesh Kumar, **Dharmveer Singh**, Deep Kumar, Devesh Kumar

Available Online at

http://www.ijcpa.in

January-March 2016

International Journal of
CHEMICAL AND PHARMACEUTICAL
ANALYSIS

eISSN: 2348-0726 ; pISSN : 2395-2466

Research Article | Volume-3 | Issue-2 | Article ID: 935

INTERACTION OF AMINO ACIDS WITH SINGLE WALLED CARBON NANOTUBE: A QUANTUM MECHANICAL STUDY

Dharmveer Singh, Asheesh Kumar, Devesh Kumar*

Department of Applied Physics, School of Physical Sciences
Baba sahib Bhimrao Ambedkar University, VidhyaVihar, Rae Bareilly Road, Lucknow, India.

***Corresponding Author:** *Email:* dkclcre@yahoo.com

Received: 18 January 2016 / Revised: 20 February 2016 / Accepted: 21 February 2016 / Available online : 31 March 2016

ABSTRACT

In the present study, the interaction of Aromatic amino acids with zig-zag Single Walled Carbon Nanotube CNT(12,0) is investigated using density of functional theory. It is found that among the four aromatic amino acid such as histidine, phenylalanine, tyrosine, tryptophan considered for the study, tryptophan has the strongest binding energy in the interior position of SWCNT than in the exterior position. The HOMO-LUMO energy gap of the complex molecular structure has been explored by B3LYP/6-31G* method before and after interaction. This work revealed that the HUMO-LUMO energy gap of the complex molecular structure with B3LYP/6-31G* method are in good agreement with the other theoretical studies. Our results are expected to serve useful insight to comprehend the binding affinity of the aromatic amino acid with zig zag CNT.

Keywords **–** DFT,Aromatic amino acids, single walled carbon nanotube, noncovalent interaction, CNT based biosensors.

1. INTRODUCTION

Carbon nanostructures (CNSs) such as graphene and carbon nanotube are one of the most important materials in the field of recent research in nano sensors. The carbon nano-structures such as graphene and carbon nanotube have emerged as the promising nanomaterials for biomedical and environmental applications due to unique physical and chemical properties such as a tunable band gap, room temperature Hall effect, high mechanical strength (200 times greater than steel), and high elasticity , thermal conductivity and high entangle network structure. The exceptional electrical properties of graphene (such as, high charge mobility and capacity, highly tunable conductance) makes it as an ideal for sensing applications.[1,2,3] Carbon nanostructures (CNSs) exhibit the non-covalent interaction such as cation-π, π-π and CH-π towards the small molecules, metal ions and bio molecules as amino acid, nucleic acids. The noncovalent interaction of amino acids with various substrates and their proton affinity values have been studied.[4,5] The importance of aromatic amino acid for the interaction between a peptide and a single walled carbon nanotube has also been studied through experiment.[6] A recent experimental study revealed that π-π noncovalent interactions between CNTs and the aromatic residue (Trp, Phe, Tyr) of the proteins were found to play a significant role in determining the strength of the CNT-protein interaction.[7]Subramanium et al. have brought out new insight to study the interaction of CNT and peptides.[8,9,10,11] The interaction between these can be seen in figure1. The study of noncovalent carbonaceous materials play a vital role in understanding various carbon nanostructures, such as diagnosis of life threatening diseases (sensors), cancers therapy (drug delivery system), DNA sequencing (personalized medicines).[12,13,14] Developing sensors based on CNT-biomolecule composites for amplified detection methods is an area of recent interest, and such sensors can be

efficiently used for the detection of various carbon nanostructures as well as different biomaterials such as DNA, protein, and so on**.**[15]Umadevi et al. investigated the adsorption of biological molecules such as amino acids, enzymes, antibodies and nucleic acids, metal ions as Na^{+}, Ka^{+}, Ca^{+2}, Mg^{+2}, Be^{+2} and small molecules as CO_2, H_2O, CO, NH_3, H_2O, CH_4 on the surface of graphene/CNTs along with thesignificant changes in the energy as well as sensitivity and specificity of biosensor.[16-20] Wang et al.[21] carried out a study to understand the affinity of the specific peptides to CNTs and delineate contribution of the constituents of amino acids to the binding strength of the peptides with CNTs. Further the studies on the structure-function-affinity of the peptides with the CNT have shown that phenylalanine has an important role to play in enhancement of the adsorption of peptides on the CNTs**.**[22] Li et al. demonstrated that polytryptophan peptides bind more strongly through their aromatic rings with the CNTs compared to the polylysine**.**[23] However, the role of interaction of these bio molecules with the CNTs and the extent to which the nanotube can be used is not understood much for these biological systems. Other studies on the adsorption of polynuclear aromatic compounds to CNTs, suggest that the π-π interactions play a critical role in the binding strength towards the nanotubes.[24,25] Dai and co-workers have investigated the potential of carbon nanotube to be used as gas sensors for detection of molecules such as NO_2 and NH_3**.**[26]Schedin et al. reported their experimental observation that graphene – based sensors could detect even the adsorption of individual gas molecules**.**[27] Carbon nanostructures can absorb a number of species such as gas molecule, metal ions, polymers, organic molecules, and bio molecules such as proteins, nucleobases and DNA on their surfaceand these adsorption properties provide opportunities for potential industrial applications**.**[28-29] Several studies have been carried out on the immobilisation of proteins and nucleic acid on nanotube.[30,31,32] However recent studies elaborate on the appreciable changes in nanotube conductivity as bio molecules which are immobilised, directly or indirectly, on the CNT sidewalls.[33,34,35] Roman et al used DFT method to investigate the adsorption of any few amino acids on (3, 3) CNT.[36] In the present work detailed theoretical calculations has been done for interaction between aromatic amino acids and single walled carbon nanotube (CNT(12, 0)) using DFT method.

2. COMPUTATIONAL DETAILS

The calculations of the interaction between CNT and phenylalanine complex system was carried out using the density functional theory. The geometry of all the structures was optimized using B3LYP/6-31G* method for isolated individual structures as well as complex structures. In this study we calculated the binding energy of the complex system using the following equation (1).

$$\text{Binding Energy} = E_{CNT\_A} - E_{CNT} - E_{A} \quad \ldots\ldots\ldots\ldots\ldots\ldots \quad (1)$$

The binding energy is defined as the difference between the total energy of the isolated individual structures (E_{CNT} and E_{A}, CNT = carbon nanotube and A = amino acids) and the total energy of the CNT-Amino acid complex (E_{CNT_A}). All calculations were done using Gaussian 09 program suit. [37] The complex structures thus generated by placing amino acid parallel to the surface of SWCNT at a distance of 3Å. These complex structures was optimized using B3LYP method and 6-31G* basis set. We also calculated the highest occupied molecular orbital (HOMO) and lowest unoccupied molecular orbital (LUMO) for the results thus obtained.

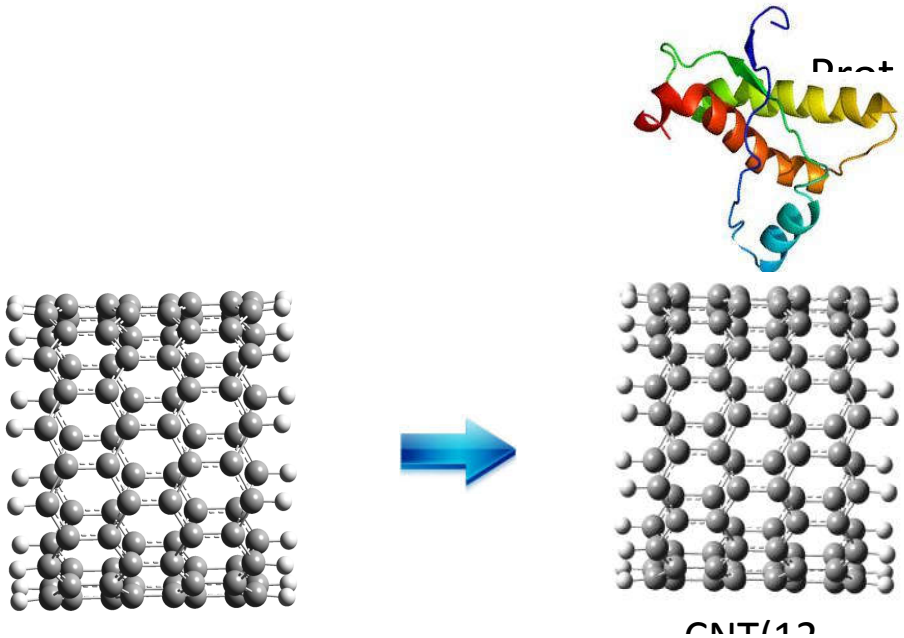

\Fig.1: The geometrical optimization of zigzag single walled carbon nanotube [CNT(12,0)] and representation of interaction of protein carbon nanotube.

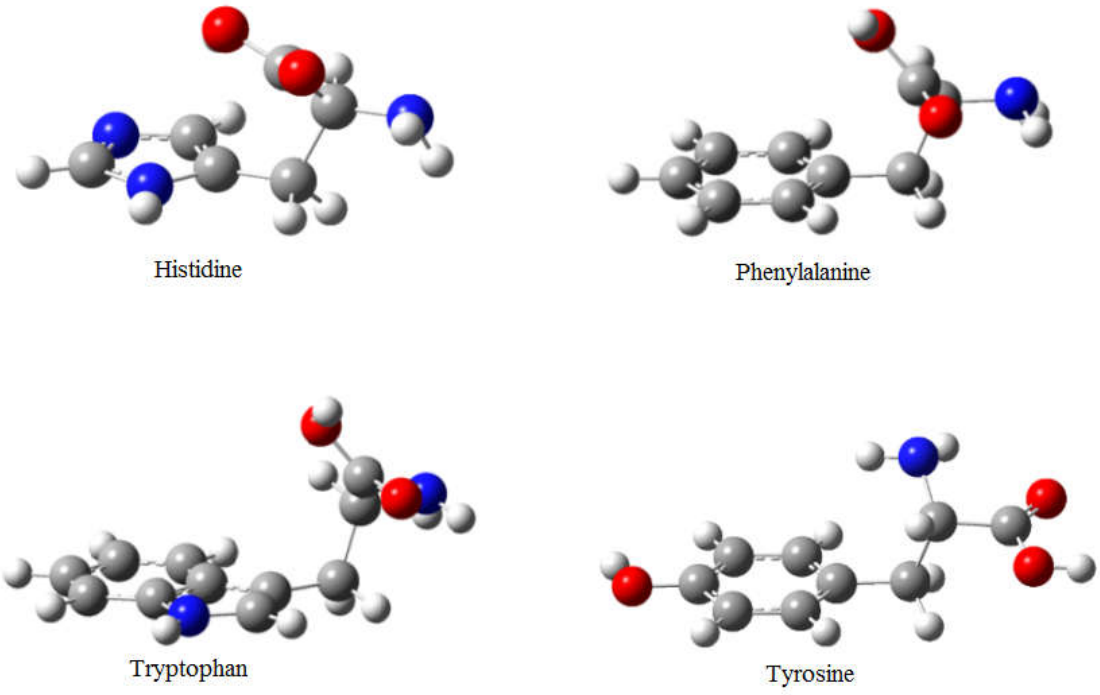

Fig. 2: The geometrical optimized geometry of aromatic amino acids.

3. RESULTS AND DISCUSSION

The optimized structure of aromatic amino acids and single walled carbon nanotube are shown in fig.1 and 2. The initial configurations of all four aromatic amino acid bases were assigned so that their aromatic rings are oriented exactly parallel to the CNT surface. The Fig 3 and Fig 4 shows the aromatic amino acid interaction in exterior and interior position of CNT (12,0). Aromatic amino acid is placed in two different positions i.e. inside the CNT and outside the CNT placed parallel to the surface of CNT at a distance of 3Å to make sure that π-π interaction takes place which plays a crucial role in the non-bonded interaction. The binding strength of all the aromatic amino acid in both the positions (i.e. interior and exterior) is found to bind with different affinity. The calculated binding energy of the aromatic amino acids such as histidine, phenylalanine, tyrosine and tryptophan in the exterior position of carbon nanotube is -7.952, -0.170, -0.649 and -0.791kcal/mole and interior position is -2.891, 4.656, 1.778 and 8.447 kcal/mole respectively. From these results it can observe that the binding strength for tryptophan is greater in interior position than in the exterior position of the CNT (12, 0). It is also observed that the binding energy of the aromatic amino acids is greater in interior position than in the exterior position of the single walled carbon nanotube (CNT (12, 0)).

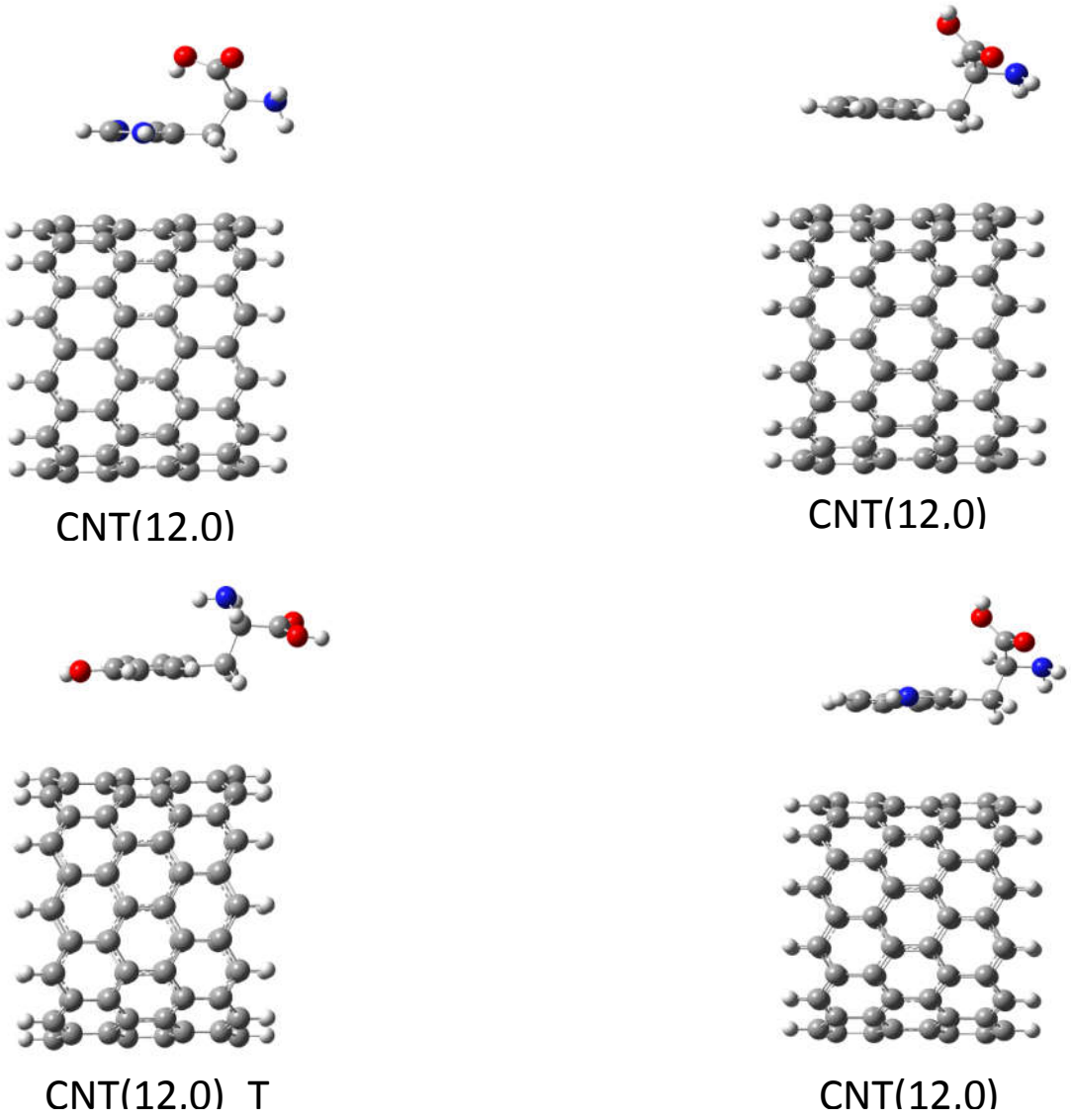

Fig. 3: Optimized geometry of four different adsorption states of aromatic amino acids on the exterior position of single walled carbon nanotube (CNT (12, 0)).

Table 1: B3LYP/6-31G* The binding Energy, HOMO-LUMO Energy Gap of the complex molecular system in the exterior postion.

Complex molecular system	Binding Energy(kcal/mole)	HOMOEnergy(eV)	LUMO Energy(eV)	HOMO-LUMO Gap(eV)
CNT(12,0)_histidine	-7.952	-3.876	-3.478	0.398
CNT(12,0)_phenylalanine	-0.170	-3.849	-3.442	0.407
CNT(12,0)_tyrosine	-0.649	-3.878	-3.474	0.404
CNT(12,0)_tryptophan	-0.791	-3.887	-3.482	0.405

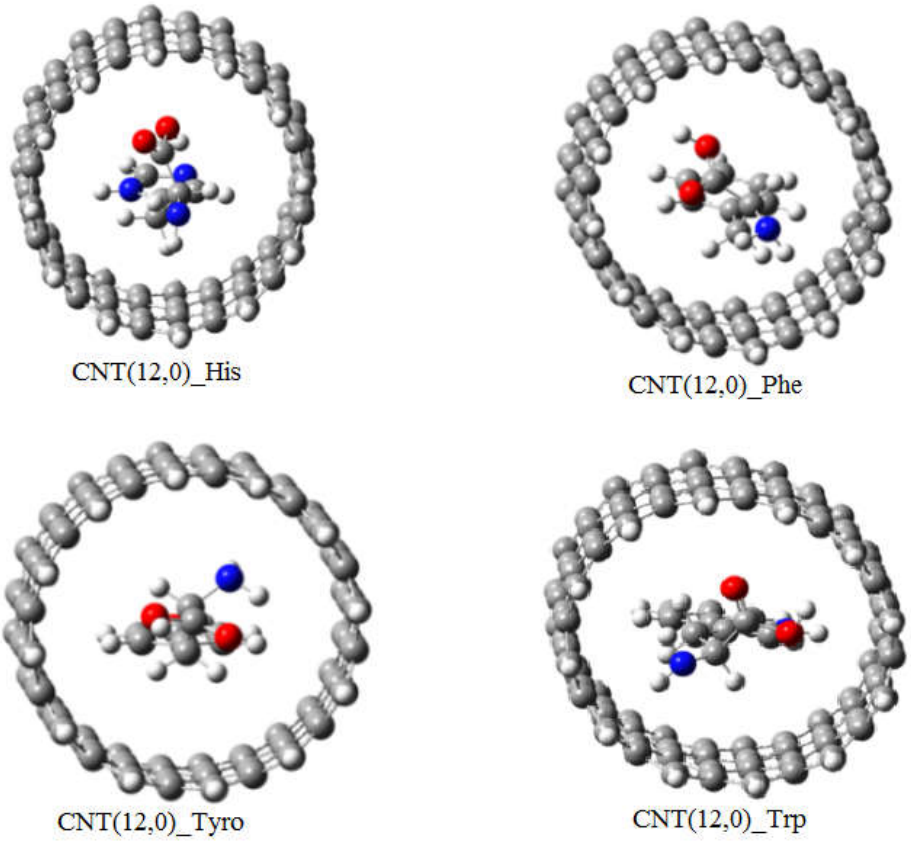

Fig. 4: Optimized geometry of four different adsorption states for aromatic amino acids in the interior position of single walled carbon nanotube (CNT (12, 0)).

Table 2: B3LYP/6-31G* The binding Energy, HOMO-LUMO Energy Gap of the complex molecular system in the interior postion of aromatic amino acid.

Complex Molecular System	Binding Energy (Kcal/mole)	HOMO Energy (eV)	LUMO Energy (eV)	HOMO-LUMO gap (eV)
Cnt(12,0)_Histidine	-2.891	-3.838	-3.481	0.357
CNT(12,0)_Phenylalanine	4.656	-3.895	-3.487	0.408
CNT(12,0)_Tyrosine	1.778	-3.839	-3.436	0.403
CNT(12,0)_Tryptophan	8.447	-3.867	-3.470	0.397

Table 1 and 2 also show the HOMO-LUMO gap of the various aromatic amino acids in exterior and interior position of single walled carbon nanotube. The HOMO-LUMO gap for the interaction of histidine with CNT(12, 0) vary from 0.357 to 0.398eV for the interior and exterior position respectively. The binding energy of histidine increases with decreasing HOMO-LUMO energy gap of CNT (12,0). The binding energy of phenylalanine and tyrosine is greater in interior position than in the exterior position of CNT(12,0) but there is no

significant change of HOMO-LUMO energy gap of CNT(12,0) with increase in binding energy for phenylalanine. On the other hand the binding energy of tryptophan vary from -0.791 to 8.447kcal/mole and the HOMO-LUMO energy gap of CNT(12,0) vary from 0.405 to 0.397eV. The binding energy of tryptophan is increasing with decrease in the HOMO-LUMO energy gap for CNT(12,0) in interior position. Therefore, we also can say that the tryptophan have strongest binding energy in interior position of single walled carbon nanotube.

4. CONCLUSION

The binding of a series of different aromatic amino acids with carbon nanotube has been comprehensively analysed. Our calculations reveal that the binding energy preferences of aromatic amino acids are different in both positions respectively i.e. in exterior and interior positions. The binding energy of aromatic amino acid is greater in interior than the exterior position of single walled carbon nanotube. For the exterior position the preferential order of the interaction for the aromatic amino acids with single walled carbon was histidine < tyrosine < tryptophan < phenylalanine while for the interior position the order is histidine < tyrosine < phenylalanine < tryptophan. The Significant changes occur in the HOMO-LUMO energy gap of the CNT(12,0) on the aromatic amino acids, which are used to design the new nano-bio composite carbonaceous material. This study can also be applied to develop novel bio- sensors, new carbon based drug delivery systems and sensing applications, focusing particularly on the mechanism of binding between biomolecule and carbon nanotube.

5. AKNOWLEDGEMENTS

DS and AK acknowledges the financial support of the University Grant Commission (UGC), Government of India, New Delhi.

6. REFERENCES

1. Dinadayalane TC and Leszczynski J, Struct. Chem., 2010, 21: 1155–1169.
2. Liang F and Chen B, Curr. Med. Chem., 2010, 17: 10–24.
3. Zhu Y, Murali S, Cai W, Li X, Suk JW, Potts JR and Ruoff RS, Adv. Mater., 2010, 22: 3906–3924.
4. Ready AS, Sastry GN, J. Phys. Chem. A., 2005, 109: 8893-8903.
5. Dinadayalane TC, Sastry GN, Leszczynski J, Int. J. Quantum Chem., 2006, 106: 2920-2933.
6. Zorbas V, Smith AL, Xie H, Ortiz-Acevedo A, Dalton AB, Dieckmann GR, Draper RK, Baughman RH, Musselman IH, J. Am. Chem. Soc., 2005, 127: 12323-12328.
7. Ge C, Du J, Zhao L, Wang L, Li Y, Yang Y, Zhou R, Chai Z, Chen C, Proc. Natl. Acad. Sci. USA, 2011, 108: 16968-16973.
8. Balamurugan K, Gopalakrishnan R, Raman SS, Subramanian V, J. Phys. Chem. B, 2010, 114: 14048-14058.
9. Balamurugan K, Singham E.R.A, Subramanian V, J. Phys. Chem. C, 2011, 115: 8886-8892.
10. Gopalakrishnan R, Balamurugan K, Singham ERA, Sundaraman S, Subramanian V, Phys. Chem. Chem. Phys., 2011, 13: 13046-13057.
11. Balamurugan K, Subramanian V, Biopolymers , 2013, 99: 357-369.
12. Liu Z , Sun X, Nakayama-Ratchford N, Dai H , ACS Nano, 2007, 1: 50-56.
13. Khan MAK, Kerman, Prtryk M, Kraatz H, Anal. Chem., 2008, 80: 2574-2582.
14. Kuang Z, Kim SN, Crookes-Goodson WJ, Farmer BL, Naik RR, ACS Nano 2010, 4: 452-458.
15. Barone PW, Baik S, Heller DA, Strano MS, Nat. Mater., 2005, 4: 86-92.
16. Umadevi D AndSastry GN, J. Phys. Chem. C, 2011, 115: 9656-9667.
17. Umadevi D, Sastry GN, J. Phys. Chem. Lett., 2011, 2: 1572-1576.
18. Umadevi D, Panigrahi S, Sastry GN, Acc. Chem. Res., 2014,47: 2574-2581.
19. Umadevi D and Sastry GN, Curr. Sci., 2014, 106: 1224.

20. Umadevi D and Sastry GN, Chem. Phys. Lett., 2012,549:39-43.

21. Kong J, Franklin NR, Zhou CW, Chapline MG, Peng S, Cho KJ, and Dai H, Science 287, 622_2000_; P. G. Collins, K. Bradley, M. Ishigami, and A. Zettl, ibid.287,1801_2000_; M. Shim, A. Javey, N. Wong Shi Kam, and H.Dai, J. Am. Chem.Soc., 2001, 123:11512.

22. Zorbas V, Smith AL, Xie H, Ortiz-Acevedo A, Dalton AB, Dieckmann GR, Draper RK, Baughman RH, and Musselman IH, J. Am. Chem. Soc., 2005, 127: 12323.

23. Lie X, Chen W, Zhan Q, Sowards L, Pender M, and Naik RR, J. Phys. Chem. B, 2006,110:12621.

24. Chen RJ, Zhan Y, Wang D, and Dai H, J. Am. Chen. Soc., 2001, 123: 3838.

25. Zhan J, Lee JK, Wu Y, and Murray RW, Nano Lett. 2003, 3: 403.

26. Kong J, Franklin N, Zhou C, Chapline M, Peng S, Cho K and Dai H, Science, 2000, 287, 622-625.

27. Schedin F, Geim AK, Morozov SV, Hill EW, Blake P, Katsnelson MI and Novoselove KS, Nature Mater., 2007,6: 652-655.

28. Chen W., Duan L, Zhu D, Environ. Sci. Technol. 2007,41: 8295.

29. Panigrahi S, Bhattacharya S, Banerjee S, Bhattacharyya D, J. Phys. Chem. C,2012, 116: 4374.

30. Balavoine F, Schultz P, Richard C, Mallouh V, Ebbesen T, Mioskowski C, Angew.
Chem. Int. Ed.,1999, 38: 1912.

31. Tsang SC, Davis JJ, Malcolm L, Green H, Allen H, Hill O, Leung YC, Sadler PJ,

32. J. Chem. Soc. Chem.Commun. 1995, 17: 1803.

33. Tsang SC, Guo Z, Chen YK, Green MLH, Allen H, Hill O, Hambley TW, Sadler PJ, Angew. Chem. Int. Ed. Engl.1997, 36: 2197.

34. Chen RJ, Bangsaruntip S, Drouvalakis KA, Kam NWS, Shim M, Li Y, Kim W, Utz P, Dai H, Proc. Natl. Acad. Sci. 2003,100: 4984.

35. Besteman K, Lee J, Wiertz FGM, Heering H, Dekker C, Nano Lett. 2003,3: 727.

36. Star A, Gabriel JCP, Bradley K, Gruner G, Nano Lett. 2003,3:459.

37. Roman T, Dino WA, Nakanishi H, Kasai H, Eur. Phys. J. D.,2006,38: 117.

38. Frisch, MJ et al., Gaussian 09, Revision C. 01, Gaussian Inc., Wallingford, CT, USA,

Bull. Mater. Sci.
DOI 10.1007/s12034-017-1478-x

Adsorption of small gas molecules on pure and Al-doped graphene sheet: a quantum mechanical study

DHARMVEER SINGH, ASHEESH KUMAR and DEVESH KUMAR*
Department of Applied Physics, School for Physical Sciences, Babasaheb Bhimrao Ambedkar University, Lucknow 226025, India
*Author for correspondence (dkclcre@yahoo.com)

MS received 26 September 2016; accepted 13 February 2017

Abstract. The interaction of small gas molecules (CCl_4, CH_4, NH_3, CO_2, N_2, CO, NO_2, CCl_2F_2, SO_2, CF_4, H_2) on pure and aluminium-doped graphene were investigated by using the density functional theory to explore their potential applications as sensors. It has been found that all gas molecules show much stronger adsorption on the Al-doped graphene than that of pure graphene (PG). The Al-doped graphene shows the highest adsorption energy with NO_2, NH_3 and CO_2 molecules, whereas the PG binds strongly with NO_2. Therefore, the strong interactions between the adsorbed gas molecules and the Al-doped graphene induce dramatic changes to graphene's electronic properties. These results reveal that the sensitivity of graphene-based gas sensor could be drastically improved by introducing the appropriate dopant or defect. It also carried out the highest occupied molecular orbital–lowest unoccupied molecular orbital energy gap of the complex molecular structure that has been explored by M06/6-31++G** method. These results indicate that the energy gap fine tuning of the pure and Al-doped graphene can be affected through the binding of small gas molecules.

Keywords. DFT; small gas molecules; graphene; aluminium-doping; non-covalent interaction; grapheme-based gas sensors.

1. Introduction

Carbon is the versatile element on the earth's crust and it is found on the earth's surface in different allotropes as graphite, diamonds, charcoal and coke, respectively. The newer allotropes of carbon were discovered such as graphene, carbon nanotubes (CNTs) and fullerenes [1–3]. Graphene is the youngest known allotrope of carbon, which is a two-dimensional and one-atom thick material consisting of sp^2 hybridized carbon atoms arranged in a honeycomb structure. These allotropes of carbon are extensively used in research, that is, from biomedical to environment applications due to their unique physical and chemical properties [4]. The exceptional properties of carbon nano materials, such as electronic, thermal, optical, mechanical and transport properties make them promising candidates for various potential applications [5–7]. From several experimental and theoretical studies it is observed that the transport and electronic properties are extremely sensitive to change in the local chemical environment [8–10]. Carbon nanostructures (CNSs) exhibit non-covalent interaction such as the XH–π, cation–π, anion–π and π–π interaction towards the small gas molecules, metal ions and bio molecules [11–15]. The XH–π weak interactions were extensively studied in recent years [16–20]. These interactions have been considered to be a unique type of hydrogen bonding interaction in which π electron acts as the proton acceptor [14]. Graphene is a sensitive nano material, which detects all the individual events when a gas molecule is adsorbed to or de-adsorbed from its surface [21]. However, it is very difficult to prepare a perfect single layer graphene with zero band gap. Doping is one of the most efficient method to improve the electronic properties of the materials. Wang *et al* have found that the sp^2 hybridization is affected and it changes the electronic properties of the system when B, N and B–N are doped with pure graphene (PG) [22]. Lherbier *et al* showed that the charge mobility and conductivity of graphene changes when B/N impurity atom is added to its surface [23]. Recently, there are several experimental studies on Al, Ga and Pd-doped graphene sheet-based gas sensor [24,25]. Interestingly, the nanoparticles such as Al, Ga and Pd incorporated the significant changes in the sensitivity and selectivity towards the gas molecules. The structure and physical properties of CNSs make them potential candidates as sensors to detect different types of gas molecules. Dai and co-workers were the first to report the gas sensors based on CNTs to detect gas molecules such as NO_2 and NH_3 [26]. Recently, Schedin *et al* experimentally reported that graphene-based gas sensors possess very high sensitivity such that the adsorption of individual gas molecules could be detected [21]. CNSs can absorb a number of species such as gas molecule, metal ions, polymers, organic molecules and biomolecules such as proteins, nucleobases and deoxyribonucleic acid (DNA) on their surface and these adsorption properties provide opportunities for potential industrial applications [27–30].

Published online: 03 October 2017

Roman *et al* studied the adsorption of few amino acids on a single-walled CNT by using the DFT method [31]. CNTs have also been found to be suitable candidates for the negative electrode of the Li-ion batteries, where the Li diffuse between the positive and negative in the ionic state [32,33]. Thus, the fundamental understanding of the interaction of metals with CNTs in the ionic state is important. It is also important to know the role of various factors such as solvent and other chemical environments, which influence such cation–π interaction [34–36]. Umadevi *et al* have found that the charge transfer between graphane and the molecules is an important factor in determining the binding strength of the complex molecular systems [37]. Zhang *et al* studied that doped graphane strongly interacts with CO, NO and NO_2 while NH_3 interacts weakly [38]. Zou *et al* found that the SiG has higher chemical reactions towards the gas molecules due to doping of silicon atom and shows the higher adsorption energy with CO, O_2, NO_2 and H_2O [39]. In the current study, the Al-doped graphene was theoretically investigated to improve its gas sensing efficiency and selectivity towards the various gas molecules. The gas molecule CCl_4, CH_4, NH_3, CO_2, CO, NO_2, CCl_2F_2, SO_2, CF_4 and N_2O, are all of great practical interest for industrial, environmental and medical applications. On the other hand, the effect of doping of the graphene sheet on the binding strength has been estimated. The charge transfer that occurred during the complex formation has also been explored. The change in the highest occupied molecular orbital–lowest unoccupied molecular orbital (HOMO–LUMO) energy gap of PG and Al-doped graphene upon the binding of these gas molecules has also been estimated.

2. Computational methods

The calculations of the interaction between PG, Al-doped graphene and gas molecule is carried out using the density functional theory. The geometrical calculations of all structures have been done by using one method B3LYP/6-31G* [40,41]. Initially, the individual gas molecule is adsorbed on the surface of PG and Al-doped graphene thereafter. Geometry optimization calculations were accomplished using Gaussian09 suite program [42]. It is important to note that complete geometrical configuration was tested but those shown are the lowest energy species feasible for the interaction of the compounds. Single point energy has been done at the M06/6-31++G** level to fine-tune the energy [43–46].

The adsorption energy (E_{ad}) of the small gas molecule (X = CCl_4, CH_4, NH_3, CO_2, N_2, CO, NO_2, CCl_2F_2, SO_2, CF_4, H_2) on the pure and Al-doped graphene is calculated by the following equation (1).

$$E_{ad} = E_{\text{graphene\_X/graphene@Al\_X}} - (E_{\text{graphene/Al@graphene}} + E_X) \quad (1)$$

Here, $E_{\text{graphene\_X/graphene@Al\_X}}$ represents the total energy of a complex molecular system. $E_{\text{graphene/graphene@Al}}$ and E_X represent the total energies of the graphene and gas molecule, respectively. The individual small gas molecule was placed parallel to the surface of graphene and doped graphene at the 3 Å distance. The variation of the charge on gas molecules as well as on pure and doped graphene when the individual gas molecules are kept at the 3 Å distance from its surface was calculated. The charge transfer has been considered as the sum of all atoms in the pure and Al-doped graphene model system. Positive charge transfer values indicate the transfer of charge from graphene to the molecules, while negative charge values indicate the transfer of charge from the molecules to the pure and Al-doped graphene. The HOMO–LUMO energy gap of pure and Al-doped graphene as well as their complexes at M06/6-31++G** level of theory were also calculated. All calculations were carried out using the Gaussian09 program package.

3. Results and discussion

The optimized structure of pure and Al-doped graphene and their complexes with small molecules are shown in figures 1, 2 and 3. The initial configuration of all small gaseous molecules were assigned so that these are oriented exactly parallel to the pure and Al-doped graphene at 3 Å from its surface. In this paper, pure and Al-doped graphene was considered to study the interaction of small gas molecules with X–π non-covalent interaction towards carbon nano materials. Tables 1 and 2 summarize our results on the adsorption energy, equilibrium graphene–molecule distance (d, defined as the distance of nearest atoms between graphene and molecule), the charge transfer (Q, mulliken charge) and HOMO–LUMO energy gap for the most stable configurations of pure and Al-doped graphene adsorbed with various gas molecules in our calculations as shown in figures 2, 3 and tables 1, 2. Subsequently, we look at the binding of the pure and Al-doped graphene with various gas molecules and the trend in the charge transfer. The HOMO–LUMO energy gap of pure and Al-doped graphene with adsorption of various gas molecules were also investigated. When one impurity atom as Al is substituted for one C atom in graphene sheet, the optimized configuration of the graphene sheet is dramatically distorted. The Al atom introduces the deformation of the six-membered ring (6MR) near the doping site to relieve stress, as a result the Al atom protrudes out of the graphene sheet. The optimized carbon–dopant atom distance (Al–C) is 1.751 Å at B3YP/6-31G*, which is in agreement with the previous study [47].

3.1 *Adsorption energy and charge transfer*

The small gas molecules form X–π type complex with the pure and Al-doped graphene that are shown in figures 2 and 3. We observed the adsorption energy of small gas

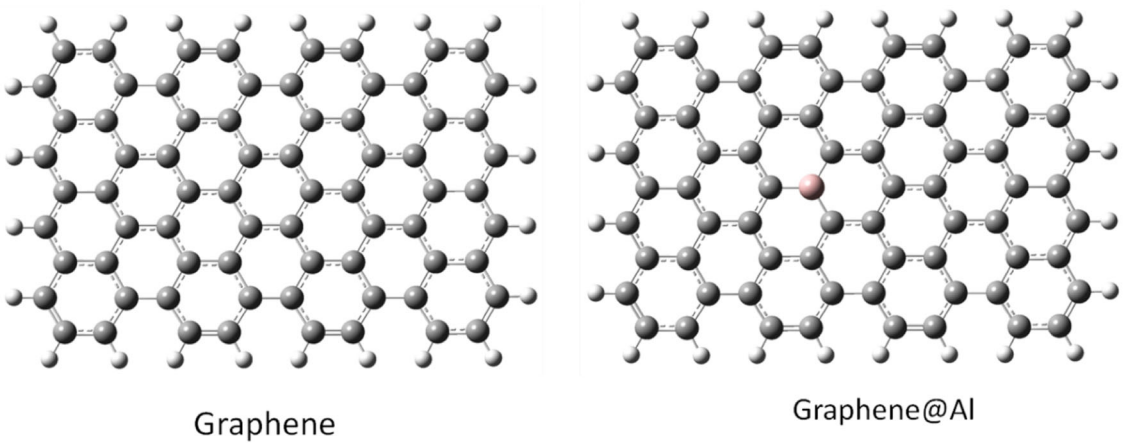

Figure 1. Top view of the optimized structure of pure and Al-doped graphene model system considered in this study.

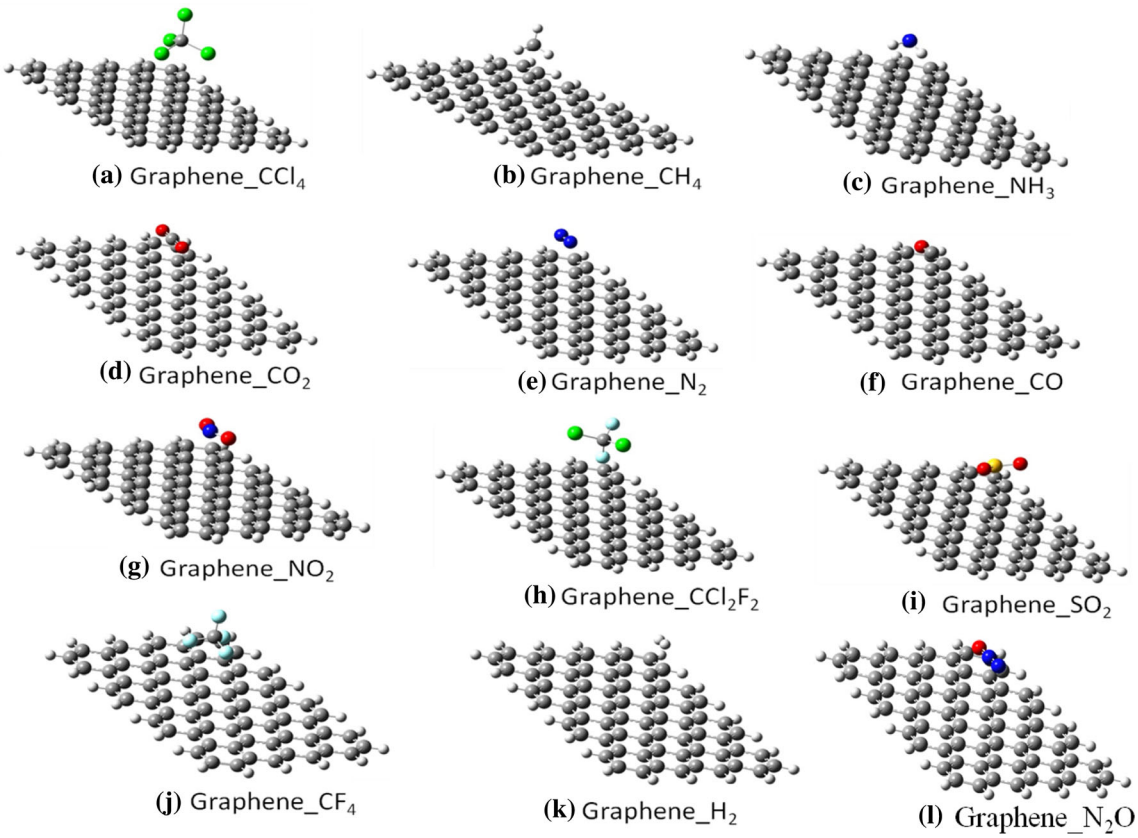

Figure 2. Optimized geometries of pure graphene with small gas molecule adsorbed (**a**) CCl_4, (**b**) CH_4, (**c**) NH_3, (**d**) CO_2, (**e**) N_2, (**f**) CO, (**g**) NO_2, (**h**) CCl_2F_2, (**i**) SO_2, (**j**) CF_4, (**k**) H_2 and (**l**) N_2O by M06/6-31++G** method.

molecule complexes with pure and Al-doped graphene when the gas molecules are kept parallel to the graphene surface at 3 Å distance. Tables 1, 2 and figure 4 display the adsorption energy, charge transfer and molecule sheet distance of the small gas molecule complexes with pure and Al-doped graphene at M06/6-31++g** level of theory.

Interestingly, a different trend in the case of small gas molecule interacting with pure and Al-doped graphene is observed, the adsorption energy of small gas molecules towards the Al-doped graphene is greater than PG. From table 2 and figure 2, the adsorption energy of all gas molecules is higher for the Al-doped graphene than that of PG.

For CCl_4 and CH_4 adsorbed on PG, the most energetically favourable configuration (Graphene_CCl_4) is also identical. The adsorption of CCl_4 and CH_4 on PG is non-covalent interaction with the adsorption energy of -0.394 and

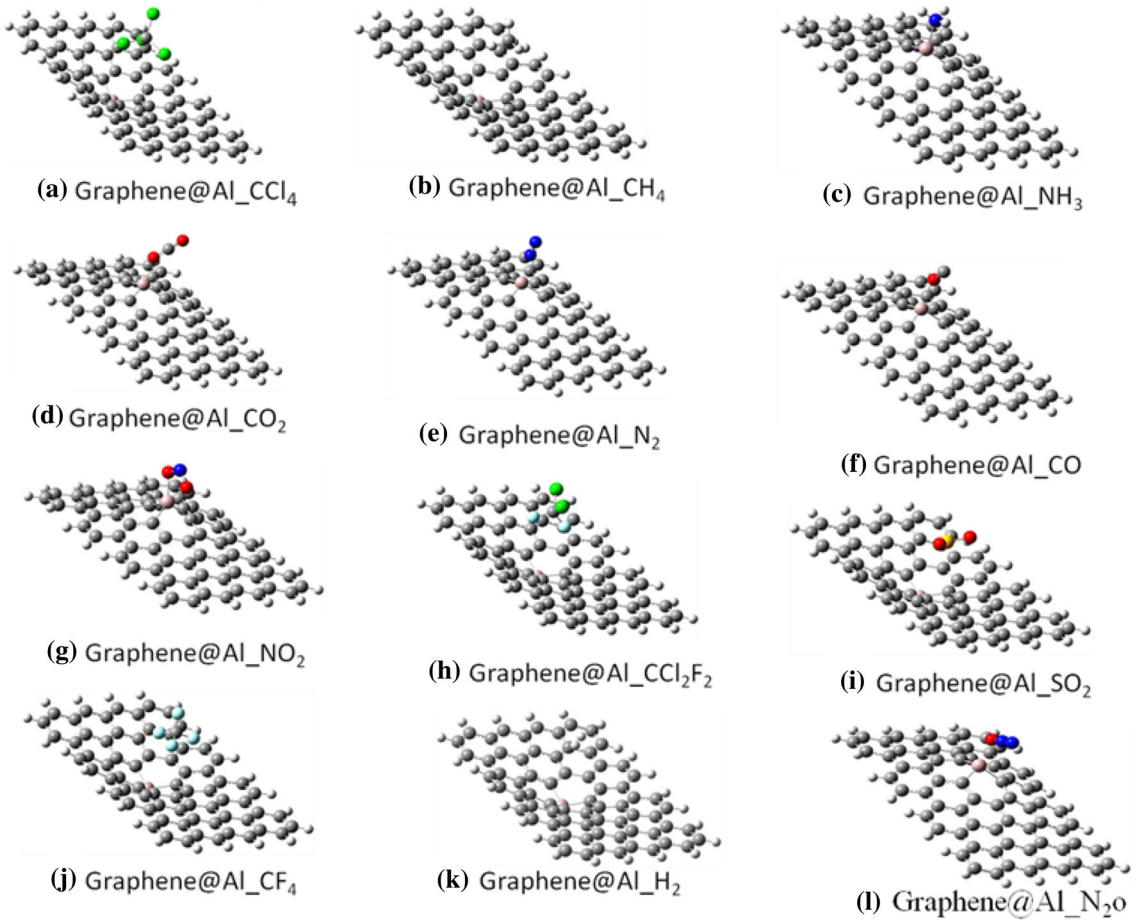

Figure 3. Optimized geometries of aluminium-doped graphene (@Al shown as Al doping in pure graphene) adsorbed with small gas molecules (**a**) CCl_4, (**b**) CH_4, (**c**) NH_3, (**d**) CO_2, (**e**) N_2, (**f**) CO, (**g**) NO_2, (**h**) CCl_2F_2, (**i**) SO_2, (**j**) CF_4, (**k**) H_2 and (**l**) N_2O by M06/6-31++G** method.

Table 1. The adsorption energy (eV), molecule sheet distance (Å), charge transfer (a.u.) and HOMO–LUMO energy gap (eV) at M06/6-31++G** level of theory.

Carbon nanomaterial	Small gas molecule	Adsorption energy (eV)	Molecule sheet distance (Å)	Charge on gas molecule (a.u.)	HOMO–LUMO gap (eV)
Graphene	CCl_4	−0.394	4.498	−0.0196	0.3339
	CH_4	−0.067	3.784	−0.0133	0.3336
	NH_3	−0.145	3.357	0.0334	0.3336
	CO_2	−0.122	3.626	0.0169	0.3336
	N_2	−0.083	3.828	0.014	0.3339
	CO	−0.110	3.732	0.0098	0.3336
	NO_2	−0.996	3.573	0.025	0.8727
	CCl_2F_2	−0.119	3.355	0.0039	0.3336
	SO_2	−0.279	3.578	0.0254	0.3339
	CF4	−0.150	3.404	0.0552	0.3336
	H_2	−0.013	4.946	0.0006	0.3339
	N_2O	−0.123	3.634	0.0180	0.3340

−0.067 eV and the molecule sheet distance of 4.498 and 3.784 Å, respectively. The charge transfer from graphene to CCl_4 and CH_4 molecule is −0.0196 and −0.0133 a.u., which indicates that the PG acts as a donor, and the gas molecule acts as an acceptor. Therefore, PG is less sensitive to the CCl_4 than CH_4 molecule. The most stable configuration of CCl_4

Table 2. The adsorption energy (eV), molecule sheet distance (Å), charge transfer (a.u.) and HOMO–LUMO energy gap (eV) at M06/6-31++G** level of theory.

Carbon nanomaterial	Small gas molecule	Adsorption energy (eV)	Molecule sheet distance (Å)	Charge on gas molecule (a.u.)	HOMO–LUMO gap (eV)
Graphene@Al	CCl_4	−1.354	3.920	−0.007	0.661
	CH_4	−1.242	4.300	0.004	0.616
	NH_3	−2.948	2.053	0.493	1.080
	CO_2	−2.019	2.158	0.423	1.574
	N_2	−1.279	2.210	0.837	0.444
	CO	−1.255	2.344	0.276	0.494
	NO_2	−3.867	1.894	−0.065	0.330
	CCl_2F_2	−1.361	3.956	0.020	0.579
	SO_2	−1.608	3.579	0.045	0.599
	CF_4	−1.354	3.920	0.138	0.662
	H_2	−1.637	6.306	0.001	1.512
	N_2O	−1.409	2.163	0.518	0.453

and CH_4 on graphene@Al is a configuration with the CCl_4 and CH_4 molecule parallel to the graphene sheet and Cl atom of CCl_4 and H atom of CH_4 adsorbed on the top of Al atom, which is shown in figure 3a and b, where the molecular sheet distance is 3.920 and 4.300 Å, respectively. The calculated E_{ad} value is −1.354 and −1.242 eV, which indicates that the graphene@Al has higher adsorption enegy than PG with CCl_4 and CH_4.

The NH_3 molecule shows different adsorption configurations on pure and Al-doped graphene, showing a more complicated adsorption mechanism than the other molecules. On the PG, the configuration with the three hydrogen atoms of NH_3 pointing towards the graphene plane is the favourable one (figure 3c), which gives an adsorption energy and molecule distance of −0.145 eV and 3.357 Å, respectively. This result is consistent with previous reports about NH_3 adsorbed on CNTs (−0.14 eV) and NH_3 adsorbed on graphene (0 ∼ −0.17 eV) [48,49], which indicates a weak interaction between NH_3 and the PG. On the Al-doped graphene, NH_3 is attached to the Al atom with the N atom pointing at the sheet, which gives an adsorption energy of −2.948 eV and an Al–N distance of 2.053 Å (as shown in figure 3c and table 2). The charge transfer from NH_3 to graphene is 0.493 a.u., which indicates that the graphene behaves as charge acceptor and NH_3 molecule as charge donor. The adsorption energy of NH_3 on Al-graphene (−2.948 eV) is much higher than that on the PG, which attributes to the strong interaction between the electron-deficient Al atom and the electron-donating N atom of NH_3. It is also investigated that the Al-doped graphene undergoes an obvious distortion upon NH_3 adsorption (figure 3c), indicating that the B site is transformed from sp^2 to sp^3 hybridization, which matched the previous study [35]. The molecular distance between Al and N is 2.053 Å. This strong interaction is also evident in the electronic total charge density on Al-doped graphene system, which shows large electron density overlap.

The adsorption energy of this complex system is –0.122 eV and molecule–sheet distance is 3.626 Å, which are shown in table 1 and figure 2d. The low adsorption energy and long molecule sheet distance indicate a weak interaction. When the CO_2 molecule is adsorbed on PG, the calculated charge transfer of CO_2 is 0.0169 a.u. In this configuration, the CO_2 molecule acts as a charge donor. When the CO_2 molecule is adsorbed on Al-doped graphene, one oxygen atom of CO_2 shows most stable configuration towards the Al atom of graphene@Al sheet. In this configuration, the adsorption energy and molecule sheet distance (O–Al) is −2.019 eV and 2.158 Å, respectively. This result indicates that the interaction of CO_2 with graphene@Al is much stronger than that of PG due to large transfer of charge. In this configuration, the charge transfer from CO_2 to the graphene@Al is 0.423 a.u., which means that the CO_2 molecule acts as a charge donor and graphene@Al acts as a charge acceptor.

In case of graphene_N_2 configuration, the N–N axis gets aligned parallel to the graphene plane along the axis of two opposite C atoms of the 6MR, which was found to be the most stable configuration. The adsorption energy and the molecule sheet distance of this complex system is –0.083 eV and 3.828 Å, respectively as shown in figure 4a, c and table 1. The charge transfer between N_2 and graphene was calculated from Mulliken population analysis, which is shown in table 1. This result indicates that the interaction is weak in nature due to very small adsorption energy and charge transfer. When adsorbed on Al-doped graphene (graphene@Al), N_2 adopts perpendicular oreintation with Al atom of the graphene sheet. In this configuration, the one N atom of N_2 and Al atom of graphene@Al is very close as shown in figure 3e. The adsorption energy and the molecule sheet distance is −1.279 eV and 2.210 Å, respectively (as shown in figures 4a and c). The charge transfer from N_2 to graphene@Al is 0.837 a.u., which indicates that N_2 acts as a charge donor. In this configuration, the adsorption energy of the complex system is higher than

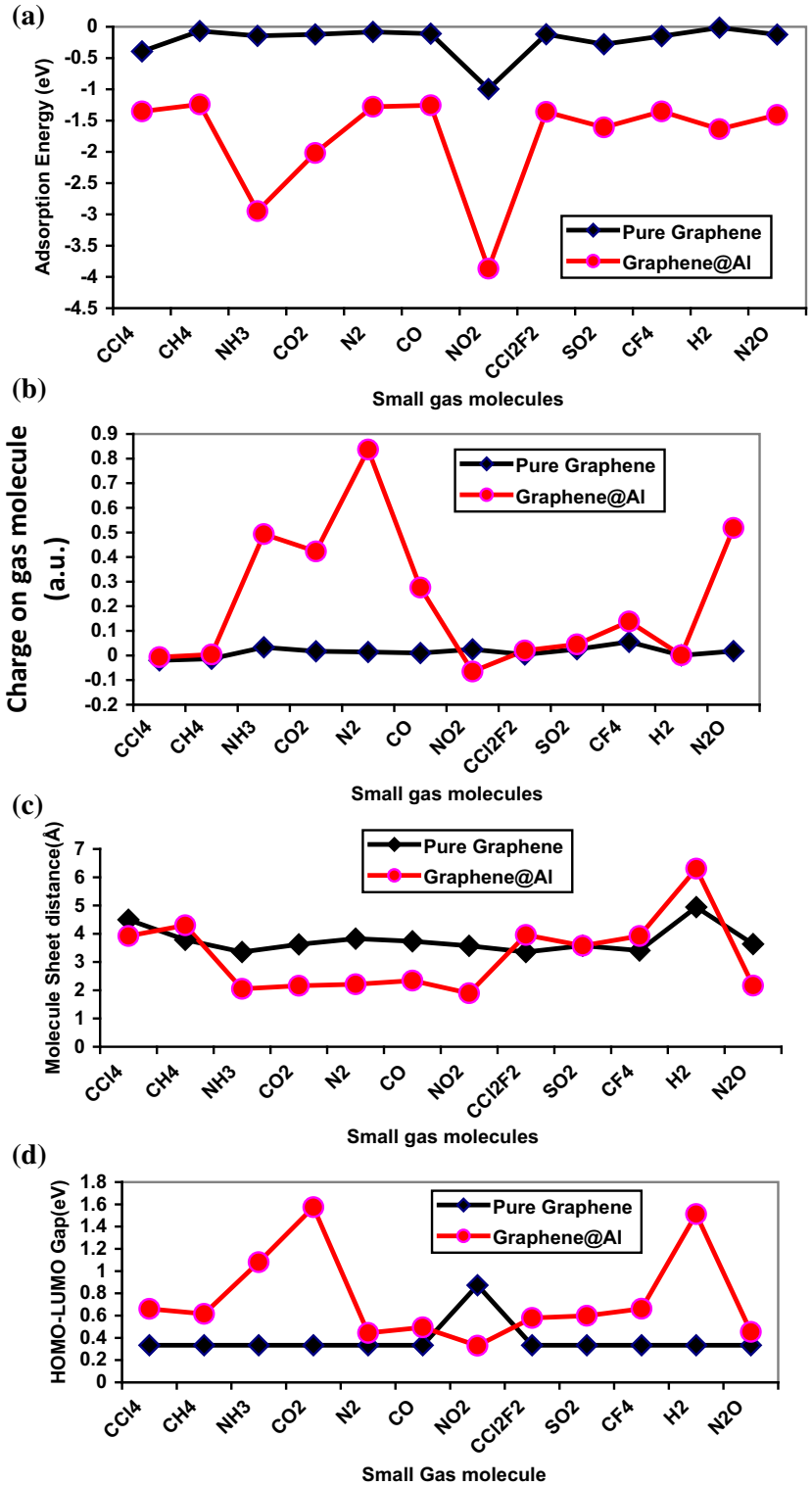

Figure 4. (**a**) The adsorption energy E_{ad}, (**b**) charge transfer, (**c**) molecule sheet distance and (**d**) HOMO–LUMO energy gap of small gas molecules with pure and Al-doped graphene complexes at the M06/-31++G** level of theory. The red line with solid red circles represents the variation for the aluminium-doped graphene whereas the black line with black solid squares represent the variation for pure graphene. The HOMO–LUMO gap for pure graphene is 0.33 eV and for Al-doped graphene is 0.22 eV without any gas molecules.

the graphene_N_2 due to large transfer of charge, which are responsible for strong interaction.

The most stable configuration of CO molecule is similar to the CO_2 and N_2, which are aligned parallel to the PG plane along the axis of two opposite C atoms of the 6MR in the complex molecular structure. The adsorption energy and molecule sheet distance is −0.110 eV and 3.732 Å, respectively (as shown in table 1). When the CO molecule is adsorbed on PG, the charge calculated on the C and O atoms of the CO molecule are 0.100 and −0.090 a.u., respectively, while there is no charge on the carbon atoms of the PG. Therefore, we can say that a very small charge is transferred from CO to the PG. The low adsorption energy and very small charge transfer indicates weak physisorption. When the CO molecule is adsorbed on Al-doped graphene, CO molecule adopts a tilted oreintation with respect to the plane of the Al-containig 6MR, with the O atom close to graphene@Al. In this complex structure, the adsorbed energy and molecule sheet distance are found be −1.255 eV and 2.344 Å, respectively. The charge transfer from CO molecule to graphene@Al is 0.275 a.u. In this configuration, the adsorption energy of graphene@Al_CO is higher than graphene_CO complex (as shown in table 2 and figure 4a).

The adsorption energy and shortest distance from PG to the nearest O atom of NO_2 are −0.996 eV and 3.573 Å, respectively, which indicates a weak interaction between the NO_2 and PG. However, the adsorption energy of NO_2 on PG can remarkably change the electronic properties of PG and the charge transferred from NO_2 to PG is about 0.02504 a.u. It is clear that PG behaves as charge acceptor. In other words, PG is more sensitive to the NO_2 molecule than any other gas molecule. For NO_2 adsorbed on AlG (Al-doped graphene), the most stable configuration (Graphene@Al_NO_2) is similar to that of graphene_NO_2. However, the oxygen atom of NO_2 is bonded to the AlG as shown in figure 2g. The O–Al bond length is 1.894 Å and the adsorption energy for Graphene@Al_NO_2 is −3.867 eV, which indicates that NO_2 is chemisorbed on the graphene@Al. In this configuration, the adsorption energy is greater than graphene_NO_2 due to large charge transferred from graphene@Al to NO_2, about −0.064582 a.u., which is shown in table 2 and figure 4b. It is clear that the graphene@Al behave as charge donor while interacting with the NO_2.

For CCl_2F_2 adsorption on PG, the most energetically favourable configuration is similar to the graphene_CCl_4 and graphene_CH_4. In this configuration, the CCl_2F_2 is adsorbed to PG with one F atom of CCl_2F_2 pointing downwards as shown in figure 2h and table 1. The adsorption of CCl_2F_2 on PG shows interaction with the adsorption energy of −0.119 eV with molecule sheet distance of 3.355 Å, indicating the weak physisorption nature. The calculated charge transfer from CCl_2F_2 is only 0.004 a.u. Therefore, the PG is not senstive to the CCl_2F_2. When the CCl_2F_2 is adsorbed on Al-doped graphene, both florine atoms of CCl_2F_2 get close to the grapehe@Al. In this configuration, the adsorption energy, molecule sheet distance and charge transfer is −1.361 eV, 3.956 Å and 0.02 a.u., respectively, which indicates that interaction is weak in nature due to very small charge transfer (as shown in figure 4b and table 2).

In the graphene_SO_2 complex structure, the S atom of SO_2 is close to the C atom of PG. The adsorption energy E_{ad} and shortest distance from PG to the S atom of SO_2 are −0.279 eV and 3.578 Å, respectively, suggesting a weak interaction between the SO_2 and PG (as shown in figure 4c, d and table 1). However, there is no change in the electronic properties of PG due to the low charge transfer, about 0.025 a.u. from SO_2 to the PG. Therefore, PG is not sensitive to the SO_2 molecule. As shown in figure 3i, the SO_2 is adsorbed on Al-doped graphene, the S atom of SO_2 gets close to the graphene@Al because the Al atom is negatively charged and S atom is positively charged. The charge on Al, S, O(98) and O(99) are −0.283, 0.796, −0.373 and −0.378 a.u., respectively, indicating that Al atom repels both oxygen atoms but attracts the S atom because S atom becomes more positively charged. In this complex structure, the adsorption energy and molecule sheet distance between S and Al is −1.608 eV and 3.579 Å as shown in figure 3i and table 2. However, the charge transfer is very low from SO_2 to grahene@Al, which is about 0.045 a.u.

For CF_4 adsorption on PG, the most energetically favourable configuration is similar to the graphene_CCl4 and graphene_CH4. In this configuration, the CF_4 is adsorbed to PG with one F atom of CF_4 pointing downward as shown in figure 2j and table 1. The adsorption of CF_4 on PG is the non-covalent interaction with the adsorption energy of −0.150 eV and the molecule sheet distance of 3.404 Å, indicating the weak physisorption. The calculated charge transfer from CF_4 is only 0.055 a.u. Therefore, PG is not senstive to CF_4. When CF_4 is adsorbed on Al-doped graphene, one florine atom of CF_4 gets close to graphene@Al. In this configuration, the adsorption energy, molecule sheet distance and charge transfer is −1.354 eV, 3.404 Å and 0.135 a.u., respectively. Therefore, we can say that graphene@Al is more sensitive than PG towards the CF_4 molecule (figure 3j and table 2). In this complex, graphene@Al acts as a charge acceptor.

The H_2 molecule was initially placed parallel to the graphene. After full relaxation, a configuration with the adsorbed H_2 axis gets aligned almost parallel to the graphene surface along the axis of two opposite C atoms of the 6MR and was found to be the most stable one for the PG. The adsorption energy of this system is −0.013 eV and the molecule sheet distance is 3.946 Å as shown in figure 3k and table 1, which are suggesting weak interaction between H_2 and graphene. The charge transfer between H_2 and graphene is 0.0007 a.u. In this configuration, PG is not sensitive towards the H_2 molecule. When adsorbed on graphene@Al, H_2 is oriented perpendicular to the Al-doped graphene plane, with one H(97) atom close to the graphene@Al. In this complex structure, the adsorption energy, molecule sheet distance and charge transfer are −1.637 eV, 6.306 Å and 0.001 a.u., respectively. Interestingly, the graphene@Al has more adsorption energy than PG.

As shown in figure 2l, the most stable configuration of N_2O adsorbed on PG (graphene_N_2O) is similar to graphene_CO_2, where the gas molecule axis is aligned parallel to the graphene plane along the axis of two opposite C atoms of the 6MR. However, the N_2O in graphene_N_2O is located above the centre of the 6MR. The calculated adsorption energy and molecule sheet distance are 0.123 eV and 3.634 Å, respectively. The low adsorption energy and long molecule sheet distance are suggesting weak physisorption. However, it is found that the interaction is significantly improved when a C atom in the PG is replaced by an Al atom. Figure 3l shows the most stable configuration of N_2O adsorbed on graphene@Al, where the oxygen atom of N_2O is close to the Al atom of graphene@Al. The adsorption energy E_{ad} for graphene@Al_N_2O is –1.409 eV, which is clearly higher than that for graphene_N_2O. The interaction distance between the N_2O molecule and the graphene@Al decreases to 2.163 Å, which indicates strong interaction. The charge transfer from N_2O to the graphene is 0.518 a.u. The large transferred charge suggests that the local electronic properties of graphene@Al is remarkably changed due to the adsorption of N_2O on graphene@Al.

The above mentioned results suggest that PG has weak interaction towards all gas molecules. Introducing dopants like Al atom into the graphene significantly increases the molecule–graphene interaction. The order of adsorption energy for small gas molecule complexes is $NO_2 > CCl_4 > SO_2 > CF_4 > NH_3 > N_2O > CO_2 > CCl_2F_2 > CO > N_2 > CH_4 > H_2$ with PG and $NO_2 > NH_3 > CO_2 > H_2 > SO_2 > N_2O > CCl_2F_2 > CF_4 > CCl_4 > N_2 > CO > CH_4$ with Al-doped graphene. Interestingly, our results predicted that Al-doped graphene are more suitable for gas sensing applications, since they have stronger interactions with all small gas molecules than PG. The Al-doped graphene particularly shows the highest sensitivity towards NO_2, NH_3 and CO_2.

3.2 *HOMO–LUMO energy gap*

The primary requisite for a material to perform as a sensor is to undergo a change in its physical property on interacting with an analyte. Such changes can be monitored and recorded to determine the presence of the analyte. The HOMO–LUMO energy gap is defined as the difference between lowest unoccupied molecular orbital and highest occupied molecular orbital. It is the electronic property of any molecular system, which is helpful to design new materials. In order to notice such a depiction in the case of carbon materials, we have calculated the HOMO–LUMO energy gap of the PG and Al-doped graphene in the free state and in the small gas molecule complexes. In general, in the case of X–π complexes, the HOMO–LUMO energy gap of single-walled carbon nanotube (SWCNT) varies with orientation of small gas molecules on the PG and Al-doped graphene. It has been shown that the energy gap of PG is not significant but when the gas molecules is adsorbed on graphene@Al then significant changes in HOMO–LUMO energy gap is observed (as shown in table 2). Therefore, we can say that the variation in HOMO–LUMO energy gap of the graphene upon binding with the various small gas molecules is significant.

4. Conclusion

The adsorption energy of various small gas molecules such as CCl_4, CH_4, NH_3, CO_2, CO, NO_2, CCl_2F_2, SO_2, CF_4 and N_2O with the pure and Al-doped graphene (graphene@Al) has been comprehensively analysed. These calculations reveal that the adsorption energy has preferences of small gas molecules with the doping in graphene as well as molecule sheet distance. It can be seen from the results that the adsorption energy of these gas molecules is higher for the Al-doped graphene than for the PG. PG shows weak sensitivity to all gas molecules. Compared with PG, graphene@Al has a higher chemical reactivity towards all gas molecules due to the doping of Al atom and shows higher adsorption energy with NO_2, NH_3 and CO_2. The strong interactions between graphene@Al and the adsorbed molecules induce dramatic changes in the electronic properties of graphene@Al and make graphene@Al a promising candidate as gas sensing materials for NO_2, NH_3 and CO_2. The Mulliken charge analysis reveals that the gas molecule acts as charge donor and acceptor in different configurations towards the pure and Al-doped graphene and influence the physical properties of carbon materials, which leads to the sensitivity. It has also been found that HOMO–LUMO energy gap of the CNT is always affected by the binding of the small gas molecules. Significant changes occur in the HOMO–LUMO energy gap on PG and graphene@Al on interacting with gas molecules, which provides a handle to tune the electronic and conductivity properties of graphene through gas molecule complexation. These studies can also be applied to develop new carbon-based materials and sensing applications, focusing particularly on the binding mechanism of various gas molecules with graphene. Developing chemical and gas sensors based on carbon materials has become an area of significant research interest since the physical and electronic properties of these materials are vulnerable to external enviroment. It is to hope that our results would be helpful to develop novel carbon material-based gas sensors.

Acknowledgements

Dharmveer Singh and Asheesh Kumar acknowledge their financial support from the University Grants Commission (UGC), New Delhi.

References

[1] Hirsch A 2010 *Nat. Mater.* **9** 868
[2] Rao C N R, Sood A K, Subrahmanyam K S and Govindaraj A 2009 *Angew. Chem. Int. Ed.* **48** 7752

[3] Iijima S 1991 *Nature* **354** 56
[4] Liu J, Cui L and Losic D 2013 *Acta Biomater.* **9** 9243
[5] Dinadayalane T C and Leszcznski J 2010 *Struct. Chem.* **21** 1155
[6] Liang F and Chen B 2010 *Curr. Med. Chem.* **17** 10
[7] Zhu Y, Murali S, Cai W, Li X, Suk J W, Potts J R *et al* 2010 *Adv. Mater.* **22** 3906
[8] Goldoni A, Larciprete R, Petaccia L and Lizzit S 2003 *J. Am. Chem. Soc.* **125** 11329
[9] Guo Z, Feng Y, He S, Qu M, Chen H, Liu H *et al* 2012 *Adv. Mater.* **25** 584
[10] Zhong J, Chiou J, Dong C, Glans P A, Pong W F, Chang C *et al* 2012 *Appl. Phys. Lett.* **100** 201605
[11] Umadevi D, Panigrahi S and Sastry G N 2014 *Acc. Chem. Res.* **47** 2574
[12] Vijay D and Sastry G N 2010 *Chem. Phys. Lett.* **485** 235
[13] Shi G, Ding Y and Fang H 2012 *J. Comput. Chem.* **33** 1328
[14] Grabowski S J and Lipkowski P 2011 *J. Phys. Chem. A* **115** 4765
[15] Mahadevi A S and Sastry G N 2016 *Chem. Rev.* **116** 2775
[16] Charlier J C 2002 *Acc. Chem. Res.* **35** 1063
[17] Huang P, Zhu H, Jing L, Zhao Y and Cao X 2011 ACS *Nano* **5** 7945
[18] Dougherty D A 1996 *Science* **271** 163
[19] Kim S K, Hu S, Tarakeshwar P and Lee J Y 2000 *Chem. Rev.* **100** 4145
[20] Ready A S and Sastry G N 2005 *J. Phys. Chem. A* **109** 8893
[21] Schedin F, Geim A K, Morozov S V, Hill E W, Blake P, Katsnelson M I *et al* 2007 *Nat. Mater.* **6** 652
[22] Wang X, Sun G, Routh P, Kim D H, Huang W and Chen P 2014 *Chem. Soc. Rev.* **43** 7067
[23] Lherbier A, Blase R X, Niquet Y, Triozon F and Roche S 2008 *Phys. Rev. Lett.* **101** 036808
[24] Lv Y-A, G-l Zhuang G-I, Wang J-g, Jia Y-B and Xie Q 2011 *Phys. Chem. Chem. Phys.* **13** 12472
[25] Cho B, Yoon J, Hahm M G, Kim D H, Kim A R, Kahng Y H *et al* 2014 *J. Mater. Chem.* **2** 5280
[26] Kong J, Franklin N, Zhou C, Chapline M, Peng S, Cho K *et al* 2000 *Science* **287** 622
[27] Umadevi D and Sastry G N 2011 *J. Phys. Chem. C* **115** 9656
[28] Umadevi D and Sastry G N 2011 *J. Phys. Chem. Lett.* **2** 1572
[29] Chen W, Duan L and Zhu D 2007 *Environ. Sci. Technol.* **41** 8295
[30] Panigrahi S, Bhattacharya S, Banerjee S and Bhattacharyya D 2012 *J. Phys. Chem. C* **116** 4374
[31] Roman T, Dino W A, Nakanishi H and Kasai H 2006 *Eur. Phys. J. D.* **38** 117
[32] Kumar A, Reddy A L M, Mukherjee A, Dubey M, Zhan X, Singh N *et al* 2011 ACS *Nano* **5** 4345
[33] Reddy A L M, Srivastav A, Gowda S R, Gullapalli H, Dubey M and Ajayan P M 2010 *ACS Nano* **4** 6337
[34] Rao J S, Zipse H and Sastry G N 2009 *J. Phys. Chem. B* **113** 7225
[35] Sharma B, Rao J S and Sastry G N 2011 *J. Phys. Chem. A* **115** 1971
[36] Mahadevi A S and Sastry G N 2011 *J. Phys. Chem. B* **115** 703
[37] Umadevi D and Sastry G N 2015 *Phys. Chem. Chem. Phys.* **17** 30260
[38] Zhang Y H, Chen Y B, Zhou K C, Liu C H, Zeng J, Zhang H L *et al* 2009 *Nanotechnology* **20** 185504
[39] Zou Y, Li F, Zhu Z H, Zhao M W, Xu X G and Su X Y 2011 *Eur. Phys. B* **81** 475
[40] Becke A D 1993 *J. Chem. Phys.* **98** 5648
[41] Ditchfield R, Hehre W J and Pople J A 1971 *J. Chem. Phys.* **54** 724
[42] Frisch M J, Trucks G W, Schlegel H B, Scuseria G E, Robb M A, Cheeseman J R *et al* 2010 Gaussian Inc., Wallingford, CT
[43] Zhao Y and Truhlar D G 2008 *Theor. Chem. Acc.* **120** 215
[44] Petersson G A, Bennett A, Tensfeldt T G, Al-Laham M A, Shirley W A and Mantzaris J 1988 *J. Chem. Phys.* **89** 2193
[45] Petersson G A and Al-Laham M A 1991 *J. Chem. Phys.* **94** 6081
[46] Frisch M J, Pople J A and Binkley J S 1984 *J. Chem. Phys.* **80** 3265
[47] Dai J Y and Yuan J M 2010 *Phys. Rev. B* **81** 165414
[48] Bai L and Zhou Z 2007 *Carbon* **45** 2105
[49] Charles W, Bauschlicher J and Ricca A 2004 *Phys. Rev. B* **70** 115409